Host-Symbiont Biomass Regulation in the Cnidarian-Dinoflagellate Symbiosis

Lucy Mae Gorman

2021

Abstract

In the cnidarian-dinoflagellate symbiosis, the regulation of host-symbiont biomass is essential for maintaining symbiosis stability and preventing cellular stress. Symbiont biomass is primarily thought to be regulated by pre-mitotic (cell-cycle arrest of the symbiont population) and post-mitotic (autophagy, apoptosis and expulsion) controls. However, there are still large knowledge gaps about the molecular events associated with this regulation, and how these events interact to generate observed patterns of host-symbiont specificity. I therefore aimed to: (1) characterise the molecular mechanisms underpinning the cell-cycle arrest of the symbiont population, and those co-ordinating host and symbiont growth *in hospite*; and (2) determine how the main regulatory mechanisms (symbiont cell-cycle arrest, host apoptosis, host autophagy and expulsion) interact during the onset, establishment and maintenance of symbioses between homologous (i.e. native) and heterologous (i.e. non-native) symbiont species.

In Chapter 2, I focused on the mechanism we know least about, cell-cycle arrest of the symbiont population. In particular, using bioinformatics, I identified which evolutionarily-conserved cell-cycle progression proteins (cyclins and cyclin-dependent kinases (CDKs)) are present in symbiotic dinoflagellates (family: Symbiodiniaceae), whether these proteins differ between species, and how the expression of Symbiodiniaceae cell-cycle genes is influenced by symbiotic state (i.e., when the dinoflagellates are in culture *versus* in the host). Cyclins and CDKs, that are related to eumetazoan cell-cycle and transcriptional cyclins and CDKs, were identified in Symbiodiniaceae, alongside several alveolate-specific cyclins and CDKs, and those related to protist and apicomplexan taxa. Alveolate-specific CDKB was proposed as a homolog to the main cell-cycle CDKs in *Saccharomyces cerevisiae*, Cdc28/Pho85, due to its phylogenetic position, conservation across Symbiodiniaceae species, and the presence of the canonical CDK motif. Symbiont species was found to influence the presence of CDK and cyclins with *Cladocopium* species and *D. trenchii* containing CDK and cyclins related to parasitic taxa, whilst a *Symbiodinium* species contained CDKs and cyclins that were all most closely related to the free-living dinoflagellate *Amphidinium*. Several alveolate-specific CDKs and two protist P/U-type cyclins exhibited altered expression when in symbiosis, suggesting that the symbiotic state influences the expression of symbiont cell-cycle genes. These findings

help us to understand the molecular mechanisms that may underpin cell-cycle arrest of the symbiont population *in hospite*.

In Chapter 3, I focused on the co-ordination between symbiont and host biomass during symbiosis and how the presence of symbionts alters the expression of host cell-cycle genes in the symbiotic gastrodermis and the asymbiotic epidermis, using pre-existing transcriptomics data for the model sea anemone *Exaiptasia pallida* ('Aiptasia') in stable symbiosis with the dinoflagellate *Breviolum minutum*. The presence of symbionts in the gastrodermis elicited host cell-cycle arrest in the G_1 phase and the inhibition of DNA synthesis and mitosis, compared with the aposymbiotic (i.e. temporarily symbiont-free) gastrodermis. As well as reducing cell-cycle progression, the presence of symbionts negatively impacted host apoptosis, with the symbiotic gastrodermis having elevated levels of host apoptotic inhibitors and depressed levels of host apoptotic sensitisers when compared with the aposymbiotic gastrodermis and the epidermis of symbiotic hosts, respectively. Also, I observed increased expression of genes associated with the persistence of non-pathogenic 'non-self' cells in symbiotic gastrodermal tissues, while genes associated with sensitivity to reactive oxygen species (ROS) were down-regulated. These events may contribute to the persistence of symbionts in the host gastrodermis. In epidermal cells, a single gene required for mitotic completion was up-regulated in symbiosis compared with aposymbiotic anemones, suggesting that the presence of symbionts in the gastrodermis stimulates mitotic completion in the epidermis, possibly through the nutritional benefits provided by the symbiosis. Microscopical analysis using the S phase indicator, EdU, confirmed that there were significantly more proliferating host cells in both the gastrodermis and epidermis in the symbiotic state compared with the aposymbiotic state, agreeing with the tissue-specific transcriptomic analysis. These findings help us to understand both how symbionts persist in a host and how symbionts stimulate the growth of the host during symbiosis on a molecular level.

In Chapter 4, I inoculated aposymbiotic Aiptasia with one of four different species of Symbiodiniaceae: homologous *Breviolum minutum* (ITS2 type B1), and heterologous *Symbiodinium microadriaticum* (A1), *Cladocopium goreaui* (C1) and *Durusdinium trenchii* (D1a). I then measured host apoptosis, expulsion and symbiont cell-cycle phase during the onset, establishment and maintenance of the symbiosis, and compared this with an

unmanipulated symbiosis (i.e. permanently symbiotic Aiptasia). The relative importance of these mechanisms shifted over time, even though they all continued to play a role. In particular, after an early peak, host apoptosis declined, but symbiont expulsion compensated for this by becoming more dominant. However, as symbiosis reached a steady state, the number of symbionts arrested in the G_1 phase of their cell cycle increased, while the number of cells cycling through their cell cycle decreased, emphasising that symbiont cell-cycle control is an important regulator of host-symbiont biomass in the stable symbiosis. Similar regulatory patterns were seen in permanently symbiotic anemones to those seen in the fully re-established symbiosis, except that permanently symbiotic hosts expelled a smaller proportion of their symbionts. Species-specific differences were apparent, however, especially with respect to rates of host apoptosis and expulsion. For instance, *D. trenchii*-colonised anemones showed the earliest decline in host apoptosis, and anemones inoculated with heterologous symbiont species consistently expelled a higher proportion of their symbiont population than those colonised by the homologous symbiont. Moreover, in the fully-established symbiosis *D. trenchii* had the highest proportion of its population arrested in the G_1 phase.

Overall, my results provide a detailed overview of the cell-cycle machinery in the Symbiodiniaceae, and highlight that symbiotic state alters the expression of both host and symbiont cell-cycle genes, so allowing growth to be co-ordinated and the symbiosis to persist. I also show that a range of regulatory mechanisms influence symbiont population density, and shift in their relative importance between the onset and full establishment of the symbiosis. Symbiont identity influences the extent to which these mechanisms are used, though not the general patterns seen over time. These findings help us to better understand the cellular events that underlie a successful symbiosis and patterns of host-symbiont specificity, with implications for the formation and persistence of novel, potentially more thermally tolerant, host-symbiont pairings in the face of climate change.

Acknowledgements

From an early age this project has always been my dream. My thanks to all the scientists who have instructed and guided me over the last four years.

Firstly, I thank Professor Simon Davy for his knowledge, expertise, support, constructive feedback and his belief in me. Secondly, my sincere thanks to Dr Clint Oakley whose mentoring and support I have very much enjoyed and appreciated. Thank you for choosing me for this experience and guiding me along the way and always offering the utmost support whenever I needed it. I could not ask for two better supervisors! Also, a big thank you goes to Dr Shaun Wilkinson who helped me so much with my bioinformatics and for taking the time to help me understand genetics. Additionally, I would like to recognise my colleagues in the Davy Lab who are wonderful people and have been with me through the highs and the lows of research, always providing support and friendship. A special shout out and thank you goes to Evan Raymond for helping me to process my autophagy samples and for helping me to optimise my western blot protocol.

Grateful thanks to my collaborators on the project, Professor Virginia Weis and Professor Arthur Grossman, for their expertise and feedback on my project over the last four years to help make my project extremely high quality. I was also lucky enough to receive funding to travel to Professor Weis' lab at Oregon State University and to work with the Weis Lab for 2 months. Virginia and everyone in the Weis lab welcomed me with open arms and made me feel part of the family through their kindness and generosity. Also I would like to acknowledge my contact with Professor Ruth Gates who was my idol and her legacy gave me the encouragement to follow my dreams.

Warm thanks to everyone who looked after me like their own daughter whilst I was in New Zealand – particularly Ron and Angie MacIntosh and Sandra Taylor. From inviting me around for dinner to going out of your way to make sure I was happy during my time in New Zealand, I thank you for being so kind and caring. I see all of you as my adopted parents in New Zealand.

Love goes out to my beautiful friends who I made before my PhD and ones who I met along my New Zealand adventure who accompanied me to festivals, coffee catchups, live musics gigs, nights out, road trips and camping. I know we will be lifelong friends.

Finally, I give thanks to my amazing family Dad Frank, Mum Lynne and brother Edward who have always supported me throughout my whole marine biology career and have been there for me with emotional and financial support.

Table of contents

List of Figures

List of Tables

Contributions and Publications

In this thesis, **Chapter 2** has recently been published (see citation and contributions below)**.** Figures and tables that were too large to include in the thesis from this publication are included in Appendix A and D.

Chapter 2 Citation: Gorman LM, Wilkinson SP, Kitchen SA, Oakley CA, Grossman AR, Weis VM, Davy SK (2020) Phylogenetic analysis of cell-cycle regulatory proteins within the Symbiodiniaceae. *Scientific Reports*, **10**, 20473.

Contributions: The study was conceptualised by L.M.G., C.A.O., A.R.G., V.M.W., and S.K.D. L.M.G. wrote the manuscript, collected and analysed the sequence and phylogenetic data, and constructed all figures (apart from figure 3) and all tables. S.P.W. helped L.M.G. with data collection and analysis. S.A.K. conducted and analysed the expression analysis, constructed figure 3, helped revise the manuscript, and advised on methods, data analysis and visualisation, C.A.O., V.M.W., S.K.D., A.R.G. helped edit and refine the manuscript. All authors reviewed the manuscript before submission.

Chapter 1: General Introduction

1.1. Symbiosis in nature

Symbiosis is classed as an intimate relationship between two or more phylogenetically dissimilar organisms that exist in close contact with one another, allowing novel biological functions to be performed (Chaston and Douglas 2012; Wernegreen 2012). Previously, it was concluded that symbioses are selected so that the host only associates with partners of high quality (those that incur little cost to the host and provide the most benefit), known as mutualistic symbioses, however, it is now widely accepted that symbioses occur on a fluid continuum scale, from parasitism to mutualism (Zook 2015). Symbioses are categorised into three forms on this fluid spectrum: mutualisms, where both partners incur a net benefit; commensalisms, where one partner benefits but provides neither a cost nor a benefit to the other partner; and parasitism, where one partner incurs a net benefit at the expense of the other partner (Redman *et al*., 2001; Roper *et al*., 2019). Environmental conditions can alter where a symbiosis lies on this spectrum, with conditions that are more favourable to the symbiont potentially promoting parasitic tendencies (Leung and Poulin 2008; Lesser *et al*., 2013; Baker *et al*., 2018).

Symbioses that exist in terrestrial biomes include the arbuscular mycorrhiza fungus-*Rhizobium*-legume symbiosis (Hayman 1986; Jennings 1995; Mergaert *et al*., 2006), the *Wolbachia* and insect symbiosis (Nikoh *et al*., 2014; Correa and Ballard 2016) and the mammal and gut bacteria symbiosis (Bäckhed *et al*., 2005; Martín *et al*., 2013). There are also symbioses that exist in the marine environment including the squid and *Vibrio* bacteria symbiosis (Nyholm and McFall-Ngai 2004; McFall-Ngai 2014) and the sponge cyanobacteria symbiosis (Wilkinson and Fay 1979; Freeman and Thacker 2011). However, perhaps the most well-known and ecologically significant symbiosis in the marine realm is that between cnidarians (e.g. hard corals, soft corals, sea anemones, jellyfish and hydrocorals) and dinoflagellate algae (Davy *et al*., 2012; Muller-Parker *et al*., 2015).

1.2. Cnidarian-dinoflagellate symbiosis

Cnidarians form symbioses with dinoflagellates from the family Symbiodiniaceae (Davy *et al*., 2012). The cnidarian-dinoflagellate symbiosis is found from temperate to tropical latitudes and from shallow to deep waters (Schlichter *et al*., 1986; Muller-Parker and Davy 2001; Rodriguez-Lanetty *et al*., 2001; Kahng and Maragos 2006; Wicks *et al*., 2010; Ziegler *et al*., 2015). It is especially important in tropical oligotrophic waters, where the nutritional benefits facilitate the growth and survival of coral reefs, though facultative symbioses also occur in nutrient-rich temperate waters (Muscatine 1990; Weis and Reynolds 1999; Dimond and Carrington 2007). Hosts can acquire their symbiont species vertically from their maternal predecessor or horizontally, from the environment (Sachs and Wilcox 2006) and are ultimately housed inside a vacuole (the 'symbiosome') in the host's gastrodermal cells (Wakefield *et al*., 2000; Wakefield and Kempf 2001) (Fig. 1.1). In the case of horizontal transmission, the host gastrodermal cell engulfs the symbiont *via* phagocytosis (Davy *et al*., 2012; Fransolet *et al*., 2012) and this phagosome is then inhibited from maturing, forming the symbiosome (Wakefield *et al*., 2000; Wakefield and Kempf 2001). Host cells most commonly contain one symbiont cell, however they have the capacity to contain up to six (Muscatine *et al*., 1998). Total densities of symbionts in a cnidarian host can vary between $1.2 – 3.6 \times 10^6$ cells *per* cm^2 host tissue (Cook and D'Elia 1987). The cnidarian provides the symbionts with protection from grazers and a stable position in the photic zone, as well as nutrients from coral waste (Weis 2008; Davy *et al*., 2012; Muller-Parker *et al*., 2015). In return, the symbiont provides the cnidarian host with photosynthetically-fixed carbon to support host growth, respiration and reproduction, and in the case of reef-building corals, stimulates skeletogenesis and the net accretion of coral reefs (Davy *et al*., 2012). This photosynthetic carbon supply promotes the assimilation and recycling of nitrogen, as well as nitrogen conservation given that the host does not need to acquire nitrogen from its own amino acid reserves (Wang and Douglas 1998). Furthermore, the nitrogen products synthesised by the symbiont from the host's waste allow access to essential amino acids that the host cannot synthesise itself, which are then translocated back to the host (Trench 1971; Wang and Douglas 1998; Kopp *et al*., 2013; Rädecker *et al*., 2015).

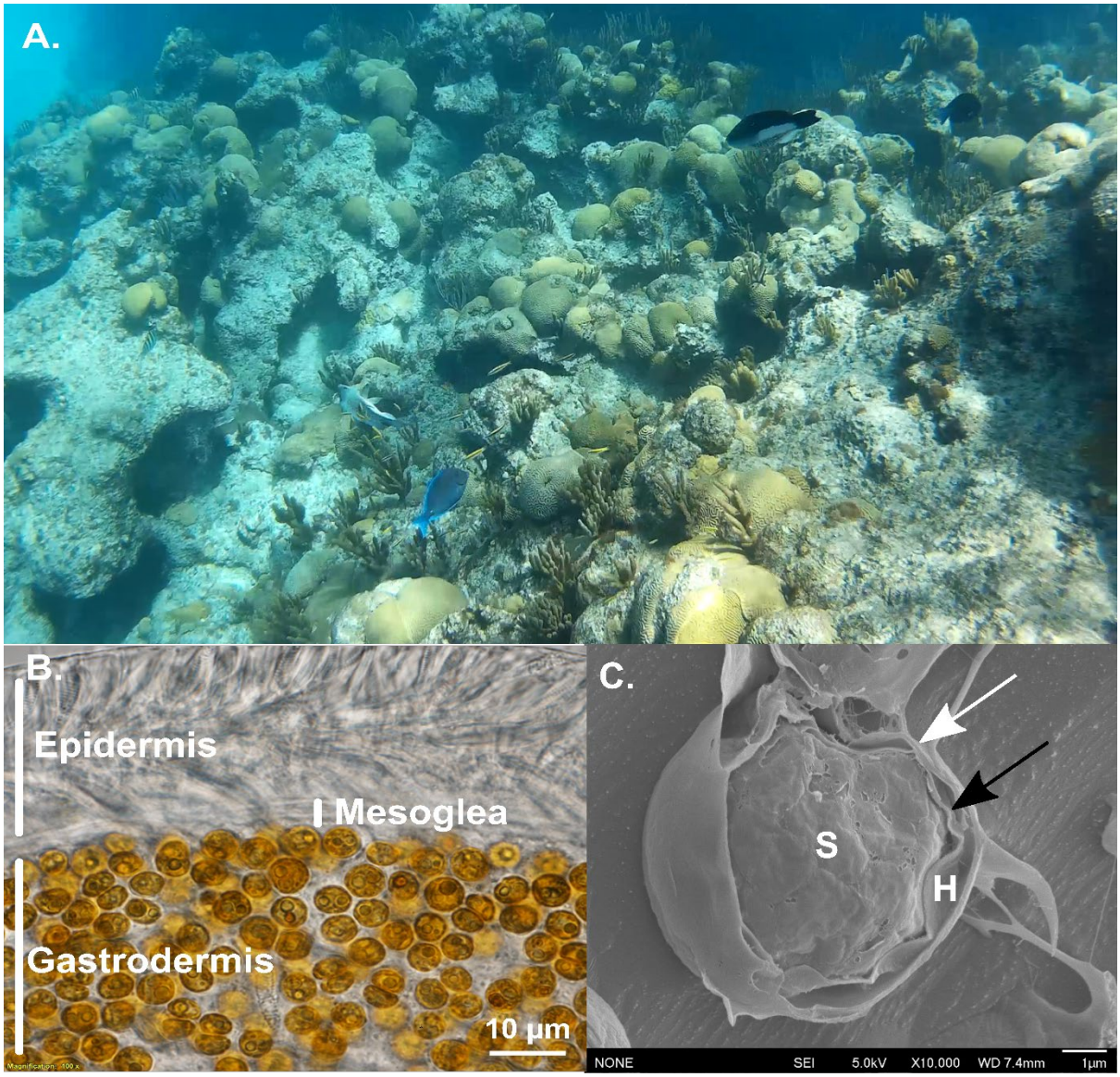

Figure 1.1. (A) Bermudian coral reef. (B) Tentacle anatomy of cnidarian *Exaiptasia pallida* (commonly referred to as 'Aiptasia') showing the symbionts located in the gastrodermis, the separation of the gastrodermis from the epidermis by the mesoglea and the asymbiotic epidermis. Magnification × 100. Photo courtesy of Amirhossein Mashini. (C) Scanning electron micrograph of *Breviolum minutum* 'S' in Aiptasia 'H' showing the symbiosome. Black arrow points to the "symbiosome membrane". White arrow points to multi-layered algal derived membranes. Magnification × 10,000. Photo taken by Lucy Gorman, Bobby Lust and Amirhossein Mashini.

1.2.1. Winnowing

The initial communication between a symbiont and its host is thought to occur at the cell-surface contact stage, which represents the start of the establishment of the symbiosis and involves the recognition between both partners and leads to winnowing of compatible symbiont species by the host (Davy *et al.*, 2012). Recognition involves a variety of cell signalling

cascades between the invading symbiont cell and the host cell (Ganot *et al*., 2011; Davy *et al*., 2012), with the host recognising the symbiont *via* specific algal glycan ligands on the symbiont's cell surface, such as α-mannose/α-glucose and α-galactose (Wood-Charlson *et al*., 2006; Logan *et al*., 2010). Host cells contain pattern recognition receptors (PRRs) on their cell surface that bind to both bacterial pathogen and symbiont ligands (McGuinness *et al*., 2003; Kvennefors *et al*., 2010). Several host PRRs have been identified in cnidarians such as Millectin from the hard coral *Acropora millepora* (Kvennefors *et al*., 2008), SLL-2 a D-galactose-binding lectin of the octocoral *Sinularia lochmodes* (Jimbo *et al*., 2000), CecL from the solitary coral *Ctenactis echinata* (Jimbo *et al*., 2010) and PdC-Lectin from the hard coral *Pocillopora damicornis* (Vidal-Dupiol *et al*., 2009). This cell-signalling interaction is also witnessed in other symbioses such as the arbuscular mycorrhiza fungus- *Rhizobium*-legume symbiosis (van Rhijn *et al*., 2001) and insects with symbiotic bacteria (Welchman *et al*., 2009). In these symbioses, the invasion of a foreign body into a host invokes an immune response which is governed by a series of signalling cascades, where host PPRs allow discrimination between pathogenic and non-pathogenic "non-self" cells (Welchman *et al*., 2009; Newman *et al*., 2013). It should be noted though, that even once the host has recognised the symbiont, efficient communication between the two partners must proceed for the symbiosis to persist. There are currently gaps in our knowledge about what molecular signals are vital to the stability of a symbiosis but recent technologies such as transcriptomics are now allowing us to investigate these molecular messages (Rosset *et al*., 2020). For instance signalling lipids, oxylipins, that usually play a role in cnidarian stress and immune responses to pathogen infection and heat stress, are down-regulated in symbiosis with a homologous (i.e. native) symbiont but not in one with a heterologous (i.e. non-native) symbiont (Lehnert *et al*., 2014; Lõhelaid and Samel 2018; Rosset *et al*., 2020). Furthermore, regulatory messengers such as non-coding RNAs (which can inhibit gene expression by binding to messenger RNA (mRNA)) are altered in their expression in the presence of compatible heterologous symbionts, particularly in the immune and stress response pathways as well as ones that are involved in the maintenance of the symbiosome membrane complex (Baumgarten *et al*., 2018; Rosset *et al*., 2020). These findings indicate the suite of molecular changes that occur as the symbiosis develops - changes that help to determine the compatibility of the symbiosis.

Once a symbiont successfully enters a host gastrodermal cell it becomes housed in the host-derived phagosome called the "symbiosome" (Wakefield *et al*., 2000; Wakefield and Kempf

2001). Usually phagosomes destroy their engulfed contents as they mature, *via* autophagy, due to fusion with lysosomes (Shui *et al*., 2008). However, the presence of the symbiont cell inhibits the fusion of the phagosome to the lysosome (Fitt and Trench 1983a), and thus inhibits its maturation, allowing the symbiont to persist. The outermost membrane of the 'symbiosome membrane complex' is host-derived and classed as the 'symbiosome membrane' with the remaining multi-layered membranes being algal-derived (Wakefield *et al*., 2000; Wakefield and Kempf 2001) (Fig. 1.1 C). The symbiosome membrane harbours molecular transporters that are integral to the efficient nutritional and communication exchange between the two partners (Peng *et al*., 2010). The following sections will describe these nutritional interactions, which are foundational to the ecological success of this symbiosis.

1.2.2. Nutritional exchange

1.2.2.1. Carbon flux

Muscatine & Hand (1958) were the first to hypothesise that symbiotic dinoflagellates provide nourishment to their hosts in the form of carbon, and it was later discovered that these symbionts *in hospite* (i.e. in the host) produce more soluble carbohydrates than those in culture (Muscatine 1967; Gordon and Leggat 2010). The resident symbionts provide most, or all, of the host's carbon requirements through photosynthetically fixing carbon, supporting the host's respiration, growth and reproduction (Muscatine 1990; Wang and Douglas 1998). The symbionts use the inorganic carbon stored in the host cytoplasm in the form of bicarbonate (HCO_3), which the host acquires from the surrounding seawater (Barott *et al*., 2015). Carbon must be concentrated as CO_2 for photosynthesis to proceed and the host aids this by acidifying the symbiosome to ~ pH 4 to increase the photosynthetic rate (Barott *et al*., 2015). Other minor sources of inorganic carbon are available to the symbiosis that include waste products from host skeletogenesis (in corals), and respiration from either partner (Harland and Davies 1995). After fixation by the symbiont, the carbon may be temporarily stored in a biochemical sink (lipid droplets and starch granules), however once required, these biochemical sinks are broken down and the carbon is ready to be translocated during night time to the host (Kopp *et al*., 2015), or released immediately (Black and Burris 1983; Muscatine *et al*., 1984). Once this photosynthate enters the host it is transported to every tissue layer (Kopp *et al*., 2015). Organic carbon products also have the capacity to be reversely translocated back to the symbionts (Cook 1972; Steen 1986). Glycerol was previously thought to be the major translocated product in the

symbiosis (Muscatine *et al*., 1967; Muscatine and Cernichiari 1969; Trench 1971), however now the current consensus is that the major product is glucose (Ishikura *et al.*, 1999; Burriesci *et al*., 2012; Hillyer *et al*., 2016). Other essential products translocated are amino acids e.g. alanine, glycolic acid (Muscatine and Cernichiari 1969), phosphorus in the form of phosphate (Godinot *et al*., 2009) and lipids (Patton *et al*., 1977; Chen *et al*., 2017).

1.2.2.2. Lipids

Lipids are the main source of energy storage in corals (Chen *et al*., 2017) and have essential roles in membrane structure and cellular communication (Dunn *et al*., 2012). Lipids are transferred to and from the symbiont in the form of lipid bodies (Leonard *et al*., 1994); these contain lipids such as wax esters, sterol esters, triglycerides, cholesterol, phospholipids and free fatty acids (Chen *et al*., 2017). Lipid bodies are a novel marker of the cnidarian-dinoflagellate symbiosis, with lipid bodies being absent from aposymbiotic cnidarians (Chen *et al*., 2015). In the symbiotic model cnidarian *Exaiptasia pallida* (commonly referred to as 'Aiptasia'), proteins that help to metabolise cholesterol to steroids (high density energy molecules) are present, reaffirming that the symbiotic state allows the host to build up energy reserves (Oakley *et al*., 2016). Lipids, which are characteristic of the symbionts' mobile products, have been found in host lipids pools in Aiptasia and *vice versa*, with lipids that are characteristic of the host's mobile products being found in symbiont lipid pools (Hillyer *et al*., 2016).

1.2.2.3. Nitrogen (recycling and conservation)

Nitrogen can be acquired as ammonium through host catabolism (Piniak *et al*., 2003) or as dissolved inorganic nitrogen from the surrounding seawater (Rädecker *et al*., 2015). The state of symbiosis promotes both nitrogen cycling and nitrogen conservation. Nitrogen conservation is when amino acid utilisation by the host decreases due to fixed carbon being translocated from the symbiont to the host, which is preferentially used as a respiratory substrate in host respiration, leading to the host conserving its own nitrogen stores (Wang and Douglas 1998). Meanwhile nitrogen recycling occurs by the symbiont extracting ammonium from the host's metabolic waste products and synthesising this ammonium into amino acids, such as histidine, isoleucine, leucine, lysine, phenylalanine, tyrosine and valine (Wang and Douglas 1999;

Tanaka *et al*., 2006). These amino acids are then translocated back to the host and used for host metabolism (Wang and Douglas 1998). Both the host and the symbiont can assimilate ammonium; however the symbiont is more efficient, being able to fix up to 23 times more than the host (Pernice *et al*., 2012). Both nitrogen transport mechanisms (ammonium transporters) and nitrogen cycling enzymes e.g. glutamate synthase are up-regulated during symbiosis (Wang and Douglas 1998; Oakley *et al*., 2016).

1.2.2.4. Phosphorus and sulphur

Alongside nitrogen, phosphorus is integral for the symbiosis as it plays a role in most biochemical mechanisms and the composition of important molecules – especially ATP, RNA, DNA and phospholipids (Godinot *et al*., 2009). Symbionts acquire dissolved inorganic phosphorus (phosphate) from the surrounding environment and hosts acquire organic phosphorus from heterotrophy (Muller-Parker *et al*., 1990). Phosphate transporters are found in both the host and its symbionts (Godinot *et al*., 2009), with the uptake of phosphorus being increased during daylight (D'Elia 1977). Phosphorus limitation/starvation has been shown to increase a coral's susceptibility to thermal bleaching (i.e. the stress-induced loss of symbionts) as it causes an imbalance in the nitrogen to phosphorus ratio (Rosset *et al*., 2017). It is now argued that nitrogen eutrophication itself does not increase a coral's susceptibility to bleaching but rather that bleaching results from the indirect effect of this process initiating phosphorus starvation (Rosset *et al*., 2017).

Little is known about sulphur fluxes in the symbiosis, but the sulphur-containing amino acid methionine is translocated from the host to the symbiont in the cnidarians *Hydra viridissima* (Muscatine and Lenhoff 1965) and Aiptasia (Cook 1971; Steen 1986) when hosts are fed ^{35}S-methionine labelled food. Steen (1986) concluded that it is reasonable to assume that most of the ^{35}S-methionine is incorporated into algal protein, as ~90% of the total sulphur in plant tissues is present in the amino acids methionine and cysteine. Along with sulphate, cultured symbiotic dinoflagellates have active transport mechanisms for cysteine, methionine and taurine (Deane and O'Brien 1981).

1.2.3. Symbiont diversity

Symbiotic dinoflagellates in corals and other marine invertebrates were originally classed as one species, *Symbiodinium microadriaticum* (Taylor 1974). Trench (1971) was the first to suggest that these algae may be the same morphologically but differ biochemically, with individual isolates translocating different amounts of photosynthate to the host. Schoenberg and Trench (1980) subsequently hypothesised that there may be other undiscovered strains or species due to the range of physiological differences found in *S. microadriaticum*. Rowan and Powers (1992) later used nuclear small subunit ribosomal (nr18S) to sequence *Symbiodinium* and split the genus into three genetic clades (A-C). Following this, the nuclear large subunit ribosomal (nr28S) was used for genetic analysis, which allowed more sensitive discretion between the genotypes (i.e. sub-clades), and led to the classification of clades A-H (Pochon *et al*., 2004) and later on, clade I (Pochon and Gates 2010). A phylogenetic analysis showed that clades evolved in the order A/E/G1 to G2/D1 to D2/I/B/F2 to F5/H/C, with A diverging the earliest from other Symbiodiniaceae, whilst C is the latest to diverge from other Symbiodiniaceae (Pochon *et al*., 2014). Recently, however, the taxonomy of these symbiotic dinoflagellates has been overhauled, with the creation of the family Symbiodiniaceae and several new genera replacing clades A-G: *Symbiodinium, Breviolum, Cladocopium, Durusdinium, Effrenium, Fugacium* and *Gerakladium,* respectively (LaJeunesse *et al*., 2018) (Figure 1.2). Moreover, a recent study described two new lineages - *Freudenthalidium* and *Halluxium* – which replace clades Fr3 and H, respectively (Nitschke *et al*., 2020; Figure 1.2). Within these two new lineages, three species were identified, meaning that there are currently 25 Symbiodiniaceae species that have been formally classified. However there are hypothesised to be potentially hundreds more that are currently unclassified (LaJeunesse *et al*., 2018; Nitschke *et al*., 2020). Hosts can associate with one or more of these species, that ultimately make up the resident symbiont community within a host (Baker 2003). The symbiont species themselves can also be generalists that associate with a wide variety of host species e.g. *C. goreaui* (C1) occupies host-symbiont communities in both the Caribbean and the Pacific, or specialists which are geographically endemic and only associate with a specific host species e.g. *Cladocopium* C27 is only found in the scleractinian coral *Pavona varians* at a depth of 10 m in the Pacific (LaJeunesse *et al*., 2003).

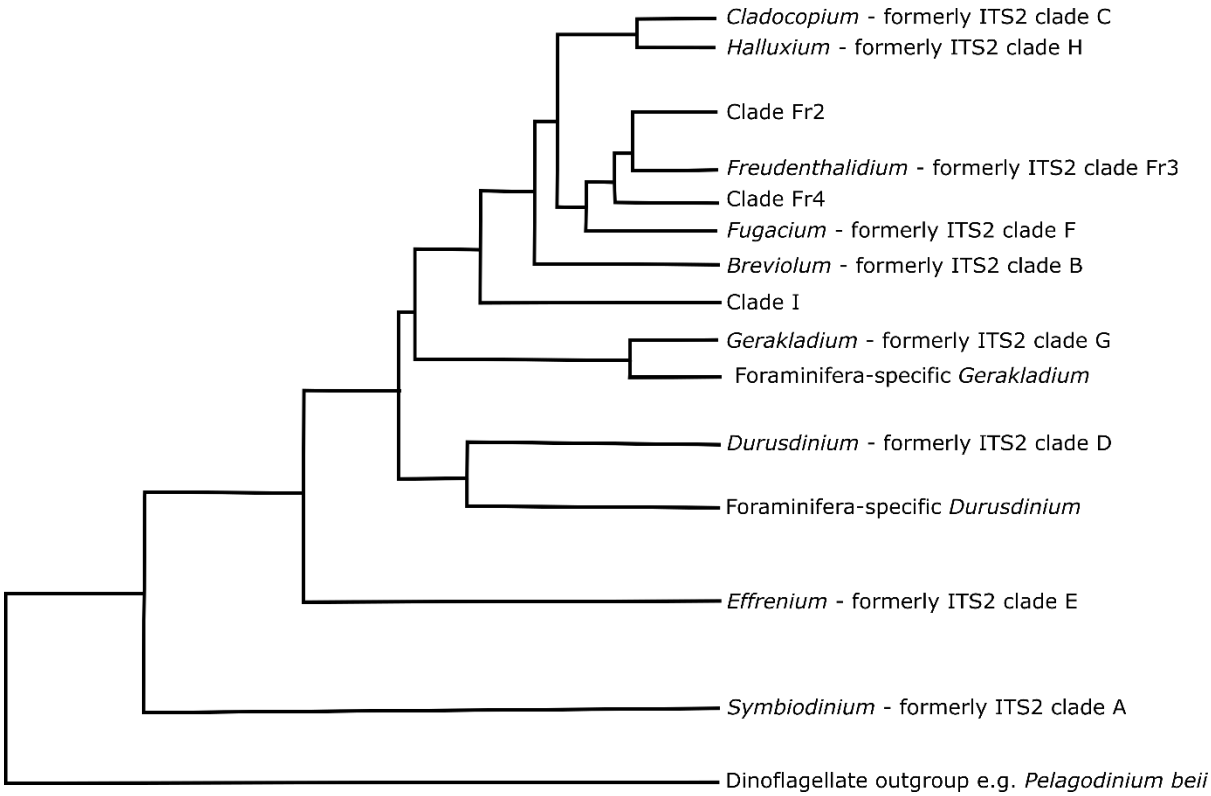

Figure 1.2. Phylogenetic tree of Symbiodiniaceae taxonomy. Adapted from Nitschke *et al*. (2020).

Irradiance (LaJeunesse *et al*., 2003), depth (Rowan and Knowlton 1995; LaJeunesse *et al*., 2003), environmental niche (Rowan *et al*., 1997; Rowan 1998; Baker 2003), and latitude (Rodriguez-Lanetty *et al*., 2001; Baker 2003) can influence the genotype of the symbiont community. Cnidarians at higher latitudes with cooler waters are normally dominated by *Symbiodinium* and *Breviolum* species, whereas cnidarians at lower latitudes are normally inhabited by *Cladocopium* and *Durusdinium* species (Baker 2003; LaJeunesse *et al*., 2003). One exception of this latitudinal rule is the Caribbean, with cnidarians containing symbiont communities more typical of higher latitudes (*Symbiodinium* and *Breviolum*) (Baker 2003; LaJeunesse *et al*., 2003). This anomaly is thought to be a result of the Plio-Pleistocene period of Northern Hemisphere glaciation, allowing cooler waters to enter the Caribbean, favouring a shift to colder water symbionts (Baker 2003).

Symbiodiniaceae differ morphologically and physiologically between genera, species and strains and this genotypic diversity corresponds to physiological diversity allowing novel host-symbiont associations to form (Parkinson *et al*., 2016; Swain *et al*., 2017; Gabay *et al*., 2018;

LaJeunesse *et al*., 2018; Matthews *et al*., 2018; Sproles *et al*., 2019). For instance, different genotypes possess different thermotolerances (Swain *et al*., 2017); different photosynthetic gene expression (Parkinson *et al*., 2016); and, different growth rates (Klueter *et al*., 2017). These different physiological characteristics influence symbiosis performance and fitness by corresponding to different nutritional statuses of the host (Trench 1971; Starzak *et al*., 2014; Oakley *et al*., 2016; Matthews *et al*., 2018), different host temperature tolerances (Stat and Gates 2010; Hume *et al*., 2013; Pettay *et al*., 2015), and different colonisation successes in host-symbiont associations (Sachs and Wilcox 2006; Dunn and Weis 2009; Gabay *et al*., 2018). For instance, in Aiptasia, heterologous *S. microadriaticum* and *D. trenchii* elicited reduced host growth and asexual reproduction compared with homologous *B. minutum*, indicating that symbiosis with *S. microadriaticum* and *D. trenchii* reduced the overall performance of the symbiosis (Gabay *et al*., 2018). It should be noted, however, that the extent to which symbiont genotype influences the host-symbiont association depends also on environmental conditions (Werner and Kiers 2015).

1.2.4. Symbiont proliferation (host-symbiont biomass control)

A key to maintaining a stable symbiosis is the delicate balance between symbiont proliferation and host cell growth, retaining enough symbionts to meet host nutritional requirements without overgrowing or inducing cellular stress in the host. Regulating the symbiont population under optimal and sub-optimal conditions is vital to the maintenance of the symbiosis (Jones and Yellowlees 1997). Once the algae reach a "steady-state" population density, their growth rate decreases by a factor of 20 compared with algae in log phase growth in the host (Berner *et al*., 1993; Baghdasarian and Muscatine 2000) and, consistent with this, symbiotic dinoflagellates have higher growth rates in areas of the host that have a lower symbiont density (Hoegh-Guldberg and Smith 1989). The symbiont density is regulated by host homeostatic processes (Jones and Yellowlees 1997). These processes are density-dependent, and can be either pre-mitotic (inhibiting symbiont cell division) (Smith and Muscatine 1999), or post-mitotic (removing newly divided symbionts either *via* degradation or exocytosis) (Table 1.1) (Jones and Yellowlees 1997; Baghdasarian and Muscatine 2000).

Table 1.1. Putative pre-mitotic and post-mitotic controls hypothesised to control resident Symbiodiniaceae populations when inside the cnidarian host.

Pre-mitotic	**Post mitotic**
Nutrients – *Pocillopora damicornis* (Hoegh-Guldberg 1994); *Myrionema ambionense* (Fitt 2000)	Degradation *via* autophagy – *Stylophora pistillata* (Titlyanov et al. 1996), *Exaiptasia pallida* (Chen *et al*., 2005; Dunn *et al*., 2007)
Lipids – cultured symbionts (Wang *et al*., 2013)	Expulsion – *E. pallida* and *P. damicornis* (Gates and Muscatine 1992)
Density-dependent feedback by symbionts - *Acropora formosa* (Jones and Yellowlees 1997)	Division of host cells (space limitation theory) - *Acropora formosa* (Jones and Yellowlees 1997)
Host division factor/ metabolite pools- *Hydra viridissima* (McAuley 1985b)	Degradation *via* apoptosis - *Fungia scutaria* (Dunn and Weis 2009); *E. pallida* (Paxton *et al*., 2013)
Reduced pH of symbiosome to divert fixed carbon to the host - *Hydra viridissima* (McAuley 1985b)	
Density-dependent inhibitor whose production ceases when host cell divides - *Hydra viridissima* (McAuley 1985b)	
Cell-cycle arrest – *E. pallida* (Smith and Muscatine 1999)	

It is still unclear which mechanisms directly control the symbiont population and their relative importance, and whether these change with symbiont genotype or over time as the symbiosis develops. The primary regulatory mechanisms of host-symbiont biomass are shown below (Figure 1.3). These include the pre-mitotic control of the cell-cycle, and post-mitotic controls – autophagy, apoptosis and expulsion (Davy *et al*., 2012). The next sections will discuss studies that have investigated host controls of the resident symbiont population.

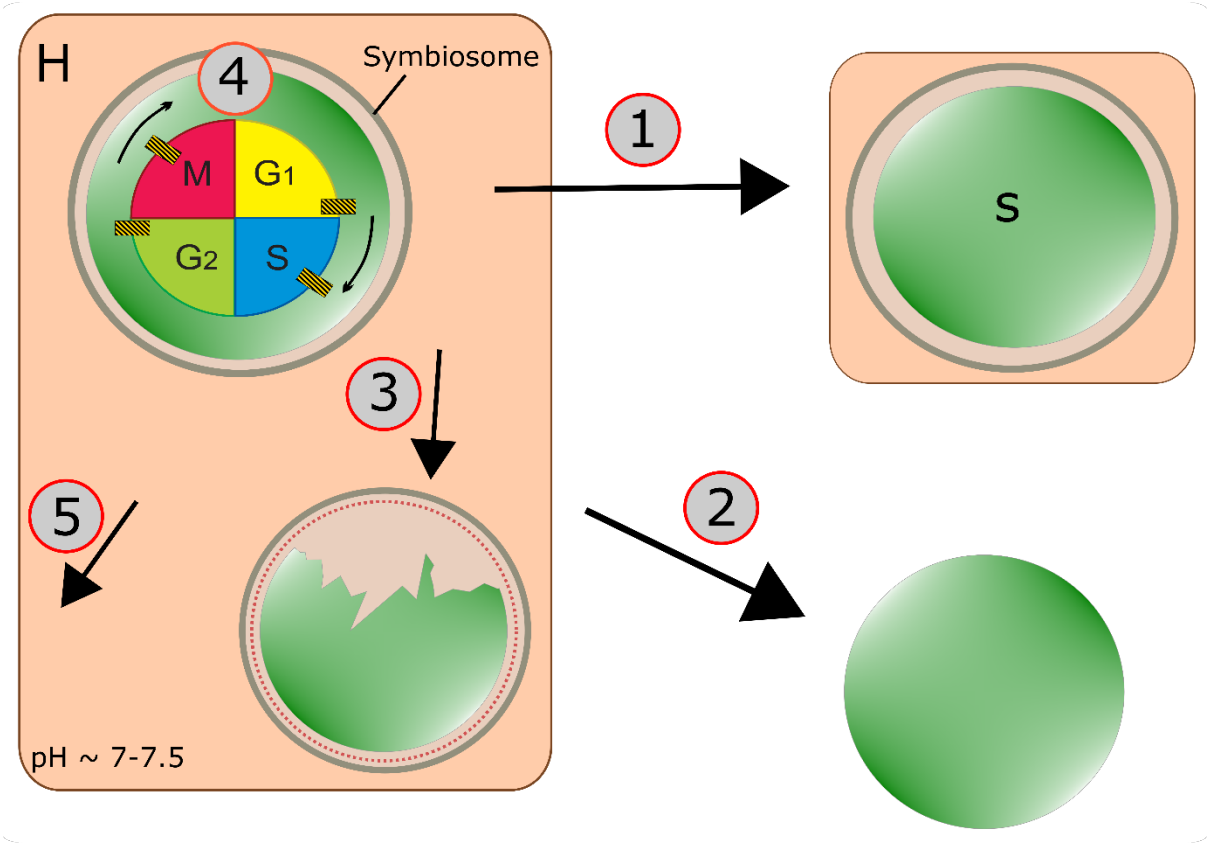

Figure 1.3. Mechanisms of host-symbiont biomass regulation. 'H' refers to host gastrodermal cell. 'S' refers to symbiont cell. (1) Expulsion of host cells containing symbionts; (2) Expulsion of symbiont cell; (3) Degradation of symbiont *via* autophagy/apoptosis of the host cell containing the symbiont cell; (4) Cell-cycle control of symbiont (arrest in G_1); (5) Control of host cell division by symbiont. Re-drawn from Davy *et al*. (2012).

1.2.4.1. Apoptosis

At any one time, it is estimated that ~1-6% of the resident symbiont population is being degraded by the host (Titlyanov *et al*., 1996). The hypothesised pathways of degradation in the host include autophagy and apoptosis (Dunn *et al*., 2007). Apoptosis is an evolutionarily conserved mechanism of 'programmed cell death' that allows the removal of aged or damaged cells (Weis 2008). Apoptosis is controlled by a series of pro-apoptotic and anti-apoptotic proteins (Dunn *et al*., 2006; Kvitt *et al*., 2016; Moya *et al*., 2016). If the pro-apoptotic genes outcompete the anti-apoptotic genes in expression levels, caspases (cysteine aspartate-specific proteases) that destroy the cell are stimulated (Kvitt *et al*., 2016). The apoptotic cascade can lead to the formation of cellular debris, chromatin condensation, DNA fragmentation and shrinking of the cell (Weis 2008). Apoptosis is a primary mechanism affecting the colonisation success of symbiotic dinoflagellates (Dunn and Weis 2009; Gates *et al*., 1992). Under stable

environmental conditions, apoptosis functions as an immune response to remove incompatible symbionts (Weis 2008; Weis *et al*., 2008; Dunn and Weis 2009), with symbionts that cause increased caspase activity in the host having reduced colonisation rates (Dunn and Weis 2009). By comparison, in symbiosis with homologous (i.e. native) symbionts, host apoptosis decreases, possibly aiding symbiont persistence (Rodriguez-Lanetty *et al*., 2006a); baseline caspase rates are therefore unique to each host-symbiont association (Tchernov *et al*., 2011; Hawkins *et al*., 2014). In addition to colonisation, apoptosis is a primary mechanism for removing incompatible symbionts during thermal bleaching episodes (Dunn *et al*., 2004; Pernice *et al*., 2011; Tchernov *et al*., 2011; Paxton *et al*., 2013; Hawkins *et al*., 2014) (see Section 1.5).

1.2.4.2. Autophagy

Autophagy is an evolutionarily conserved process that occurs during cellular starvation or disease and allows an animal to digest its own cells (Ao *et al*., 2014). Autophagy is also integral to the differentiation, structure, growth control and immune response within cells (Weis 2008). The autophagic pathway involves three main steps: autophagosome formation; autophagosome-lysosome fusion followed by autophagosome maturation; and finally, degradation (Tanida 2011; Ao *et al*., 2014). In the cnidarian-dinoflagellate symbiosis, autophagy has been reported to play a role in the regulation of the symbiont population by the host and has shown to be interconnected with the apoptotic pathway, with one's inhibition resulting in the other's initiation (Dunn *et al*., 2007). Under non-stressful conditions, an autophagy promoter led to the increased bleaching in Aiptasia (Dunn *et al*., 2007), whereas under heat and light stress in the coral *Pocillopora damicornis*, an increase in autophagic structures and enzymes associated with late endosome transport in autophagy were observed (Downs *et al*., 2009).

In cnidarians, the genes that function in the autophagic pathway are starting to be investigated. For instance, a recent study using cell-specific transcriptomics confirmed that symbiosis inhibits host autophagy, possibly through the highly-conserved mTORC1 (mechanistic target of rapamycin complex 1) (Voss *et al*., 2019). This finding is unsurprising, since in the symbiosis, symbionts are housed in host autophagolysosomes that are prevented from maturing by the presence of the symbiont (Karakashian and Karakashian 1973; Karakashian and

Rudzinska 1981; Fitt and Trench 1983a). In eukaryotes, mTORC1 links environmental cues such as growth factors, amino acids and oxygen to metabolic processes such as cell growth. As well as co-ordinating cell growth in stable conditions, under stressful conditions mTORC1 can stimulate the formation of autophagic complexes that lead to the autophagic cascade (Lane *et al*., 2017). Another protein involved in autophagy in eukaryotes is the microtubule-associated protein 1A/1B-light chain 3 (LC3). Upon an autophagic signal, LC3 becomes localised to the autophagosome membrane, so the quantity of LC3 in an organism is directly correlated with the number of autophagosomes (Kabeya *et al*., 2000). When mouse cells were transfected with EFGP vectors containing the Aiptasia LC3 gene sequence, a similar autophagosome localisation was observed to those transfected with human LC3 (Flesher 2013), highlighting the conservation of the autophagy pathway in eukaryotes. Furthermore, the treatment of Aiptasia with rapamycin (a known autophagy inducer) caused a significant increase in the mRNA levels of LC3 (Bailey *et al*., 2020).

In addition to mTORC1 and LC3, a set of genes associated with autophagy, Rab GTPases, have been found to be associated with the cnidarian-dinoflagellate symbiosis (Chen *et al*., 2005). Rab GTPases play a pivotal role in the vesicle transport process of autophagy, acting as 'molecular switches' for the transport, tethering and fusion of proteins (Ao *et al*., 2014). Two of these Rab GTPases (5 and 7) are associated with the early endocytotic pathway and late endosome transport in autophagy, respectively (Ao *et al*., 2014). *In hospite*, healthy symbionts have a higher association of ApRab5 with the symbiosome and a lower association of ApRab7 than photosynthetically-damaged symbionts (Chen *et al*., 2003, 2004). A later study (Chen *et al*., 2005) investigated the levels of a Rab GTPase associated with recycling endosomes, Rab11, in Aiptasia and found that healthy symbionts had a lower percentage of ApRab11-positive phagosomes than unhealthy symbionts.

1.2.4.3. Expulsion

Expulsion is a mechanism where the host removes healthy and non-healthy symbionts into the surrounding environment by exocytosis (Steele 1977). During expulsion, symbionts are ejected through the gastrovascular cavity (Steen and Muscatine 1987). Expulsion is a major regulatory mechanism in cnidarians, with rates of 0.1-4.6% of the resident symbiont population being expelled *per* day in the hard and soft corals *Astrangia poculata, Acropora formosa, Xenia*

maerospiculata, Heteroxenia fuscescens, Stylophora pistillata and *Millepora dichotoma* (Hoegh-Guldberg *et al*., 1987; Jones 1997; Baghdasarian and Muscatine 2000; Dimond and Carrington 2008). Symbionts with increased growth rates are preferentially expelled from the host (McCloskey *et al*., 1996), possibly due to increased growth rates being more likely to exhaust host energy reserves, leading to host mortality and collapse of the symbiosis (Sachs and Wilcox 2006). In addition to autophagy and apoptosis, the expulsion of symbionts increases with factors that allow proliferation of the symbiont population, e.g. moderate temperature increase (Baghdasarian and Muscatine 2000). In *Cassiopea xamachana*, the mode of symbiont acquisition also affects its expulsion rate from the host, with horizontally transmitted symbionts being preferentially expelled over vertically transmitted counterparts (Sachs and Wilcox 2006). This could be due to the difference in colonisation success with horizontally transmitted symbionts reaching higher population densities in *Cassiopea xamachana* (Sachs and Wilcox 2006). Currently, it is still debated whether expulsion solely involves symbiont cells, or also involves the expulsion of host cells containing intact symbionts, as host cells may disintegrate rapidly *ex vivo*, leaving only the intact symbionts - making this distinction difficult to measure (Gates *et al*., 1992; Baghdasarian and Muscatine 2000). However, expulsion is likely to involve exocytosis of both individual symbiont cells and host cells containing intact symbionts, with histological staining of corals during a bleaching event in the field showing signs of expulsion of host endodermal cell membrane surrounding intact symbiont cells (Brown *et al*., 1995).

1.2.4.4. Cell-cycle regulation

The mitotic cell cycle is a biological process that allows eukaryotic organisms to renew, repair and grow their tissues (Neufeld and Edgar 1998; Orford and Scadden 2008; Hustedt and Durocher 2017). The cell cycle results in a mother cell dividing and producing two genetically identical daughter cells (D'Erfurth et al. 2009). The mitotic cell cycle involves a first gap phase (G_1) where cells grow, a DNA synthesis phase (S), a second gap phase (G_2) and finally a mitotic phase (M) where two sets of genetic information are divided between the two daughter cells (Malumbres and Barbacid 2009). Following mitosis, the cytoplasm splits during a process known as cytokinesis and this produces two individual cells. Several checkpoints are present during the cell cycle (Figure 1.4) to stop damaged and deformed cells replicating and/or stop cells replicating in unfavourable environments (Clercq and Inzé 2006). The checkpoints require

several environmental and physiological criteria to be met before the cell can progress onto the next stage (Figure 1.4); otherwise the cell will be arrested (Hartwell and Kastan 1994; Kastan and Bartek 2004; Malumbres and Barbacid 2009).

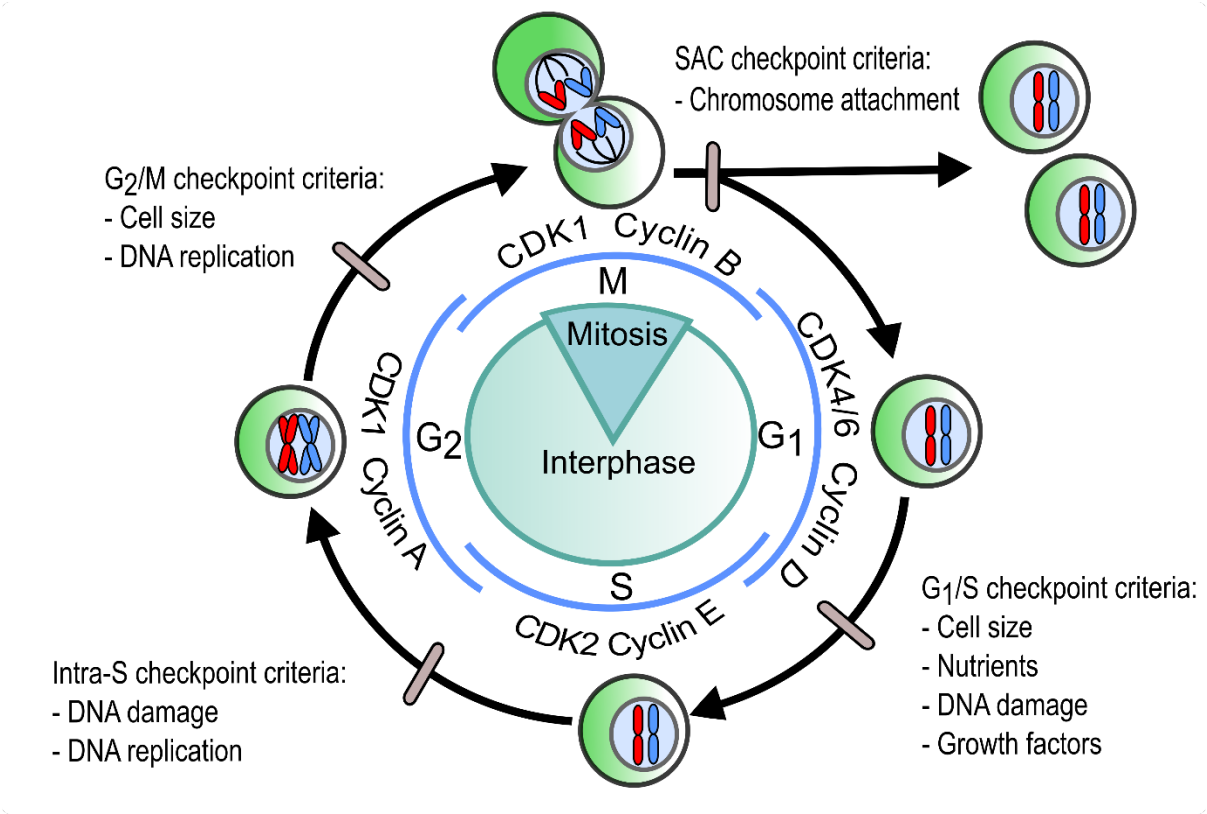

Figure 1.4. The generalised cell cycle in eumetazoans. Cell-cycle phase (G_1, S, G_2, M), regulatory checkpoints (grey ovals) and the criteria that must be met for the cell cycle to progress in eukaryotes. Cyclin-dependent kinase (CDK)-cyclin complexes within *Homo sapiens* that are formed at specific points in the cell cycle (blue lines) for the cell to progress to the next phase. SAC – Spindle Assembly Checkpoint.

In the cnidarian-dinoflagellate symbiosis the host has been shown to inhibit the cell cycle of its symbionts, with ~80% of symbionts arrested in the G_1 phase compared with 40-55% when in culture (Smith and Muscatine 1999). The cell cycle in cultured symbiotic dinoflagellates is stimulated by light-dark photoperiods (Wang *et al.*, 2008), with light stimulation driving symbiont cells through the G_1 phase to the S phase. The dark phase is then required for the initiation of the G_2/M phase and ultimately mitotic exit, with newly divided cells returning to the G_1 phase for the start of the light period. In this same study, symbiont photosynthetic efficiency also changed in relation to cell-cycle phase, with the highest photosynthetic rates in

the G_1 phase and the lowest in the G_2/M phase. Therefore, alongside symbiont density regulation, G_1 arrest phase may be enforced by the host to increase photosynthetic efficiency (and thus carbon translocation) from its symbionts. Different genotypes of Symbiodiniaceae have been shown to have this same cell-cycle progression with all species progressing through each cell-cycle phase at the same time (Fujise *et al*., 2018), probably due to their synchronicity with the light-cycle (Wang *et al*., 2008). However, different symbiont genotypes did have different proportions of the population in specific cell-cycle phases (Fujise *et al*., 2018), implying that different genotypes have different amounts of cycling cells in the population at a given time, contributing to different growth rates between genotypes. This finding agrees with a recent study (Tivey *et al*., 2020), which compared the cell cycle *in hospite* between two *Breviolum* species in Aiptasia and found that the two species had different proportions of their population in cell-cycle phases at a steady-state symbiosis.

A handful of studies have focused on investigating factors which may allow the host to control the symbiont cell cycle *in hospite,* such as photosynthetic pigments (Fitt and Cook 2001), nutrient levels (Cook *et al*., 1988; Hoegh-Guldberg 1994; Wang *et al*., 2013) and co-ordination with host cell division (McAuley 1985b; Fitt 2000; Tivey *et al*., 2020). One consensus is that the host controls symbiont division through depriving the symbionts of essential nutrients (primarily nitrogen). It is well known that the symbionts in cnidarian hosts are nitrogen depleted, with the higher population density of symbionts in the host's tissues than the surrounding water column increasing nutrient demand considerably (Cook and D'Elia 1987). Additionally, carbon to nitrogen ratios of symbionts in the field *in hospite* are intermediate between symbionts in nutrient-replete and nutrient-depleted hosts in experimental conditions (Cook *et al*., 1988), highlighting that in the field symbionts are likely to be nitrogen limited. Consequently, the addition of exogenous nitrogen to the holobiont has been shown to: increase the proportion of dividing symbiont cells (Cook *et al*., 1988; Muscatine *et al*., 1989; Stimson and Kinzie 1991; Hoegh-Guldberg 1994); increase both symbiont and host biomass (Hoegh-Guldberg and Smith 1989; Muller-Parker *et al*., 1994); and control the periodicity of the symbiont cell cycle *in hospite* (Fitt and Trench 1983b; Hoegh-Guldberg 1994; Fitt 2000).

In addition to exogenous nitrogen, feeding of the host has been shown to initiate symbiont cell division due to the co-ordinated growth of the two partners (McAuley 1985b; Smith and

Muscatine 1999; Tivey *et al*., 2020). The co-ordination of cell division between host and symbiont *in hospite* requires an external food source, a lag time for host digestion, and a light period (Fitt 2000). Fitt (2000) concluded, following studies conducted on *Hydra viridissima* (McAuley 1985b) and his own findings on the hydroid *Myrionema ambionense*, that host cells divide 12-24 hours after host feeding, and that the resident symbiont population divides 12-24 hours after this host cell division (24-48 hours post host feeding) (Fitt 2000). Moreover, the co-ordination between symbiont and Aiptasia host cell division (Figure 1.5) has been recently investigated (Tivey *et al*., 2020), where the presence of symbionts elicited the proliferation of host cells in both the gastrodermis and the asymbiotic ectodermis. The *in hospite* environment invoked more symbionts in the S-phase, with fewer progressing to the G_2/M phase compared with symbionts in culture (Tivey *et al*., 2020). When the symbionts were in starved hosts, more of the symbiont population was arrested in the G_1 phase and fewer were found in the G_2/M phase compared with fed anemones, highlighting that fewer symbionts were dividing in starved hosts. However, the difference between the proportion of the symbiont population in the G_2/M phase of fed and starved Aiptasia was small: 1.5% *versus* 0.9%, respectively (Tivey *et al*., 2020). These findings are consistent with field observations, where seasonal increases in food availability were observed to elicit both increased host and symbiont cell growth in the sea

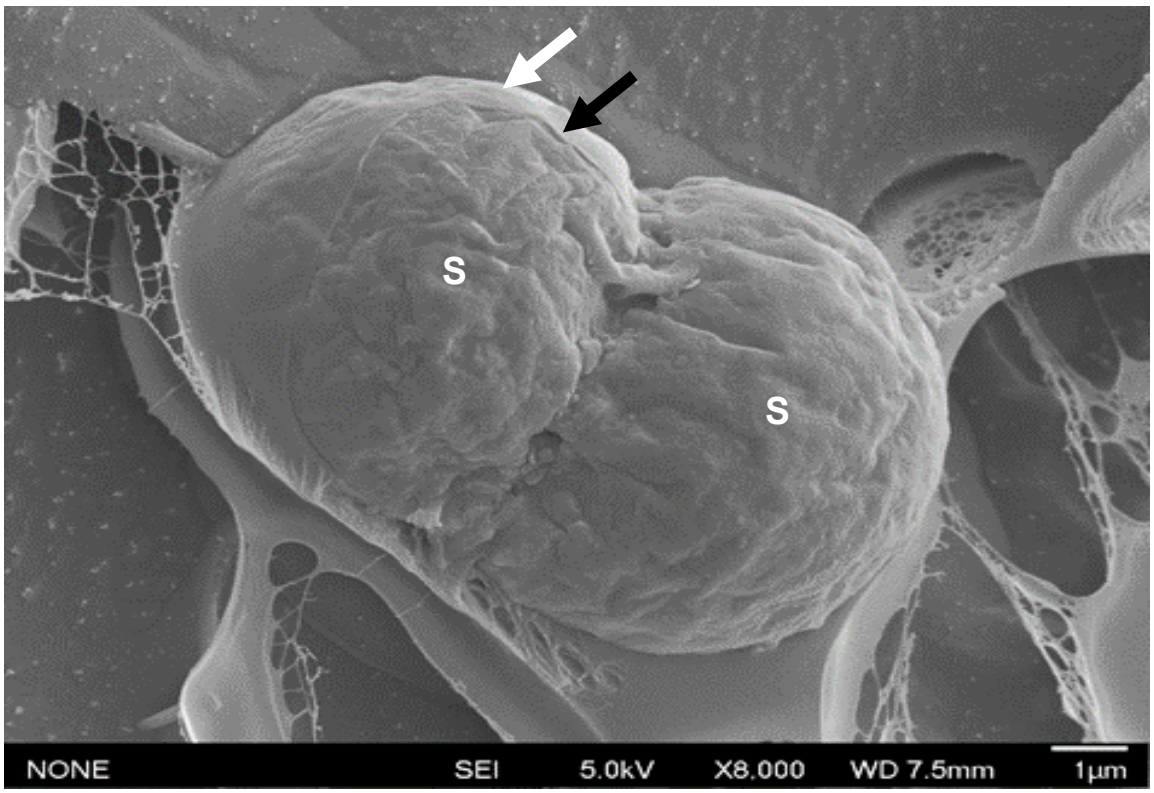

anemones *Anthopleura elegantissima* and *Stichodatyla helianthus* (Dimond *et al*., 2013).

Figure 1.5. Scanning electron micrograph of symbiont cell (*Breviolum minutum*) dividing during cytokinesis in the gastrodermis of Aiptasia. White arrow points to host cell stretched over symbiont cells ('S'). Black arrow points to symbiosome membrane. Photo taken by Lucy Gorman, Bobby Lust and Amirhossein Mashini.

Although nitrogen addition and host feeding do release the resident symbiont population from host-controlled growth arrest, the growth rate of nitrogen-replete symbionts *in hospite* is <20% that in culture or at low population densities in the host (Smith and Muscatine 1999). This emphasises that, although nutrient limitation is probably the primary control of symbiont growth, it is not the sole factor controlling the symbiont cell-cycle *in hospite*. Other growth-limiting factors in the symbiosis could include lipids, as the addition of a lipid synthesis inhibitor led to cell-cycle arrest in cultured symbionts (Wang *et al*., 2013). Also, the symbiotic environment could cause a decrease in growth rate due to lower light levels reaching the symbionts (Fitt and Cook 2001). For instance, in the hydroid *Myrionema amboinense*, light levels *in hospite* are <50% of those in culture (Fitt and Cook 2001). Furthermore, when a blue-light absorbing photopigment was added to the coral *Euphyllia glabrescens*, the proliferation of its symbionts ceased (Fitt and Cook 2001).

Despite the evidence for the potential mechanisms by which host and symbiont cell growth are regulated, there are still major knowledge gaps. For example, we know almost nothing about the symbiont genes and proteins targeted in cell-cycle arrest by the host, though very recently Cato and co-workers (Cato *et al*., 2019) investigated the presence of cell-cycle checkpoint proteins (cyclins and cyclin-dependent kinases) in *Breviolum minutum* and monitored their expression in relation to cell-cycle phase when in culture. Their study found 15 putative cyclins and 10 putative CDKs in *B. minutum*, while they proposed that a CDK1/cyclin B2 complex is required for G_1/S transition.

1.2.5. Coral bleaching

Coral reefs are the marine ecosystem most significantly impacted by climate change (Duarte *et al*., 2020), with even conservative predictions of global warming of 1.5 °C by 2100 causing predicted losses of 70-90% of coral reefs globally (Hoegh-Guldberg *et al*., 2018). One mechanism proposed by which corals might adapt to this stress and potentially survive is *via* changing their resident symbiont population for a more thermally-resistant cohort (Kemp *et al*., 2014; Thornhill *et al*., 2017), yet data from ancient octocoral DNA has indicated that certain

cnidarian hosts have had a consistent symbiotic partner for centuries (Baker *et al*., 2013a). Clearly therefore, we need to understand better the limitations on establishing novel host-symbiont partnerships, both in terms of cellular integration and holobiont fitness, to predict future trajectories on coral reefs better.

Bleaching is often referred to as the discolouration of corals due to the expulsion of their resident symbionts or the reduction in their photopigments after photosystem damage under suboptimal environmental conditions, e.g. high temperatures (Baker *et al*., 2008). Currently the molecular pathway underpinning bleaching is not completely understood (Oakley and Davy 2018). Most widely known is the oxidative theory of bleaching (Lesser *et al*., 1990; Downs *et al*., 2002). Here, ROS generation surpasses ROS detoxifying mechanisms, e.g. the enzyme ascorbate peroxidase which converts ROS to oxygen and water, causing the ROS to leak from the cell, ultimately triggering a bleaching cascade that leads to host cell apoptosis (Dunn *et al*., 2004; Weis 2008; Saragosti *et al*., 2010; Paxton *et al*., 2013; Oakley and Davy 2018). Unsurprisingly, caspase levels, and therefore apoptotic sensitivity, is one of the indicators of bleaching susceptibility (Tchernov *et al*., 2011) and corals can actively reduce their caspase activity, presumably to avoid bleaching (Tchernov *et al*., 2011). The addition of exogenous ROS increases host caspase activity 40-50 fold (Tchernov *et al*., 2011), and the inhibition of apoptosis reduces the rate of bleaching under temperature stress (Tchernov *et al*., 2011).

In hospite symbiont apoptosis has been shown to be 8 fold higher than in culture when exposed to thermal stress at 33 °C (Paxton *et al*., 2013), however it is still unknown whether the host and/or the symbiont initiates the bleaching cascade, but both partners can produce and ameliorate ROS (Weis *et al*., 2008; Paxton *et al*., 2013). In the symbiont, photodamage leads to the build-up of excess energy which triggers the release of ROS, mainly due to over-excitation of the photosynthetic apparatus (Rehman *et al*., 2016). However, in the host the mitochondrion is hypothesised to be the source of ROS generation, as in other non-photosynthetic organisms (Chance *et al*., 1979; Blackstone 2009; Dunn *et al*., 2012; Oakley and Davy 2018). Furthermore, along with its effect on host fitness, symbiont genotype has been hypothesised to contribute to the bleaching susceptibility of its host (Sampayo *et al*., 2008; Tchernov *et al*., 2011; Silverstein *et al*., 2017), with different genotypes producing different levels of ROS under the same conditions in culture (Suggett *et al*., 2008).

Other possible mechanisms involved in the bleaching cascade have been suggested due to being up-regulated under bleaching conditions, such as nitric oxide (NO)-mediated apoptosis (Weis *et al*., 2008; Hawkins and Davy 2012; Hawkins *et al*., 2013). NO can cross membranes, leak from one organism to another due to its lipophilic nature and can react with superoxide (O_2-) to form toxic peroxynitrite that inhibits electron transport, however its role in bleaching is unclear (Hawkins and Davy 2013; Oakley and Davy 2018). When symbiotic Aiptasia were exposed to elevated temperature or incubated with a NO donor under non-stressful temperatures, bleaching of their symbionts *via* expulsion (Perez and Weis 2006) and caspase-activated apoptosis (Hawkins and Davy 2013) was observed.

During a bleaching episode, cnidarian hosts have a limited window of time to replace any lost symbionts, with failure in this endeavour leading to hosts exhausting their own energy reserves and ultimately death. The 'adaptive bleaching hypothesis' (Buddemeier and Fautin 1993) suggests that corals bleach to acquire new symbionts in suboptimal environmental conditions, and are therefore more likely to survive (see Baker 2001). However, the data to support this hypothesis are limited (Hoegh-Guldberg *et al*., 2002; Douglas 2003). There are two methods proposed by which hosts can regain symbionts. One route is referred to as 'symbiont shuffling' (Baker 2003). Symbiont shuffling occurs during suboptimal conditions, where hosts may shuffle their dominant symbiont to a subordinate co-occurring symbiont (i.e., that usually inhabits the host at low densities under stable conditions) if this symbiont is better suited to the new conditions (Jones *et al*., 2008; Kemp *et al*., 2014; Silverstein *et al*., 2015; Bay *et al*., 2016). However, laboratory and field experiments with cnidarians associated with thermally-tolerant species such as *D. trenchii* have documented physiological trade-offs such as reduced photosynthate translocation, lower host growth rates, and lower calcification rates (Cantin *et al.*, 2009; Jones and Berkelmans 2010; Stat and Gates 2010; Pettay *et al*., 2015; Gabay *et al*., 2018). Another route is known as 'symbiont switching', where the host acquires a novel heterologous symbiont (i.e. not usually found in association with a specific host) horizontally from the environment (Baker 2003). Many studies have shown the physiological costs incurred to the host by horizontally acquired (Sachs and Wilcox 2006) and/or heterologous symbionts (Matthews *et al*., 2018; Rädecker *et al*., 2018; Medrano *et al*., 2019; Sproles *et al*., 2019), so it is perhaps not surprising that switching has not been documented in the field during bleaching

events (Jones *et al*., 2008; but see Boulotte *et al.*, 2016; Huang *et al*., 2020). Further information about the capacity to take up new symbionts and regulate heterologous symbiont populations will shed further light on the potential for partner switching and the limitations upon this potential adaptive mechanism.

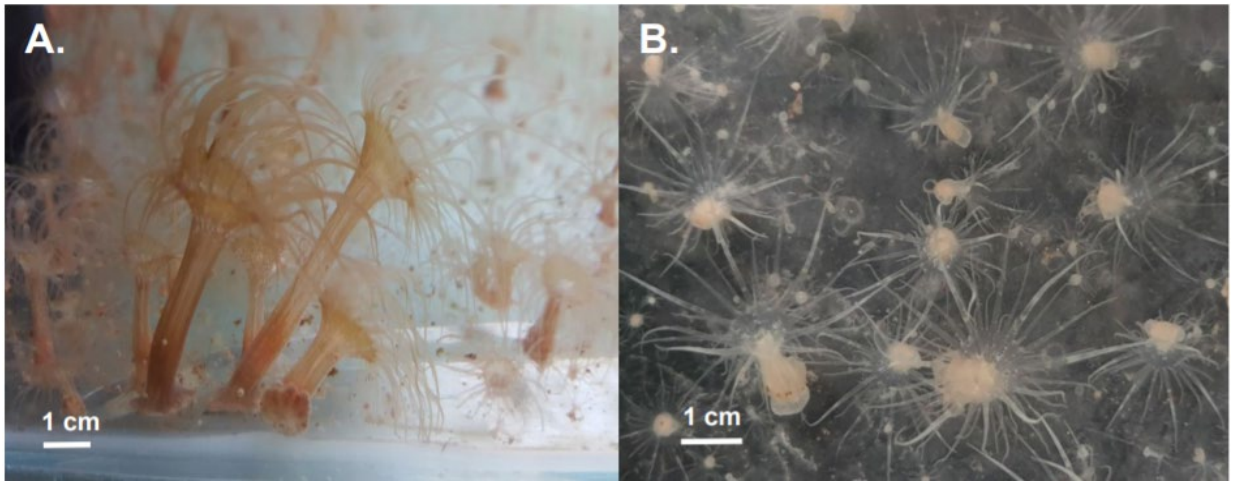

Figure 1.6. *Exaiptasia pallida* 'Aiptasia' (strain NZ-1) clonal individuals. (A) Symbiotic Aiptasia. (B) Aposymbiotic Aiptasia.

To understand fully the fundamental biology behind the cnidarian-dinoflagellate symbiosis, a model systems approach using *Exaiptasia pallida* ('Aiptasia') (Figure 1.6) has been commonly used (Weis *et al*., 2008; Hawkins and Davy 2013; Gabay *et al*., 2018; Matthews *et al*., 2018; Sproles *et al*., 2019; Tivey *et al*., 2020). The Aiptasia model provides a robust, plastic and highly reproducible model to use when investigating symbiosis onset, establishment, maintenance, and dysfunction. This is because Aiptasia can be easily bleached using menthol to render them aposymbiotic, and can exist in this aposymbiotic state for prolonged periods if fed (Matthews *et al*., 2016). After bleaching, Aiptasia can be horizontally infected by a range of different symbiont species, including various heterologous ones (Schoenberg and Trench 1980; Starzak *et al*., 2014: Chen *et al*., 2016; Hawkins *et al*., 2016; Gabay *et al*., 2018), allowing genotypic differences in host-symbiont associations to be measured.

1.3. Aims and objectives

While we are steadily discovering more about the regulatory processes in the cnidarian-dinoflagellate symbiosis, we still have much to learn, with the mechanism of cell-cycle

regulation in particular being very poorly understood. Moreover, to date, no studies have measured all possible host regulatory mechanisms (cell-cycle, expulsion, apoptosis and autophagy) simultaneously to assess their relative importance during the onset, establishment and maintenance of the symbiosis. The importance of measuring all host-symbiont biomass regulatory mechanisms simultaneously was highlighted by Dunn *et al*. (2007), who manipulated autophagic and apoptotic mechanisms in Aiptasia and found that if just one of these pathways was inhibited, there was no significant drop in the bleaching of Aiptasia under thermally stressful conditions. This indicates that there is not a sole regulatory pathway but rather a network of interlinked pathways. Furthermore, other studies have shown that symbiont genotype affects the activation of these mechanisms (Dunn and Weis 2009; Tivey *et al*., 2020), highlighting their role in determining patterns of host-symbiont specificity and the capacity for new symbioses to form. This latter point is especially important in the context of climate change, given the proposal for adaptation of reef corals through the establishment of novel, more thermally-tolerant host-symbiont associations (Cumbo *et al*., 2018).

The aim of the current study was to characterise the molecular processes that underpin regulation of cell-cycle progression in the cnidarian-dinoflagellate symbiosis, and to determine how symbiont identity influences patterns of biomass regulation in the host, thereby assessing the relative importance of these regulatory processes during the onset, establishment and maintenance of the symbiosis. To satisfy this aim, the study had three specific objectives:

1. **To characterise cell-cycle proteins in Symbiodiniaceae and their evolution with respect to other eukaryotes, and determine whether symbiotic state changes the expression of these proteins.**

The hypotheses were:

a) cell-cycle proteins will be highly conserved across eukaryotes (from humans to Symbiodiniaceae);

b) some cell-cycle proteins will be specific to particular species or genera of Symbiodiniaceae;

c) the symbiotic state will cause symbiont cell-cycle protein expression to change.

2. **To determine how the presence of a symbiont alters the expression of host cell-cycle genes and genes related to persistence of the symbiont, in a host.**

The hypotheses were:

a) cell-cycle genes that promote growth in host tissues will be up-regulated in the symbiotic *versus* aposymbiotic state;

b) cell-cycle gene expression will differ between host tissues (gastrodermis *versus* epidermis), with gastrodermal tissues progressing at a slower rate due to the presence of symbionts within them compared with asymbiotic epidermal cells;

c) the presence of a symbiont will influence host genes in the gastrodermis that are involved in host immunity.

3. **To measure the relative importance of host-symbiont regulatory processes during the establishment and maintenance of the cnidarian-dinoflagellate symbiosis, and assess how these processes are influenced by symbiont identity and time.**

The hypotheses were:

a) the relative importance of different regulatory mechanisms will shift during the onset, establishment and maintenance of symbiosis;

b) the relative importance of different regulatory mechanisms will differ between heterologous (i.e. non-native) and homologous (i.e. native) symbiont species, though any observed differences will become less pronounced over time in symbiosis.

Chapter 2: Phylogenetic analysis of cell-cycle regulatory proteins within the Symbiodiniaceae

2.1. Abstract

In oligotrophic waters, cnidarian hosts rely on symbiosis with their photosynthetic dinoflagellate partners (family Symbiodiniaceae) to obtain the nutrients they need to grow, reproduce and survive. For this symbiosis to persist, the host must regulate the growth and proliferation of its symbionts. One of the proposed regulatory mechanisms is arrest of the symbiont cell cycle in the G_1 phase, though the cellular mechanisms involved remain unknown. Cell-cycle progression in eukaryotes is controlled by the conserved family of cyclin-dependent kinases (CDKs) and their partner cyclins. I identified CDKs and cyclins in different Symbiodiniaceae species and examined their relationship to homologs in other eukaryotes. Cyclin proteins related to eumetazoan cell-cycle-related cyclins A, B, D, G/I and Y, and transcriptional cyclin L, were identified in Symbiodiniaceae, alongside several alveolate-specific cyclin A/B proteins, and proteins related to protist P/U-type cyclins and apicomplexan cyclins. The largest expansion of cyclins was within the P/U-type cyclin groups. Proteins related to eumetazoan cell-cycle-related CDKs (CDK1) were identified as well as transcription-related CDKs. The largest expansion of CDK groups was, however, in alveolate-specific groups which comprised 11 distinct CDK groups (CDKA-J) with CDKB being the most widely distributed CDK protein. As a result of its phylogenetic position, conservation across Symbiodiniaceae species, and the presence of the canonical CDK motif, CDKB emerged as a likely candidate for a *Saccharomyces cerevisiae* Cdc28/Pho85-like homolog in Symbiodiniaceae. Similar to cyclins, two CDK-groups found in Symbiodiniaceae species were solely associated with apicomplexan taxa. A comparison of *Breviolum minutum* CDK and cyclin gene expression between free-living and symbiotic states showed that several alveolate-specific CDKs and two P/U-type cyclins exhibited altered expression *in hospite*, suggesting that symbiosis influences the cell cycle of symbionts on a molecular level. These results highlight the divergence of Symbiodiniaceae cell-cycle proteins across species. These results have important implications for host control of the symbiont cell cycle in novel cnidarian-dinoflagellate symbioses.

2.2. Introduction

Many cnidarians in the marine environment, including reef-building corals, form symbiotic relationships with photosynthetic dinoflagellates from the family Symbiodiniaceae (Davy *et al*., 2012). These dinoflagellate symbionts are located in host gastrodermal cells inside symbiosomes, (vacuoles consisting of a host-derived membrane) (Wakefield and Kempf 2001). This closely integrated intracellular relationship indicates that symbiont population maintenance by the host was probably integral to the evolution of the symbiosis (Jones and Yellowlees 1997; Davy *et al*., 2012). To date, most studies examining symbiont cell division *in hospite* have focused on nutrient availability (Hoegh-Guldberg and Smith 1989; Hoegh-Guldberg 1994; Muller-Parker *et al*., 1994; Smith and Muscatine 1999; Fitt 2000; Xiang *et al*., 2020). However, symbiont growth rate appears to be controlled by more than nutrient limitation, as nutrient-replete symbionts *in hospite* still have a growth rate that is less than 20% of symbionts *ex hospite* (Hoegh-Guldberg 1994).

Besides nutrient control, other proposed host regulatory mechanisms of symbiont growth and proliferation include pre-mitotic cell cycle control and post-mitotic autophagy, expulsion and apoptosis (Smith and Muscatine 1999; Baghdasarian and Muscatine 2000; Dunn *et al*., 2007; Davy *et al*., 2012). However, the contribution of each mechanism towards the regulation of symbiont biomass, from the onset to the stabilisation of the symbiosis, is unknown. Smith and Muscatine (1999) proposed that the main control of a dampened symbiont growth rate *in hospite* is from the cnidarian host arresting the cell cycle of its resident symbionts. In the eukaryotic cell cycle there are four cycling phases: G_1 (gap 1) where cells grow and are sensitive to extracellular cues such as growth factors (Pardee 1989); S (synthesis) where genomic DNA is replicated and synthesised (Nishitani and Lygerou 2002); G_2 (gap 2), where DNA breaks that occur during the S phase are repaired before mitosis (Stark and Taylor 2004); and M (mitosis), where two equal copies of the chromosomes are distributed between the two cells (Nishitani and Lygerou 2002). There is also a quiescent phase (G_0) where the cells stop progressing through their cell cycle and become dormant (Nishitani and Lygerou 2002). A cell can enter this phase at any point in the cell cycle. In the sea anemone *Exaiptasia pallida* (‘Aiptasia’), 80% of the resident symbionts were shown to be arrested at the G_1 phase compared with 40-55% in culture (Smith and Muscatine 1999).

Once a cell enters the cell cycle, it can be arrested at a series of cell-cycle checkpoints (Fig. 1.4). These checkpoints monitor the integrity and correct progression of the cell cycle with each checkpoint containing criteria that must be met for a cell to progress to the next stage of the cycle (Houtgraaf *et al*., 2006; Barnum and O'Connell 2014). Each checkpoint is regulated by cyclin-dependent kinases (CDKs) and their partner cyclins (Malumbres and Barbacid 2009). Once a cell meets its checkpoint criteria, cyclins are synthesised and bind to their partner CDKs (Malumbres and Barbacid 2009). Cyclins regulate the catalytic activity of CDKs (Lim and Kaldis 2013). These CDK-cyclin complexes can directly trigger cell-cycle progression (Fig. 1.4) or indirectly trigger cell-cycle progression through a variety of other downstream events such as transcription, DNA damage repair, proteolytic degradation and metabolism (Vermeulen *et al*., 2003). Table A1 summarises the cell-cycle stage and roles of individual CDK and cyclin proteins. CDK-cyclin complexes in *Homo sapiens* are shown in Figure 1.4; however, the type and quantity of CDKs and cyclins are specific to a particular species (Malumbres and Barbacid 2009).

Identification of cell-cycle proteins within Symbiodiniaceae is just beginning, with a study by Cato *et al.* (2019) finding 10 distinct CDKs and 15 distinct cyclin genes in the genome of *Breviolum minutum,* several of which are phylogenetically related to other eukaryotes. In the same study (Cato *et al*., 2019), qPCR analysis revealed that a cyclin B2/CDK1 pair was expressed during the G_1/S phase transition in cultured *B. minutum*. As there are at least nine genera of Symbiodiniaceae (LaJeunesse *et al*., 2018; Nitschke *et al*., 2020), determining whether cell-cycle proteins present in *B. minutum* are conserved across the Symbiodiniaceae will inform our understanding of cell-cycle progression and cellular growth rates in this family. For example, a recent study (Fujise *et al*., 2018) comparing cell-cycle progression between four Symbiodiniaceae genera (*Symbiodinium, Breviolum, Cladocopium* and *Durusdinium*) in culture, found that the proportion of the population progressing through the cell cycle was different between genera, resulting in differing growth rates. Similarly, different Symbiodiniaceae species have been shown to have different proliferation rates and to reach different densities within the same host (Starzak *et al*., 2014; Yuyama and Higuchi 2014; Leal *et al*., 2015; Gabay *et al*., 2018), with inherent differences in cell-cycle machinery between species being one possible explanation. The current study represents the first attempt to identify

and describe cell-cycle proteins across diverse Symbiodiniaceae species and provides a basis for future research.

2.3. Materials and methods

2.3.1. Identification of Symbiodiniaceae *CDKs and cyclins*

Twenty-seven Symbiodiniaceae transcriptome and genome databases were acquired from publicly available sources (Table A2). Cyclins and CDKs from two free-living Symbiodiniaceae species, *Effrenium voratum* (Jeong *et al*., 2014) and *Fugacium kawagutii* (Liu *et al*., 2018), were compared with symbiotic species (*Symbiodinium microadriaticum*, *S. tridacnidorum, Breviolum minutum, B. aenigmaticum, B. pseudominutum, B. psygomophilum, Cladocopium goreaui, Cladocopium* genotypes C15 and C92 and *Durusdinium trenchii*). Profile hidden Markov models (pHMMs) were obtained from the PFAM 31.0 database for the cyclin N terminal domain (PF00134) and CDK conserved domain (PF00069). The pHMM models were re-trained using CDKs and cyclins from eukaryotic organisms closely related to Symbiodiniaceae (e.g. Apicomplexa) using the aphid R package (Wilkinson 2019).

The Symbiodiniaceae databases were then queried with the updated pHMM models using an optimal alignment homology search to find putative Symbiodiniaceae cyclin and CDK sequences (Fig A1). Sequences with log-odds similarity scores >50 were retained for cyclins and CDKs. The cyclin model returned 119 sequences and the CDK model returned 6032 sequences. Due to the high abundance of Symbiodiniaceae CDK sequences returned from the model, the collected CDK sequences from the pHMM model were examined further using conserved CDK motifs (Table A3) (Joubs *et al*., 2000; Corellou *et al*., 2005; Malumbres and Barbacid 2005; Talevich *et al*., 2011). If the CDK contained a motif that when BLASTp searched against the NCBI non-redundant database matched to a CDK, the sequence was retained for further analysis. All 119 cyclins retrieved by the model were also searched, and were included in the analysis if the highest-scoring sequence was annotated as a cyclin or CDK and had an E value $\leq 1 \times 10^{-5}$. Owing to the lack of information available for CDKs and cyclins in other unicellular marine eukaryotes, several taxa (Table A5) were chosen for screening through the trained pHMM models to identify putative cyclin and CDK sequences, allowing possible alveolate-specific groups to be identified.

2.3.2. Sequence alignment and phylogenetic analysis

Phylogenetic trees were generated twice. The sequence alignment for the first set of trees was aligned to just the conserved cyclin N (PFAM ID:PF00134) and protein kinase domains (PFAM ID: PF00069), which were used to determine distinct phylogenetic groups of Symbiodiniaceae cyclins and CDKs. These were later used to identify other similar sequences from the Symbiodiniaceae databases.

The first trees were generated by aligning the putative CDK and cyclins in the aphid R package (Wilkinson 2019) (along with other eukaryotic cyclins and CDKs) and the best substitution model was selected by ProTest (v3.4) (Darriba *et al*., 2011). Both alignments had an appropriate evolutionary model of PROTOGAMMAAUTO, which was then used to infer maximum-likelihood trees in RAxML (v8.2.12) (Stamatakis 2014). Bootstrap support was used to find the distinct phylogenetic groupings among Symbiodiniaceae CDKs and cyclins (n =1000) by using the topology of the tree with the highest log-likelihood score. Trees were rooted using the *H. sapiens* MAPK (NP_002737.2) gene for the CDK tree and *H. sapiens* CABLES1 (NP_112492.2) and *H. sapiens* CABLES2 (NP_001094089.1) for the cyclin tree based on a previous study on animal cyclins and CDKs (Cao *et al.*, 2014). Symbiodiniaceae candidate proteins from distinct phylogenetic CDK and cyclin groups were used to perform custom BLASTp searches (Table A4) in Geneious v.11.1.5 against the 27 Symbiodiniaceae databases used in this study, to ensure that all putative CDKs and cyclins were identified. The first 10 Symbiodiniaceae proteins with the highest E-value ($\leq 1 \times 10^{-5}$) that were not previously identified by the pHMM model, and that identified a CDK or cyclin on the NCBI nr database in BLASTp searches, were collected from each Symbiodiniaceae database for each of the candidate proteins. These newly identified Symbiodiniaceae sequences were added to the previously collected sequences through the pHMM models and together these were entered into CD-Hit v4.8 (Li *et al*., 2001) to remove isoforms and redundant proteins using a similarity threshold of 90%.

Once redundant proteins and isoforms were removed, Symbiodiniaceae sequences were submitted to InterProScan (Quevillon *et al*., 2005) to identify CDK and cyclin domains. Due to the low-quality annotations in Symbiodiniaceae databases (Chen *et al*., 2020), many sequences contained regions that coded other proteins, therefore the alignments were trimmed manually in Geneious v.11.1.5 to CDK- (PFAM ID: PF00069; PANTHER ID: PTHR24056) and cyclin- (PFAM ID:PF00134, PF02984, PF16899 and PF08613; PANTHER ID: PTHR10177) annotated domains. The final CDK alignment for the second phylognetic analysis was 465 amino acids (aa) long, and contained 177 Symbiodiniaceae sequences and 50 CDKs from other eukaryotes, whereas the cyclin alignment was 395 aa long and contained 191 Symbiodiniaceae sequences and 54 cyclins from other eukaryotes. All CDK and cyclin families from *Homo sapiens* were included in the trees to create the correct topologies, and CDKs and cyclins from other model organisms, including *Saccharomyces cerevisiae* and *Arabidopsis thaliana,* were only included if Symbiodiniaceae proteins were related to them, otherwise they were removed to simplify the tree.

Final CDK and cyclin alignments were run through ProTest (v3.4) (Darriba *et al*., 2011) as described previously. Maximum-likelihood trees were then run in PhyML (v3.1) (Guindon and Gascuel 2003) using the Akaike information criterion which corresponded to the LG+I+G+F model for the CDK alignment with a proportion of invariable sites of 0.039 and a gamma shape parameter of 1.195 and the LG+G+F model for cyclin alignments with a gamma shape parameter of 2.331. Due to the quantity of sequences in the tree, an approximate likelihood ratio test (aLRT) was used for branch support instead of bootstrap support (Anisimova and Gascuel 2006), however it has been shown to be very similar in calculating correct branch supports (Guindon *et al*., 2010). Based on a comparison of correct branch topologies determined by bootstrap support and SH-values (Guindon *et al*., 2010), true Symbiodiniaceae CDK and cyclin homologs were determined by branches containing an SH-value > 0.8. Trees were rooted as described previously. Trees were edited in the Interactive Tree of Life (iToL) software v.5.6.3 (Letunic and Bork 2019). The nomenclature of protein groups that did not phylogenetically group with other well-classified CDKs or cyclins was attributed by using BLAST searches against the NCBI nr database.

2.3.3. Cyclin and CDK gene expression of B. minutum

To explore expression of cyclins and CDKs in Symbiodiniaceae, RNA-Seq reads were analysed from a recent study by Maor-Landaw *et al.* (2020) on the expression of cultured (n = 3) and freshly isolated *B. minutum* (n = 3) from the sea anemone *Exaiptasia diaphana* (= *pallida*) (SRA PRJNA544863). Reads were aligned to the *B. minutum* genome assembly (Shoguchi *et al*., 2013) using STAR v2.7.1a in two-pass mode (Dobin *et al*., 2013) and read counts were extracted from the alignments with featureCounts v1.6.3 (Liao *et al*., 2014). Differential expression analysis was completed using the exact test in EdgeR (Robinson *et al*., 2010) on TMM normalized counts of the cultured and isolated *B. minutum* . Differentially expressed genes (DEGs) were those with Benjamini-Hochberg adjusted p-values < 0.05. Cyclins and CDKs identified in *B. minutum* were selected from the list of DEGs to generate a heat map in the R environment (Team 2020), using the mean-variance modelling at the observational level (voom) (Law *et al*., 2014) of $\log_2$-transformed counts *per* million (CPM).

2.4. Results and Discussion

2.4.1. Characterisation and phylogenetic positioning of Symbiodiniaceae CDK sequences

Eukaryotic organisms contain different numbers of CDK proteins, ranging from three in premetazoans, to 20 in eumetazoans such as *Homo sapiens* (Cao *et al*., 2014). A total of 177 unique Symbiodiniaceae CDK gene copies were identified across six genera (Table 2.1). CDK gene copy numbers were the highest in *Cladocopium goreaui* which contained 16 CDK copies. Interestingly, no CDKs related to the CDK4/6 family nor their cyclin partners (cyclin E) were found in Symbiodiniaceae using the databases referenced in this study (Fig. 2.1). This agrees with findings for plants and many protists in which there is also an absence of the CDK4/6 family and cyclin E in most non-metazoan lineages (Cao *et al*., 2014).

Table 2.1. Gene copies of CDKs within Symbiodiniaceae. 'G' refers to genome and 'T' refers to transcriptome.

	Source of database	CDK1/2/3 subfamily	CDK4/6 subfamily	CDK5 subfamily (CDK5/14/15/Pho85)	CDK7	CDK8 subfamily (CDK8/19)	CDK9 subfamily (CDK9/12/13)	CDK10/ CDK11 subfamily	CDK20	Alveolate-specific CDKA	Alveolate-specific CDKB	Alveolate-specific CDKC	Alveolate-specific CDKD	Alveolate-specific CDKE	Alveolate-specific CDKF	Alveolate-specific CDKG	Alveolate-specific CDKH	Alveolate-specific CDKI	Alveolate-specific CDKJ	Parasitic CDKA	Apicomplexan Cdc2-like CDK	Total
S. microadriaticum	G				1				1	1	1	1	1		1	1	1	1	1			11
S. tridacnidorum	G				1		1	1		1	1	1	1	1	1		1	1	1			12
***Symbiodinium* sp. #1**	T				1		1	1			1	1	1	1	1	1		1				10
***Symbiodinium* sp. #2**	T				1			1			1			1				1				5
B. minutum	G				1		1	1	1	1	1	1	1	1	1	1	1	1	1			14
B. aenigmaticum	T				1		1	1			1	1	1	1	1		1	1	1			11
B. pseudominutum	T				1		1	1		1	1	1	1	1	1	1		1	2			13
B. psygomophilum	T				1		1	1		1	1	1	1	1	1	1	1	1	1			13
***Breviolum* sp. #1**	T				1		1	1		1	1	1	1	1	1		1	1	2			13
C. goreaui	G	1		1	1		1	1		1	1	1	1	1	1	1		1	2		1	16
***Cladocopium* sp. C15**	T				1						1	1	1	1	1		1	1	1			9
***Cladocopium* sp. C92**	G						1		1		1	1	1	1	1	1	1		1			10
***Cladocopium* sp. #1**	T										1			1						1		3
***Cladocopium* sp. #2**	T				1		1	1			1	1	1	1	1		1	1				10
***Cladocopium* sp. #3**	T										1	1		1								2
D. trenchii	T			1							1	1	1	1						1		6
***Durusdinium* sp. #1**	T									1		1		1				1	1			4
Effrenium voratum	T										1	1	1	1	1			1	1			7
Fugacium kawagutii	G				1			1	1	1	1	1										5
TOTAL		1	0	2	13	0	10	11	4	9	18	17	14	17	13	7	9	14	15	2	1	177

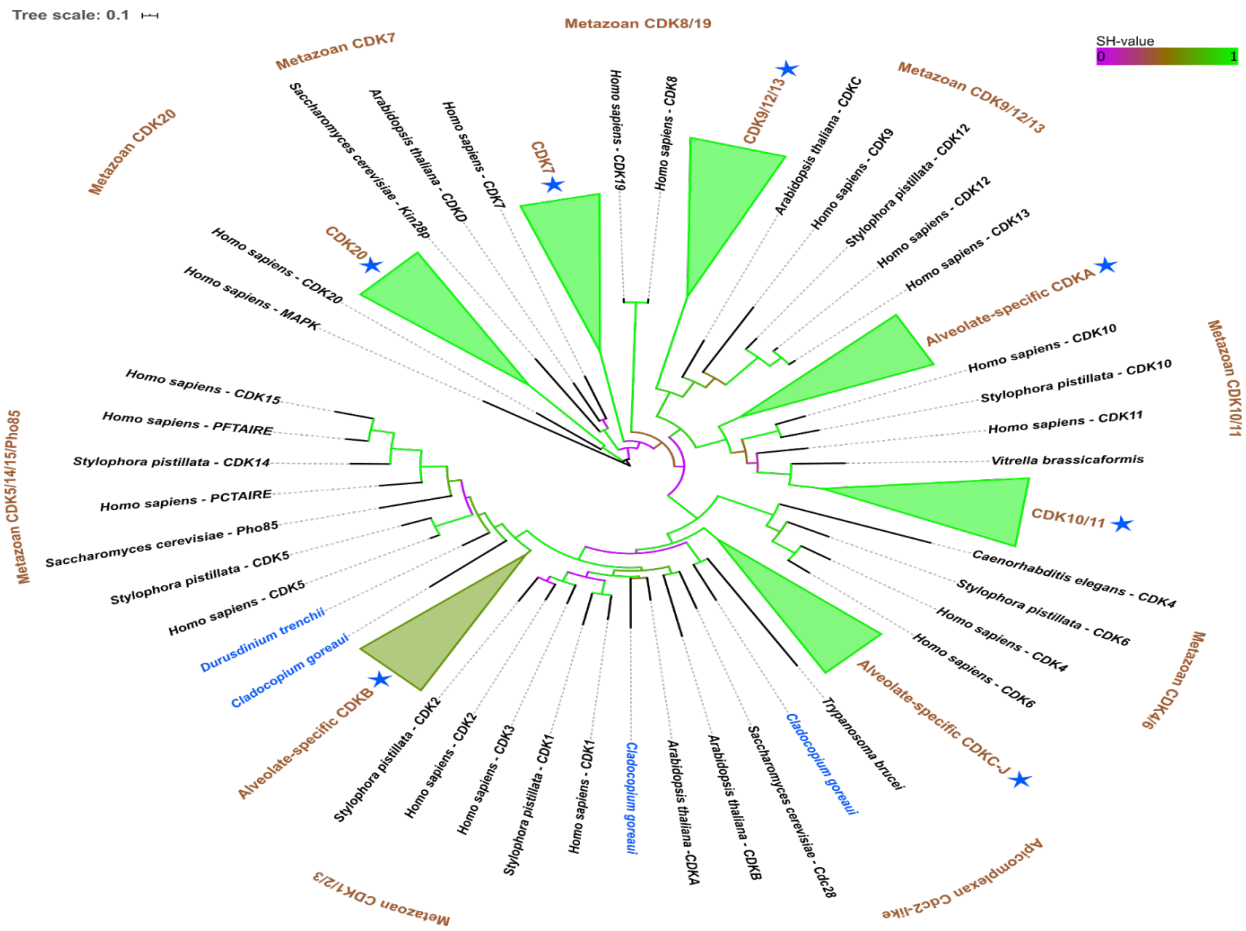

Figure 2.1. Collapsed phylogenetic tree of CDKs within Symbiodiniaceae. Colour of branches corresponds to aLRT support (SH-value). Purple branches correspond to SH-values below 0.5, brown branches correspond to SH-values near 0.5 and green branches correspond to SH-values close to 1. Symbiodiniaceae species are written in blue with blue stars depicting collapsed branches containing Symbiodiniaceae species. The phylogenetic tree was made using PhyML(v3.1) (Guindon and Gascuel 2003) and visualised using the Interactive Tree of Life software (v5.6.3) (Letunic and Bork 2019).

Some of the Symbiodiniaceae CDKs showed high sequence similarity to eumetazoan CDKs however, the largest expansion of CDKs was within the alveolate-specific CDK groups (Table 2.1; Fig. 2.1). A previous study (Cato *et al*., 2019) investigating Symbiodiniaceae cell-cycle proteins found four *B. minutum*-specific CDKs. Here I show that three of those four CDKs are also present across other Symbiodiniaceae species (alveolate-specific CDKG/H/J – Table 2.1; Fig. D1). In the previous study (Cato *et al*., 2019), the *B. minutum* CDKs (alveolate-specific CDKG/H/J) did not change their expression with cell-cycle phase when in a free-living state. However, our analysis of the previously published RNA-Seq data (Maor-Landaw *et al*., 2020) shows that symbiosis alters the expression of *B. minutum* CDKG and CDKH, which were both up-regulated *in hospite* compared with when in culture (Table A6; Fig. 2.2).

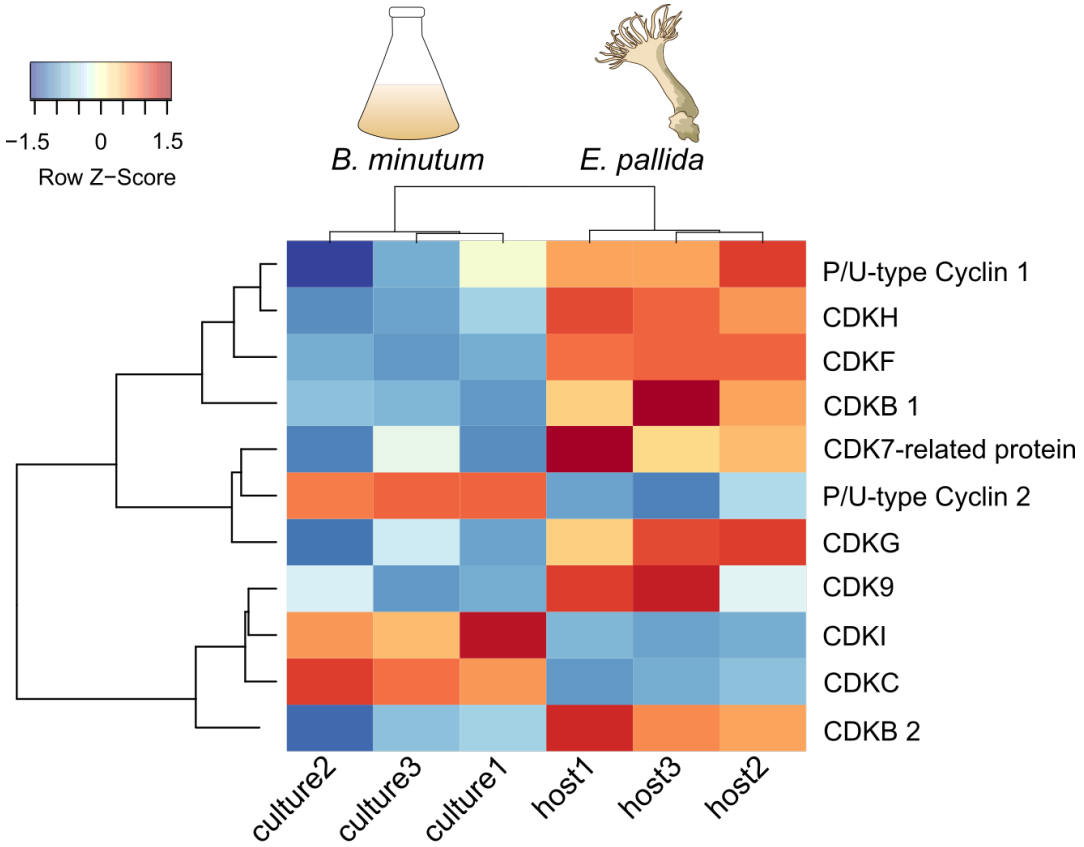

Figure 2.2. Heat map comparison of *B. minutum* cyclin and CDK gene expression between cultured cells and cells freshly isolated from *E. pallida*. Red corresponds to a higher Z-score and gene up-regulation whilst blue corresponds to a lower Z-score and down-regulation.

The most common CDK identified in Symbiodiniaceae was an alveolate-specific CDK (CDKB) with gene copies found across 18 species in the five Symbiodiniaceae genera examined (Table 2.1). Symbiodiniaceae proteins in the CDKB group contained the canonical

CDK motif PSTAIRE (Table 2.2). The CDKB sister clade is the Pho85/CDK5 subfamily (SH-value 0.95), which is sister to the metazoan CDK1/*S. cerevisae* Cdc28, with strong branch support (SH-value = 1; Fig. D1). CDK1/Cdc28 is the primary cell-cycle regulator from yeast to humans (Lee and Nurse 1987; Mendenhall and Hodge 1998; Santamaría *et al*., 2007), however Pho85 has been shown to have overlapping roles with Cdc28, phosphorylating many of the same substrates (Huang *et al*., 2007). The primary roles of Pho85 include responding to environmental cues *via* the induction of signals that inform the cell whether conditions are adequate for cell division and nutrient metabolism (Carroll and O'Shea 2002). As Symbiodiniaceae proliferate in response to increased nutrients (Hoegh-Guldberg 1994), they may have evolved CDKs that possess similar functions for linking external stimuli (e.g. environmental nitrogen and phosphorus levels) to cell-cycle progression. Furthermore, our analysis of the RNA-Seq data comparing cultured *versus* freshly-isolated *B. minutum* (Maor-Landaw *et al*., 2020) suggests that two CDKB genes are up-regulated in symbiosis (Table A6; Fig. 2.2). I hypothesise that, due to its phylogenetic grouping, conserved motif, widespread presence across Symbiodiniaceae and up-regulation in the symbiotic state, CDKB may be a homolog of Cdc28/Pho85 and a primary cell-cycle regulator in Symbiodiniaceae. This hypothesis requires confirmation.

Proteins related to eumetazoan transcriptional CDK subfamilies (CDK9/12/13 (SH-value = 0.89), CDK10/11 (SH-value = 0.89) and CDK20 (SH-value = 0.93)) were also present in Symbiodiniaceae (Table 2.1; Fig. D1). Amongst transcriptional roles, the CDK10/11 subfamily has also been proposed to have roles in cell-cycle progression during the G_2/M phase (Table A1) (Li *et al*., 1995). However, in *B. minutum,* CDK20, CDK9 and CDK11 expression did not change with cell-cycle phase (Cato *et al*., 2019), highlighting their similarity to metazoan CDK20, CDK9 and CDK11, which are predominantly transcriptional CDKs and indirectly related to the cell-cycle (Malumbres 2014). Previous studies (Cato *et al*., 2019) have reported an absence of CDK7 in *B. minutum*, however this study found a CDK7-related gene (confirmed *via* BLAST searches on the NCBI nr database) across 13 different Symbiodiniaceae species (Fig. D1). The difference in results may be, in part, explained by the Symbiodiniaceae CDK7 being phylogenetically distant from the metazoan CDK7 and yeast CDK7 homolog (Kin28p), grouping separately and with no concrete relationship to any other CDK included in this study, possibly owing to its divergence. CDK7 has been discovered in other non-metazoans, such as the amoebozoan *Dictyostelium purpureum* (Ma *et al*., 2013). In metazoans, CDK7 forms part

of the cyclin kinase-activating (CAK) complex that activates other CDKs by phosphorylating their T-loop (Schachter *et al*., 2013), and inhibition of CDK7 led to the arrest of the cell cycle in proliferating cells (Larochelle *et al*., 2007). The previously published RNA-Seq data (Maor-Landaw *et al*., 2020) show that the CDK7-related gene was up-regulated in symbiotic *B. minutum* (Table A6).

Table 2.2. Conserved motifs found in Symbiodiniaceae CDK genes

CDK group	**Symbiodiniaceae motif**
CDK1/2/3 subfamily	PSTALRE
CDK4/6 subfamily	N/A
CDK5 subfamily (CDK5/14/15/Pho85)	PCTAIRE
CDK7	(G/S)TALRE
CDK8 subfamily (CDK8/19)	N/A
CDK9/12/13	P(A/T/S)T(S/A/C)(I/V)RE
CDK10/11	P(V/S)(P/A/S)S(L/I)RE
CDK20	PWFSAERE
Alveolate-specific CDKA	P(K/R)(I/S)SLRE
Alveolate-specific CDKB	PSTAIRE
Alveolate-specific CDKC	PSTAIRE
Alveolate-specific CDKD	PSTALRE/EHQLRRE
Alveolate-specific CDKE	P(G/S)TA(I/L)RE
Alveolate-specific CDKF	(S/P)(A/P)(T/H/Y/Q)(T/A/V)(I/L)RE
Alveolate-specific CDKG	S(A/T)Q(V/A)LRE
Alveolate-specific CDKH	(S/T)S(Y/F)(S/A)(L/I)RE
Alveolate-specific CDKI	P(T/A)(T/A)(S/T/A)(I/L)RE
Alveolate-specific CDKJ	P(T/A)TALRE; PAVA(L/M)RE
Parasitic CDKA	PSTAIRE
Apicomplexan Cdc2-like CDK	PQTALRE

Symbiodinium sp. #2 contained CDKs and cyclins that are more similar to those of the free-living dinoflagellate *Amphidinium* (SH-value > 0.95) than to other Symbiodiniaceae species (Fig. D1). CDKs and cyclins that are not present in *Amphidinium* sp. but are present in *Symbiodinium* sp. #2 grouped next to, not with, the other Symbiodiniaceae species (SH-value > 0.78). This placement may reflect the early divergence of *Symbiodinium* within the Symbiodiniaceae (LaJeunesse *et al*., 2018).

Several Symbiodiniaceae species contained CDKs found in parasitic taxa. A CDK protein that is related to a gene present in the free-living, facultative pathogenic marine ciliate *Pseudocohnilembus persalinus,* was found in both *D. trenchii* and *Cladocopium* sp. #1 (SH-value = 1), while *C. goreaui* harbours a CDK related to Cdc2-related kinase 6 (CRK6) from *Trypanosoma brucei* (SH-value = 0.97) (Fig. 2.1, Fig. D1). Studies (Jones *et al*., 2014; Tu and Wang 2005) have shown that the loss of *T. brucei* CRK6 slows the growth of *T. brucei* but does not inhibit the cell cycle (contrasting with cell-cycle indispensable CRK3 and CRK1), highlighting a function of CRK6 that may not be directly associated with the cell cycle.

2.4.2. Characterisation and phylogenetic positioning of Symbiodiniaceae cyclin sequences

Similar to CDKs, the number of cyclins differs across eukaryotes – from eight in premetazoans to 29 in *Homo sapiens* (Cao *et al*., 2014). Across the six Symbiodiniaceae genera examined, 191 cyclins were identified (Table 2.3; Fig. 2.3). *C. goreaui* contained the most cyclin gene copies, harbouring 19 distinct copies. Differences in abundance of cell-cycle proteins (cyclins and CDKs) between different Symbiodiniaceae species could be a result of the different database information provided (genomes *versus* transcriptomes), as if CDKs and cyclins were not expressed at the time of transcriptomic analysis, these may have been missed, thus producing a bias towards genomes harbouring more cyclin and CDK gene copies. Another possible reason for the difference in cyclin and CDK gene copies in the Symbiodiniaceae, is gene duplication events which are followed by genetic drift over time, causing the formation of cell-cycle paralogs with functional divergence in the family.

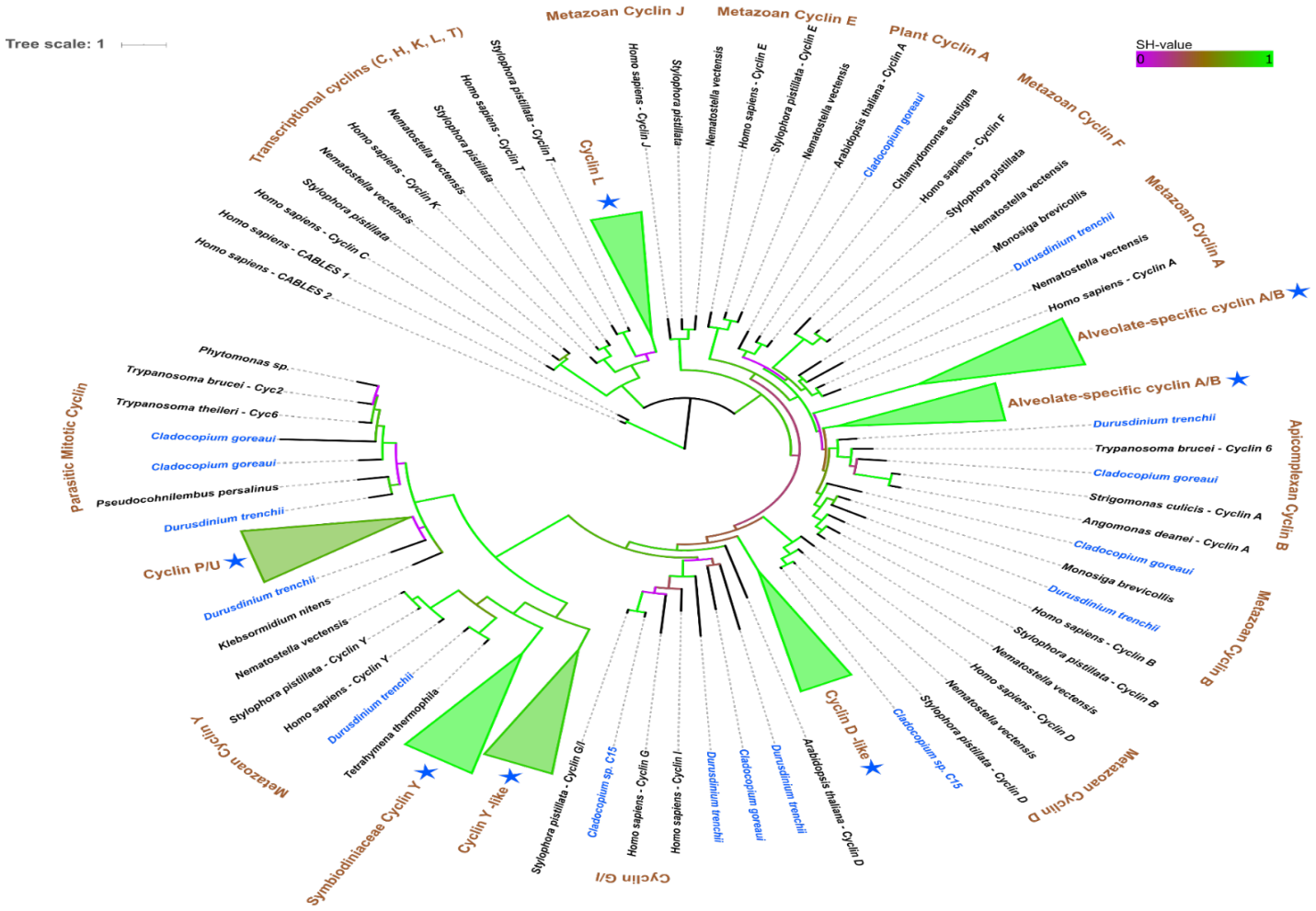

Figure 2.3. Collapsed phylogenetic tree of cyclins within Symbiodiniaceae. Colour of branches corresponds to aLRT support (SH-value). Purple branches correspond to SH-values below 0.5, brown branches correspond to SH-values near 0.5 and green branches correspond to SH-values close to 1. Symbiodiniaceae species are written in blue with blue stars depicting collapsed branches containing Symbiodiniaceae species. The phylogenetic tree was made using PhyML(v3.1) (Guindon and Gascuel 2003) and visualised using the Interactive Tree of Life software (v.5.6.3) (Letunic and Bork 2019).

Table 2.3. Gene copies of cyclins within Symbiodiniaceae and complementary conserved motifs.

	Cyclin type	**Symbiodiniaceae Motif**	*Symbiodinium microadriaticum*	*Symbiodinium triacnidorum*	*Symbiodinium* sp.#1	*Symbiodinium* sp. #2	*Breviolum minutum*	*Breviolum aenigmaticum*	*Breviolum pseudominutum*	*Breviolum psygomophilum*	*Breviolum* sp. #1	*Cladocopium goreaui*	*Cladocopium* sp. C15	*Cladocopium* sp. C92	*Cladocopium* sp. #1	*Cladocopium* sp.#2	*Cladocopium* sp. #3	*Durusdinium trenchii*	*Durusdinium* sp.#1	*Effrenium voratum*	*Fungacium kawagutii*	Total
Eumetazoan and plant cell cycle cyclins	Cyclin A	(M/L)R(A/V)(I/A)L(V/I)DWL										1						1				2
	Cyclin B	YRTKIVNWM; NLAVLHDWL										1						1				2
	Cyclin D	MRRMVTSWM											1									1
	Plant Cyclin D-like	ERALAVDWL; DRQETLTWM; RRLDALEWL	1	1	1		2	2	2	2	1	2	2	2				1		1		20
	Cyclin E																					0
	Cyclin G/I	GRRDLMIWL;QRDNITTFM;(W/N)R(R/D)(Q/D)(M/S)(I/T)(E/V)(W/F)(C/I)										1	1					2				4
	Cyclin J/O																					0
	Cyclin F																					0
Eumetazoan transcriptional cyclins	Cyclin C																					0
	Cyclin H																					0
	Cyclin K																					0
	Cyclin L	LR(R/A)FG(V/G/N/S)VL(I/L)	2	1	1	1	2		2	2	2	2	1	2								18
	Cyclin T																					0
	Cyclin Y-like	LADEIYELL; S(K/T)E(T/A)ILDFL; REMVLDFL; HEAVL(T/A)FL		2	2		1		1	1	1	1		1		1		1	1	2		15
	Cyclin Y	TVDNIYEFM; ----IYDFL	1	1		1	1				1	1								1		7

Table 2.3. continued.

Protist A/B cyclins	Cyclin A/B	MR(G/A)ILVDWL; ER(A/G)(L/T/A/S/C/I)(A/V)(A/D/N)W(L/M); (S/Q)RA(V/T)(Q/L)(I/V)D(F/M)(M/I)	2	4	3	2	3	4	3	3	3	3	3	3	2	4	1	2	2	5	2	54
	Apicomplexan cyclin B	MR(T/I)ILVDWL										1						1				2
	Parasitic mitotic cyclin	PSINVADYL; PGITMPDFF; PPLSLADLG										2						1				3
	P/U cyclin	PSISVRSYL; PPIT(V/L)(R/K)DY(V/L); (E/D)PPDI(S/N)(A/Y/S)(Y/F)(I/V); (K/S)(N/A)MDLDDFI; E(S/T)(S/Q/V)DIEEYI; P(T/S)I(S/G)(V/I)(G/E)(E/D)YL; PKISV(R/L)(D/N)YL; PGIG(V/A/I)(A/E)(A/Q/L/V)YL; P(G/T/S)I(P/S)V(D/Q)(K/Q)YL	5	5	4		4	4	4	4	4	4	2	3	2	6	1	2	1	6	2	63
Total			11	14	11	4	13	10	12	12	12	19	10	11	4	11	2	12	4	15	4	191

All the cyclins found in the Symbiodiniaceae contained one of three distinct domains (Fig. 2.4): the conventional cell-cycle cyclin N and C domains; a cyclin N domain found nearer the amino terminus than the position of the conventional cell-cycle cyclin N domain which corresponded phylogenetically to transcriptional cyclins (specifically cyclin L); and a single plant P/U cyclin domain that is phylogenetically related to the analogous domain of the Pho80p cyclin in *S. cerevisiae*.

Proteins related to eukaryotic cell-cycle cyclins A, B, D and G/I, and transcriptional cyclin L were identified in the Symbiodiniaceae, along with proteins related to plant cyclin D, protist/plant P/U-type cyclin and cyclin Y, as well as genes related to Cyc2 and mitotic Cyc6 from the sister taxon Apicomplexa (Fig. 2.3; Fig. D2). Three phylogenetically distinct groups of cyclins were also present in Symbiodiniaceae that, upon searching the NCBI nr database, matched to alveolate-specific cyclins A/B (Fig. D2). Two cyclins previously reported to be *B. minutum*-specific (Cato *et al*., 2019) were found in other Symbiodiniaceae species and belong to the "Plant Cyclin D-like" grouping (Table 2.3; Fig. D2). In metazoans and plants, cyclin D is required for G_1 phase progression (Ortega *et al*., 2002).

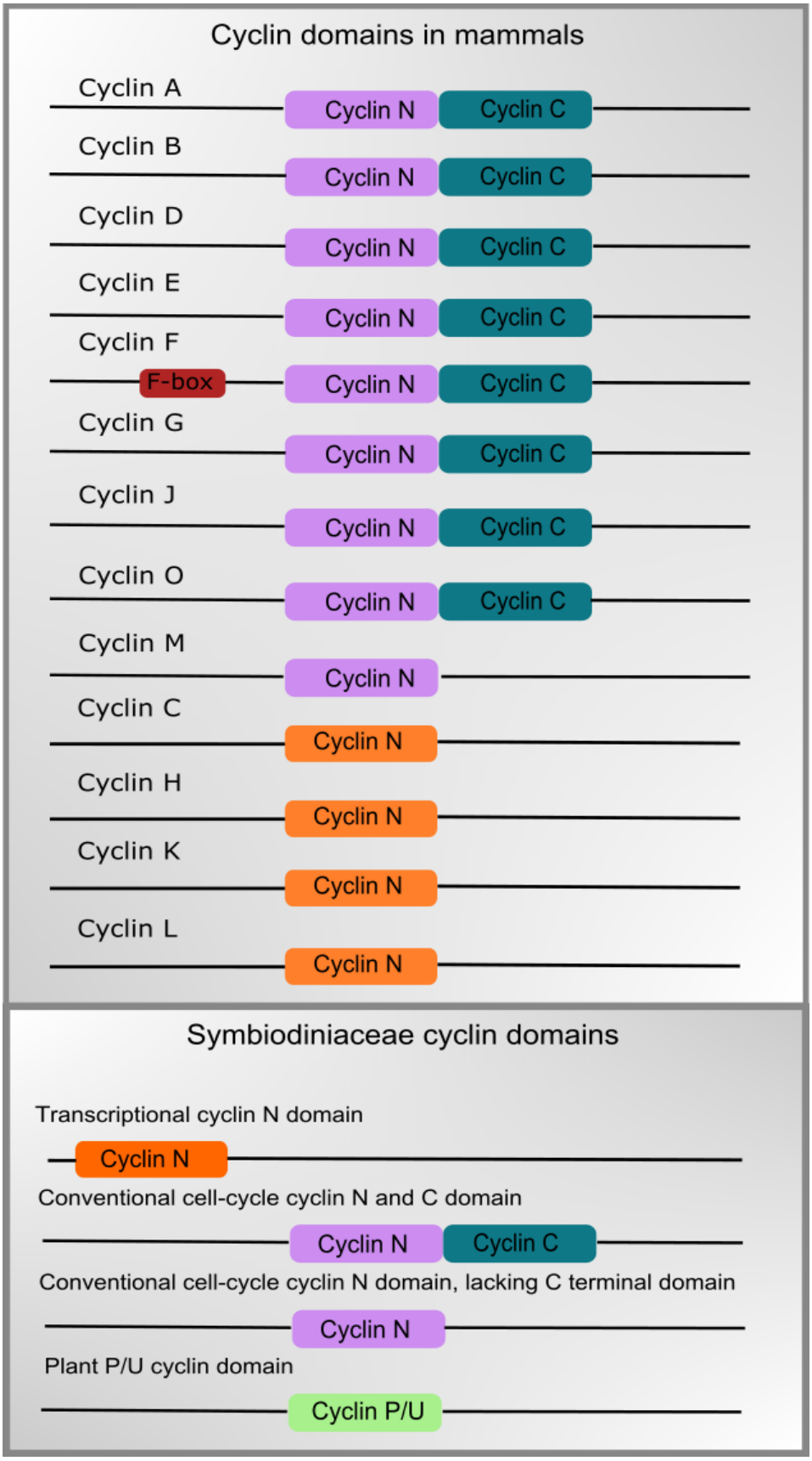

Figure 2.4. Domain structure of mammalian cyclin proteins compared with those in Symbiodiniaceae.

An expansion of the protist/plant P/U-type cyclin groups was found within Symbiodiniaceae, with 63 gene copies being present across six Symbiodiniaceae genera (Fig. 2.3, Fig. D2). This finding agrees with the previous study (Cato *et al*., 2019), which found P-type cyclins in *B. minutum.* Genes within these groups were related to the *S. cerevisiae* Pho80p cyclin. In *S. cerevisiae,* the Pho80 subfamily of P/U-type cyclins (Pho80, Pcl6, Pcl7, Pcl8 and Pcl10 (Huang *et al*., 2007)) link nutrient availability with cell-cycle progression (Roques *et al*., 2015). In *A. thaliana,* P/U-type cyclins are implicated in the switch from heterotrophic to autotrophic growth (Peng *et al*., 2014). RNA-Seq data (Maor-Landaw *et al*., 2020) revealed that two of these P/U type cyclins had contrasting expression (one being up-regulated whilst the other was down-regulated) *in hospite versus* in culture in *B. minutum* (Table S6; Fig. 2.2). Given that nutritional exchange is a fundamental feature of the cnidarian-dinoflagellate symbiosis (Davy *et al*., 2012), and that P/U cyclins are involved in glycogen metabolism and carbon source utilisation (Huang *et al*., 1998; Carroll and O'Shea 2002), the differential expression of these cyclins *in hospite* is unsurprising. Whether the difference in expression is a response to environmental stimuli exclusively experienced in symbiosis, e.g. host-associated factors such as the pH of the symbiosome in which the alga resides (Barott *et al*., 2015), requires further study. Similar to Symbiodiniaceae, the apicomplexan *T. gondii* also lacks a cyclin E homolog and instead uses a P-type cyclin for G_1 phase progression (Alvarez and Suvorova 2017). Symbiodiniaceae may also use P-type cyclins in place of eumetazoan cyclin E, however this requires confirmation.

Twenty-two cyclin Y-like gene copies were found across the Symbiodiniaceae. These encompassed two phylogenetic groups, one termed "Cyclin Y" which grouped with eumetazoan Cyclin Y (SH-value = 0.93), and one group of cyclins that grouped with the conventional eumetazoan Cyclin Y (SH-value = 0.80) that were termed "Cyclin Y-like" (Fig. 2.3, Fig. D2). Cyclin Y is absent in plants and fungi (being replaced by the Pcl class of cyclins in fungi) but is present in animals and protists (Ma *et al*., 2013). In eumetazoans and fungi, cyclin Y and Pcl1 cyclins are the binding partners of CDK14 and Pho85, respectively (Measday *et al*., 1997; Jiang *et al*., 2009). In yeast, the cyclin Y homolog, Pcl1, is expressed during the G_1 phase of the cell cycle (Measday *et al*., 1997) and provides information to the cell, determining whether it passes the START checkpoint, where the yeast cell commits to mitosis (Carroll and O'Shea 2002). In *Drosophila*, cyclin Y is required for Wnt signalling by localising the CDK14 kinase to the cell membrane (Sun *et al*., 2014). As Wnt signalling is an

indispensable pathway for the long-term viability of cells (MacDonald *et al*., 2009), the presence of cyclin Y and cyclin-Y like genes in most eukaryotes is predicted.

Uniquely, *C. goreaui* and *D. trenchii* both contain cyclins present in two phylogenetic groups that cluster with mitotic cyclins from the dinoflagellate sister taxon, the apicomplexans (Leander and Keeling 2004) (Fig. 2.3). One group is related to the B-type G_2/M phase-specific cyclin, Cyc6, in the apicomplexans (SH-value > 0.98), while the other clusters with Cyc2-like from *T. brucei*, which is involved in transition from both the G_1 to S and G_2 to M phases (Liu *et al*., 2013) (Fig. 2.3). The correlation in cell-cycle machinery of both cyclins and CDKs between pathogenic protists and *D. trenchii,* which is reported to colonise hosts during heat stress opportunistically (Stat and Gates 2010; Leal *et al*., 2015), and has a fast growth rate *versus* other Symbiodiniaceae species in culture (Fujise *et al*., 2018), is noteworthy and warrants future investigation.

Cladocopium sp. C15 harbours two cyclins (cyclin D and cyclin G/I) that are related to a symbiotic coral (*Stylophora pistillata*), with strong support (SH-value = 1). Both *Cladocopium* sp. C15 cyclin D and G/I share a close identity (92.1% and 74.5%, respectively) and similarity (95.7% and 91.6%, respectively), across the full sequence length to *S. pistillata* cyclins. To account for possible contamination of host material in the *Cladocopium* sp. C15 transcriptome, the origin of this symbiont was traced (MMETSP (Keeling *et al*., 2014)). The *Cladocopium* sp. C15 was found to have been freshly isolated from its host *Porites compressa,* so host contamination cannot be excluded. This being said, symbiosis has been suggested to drive the formation of paralogous genes involved in host-symbiont interactions due to selective pressure for a more mutualistic partnership between host and symbiont (Duncan *et al*., 2016). How the evolution of cell-cycle proteins that share a high similarity between host and symbiont affects biomass co-ordination is deserving of future attention.

2.5. Conclusions

Our study shows the divergence of cell-cycle proteins in the Symbiodiniaceae family and demonstrates that there are several conserved CDK and cyclin groups across the Symbiodiniaceae, though also that there are marked species-specific differences. Which of

these conserved cell-cycle proteins are indispensable for cell-cycle progression and which species-specific proteins influence proliferation rates in symbiosis remains unknown. Further study will be required to clarify which CDKs and cyclins are required for Symbiodiniaceae cell-cycle progression, and whether this differs between species and symbiotic states. As annotation of Symbiodiniaceae genomes is challenging (Chen *et al*., 2020), future studies should aim to apply the same comparative analysis across new Symbiodiniaceae genomes to inform cyclin and CDK gene prediction accurately.

Chapter 3: Symbiosis with dinoflagellates alters cnidarian cell-cycle gene expression

3.1. Abstract

In the cnidarian-dinoflagellate symbiosis, hosts show altered expression of genes involved in growth and proliferation when in the symbiotic state, but little is known about the molecular mechanisms that underlie the host's altered growth rate. Using pre-existing tissue-specific transcriptomics, I determined how symbiosis affects expression of cell cycle associated genes, in the model symbiotic cnidarian *Exaiptasia diaphana* ('Aiptasia'). The presence of symbionts within the gastrodermis elicited host cell cycle arrest in the G_1 phase and the inhibition of DNA synthesis and mitosis, compared with the aposymbiotic gastrodermis. Host apoptotic inhibitors (Mdm2) were elevated while host apoptotic sensitisers (c-Myc) were depressed in the symbiotic gastrodermis when compared with the aposymbiotic gastrodermis and epidermis of symbiotic hosts, respectively. This indicates that the presence of symbionts negatively regulates host apoptosis, possibly contributing to their persistence within a host. Transcripts associated with the persistence of 'non-self', non-pathogenic cells (SMAD4) increased in symbiotic gastrodermal tissues while transcripts (ATM/ATR) associated with sensitivity to reactive oxygen species (ROS) were down-regulated. In epidermal cells, a single gene (Mob1) required for mitotic completion was up-regulated in symbiotic anemones compared with aposymbiotic anemones, suggesting that the presence of symbionts in the gastrodermis stimulates mitotic completion in the epidermis, possibly through the nutritional benefits provided by the symbiosis. To corroborate further this hypothesis, I analysed pre-existing data from microscopical analysis that used an S phase indicator (EdU) to measure cell cycling in host cells. The results confirmed that there were significantly more proliferating host cells in both the gastrodermis and epidermis in the symbiotic state compared with the aposymbiotic state. These results contribute to our understanding of the influence of symbionts on mechanisms of cnidarian cell proliferation and mechanisms associated with symbiont maintenance.

3.2. Introduction

Coral reefs are one of the most negatively impacted ecosystems on our planet (Parmesan 2006), a consequence of anthropogenic climate change that has led to ocean warming and acidification (Hughes *et al*., 2003; Hoegh-Guldberg *et al*., 2007). Reef-building scleractinian corals and

other cnidarians (soft corals, sea anemones, jellyfish and hydrocorals) form symbioses with dinoflagellates of the family Symbiodiniaceae (Davy *et al*., 2012), which are located in the host's gastrodermal cells, within host-derived vacuolar compartments known as "symbiosomes" (Wakefield *et al*., 2000; Wakefield and Kempf 2001). During stable environmental conditions, this symbiosis is mutualistic, with the major benefit being the exchange of nutrients (Kopp *et al*., 2015). In particular, fixed carbon is translocated from the algae to the host, often in the form of glucose (Burriesci *et al*., 2012; Hillyer *et al*., 2016), while inorganic nitrogen is released to the algae by the host (Muscatine and Hand 1958; Rädecker *et al*., 2015). This nutritional interplay underlies the success of coral reefs in nutrient-poor tropical waters (Roth 2014).

Evolved interactions between the resident symbiont and the host are integral for controlling the metabolic integration, the nutritional state and the co-ordinated growth of the symbiont and host (Jones 1997). The host has evolved several homeostatic mechanisms to regulate the steady-state symbiont density, including pre-mitotic mechanisms such as cell cycle arrest (Smith and Muscatine 1999) and post-mitotic mechanisms such as autophagy (Dunn *et al*., 2004; Chen *et al*., 2005; Dunn *et al*., 2007), apoptosis (Gates *et al*., 1992; Dunn *et al*., 2007; Dunn and Weis 2009) and expulsion (Hoegh-Guldberg *et al*., 1987; Jones and Yellowlees 1997; Baghdasarian and Muscatine 2000; Dimond and Carrington 2008). These host regulatory processes have been shown to be up-regulated when: conditions favour symbiont growth and are suboptimal to the host e.g. increased temperatures (Baghdasarian and Muscatine 2000; Dunn *et al*., 2007; Paxton *et al*., 2013); the host associates with heterologous symbiont types (Dunn and Weis 2009); and during the association of the host with symbionts that have increased growth rates (McCloskey *et al*., 1996; Sachs and Wilcox 2006).

Cell-cycle control has been proposed as one of the dominant mechanisms for regulating symbiont biomass in the cnidarian-dinoflagellate symbiosis, with arrest of the cell cycle of the majority of symbionts in the G_1/S phase, compared with symbionts in culture (Smith and Muscatine 1999; Tivey *et al*., 2020). The mitotic cell cycle is a biological process that allows eukaryotic organisms to renew, repair and grow their tissues (Neufeld and Edgar 1998; Orford and Scadden 2008; Hustedt and Durocher 2017). It involves a first gap phase (G_1) where cells grow (Pardee 1989), a DNA synthesis phase (S) where DNA is replicated (Nishitani and

Lygerou 2002), a second gap phase (G_2) where DNA damage is repaired before mitosis (Stark and Taylor 2004), and finally a mitotic phase (M) where cells divide (Malumbres and Barbacid 2009). Checkpoints within the specific cell-cycle phases control cell proliferation during unfavourable environmental conditions and prevent damaged cells from propagating (Clercq and Inzé 2006).

Co-ordination of host and symbiont growth is vital for maintaining optimal functioning between the biological partners in a dynamic environment (both biotic and abiotic) which can shift the metabolic equilibrium and help to sustain the association. The symbiotic state elicits proliferation of host cells in both the epidermis and gastrodermis, with proliferation most pronounced in host cells closest to the symbionts (<13 μm) (Tivey *et al*., 2020). In contrast, reduced proliferation of symbiont cells *in hospite* during colonisation (compared with log phase growth in culture) appeared to be the result of altered progression of the symbiont cell-cycle through arrest of the symbionts in the S phase, which causes fewer cells to enter the G_2/M phase and thus to divide (Tivey *et al*., 2020). It is unclear whether the proportion of the symbiont population within the different phases of the cell cycle change after the symbiont reaches a steady-state population within the host. In the hydroid *Myrionema ambionense,* measurement of the mitotic index using a microscope indicated that symbiont biomass becomes synchronised with the biomass of the host once the symbiont population reaches a steady-state, with the host cells dividing after host feeding, and the symbiont cells dividing 10-12 hours following host cell division, but only if kept in ample light (Fitt 2000).

The molecular mechanisms that underlie host-symbiont co-ordination and synchrony are only now being described. Previous transcriptomic studies have shown that the symbiotic state changes the expression of 920 and 91 host genes in the sea anemones *Exaiptasia pallida* (commonly referred to as ‘Aiptasia’) (Lehnert *et al*., 2014) and *Anthopleura elegantissima* (Rodriguez-Lanetty *et al*., 2006a), respectively. Furthermore, the symbiotic state also caused a shift in the rhythms of host gene expressions in Aiptasia, with 10% changing their periodicity from 12 to 24 hour rhythms (Sorek *et al*., 2018). In this latter study, one of the top five canonical pathways that changed its periodicity was the mammalian target of rapamycin (mTOR) pathway. This pathway combines nutrient and mitogenic signals to integrate cell growth/size (Schmelzle and Hall 2000; Fingar *et al*., 2004), an important factor when determining

progression through cell-cycle checkpoints (Abraham 2001). In *A. elegantissima,* the presence of symbionts resulted in a decrease in the expression of four host genes involved in host cell apoptosis and an increase in the expression of one host gene involved in host cell proliferation, through an impact on the sphingosine-1-phosphate (S1P) and prohibitin pathways (Rodriguez-Lanetty *et al*., 2006a). In Aiptasia, S1P has been shown to promote host cell survival both during association with symbionts (Kitchen *et al*., 2017) and through periods of host stress (Kitchen and Weis 2017). We still have a long way to go to understand which host genes are altered in their expression in the presence of symbionts and how this induces downstream effects on host growth.

The development of the Aiptasia model system and the advancement in 'omic' technologies have played a significant role in describing the molecular differences in the cnidarian host elicited by the establishment of the symbiotic state (Ganot *et al*., 2011; Lehnert *et al*., 2014; Oakley *et al*., 2016; Matthews *et al*., 2017; Baumgarten *et al*., 2018; Sorek *et al*., 2018). I expanded on these pioneering studies to further our understanding of cell-cycle regulation in the cnidarian-dinoflagellate symbiosis, by analysing a cnidarian tissue-specific transcriptomic dataset that compared differences in expression of host cell-cycle genes between symbiotic states (aposymbiotic *versus* symbiotic) and host tissue types (epidermis *versus* gastrodermis). Following the findings of the gene-expression changes a microscope method was developed to quantify the number of proliferating host cells in the gastroderm and epiderm of *E. diaphana* in aposymbiotic, recently inoculated (two days post-inoculation), and stably symbiotic, hosts with heterologous *Breviolum minutum.*

3.3. Materials and Methods

3.3.1. Tissue-specific transcriptomics

3.3.1.1. Animal maintenance and laser microdissection

Symbiotic and aposymbiotic Aiptasia (strain CC7) were kept in replicate-specific tanks on a 12 h:12 h light: dark cycle with ~40 µmol photons $m^{-2}s^{-1}$ of photosynthetically active radiation and fed with freshly hatched brine shrimp, *Artemia* sp. nauplii, approximately three times *per* week. One anemone from each tank was collected after 6 hours in light period, snap-frozen in liquid nitrogen immediately, and embedded with Tissue Freezing Medium (Electron

Microscopy Science, USA). The embedded samples were stored in -80 °C before cryosection. The cryostat (Leica Biosystems, Germany) was pre-chilled to a chamber temperature of -23 °C. Samples were equilibrated to the chamber temperature for 20 mins, then for each replicate, a layer of tissue was cut from the top to the bottom of the animal and dissected at a thickness of 8 µm. Tissue sections were placed on microscope slides (1-3 *per* slide), and the gastrodermis and epidermis were identified using Leica LMD 6000 microscope (Leica Microsystems, Germany) and the Leica filter cube B/G/R and A (Leica Microsystems, Germany). Regions of interest were traced by LMD software and dissected using the ultraviolet laser beam. The dissected tissues were collected in caps containing 40 µl RNA extraction buffer from Arcturus PicoPure RNA isolation kit (Thermo Fisher Scientific, USA). The harvested cells were lysed at 42 °C for 30 mins, vortexed briefly, then kept at -80 °C until further processing.

3.3.1.2. Tissue-specific RNA-seq

Total RNA from the cell lysates was extracted using Arcturus PicoPure RNA Isolation Kit following the protocol for use with CapSure Macro LCM Caps. Quality of RNA samples were assessed using Agilent RNA 6000 Pico Kit on Agilent 2100 Bioanalyzer (Agilent Technologies, USA). cDNA was synthesized using Ovation RNA-seq System V2 kit (NuGen, USA) following manufacturer's instructions. The amplified cDNA was processed for library preparation using NEBNext Ultra II DNA Library Prep Kit (NEB, USA) for Illumina sequencing. The samples were pooled and sequenced on four lanes of the Illumina HiSeq 2000 platform (Illumina, USA) to generate paired-end reads. . Symbiont-originated reads were found in the symbiotic gastrodermal samples, however there were not enough reads to analyse the expression profile of the symbionts. The expression levels of revised Aiptasia gene models (Cziesielski *et al*., 2018; Cui *et al*., 2019) were quantified using kallisto (Bray *et al*., 2016). Differential expression analysis was performed using sleuth (Pimentel *et al*., 2017). GO enrichment analysis was conducted on the differentially expressed genes using topGO (Alexa *et al*., 2006). It should be noted that KEGG pathway analysis within this study was based on mammalian and yeast genes due to the lack of KEGG pathway data for Aiptasia.

3.3.1.3. Data accession

The tissue-specific transcriptome method described in this current study, and the cell-cycle transcript data collected, are part of a wider transcriptome dataset collected by Cui *et al*. (in

prep.). The full transcriptome dataset can be accessed at the NCBI database (accession number: PRJNA631577).

3.3.2. Microscopic analysis of host cell proliferation

3.3.2.1. Modification of Aiptasia symbiotic state

In this study, clonal Aiptasia were used in three different symbiotic states: fully symbiotic; symbiont-free (i.e. aposymbiotic); and, two days post-inoculation with cultured symbionts. In total 45 anemones were used in this study, placing 15 animals *per* symbiotic state, three biological replicates *per* well into three 6-well plates. All animals were then kept at 25 °C in autoclaved sea water from the Red Sea with salinity adjusted to ~37 ppt, and a 12-h light/12-h dark cycle and irradiance of ~40 µmol photons $m^{-2}s^{-1}$. All animals were fed with freshly hatched *Artemia* sp. nauplii approximately three times a week, with a water change on the day after feeding. The last feeding occurred two days before EdU imaging, so that feeding did not affect host cell proliferation rates (Smith and Muscatine 1999). Aposymbiotic anemones for this experiment were obtained *via* cold shock treatment in combination with the photosynthetic inhibitor diuron (Sigma-Aldrich) (Baumgarten *et al*., 2015; Cui *et al*., 2019). After removal of symbionts, aposymbiotic animals were kept under the same conditions as the symbiotic anemones for at least three months. To ensure the absence of symbionts, anemones were examined for the presence of chlorophyll autofluorescence once a week and on the day of the experimental setup using a fluorescent microscope (Leica DMI3000 B). Recently inoculated hosts were obtained by inoculating aposymbiotic anemones with laboratory cultured heterologous *Breviolum minutum* (previously known as *Symbiodinium* clade B strain SSB01) two days before the sample processing to represent an early symbiotic state.

3.3.2.2. Visualisation of cell proliferation

To observe cell proliferation in Aiptasia tissues, the incorporation of a thymidine nucleotide substitute 5-ethynyl-2'-deoxyuridine (EdU) into the DNA (Click-iT®EdU imaging kit, Invitrogen) was measured. Animals were exposed to 10 µM EdU concentration (solvent DMSO) for 48 h (Fransolet *et al*., 2013, 2014). After incubation, an equal volume of 3.7% $MgCl_2$ solution was added to seawater and this mixture was used to anesthetize anemones for 30 min. To initiate fixation of the specimens, they were held in 4% paraformaldehyde at 4 °C overnight. Fixation was followed by washing the specimens twice with phosphate buffer saline

(PBS) and dehydration with ethanol. Dehydration was performed by transferring animals into 50%, 60%, 70%, 80% and 95% EtOH for 10 minutes at each concentration. Following this incubation, animals were transferred into absolute EtOH twice for 15 minutes and then into m-Xylene twice for 15 minutes. Specimens were then embedded in paraffin, sectioned with a rotary microtome to a thickness of 7 µm, and the sections were gently positioned on glass slides. A minimum of three slides were analysed *per* individual. The paraffin was then carefully removed and the samples were re-hydrated by placing them in m-Xylene for 15 minutes. After the m-Xylene incubation, the slides were transferred to 100%, 80%, 60% and 50% EtOH and incubated for 7 minutes in each concentration. After rehydration slides were washed once with PBS, a blocking solution of 3% bovine serum albumin (BSA) in PBS was used before permeabilizing the samples with 0.5% Triton X-100 in PBS. Additional washes with the blocking solution (3% BSA in PBS) and then with PBS were performed. Samples were treated with Click-iT® EdU reaction cocktail, prepared according to the manufacturer's recommendations, and incubated at room temperature for 30 min in the dark. A negative control, without Click-iT® reaction, was also imaged (n = 3-4 *per* symbiotic state). After the 30 min incubation, the reaction mixture was washed with PBS, followed by Hoechst 33342 staining at a final concentration of 3 µg/mL for 10 min in the dark to visualize all nuclear DNA. Slides were thoroughly washed once more with PBS, and then mounted and imaged.

A Leica SP8 TCS STED 3X confocal microscope was used to observe the EdU and Hoechst 33342 fluorescent signals. Images were taken where gastrodermal and epidermal tissues could be identified in up to three random areas. Acquired pictures were analysed with Cell Profiler 3.1.9 (McQuin *et al*., 2018) using an adapted pipeline for particle counting from the manufacturer. Nuclei from both epidermal and gastrodermal tissue layers were counted together, as tissue differentiation was not possible *via* this method. Unfortunately, not every biological replicate produced good quality pictures, which led some of the individuals not to be used for further analysis. Altogether, 10 aposymbiotic individuals, 12 inoculated individuals and 14 hosts in a stable symbiosis were analysed for EdU. Proliferating cell counts obtained from Click-iT® EdU stained cells were normalized to Hoechst 33342-stained nuclei number, as a proxy for total cell number. Mean values of nuclei count *per* sample were calculated based on the counts from two to three images, depending on image quality. Statistical analysis was performed using R version 3.5.2 (Team 2020). The normality of the data distribution was determined with the Shapiro-Wilk test. Outlier values found in the datasets were removed from

further analysis. Evaluation of homogeneity of variances was conducted using Levene's test, followed by a Student t-test for independent samples to compare between different conditions. A p-value < 0.05 was classed as statistically significant.

3.4. Results and Discussion

Altogether, 24 genes differed in expression with symbiotic state and tissue type (Table 3.1).

Table 3.1. Differentially expressed host cell-cycle genes between symbiotic states and host tissues in Aiptasia. Red represents genes significantly up-regulated and blue represents genes significantly down-regulated. Numbers within boxes represent log-fold change in expression between samples.

Gene	Role	Symbiotic Gastrodermis vs Aposymbiotic Gastrodermis	Symbiotic Gastrodermis vs Epidermis of Symbiotic Hosts	Epidermis of Symbiotic vs Aposymbiotic Hosts	Gastrodermis vs Epidermis of Aposymbiotic Hosts
ATM, ATR	DNA damage response		-0.821		
Bubr1	SAC protein that inhibits APC/C(Cdc20) activity in interphase allowing accumulation of cyclin B in the G_2 phase	-0.833			
Cdc14 phosphatase	Essential for the exit from mitosis	1.492			-0.584
Cdc20	Destroys cyclin B; chromosome separation; exit from mitosis	-1.489			
Cdc25B,C	Mitosis G_2/M; activates cyclin B-CDK1 complexes	-1.022			

Table 3.1. continued.

Cyclin B	Forms complex with CDK1 in mitosis. Required for the progression through the M phase.	-1.255			
CDK1	G_2/M phase. Forms complex with cyclin A in G_2 phase to fortify cells for commitment to mitosis; forms complex with cyclin B in M phase for mitotic progression	-1.644			
CDK4,6	Regulator of restriction point in G_1	-0.782			
c-Myc	Cell cycle entry of G_0 cells; Cell-cycle progression; Apoptotic Sensitivity		-1.052 — 3.550		
Dp-1,2	Makes complex with E2F transcription factors that bind to different proteins and change their function for cell-cycle progression	1.439	1.881		
E2F1,2,3	G_0 to S phase progression; DNA stability; Transcriptional activators of essential cell-cycle genes		1.287		
GADD45	Inhibitor of cyclin B/CDK1; apoptosis; cell-cycle arrest	0.914			
HDAC	Deacetylates key cell-cycle proteins	0.713			
Mcm3	Forms MCM helicase complex that is required during DNA replication; unwinds DNA; elicits replication elongation.	-0.675	-0.799		
Mcm6		-0.859			
Mdm2	Controls p53; Delays cell-cycle progression in G_2/M phase	1.111	0.889		
Mob1	Cell polarity marker that plays role in mitotic exit pathway			0.979	
Mps1	Phosphorylates components of the SAC that recruits other proteins to inhibit the APC/C(Cdc20) complex	-0.920			

Table 3.1. continued.

ORC3	Forms the ORC (origin of replication complex). Marks the replication point on DNA and allows the attachment of other replication proteins e.g. MCM-helicase				**-0.675**
PIK1	Promotes mitotic entry by inducing the phosphorylation of Cdc25B/C	**-0.583**	**-2.327**		
p27 kip1	CDK inhibitor that binds to CDK 2-cyclin E complexes at the G_1/S phase to inhibit cell-cycle progression				**-0.770**
SCF (Skp1/cullin/F-box protein)	Degrades cell-cycle blockers allowing progression of the cell cycle	**0.504**			
Smad4	Cell-cycle arrest in G_1; Main regulator of TGF-β		**0.840**		**0.809**
14-3-3 protein associated with Cdc25B/C	Regulates Cdc25B/C	**-0.479**			

3.4.1. Symbiotic gastrodermis versus *aposymbiotic gastrodermis differentially expressed genes (DEGs)*

The levels of seventeen transcripts differed between the gastrodermis with and without symbionts. Six transcripts showed elevated expression - Dp-1, 2, SCF, HDAC, GADD45, Mdm2 and Cdc14 (Table 3.1; Fig. 3.1) and the remaining 11 showed a decrease in expression in the symbiotic gastrodermis when compared with the aposymbiotic gastrodermis. The up-regulated genes of the gastrodermis included some genes involved in G_0 to G_1 phase transitions, whereas most of the down-regulated genes are involved in DNA synthesis and mitosis. These results suggest that the presence of symbionts in the gastrodermis may arrest host cells at the G_1/S phase checkpoint and may inhibit their mitotic progression and completion (Fig. 3.2).

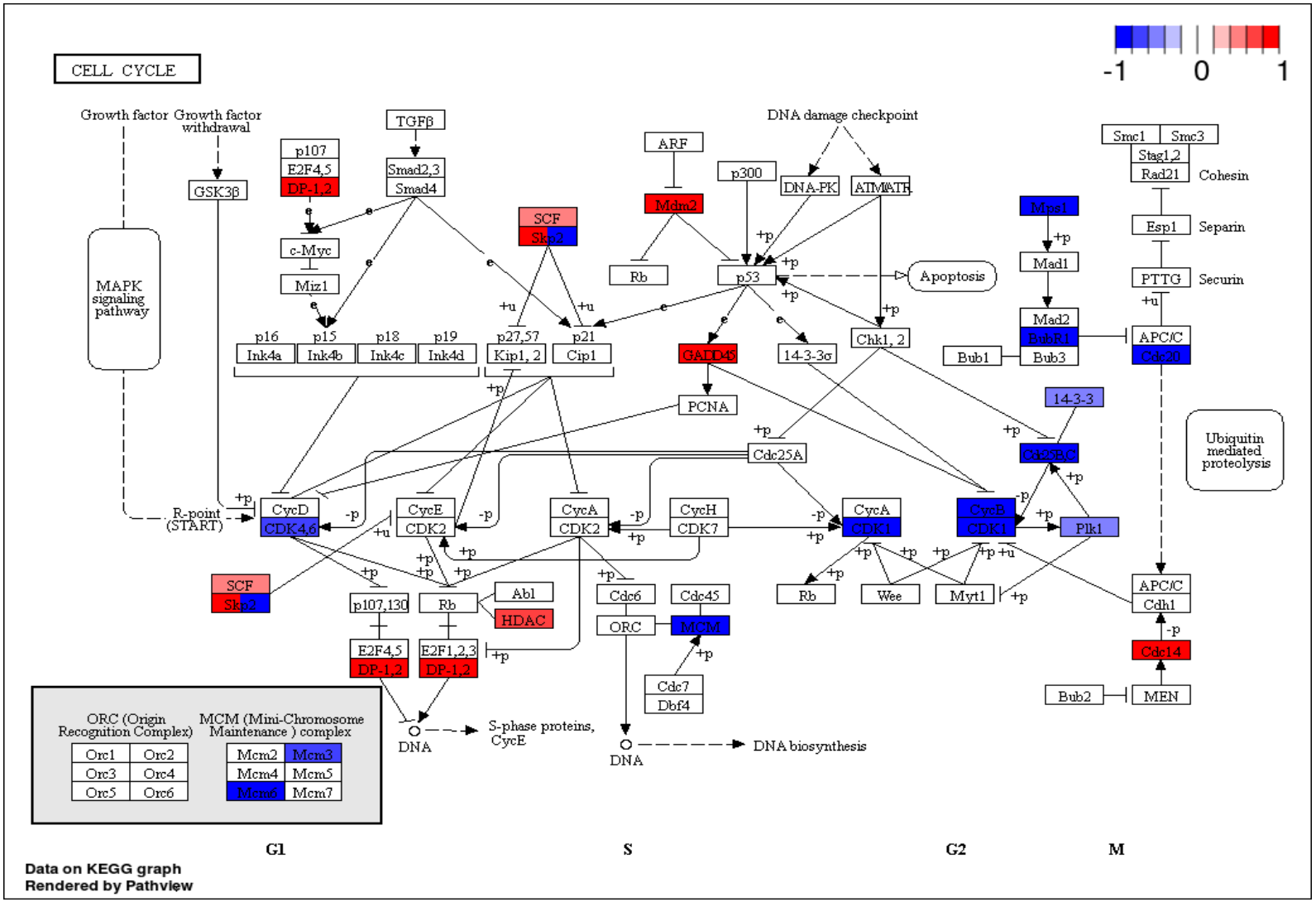

Figure 3.1. Differentially expressed host cell-cycle genes between the symbiotic gastrodermis when compared with the aposymbiotic gastrodermis Scale represents the fold-change in expression. Blue signifies down-regulation and red signifies up-regulation.

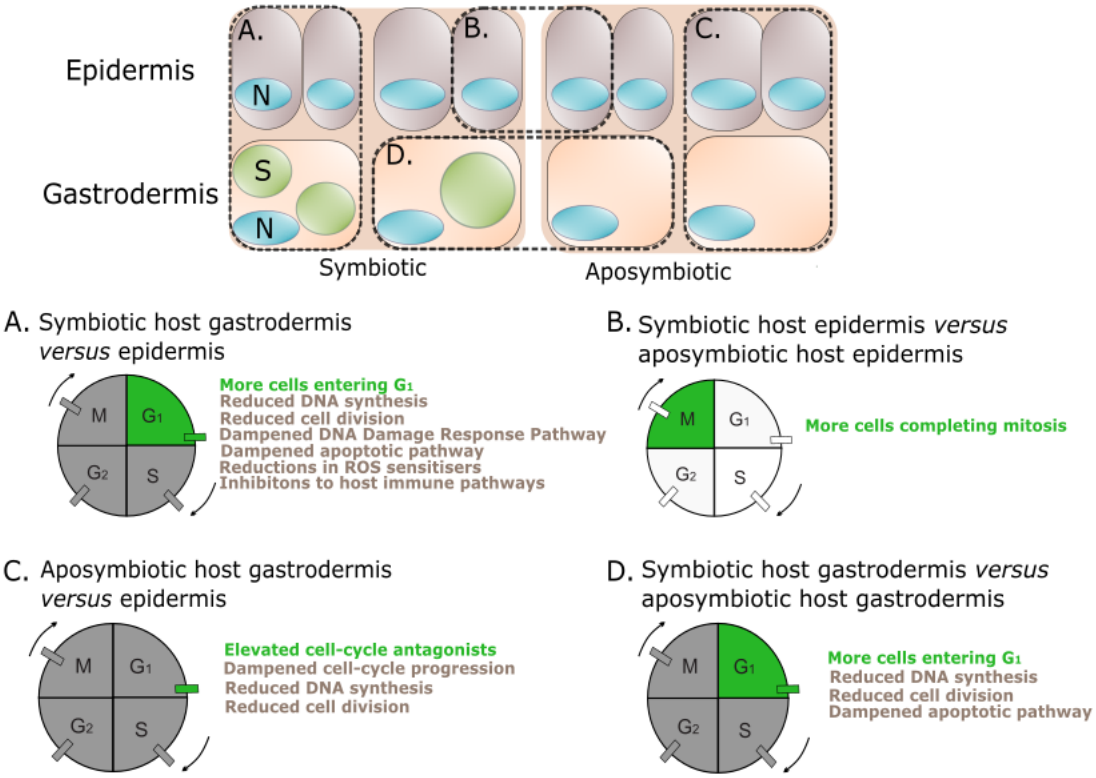

Figure 3.2. Differences in host cell-cycle gene expression and progression between symbiotic states and tissue types in Aiptasia. Green symbolises up-regulated and grey represents down-regulated cell-cycle phases, whilst white represents no recorded changes to cell-cycle phase in the respective comparisons. 's' refers to symbiont; 'n' refers to host nuclei and 'm' refers to mesoglea.

3.4.1.1 G_1 phase genes

The SCF (Skp1-Cul1-F-box protein) was up-regulated in the symbiotic gastrodermis. SCF and APC/C (anaphase-promoting complex or cyclosome) are the two major E3 ubiquitin ligases involved in controlling the cell cycle (Nakayama and Nakayama 2005). E3 ubiquitin ligases transfer a ubiquitin molecule onto a lysine residue on the target substrate which promotes the unfolding of a protein and its subsequent degradation by a proteasome (Ang and Harper 2005). SCF acts throughout the cell cycle and its substrates mostly include cell-cycle antagonists that inhibit cell-cycle progression (p57, p27, p21, Wee1 and Emi1) (Vodermaier 2004; Ang and Harper 2005). Thus, its elevation favours the degradation of cell-cycle antagonists and promotes cell-cycle progression. Skps2 and Cks1 are the substrate targeting subunits of the SCF (Bashir *et al*., 2004). SCF regulates entry into the S phase, with increasing levels of Skps2 and Cks1 destroying S phase antagonists p21 and p27, allowing the cells to enter the S phase (Bashir *et al*., 2004).

CDK4/6 was down-regulated in the symbiotic gastrodermis. Cyclin-dependent kinases (CDKs) are the main regulators of the cell-cycle through checkpoints (Malumbres *et al*., 2009). CDK4/6 is active in the G_1 phase and their function is to phosphorylate the Rb-E2F complex at the restriction checkpoint (Giacinti and Giordano 2006). Until phosphorylation by CDK4/6, the Rb-E2F complex represses the transcription factor complex, E2F-Dp, by histone deacetylase (HDAC) activity (Rogers *et al*., 1996; Luo *et al*., 1998; Zhang *et al*., 1999; Siddiqui *et al*., 2003). HDACs repress transcription through the deacetylation of lysine residues on histones, changing chromatin conformation and actively stopping protein function (Telles and Seto 2012). This gene suppression negatively regulates the G_1/S transition (Rubin *et al*., 2005). As HDACs were up-regulated in the symbiotic gastrodermis and CDK4/6 was down-regulated, it suggests that HDACs were inducing the arrest of the gastrodermal cells at the restriction point in the G_1 phase.

Dp1 and Dp2 levels increased in the symbiotic gastrodermis. Dp proteins form complexes with transcription factor E2F (Dimova *et al*., 2003). There are several types of E2F that have different functions: E2F1-3 are transcriptional activators whereas E2F4-5 are transcriptional suppressors (Dimova *et al*., 2003). As it is unknown whether the Dp proteins associated with the transcriptional suppressors (E2F4-5) or activators (E2F1-3), it is hard to draw conclusions on what this finding may mean. However, as genes involved in transcriptional suppression were up-regulated (HDAC) and genes involved in G_1 progression were down-regulated (CDK4/6), it is fair to assume that the up-regulated Dp genes do not lead to cell-cycle progression.

3.4.1.2. S phase genes

Two important genes involved in DNA synthesis were down-regulated in the symbiotic gastrodermis: Mcm3 and Mcm6. The mini-chromosome maintenance proteins (Mcm2-7) are essential for the initiation of DNA replication during the S phase, as their function is to identify chromatins that can duplicate in the G_2/M phase (Labib and Diffley 2001). Mcm3 and Mcm6 are loaded onto chromatin by the origin of replication complex (ORC) at the sites of replication during the G_1 phase and, together with the proteins Cdc6 and Cdt1, form the pre-replication complex (PRC) (Liang and Stillman 1997; Kelly and Brown 2000; Labib and Diffley 2001; Duncker *et al*., 2009). Mcm3 enters the nucleus towards the end of mitosis and persists through the G_1 phase, disappearing from the nucleus after the start of the S phase (Yan *et al*., 1993).

This strict localisation has been hypothesised to ensure that DNA replication only occurs once *per* cell cycle (Yan *et al*., 1993). Mcm3 inhibition leads to the arrest of cells in G_1 with un-duplicated DNA (Dalton and Whitbread 1995). The down-regulation of Mcm3 and Mcm6 suggests that, in the presence of symbionts, fewer gastrodermal host cells synthesise DNA. This may be a regulatory path elicited by the presence of the symbiont to allow algal proliferation while slowing the proliferation of host cells, as it has been shown that in certain viral infections, the down-regulation of the host's PRC facilitates proliferation of the viral infection (Braun *et al*., 2012).

3.4.1.3. G_2/M phase genes

Multiple kinases (BubR1, Plk1, Mps1, Cdc20 and CDK1) and proteins (cyclin B) involved in mitotic progression were down-regulated in the symbiotic gastrodermis. Cyclin A-CDK1 prepares cells for commitment to mitosis, as it is an upstream regulator of Plk1 (polo-like kinase 1) (Gheghiani *et al*., 2017). Plk1 is activated in G_2 and promotes mitotic entry by inducing the phosphorylation of Cdc25B/C (Gheghiani *et al*., 2017). The phosphorylation of Cdc25B then activates the cyclin B-CDK1 complexes whose activity remains high until anaphase (Peng *et al*., 1997; Timofeev *et al*., 2010). During anaphase the APC/C complex destroys cyclin B and inactivates CDK1, allowing the exit from mitosis and the completion of the cell cycle (Wong and Fang 2007; Maciejowski *et al*., 2010).

The APC/C is inhibited from destroying cyclin B until anaphase by the mitotic checkpoint complex (MCC), which inhibits the activator of APC/C, Cdc20 (Kramer *et al*., 2000; Malureanu *et al*., 2009; Maciejowski *et al*., 2010; Bolanos-Garcia and Blundell 2011; Lee *et al*., 2012). The MCC is initiated by CDK1/cyclin B phosphorylating the BubR1 kinase (Wong and Fang 2007) and this promotes Plk1 recruitment which further phosphorylates BubR1, leading to a BubR1 upshift (Elowe *et al*., 2007; Maciejowski *et al*., 2010). Along with BubR1, cells recruit a series of proteins including BubR3, Mad2 and Cdc20 to form the MCC (Bolanos-Garcia and Blundell 2011). The MCC produces the "wait anaphase" signal and inhibits APC/C activity until the final chromatids have joined in metaphase (Malureanu *et al*., 2009). The MCC achieves this by the Mps1 kinase recruiting Cdc20 inhibitors (BUBR1, BUBR3 and MAD2), which inhibit Cdc20 from forming a complex with APC/C (Kramer *et al*., 2000; Malureanu *et al*., 2009; Maciejowski *et al*., 2010; Bolanos-Garcia and Blundell 2011; Lee *et al*., 2012). This stops the APC/C degrading mitotic cyclins (mainly cyclin B) at the end of mitosis (Golan *et*

al., 2002), and therefore inhibits the mitotic exit. As the CDK1 was down-regulated in the symbiotic gastrodermis and is the upstream regulator of the mitotic cascade (through regulating Plk1), it is not surprising that genes involved in mitosis were also all down-regulated.

Two antagonists of the cyclin B-CDK1 complex were simultaneously up-regulated in the symbiotic gastrodermis: GADD45 and Cdc14. GADD45 is a protein often induced by cellular stress, such as DNA damage, cell injury, apoptosis and cell-cycle checkpoint maintenance in growth arrest (Salvador *et al*., 2013) (Fig. 3A). GADD45 is an extremely strong inhibitor of the mitotic CDK1/ cyclin B complex (Zhan *et al*., 1999; Salvador *et al*., 2013) and can block Cdc25B/C (Reinhardt *et al*., 2010). The up-regulation of GADD45 may therefore explain the down-regulation of CDK1, cyclin B (and presumably the CDK1/cyclin B complex) and Cdc25B/C in the symbiotic gastrodermis. Furthermore, the 14-3-3 protein which binds to Cdc25B/C was also down-regulated.

GADD45 can also induce an apoptotic cascade by p38 activation, which in turn activates the tumour suppressor gene p53 and creates a positive feedback loop (Salvador *et al*., 2013) (Fig. 3.3A). However, p53 expression remained unchanged, and instead we saw its antagonistic controller Mdm2 being up-regulated (Haupt *et al*., 1997; Wasylyk and Wasylyk 2000; Clair *et al*., 2004). Once activated, p53 can cause apoptosis, cell cycle arrest and DNA damage repair (Shi and Gu 2012). Mdm2 monoubiquitinates p53 and inhibits its role in apoptotic initiation and G_1 arrest (Chen *et al*., 1996). This suggests that the end point of the GADD45 up-regulation was likely to be due to the down-regulation of the cyclin B-CDK1 complex rather than p53 activation (Figure. 3.3A). This finding agrees with a past study investigating gene expression changes in the symbiotic state (Lehnert *et al*., 2014), that found symbiosis in Aiptasia elicited the up-regulation of GADD45 by 5.1-fold. Furthermore, the same study identified the apoptotic pathway as one of the main cellular functions that differed between symbiotic states, with 13 genes significantly changing their expression (Lehnert *et al*., 2014). The up-regulation of Mdm2 suggests that the presence of compatible symbionts reduces apoptotic rates in host cells, agreeing with a past study (Rodriguez-Lanetty *et al*., 2006a), which found decreases in host apoptosis in the presence of homologous symbionts compared with aposymbiotic hosts under stable conditions.

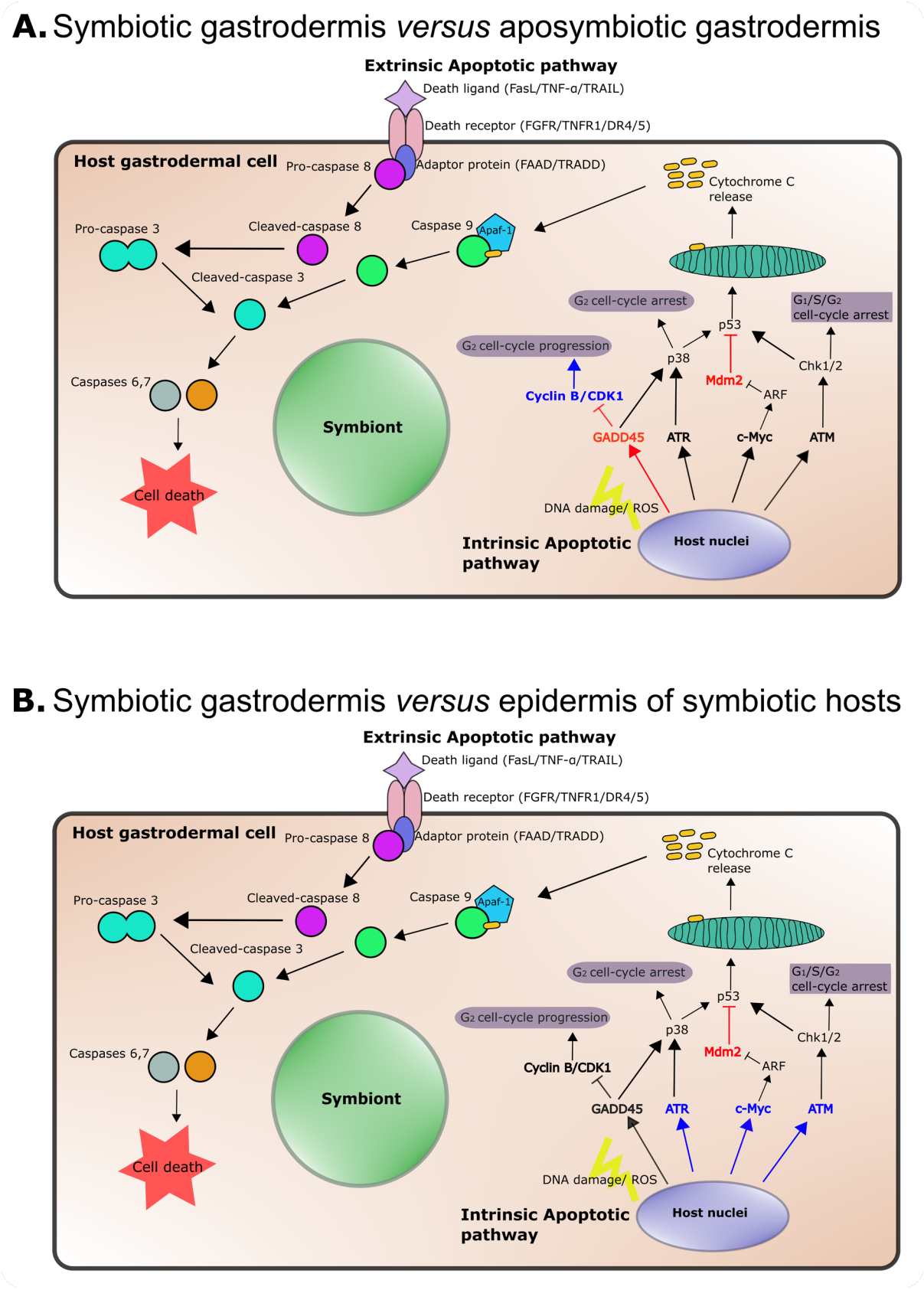

Figure 3.3. Apoptosis pathway changes in the host elicited by the presence of the symbiont in the gastrodermal tissue. Red text and arrows refer to up-regulated genes and blue text and arrows refer to down-regulated genes.

A triggering of an apoptotic cascade by the host in the presence of symbionts is consistent with this post-phagocytotic mechanism controlling the symbiont population, as had been suggested previously during symbiosis onset, and homeostatic and stress-induced regulation of symbiont population in the full symbiotic state (Dunn and Weis 2009; Davy *et al*., 2012; Paxton *et al*., 2013). Therefore, it favours the symbiont to block host apoptotic mechanisms to allow persistence within the host. Along with apoptosis regulation, Mdm2 also delays cell-cycle progression through the G_2/M phase by degrading Cdc25C (Giono *et al*., 2017). This agrees with the rest of the G_2/M phase genes that allow M phase progression to be down-regulated.

Along with GADD45, Cdc14 is another antagonist of the CDK1-cyclin B complex. Cdc14 is a phosphatase that participates in the regulation of the G_2/damage checkpoint, and its release from the nucleolus promotes mitotic exit *via* the dephosphorylation of CDK1 substrates - mitotic cyclins (Morgan 1999; Bassermann *et al*., 2008; Bremmer *et al*., 2012). The degradation of mitotic cyclins resets the cell cycle to the G_1 phase (Manzoni *et al*., 2010). Thus, the up-regulation of both Cdc14 and GADD45 makes the subsequent down-regulation of the cyclin B-CDK1 complex unsurprising.

3.4.2. Symbiotic gastrodermis versus *epidermis of symbiotic hosts differentially expressed genes (DEGs)*

In the current study, four genes were differentially up-regulated, Dp1, 2, Mdm2, Smad4, and E2F1, 2, 3, while four were down-regulated, ATM/ATR, PIK1, Mcm3, and c-Myc in the symbiotic gastrodermis when compared with the symbiotic epidermis (Fig. 3.4; Table 3.1).

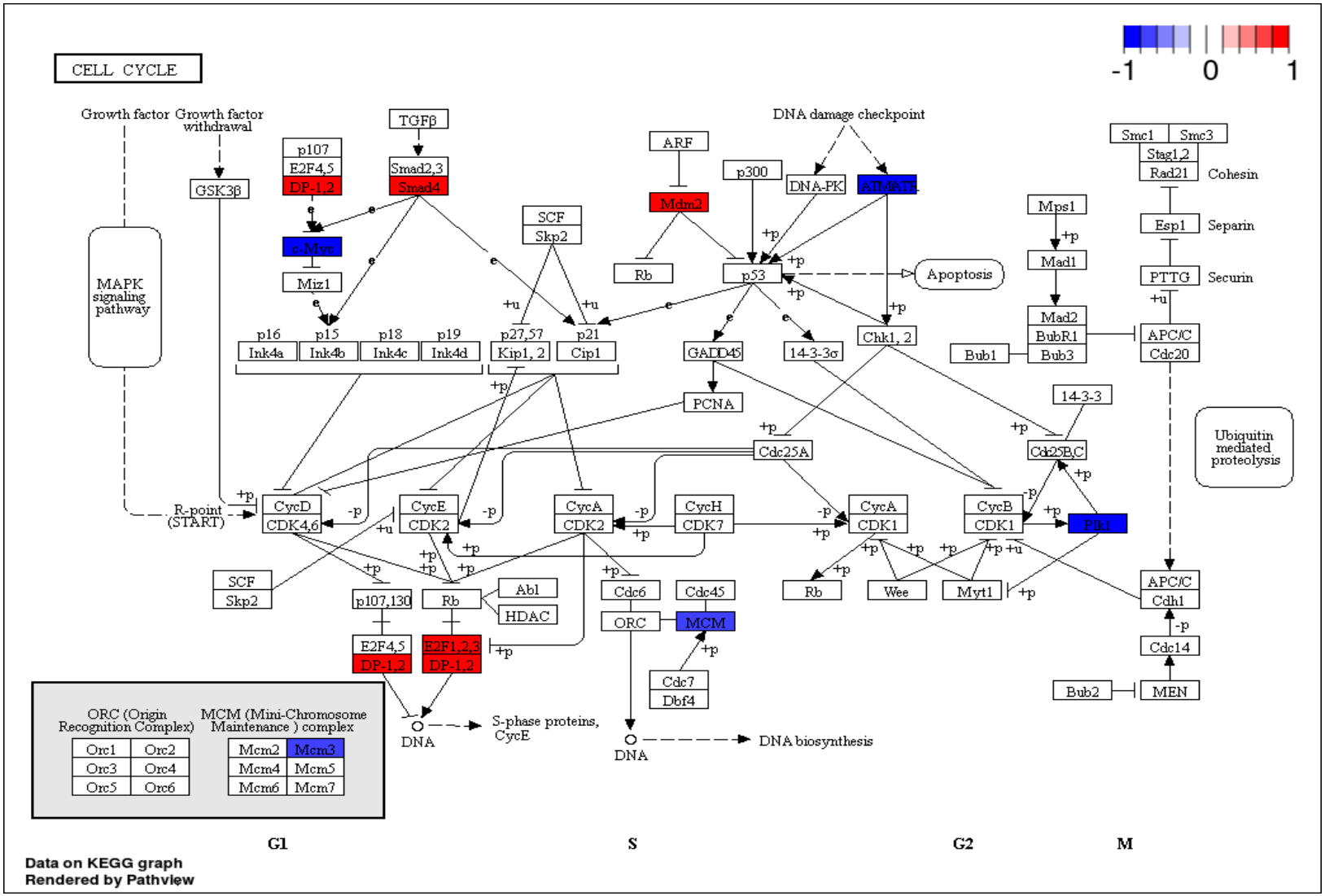

Figure 3.4. Differences in host cell cycle gene expression in the symbiotic gastrodermis when compared with the epidermis of symbiotic hosts. Scale represents the fold-change in expression. Blue signifies down-regulation and red signifies up-regulation.

3.4.2.1. G_1 phase genes

Dp1, 2 levels were up-regulated in the symbiotic gastrodermis *versus* the symbiotic epidermis as with the symbiotic gastrodermis *versus* aposymbiotic gastrodermis. The partners of Dp1, E2F1-3, were also up-regulated. E2F1-3 are transcriptional activator genes that form a complex with Dp1, 2 (Ren *et al*., 2002). This complex has cyclical interactions with important regulators of the cell cycle, e.g. cyclin A (Ren *et al*., 2002; Stevaux and Dyson 2002). The up-regulation of the E2F-Dp complex points to increased numbers of cells transcribing genes for cell-cycle progression in the G_1/ S phase transition (Bertoli *et al*., 2013), compared with epidermal cells (Fig. 3.2).

Proteins involved in the DNA damage response pathway, including ATM and ATR were down-regulated in the symbiotic gastrodermis relative to the epidermis of symbiotic anemones. Activation of the ATM (Chk2) kinase leads to apoptosis, cell-cycle arrest at the G_1/S checkpoint and DNA repair (Abraham 2001; Blackford and Jackson 2017). ATM is the kinase responsible for a variety of events that follow double-stranded DNA breaks initiating down-stream pathways e.g. DNA repair and checkpoint activation (Blackford and Jackson 2017) (Fig. 3.3B).

Another gene functioning in apoptosis, c-Myc, was also down-regulated in the symbiotic gastrodermis relative to the symbiotic epidermis. c-Myc functions in a variety of processes including the cell-cycle entry of quiescent (G_0) cells and increasing apoptotic sensitivity (Dang 1999; van der Sman *et al*., 1999; Tanaka *et al*., 2002; Hoffman and Liebermann 2008; Bretones *et al*., 2015). c-Myc expression amplifies death receptor pathways, increasing the apoptotic sensitivity of an organism (Hoffman and Liebermann 2008) (Fig. 3.3B). In cnidarians, apoptosis has been shown to influence the colonisation success of symbionts within a host, with high levels of apoptosis reducing the colonisation success (Dunn and Weis 2009). Likewise, host apoptosis has been shown to increase and to contribute to the bleaching of the resident symbiont population during host stress (Dunn *et al*., 2007; Kvitt *et al*., 2016). Furthermore, previous studies have shown that host apoptotic gene expression decreases in the presence of symbionts (Rodriguez-Lanetty *et al*., 2006a) and that the inhibition of host apoptosis allows the recolonisation of hosts by symbionts during thermal stress (Kvitt *et al*., 2016). Altogether these findings, along with the findings in this current study, suggest that host apoptosis is a major regulatory mechanism of the symbiont population that is influenced by both the host's symbiotic state and stress, with decreases in apoptosis allowing colonisation,

persistence, and proliferation of a symbiont population within the host, whilst increases in apoptosis contribute to the bleaching of a symbiont population and unsuccessful host colonisation.

c-Myc transcription is inhibited by the TGF-β-Smad4-Dp1-E2F4/5 -p107 complex which inhibits cell proliferation (Yagi *et al*., 2002; Massagué *et al*., 2005; Lim and Hoffmann 2006). One of the components of this complex, SMAD4, a transcriptional activator that is the main mediator of TGF-β (Zawel *et al*., 1998; Le Dai *et al*., 1999; Zhao *et al*., 2018), was up-regulated in the gastrodermis *versus* in the epidermis of symbiotic anemones. This may explain the mechanism of c-Myc down-regulation. TGF-β functions in inhibiting cell-cycle progression at the G_1/S checkpoint and in cellular immunity to maintain tolerance *via* the regulation of lymphocytes (Le Dai *et al*., 1999; Li *et al*., 2006). TGF-β allows the host to develop immuno-pathology to its own or non-pathogenic cells, without removing the immune response to pathogens (Li *et al*., 2006). In cnidarian hosts, TGF-β has been shown to help hosts to withstand invading microbes, and studies have shown TGF-β is influenced by the symbiotic state, becoming up-regulated in the host during symbiont colonisation (Berthelier *et al*., 2017; Baumgarten *et al*., 2018). The inhibition of TGF-β resulted in unsuccessful colonisation by symbionts (Detournay *et al*., 2012). Therefore, SMAD4's up-regulation may be another mechanism altered by symbionts to allow for persistence in host tissues.

3.4.2.2. S phase genes

Mcm3 (required for distinguishing chromatins that can duplicate in the G_2/M phase (Labib and Diffley 2001)), was down-regulated in the gastrodermis *versus* the symbiotic epidermis of symbiotic anemones, as with the symbiotic *versus* aposymbiotic gastrodermis, suggesting larger reductions in DNA synthesis in the symbiotic gastrodermis. The reduction in DNA synthesis also correlates with the down-regulation of c-Myc expression and up-regulation of SMAD4 expression, suggesting a reduction in cellular proliferation in the symbiotic gastrodermis (Fig. 3.2).

3.4.2.3. G_2/M phase genes

Mdm2, the antagonistic controller of p53 and G_2/M phase inhibitor, was up-regulated in the symbiotic gastrodermis when compared with the epidermis in the symbiotic state, as well as in the aposymbiotic gastrodermis (Fig. 3.3B). Furthermore Plk1, which promotes mitotic entry (Gheghiani *et al*., 2017) and is the kinase required for mitotic spindle function in chromosome

separation (Golsteyn *et al*., 1995), was also down-regulated. This suggests that there is a down-regulation in the host apoptotic pathway and fewer cells progressing through mitosis in the symbiotic gastrodermis.

ATR is one of the three kinases (the others being ATM and DNA-PK) that control the DNA damage response (DDR) pathway in cells (Blackford and Jackson 2017). ATR controls the intra-S and G_2/M checkpoints, and responds to a larger array of genotoxic agents than ATM (Blackford and Jackson 2017). The down-regulation of ATM and ATR may be another method employed by the symbiont to allow its persistence and proliferation. Viruses have been shown to inhibit ATM/ATR, as viral proliferation induces the DDR pathway which would limit the proliferation of the infection through up-regulating cell checkpoint pathways (Awasthi *et al*., 2015; Blackford and Jackson 2017). Interestingly, ROS have also been shown to induce ATM activation (Alexander *et al*., 2010). Thus, by down-regulating ATM/ATR, the symbiont may reduce the host's sensitivity to ROS, with ROS being a known driver for coral bleaching and the subsequent expulsion of symbionts (Downs *et al*., 2002). This agrees a past study (Rodriguez-Lanetty *et al*., 2006a) that found that, in the symbiotic state, host ROS scavengers are reduced in their expression. This suggests that the symbiont may down-regulate both host ROS scavenging and sensitising mechanisms.

3.4.3. Epidermis of symbiotic hosts versus *the epidermis of aposymbiotic hosts differentially expressed genes (DEGs)*

Only one gene was differentially expressed in the epidermis of symbiotic *versus* aposymbiotic anemones: Mob1 (Table 3.1; Fig. 3.5).

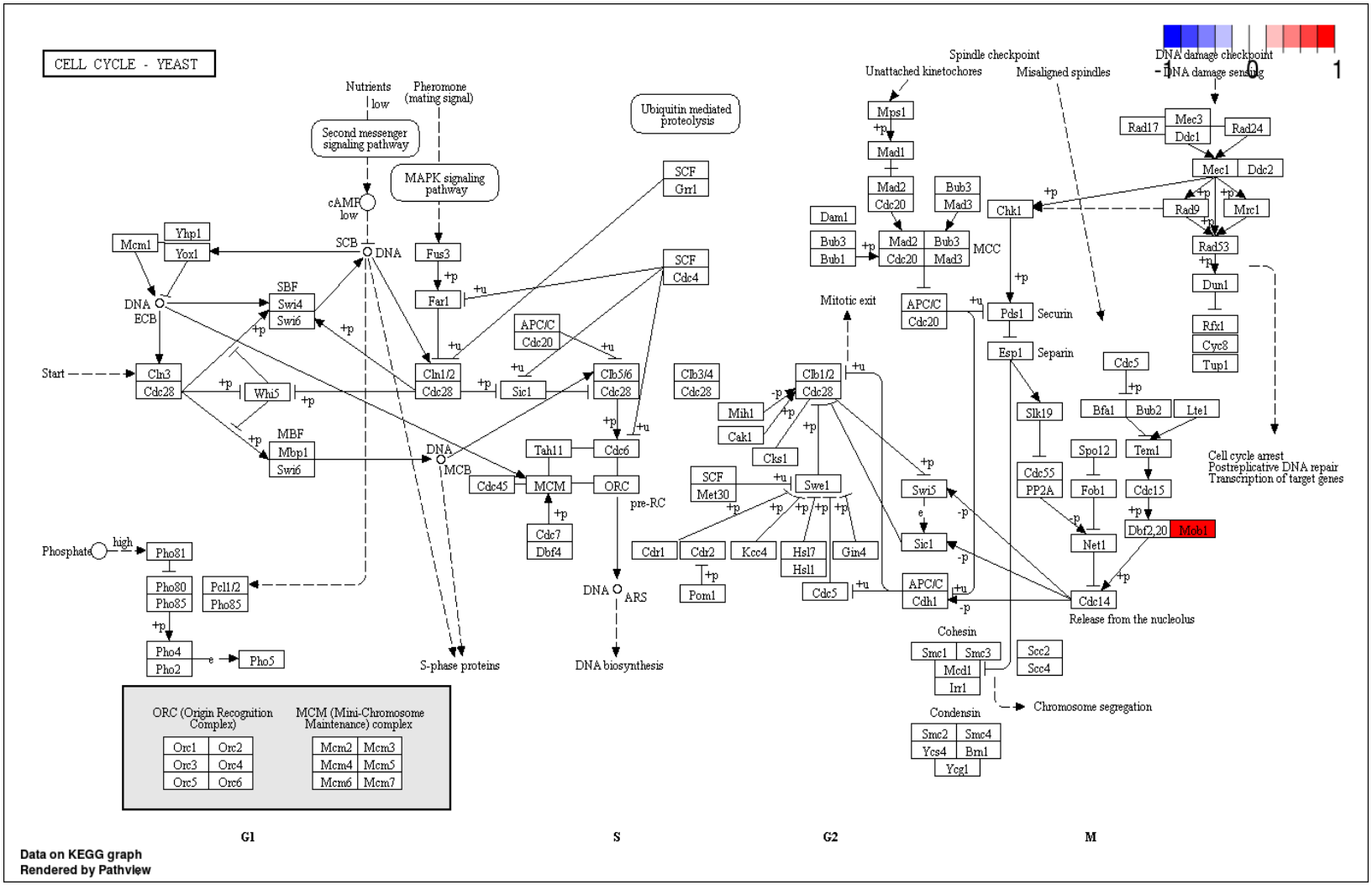

Figure 3.5. Differences in host cell cycle gene expression in the epidermis of symbiotic compared with aposymbiotic anemones. Scale represents the fold-change in expression. Blue signifies down-regulation and red signifies up-regulation.

Mob1 is involved in the mitotic exit network (MEN) signalling cascade and associates with spindle pole bodies throughout the cell cycle (Bardin and Amon 2001). The up-regulation of Mob1 may highlight that more host cells are exiting mitosis in the epidermis during the symbiotic state (Fig. 3.2). This finding agrees with both the cell proliferation rates found in the current study (Fig. 3.8), which revealed that host cell proliferation was the lowest in aposymbiotic hosts, and findings from a previous study which showed that host cell division was up-regulated in the presence of symbionts (Tivey *et al*., 2020).

It is well known that symbiotic algae translocate photosynthetic products to their cnidarian hosts, supporting the host's metabolism, growth and reproduction (Yellowlees *et al*., 2008; Bingham *et al*., 2014). Consequently, growth rates in symbiotic hosts are higher than those in aposymbiotic hosts, even with host feeding (Habetha *et al*., 2003; Gabay *et al*., 2018), with enhanced growth presumably occurring in all tissues irrespective of whether symbionts are present or not (Tivey *et al*., 2020).

3.4.4. Aposymbiotic gastrodermis versus *epidermis of aposymbiotic hosts differentially expressed genes (DEGs)*

In the aposymbiotic state only four genes were differentially expressed in the gastrodermis compared with the epidermis: SMAD4, $p27^{kip1}$, ORC3 and Cdc14 (Table 3.1; Fig. 3.6).

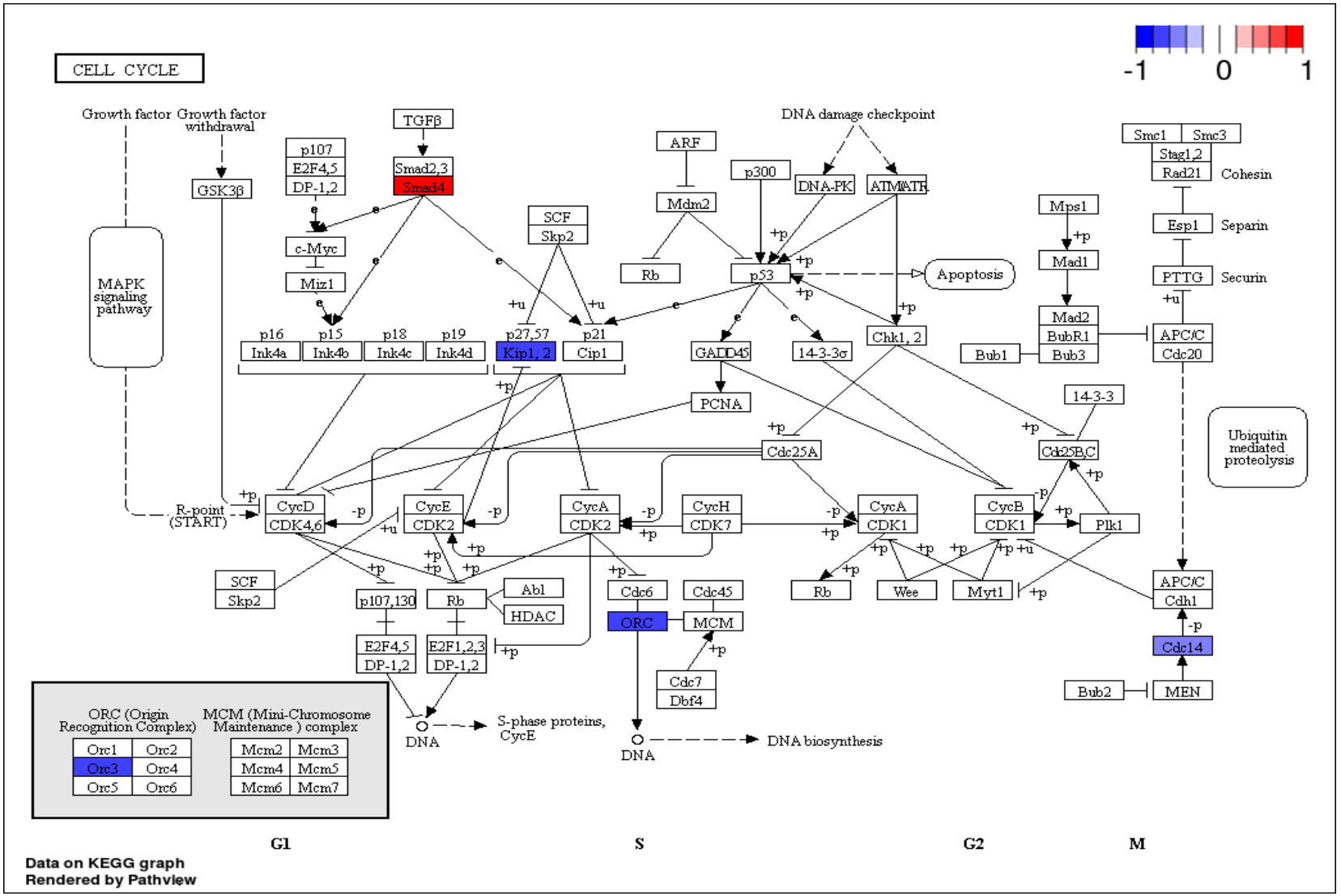

Figure 3.6. Differences in host cell cycle gene expression in the gastrodermis when compared with the epidermis of aposymbiotic anemones. Scale represents the fold-change in expression. Blue signifies down-regulation and red signifies up-regulation.

Similarly to the gene expression differences recorded in the symbiotic gastrodermis *versus* the epidermis of hosts harbouring symbionts (see section 3.4.2), the aposymbiotic gastrodermis also has an up-regulation of SMAD4 compared with the epidermis of symbiont-free hosts. As SMAD4 is known to elicit cell-cycle arrest in the G_1 phase by transcribing genes primarily involved in growth arrest and apoptosis (Zhao *et al*., 2018), this suggests that as with the symbiotic state, fewer gastrodermal cells were progressing through the cell cycle compared with epidermal cells in the aposymbiotic state also (Fig. 3.2). This highlights that the epidermis, regardless of symbiotic state, has an elevated host cell turnover compared with the gastrodermis, agreeing with past studies that have recorded higher baseline rates of proliferation in the epidermis compared with the gastrodermis in cnidarians (Passamaneck and Martindale 2012; Fransolet *et al*., 2013; Lecointe *et al*., 2016; Tivey *et al*., 2020).

As SMAD4 primarily arrests cells at the G_1/S checkpoint (Massagué and Blain 2000), this probably explains the down-regulation of both antagonistic ($p27^{kip1}$) and synergistic (ORC3 and Cdc14 phosphatase) downstream cell-cycle genes. $p27^{kip1}$ is a cyclin-dependent kinase inhibitor that binds to CDK 2-cyclin E complexes at the G_1/S phase of the cell-cycle to inhibit cell-cycle progression (Sherr and Roberts 1995; Warner *et al*., 1999). Its down-regulation is probably attributed to the reduction in proliferation of gastrodermal cells due to the up-regulation of SMAD4. Likewise, the phosphatase required for mitotic exit, Cdc14 (Visintin *et al*., 1998), and a protein essential for DNA replication (ORC3) (Liang *et al*., 1995; Lipford and Bell 2001), were both also down-regulated in the aposymbiotic gastrodermis. The ORC is a sequence specific DNA binding protein that contains six subunits (ORC1-6) that bind to replicating sequences in the chromatin and determine the origins of DNA replication during the S phase of the cell cycle (Liang and Stillman 1997). Furthermore, the ORC is essential in recruiting the other proteins that make up the pre-RC to the origin (Kelly and Brown 2000). Along with mitotic exit, Cdc14 has also been suggested to have an indirect role during DNA replication by supressing CDKs upon mitotic exit, with this CDK suppression allowing the effective formation of pre-RC complexes during the S phase (Stark *et al*., 2016). Thus, the down-regulation of Cdc14 and the concurrent depression of a gene also involved in recruiting proteins to the pre-RC (ORC3), is unsurprising and indicates reduced DNA replication in the gastrodermal cells (Fig. 3.2).

3.4.5. Cell proliferation in different symbiotic states

Following the findings from the transcriptomic analysis, the host cell proliferation of Aiptasia in different symbiotic states was assessed to measure whether the presence of symbionts did cause an increase in cell-turnover in cnidarian hosts. Microscopic analysis revealed that the EdU nucleotide was successfully incorporated into both gastrodermal and epidermal cells of all animals, irrespective of symbiotic state (Fig. 3.7). Samples that were not treated with the Click-iT® EdU reaction mix showed no EdU signal (data not shown), confirming EdU incorporation specificity and absence of significant autofluorescence from tissues.

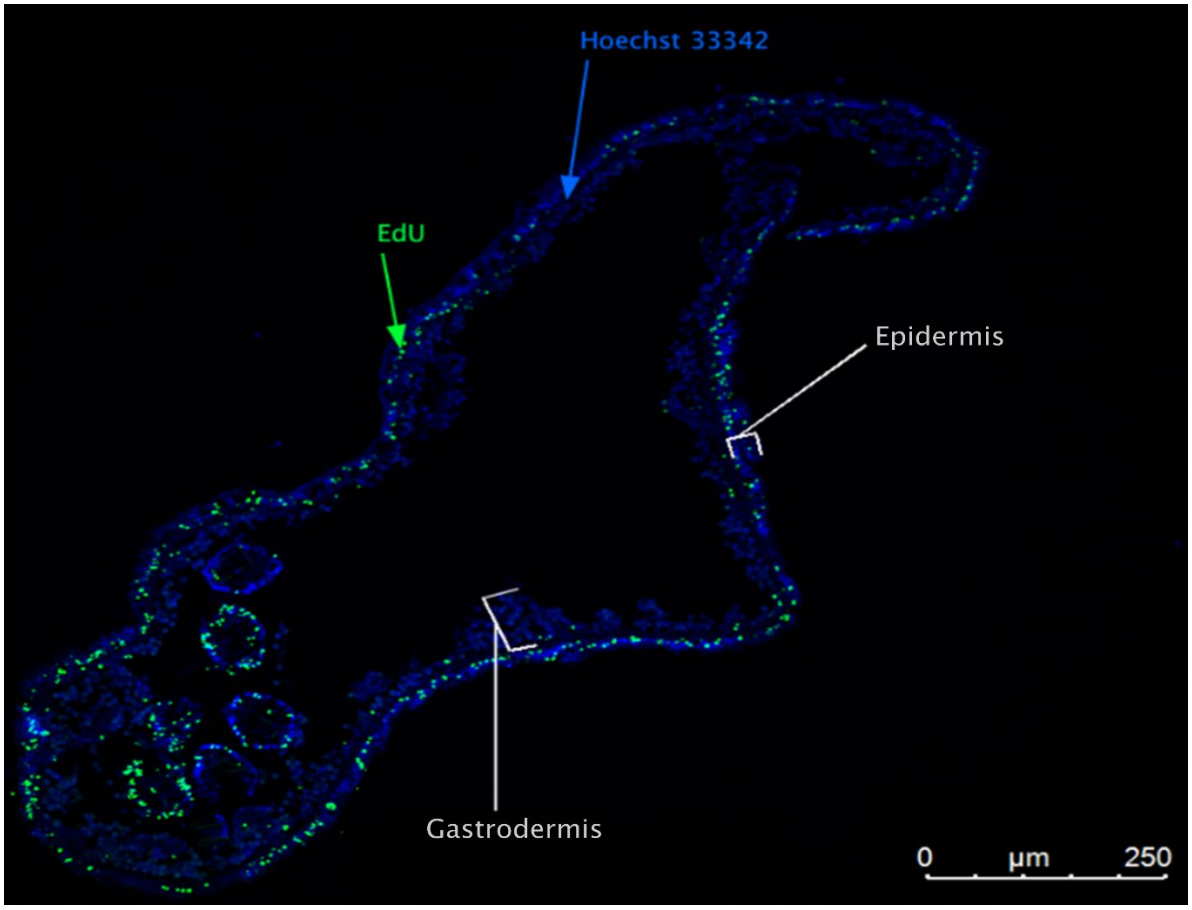

Figure 3.7. Transverse section of symbiotic Aiptasia column. Section is stained with Hoechst 33342 (blue) and EdU (green), visualized under fluorescent microscope. Blue cells indicate all non-cycling Aiptasia cells present, whereas green cells indicate the proliferating (cycling) Aiptasia cells through the incorporation of EdU into cells progressing through their cell-cycle during DNA synthesis (S phase).

The presence of symbionts significantly changed the proliferation rates of host cells (One Way ANOVA, $F(2, 32) = 5.295$, $p = 0.01$), with fully symbiotic anemones (stable symbiotic) having a significantly higher host proliferation rate (0.39 ± 0.04 $Edu^{+}/Hoechst^{+}$ cells) than

aposymbiotic anemones (0.24 ± 0.03 Edu^{+}/$Hoechst^{+}$ cells) (Tukey post-hoc, p = 0.008; Fig. 3.8). However, there was no statistical difference between inoculated Aiptasia and aposymbiotic anemones (Tukey post-hoc, p = 0.388), which could be due to the relatively short incubation time with EdU (48h).

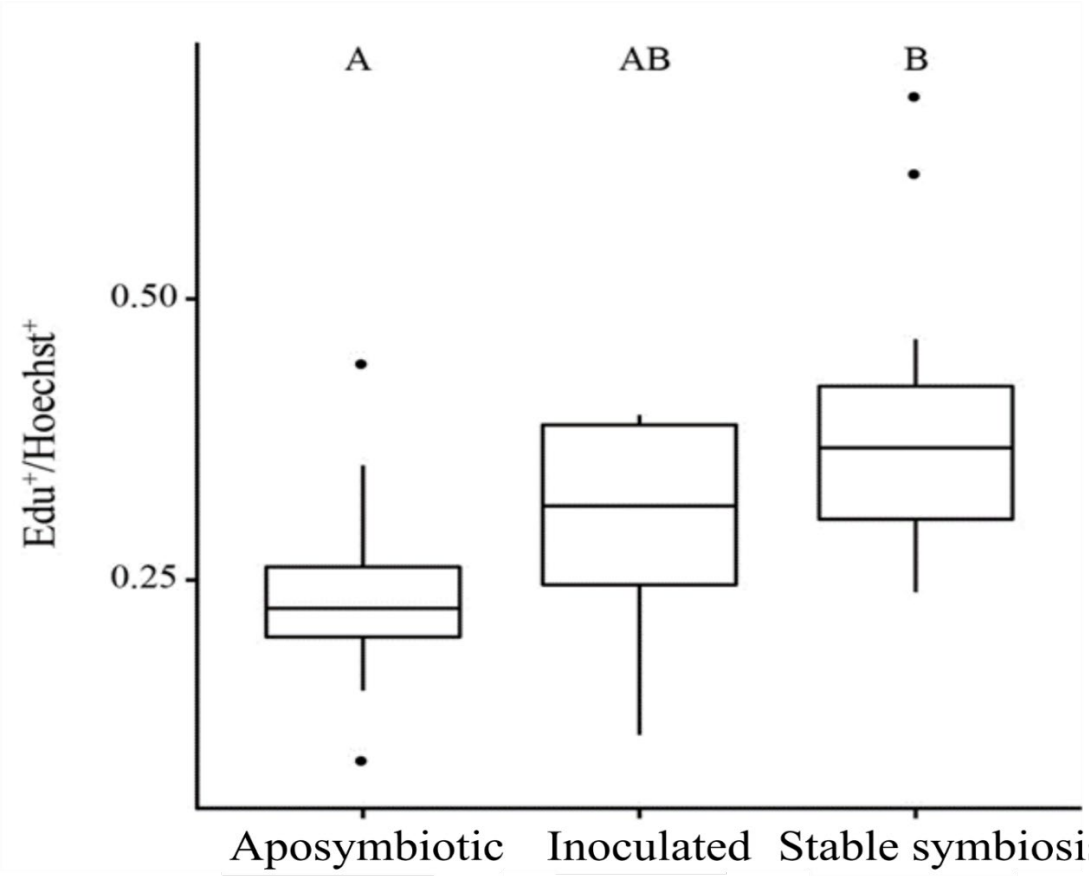

Figure 3.8. Cell proliferation rates calculated as the proportion of Hoechst-positive: EdU-positive in aposymbiotic (n = 10), recently inoculated (n = 12) and stably symbiotic (n = 14) hosts. Ratios were calculated *via* quantifying the number of Hoescht and EdU stained nuclei in microscope images (n = 2-3 *per* host) where gastrodermal and epidermal tissues could be identified. Statistical significance of pairwise comparisons was calculated using Student's t-test and is indicated by letters above the boxplots. Statistical significance of difference among the three groups was calculated by one-way ANOVA, p = 0.013.

Although not quantified, during microscope imaging it was observed that, in symbiotic anemones, the epidermis had a greater number of proliferating cells than the gastrodermis (Fig. 3.7). This finding is consistent with the results from the differentially expressed gene analysis, suggesting a reduced proportion of gastrodermal cells progressing through mitosis (Table 3.1; Fig. 3.2 and 3.4). This finding agrees with a recent study investigating the proliferation rate of host cells after symbiont colonisation (Tivey *et al*., 2020), which also reported a higher

proliferation rate in the host epidermis (58.3% of cells) than the gastrodermis (41.7% of cells). Furthermore, in adult corals the epidermis has been shown to have a faster proliferation rate in the symbiotic state than the gastrodermis (Lecointe *et al*., 2016).

3.5. Conclusion

The presence of symbionts in gastrodermal cells is associated with a down-regulation of host apoptotic initiators and sensitizers; the down-regulation of ROS sensitizers; the up-regulation of genes that function in cellular immunity to help hosts withstand 'non-self' non-pathogenic cells; the down-regulation of genes that function in G_1 and mitotic progression; and, the down-regulation of genes involved in DNA synthesis, when compared with both aposymbiotic gastrodermal cells and epidermal cells in symbiotic hosts. These may be mechanisms of inter-partner regulation by the symbiont to aid it in persisting and proliferating within the host. In contrast to reduced mitotic progression and DNA synthesis in gastrodermal cells, our observations in the epidermal cells of symbiotic anemones suggests that the presence of symbionts in the gastrodermis increases rates of mitotic completion and host cell proliferation, possibly due to the translocation of photosynthetic products from the symbionts to the host. The findings in this study point to which host genes play a role in symbiont persistence within the host cell and also which genes are involved in host cell proliferation in the symbiotic state, helping us further our knowledge in understanding host-symbiont biomass co-ordination in a stable symbiosis on a molecular level.

Chapter 4: Symbiont identity influences symbiont biomass regulatory mechanisms in a cnidarian host

4.1. Abstract

Regulation of the resident symbiont population by the host is likely to be central to maintaining the stability of the cnidarian-dinoflagellate symbiosis. Host regulatory mechanisms are thought to be comprised of both pre-mitotic (cell-cycle arrest) and post-mitotic (autophagy, apoptosis and expulsion) mechanisms. However, the relative importance of these mechanisms during establishment and maintenance of the symbiosis, and in response to different symbiont species, is unknown. In this study I inoculated a symbiont-free (aposymbiotic) model cnidarian (*Exaiptasia pallida,* commonly referred to as 'Aiptasia') with four different species of Symbiodiniaceae: homologous *Breviolum minutum* (ITS2 type B1), and heterologous *Symbiodinium microadriaticum* (A1), *Cladocopium goreaui* (C1) and *Durusdinium trenchii* (D1a). I then measured host apoptosis, expulsion and symbiont cell-cycle phase during the onset, establishment and maintenance of the symbiosis, to compare with an unmanipulated symbiosis (i.e. permanently symbiotic Aiptasia). *B. minutum* colonised Aiptasia fastest and reached the highest cell density throughout the experiment. Of the heterologous symbionts, *D. trenchii* colonised Aiptasia fastest during the first month of colonisation, while *C. goreaui* colonised slowest; however, *D. trenchii* ultimately achieved the lowest cell density. At Week 4, there was a rapid increase in the cell density of all symbiont species, which was positively correlated with the number of symbionts expelled from the host. Expulsion differed between symbiont species, with anemones colonised by heterologous species expelling the highest percentage of their symbiont population (*C. goreaui*-inoculated anemones expelling most at Week 1, and *D. trenchii*-inoculated anemones expelling most at Weeks 4 and 24) even though hosts inoculated with homologous *B. minutum* contained higher cell densities. Host apoptosis was dampened in all hosts at Week 4, irrespective of symbiont species, however this occurred earlier in *D. trenchii*-colonised Aiptasia (Week 1) than in anemones colonised by other symbiont species. All inoculated Aiptasia showed a negative correlation between host apoptosis and symbiont cell density. *B. minutum*-colonised anemones had the greatest number of symbiont cells cycling through their cell cycle during the first month of colonisation compared with heterologous symbiont species. All symbiont species showed the same pattern of cell-cycle arrest, with a greater proportion of the symbiont population becoming arrested in

the G_1 phase as time in symbiosis increased. However, hosts colonised by *D. trenchii* had a larger proportion of their symbiont population in the G_1 phase at Week 24 than the other symbiont species, emphasising that cell-cycle control is, in part, symbiont species-specific. These results highlight that, during the onset and establishment of the symbiosis, dampening of host apoptosis and high rates of symbiont cell-cycling allow the rapid proliferation of the symbiont population. Therefore, during this time, expulsion becomes a dominant regulatory mechanism. However, as the symbiosis reaches a steady state, the number of symbionts arrested in the G_1 phase of their cell cycle increases, while the number of cells cycling through their cell cycle decreases, emphasising that symbiont cell-cycle control is an important regulator of a stable symbiosis. Alongside cell-cycle control, an increase in host apoptotic rate was observed, following initial colonisation, and a notable proportion of the symbiont population was expelled in the steady state symbiosis, highlighting that all mechanisms ultimately play a role in maintaining symbiosis stability.

4.2. Introduction

Cnidarians (hard corals, soft corals, sea anemones, jellyfish and hydrocorals) form symbiotic partnerships with members of the dinoflagellate Symbiodiniaceae family (Davy *et al*., 2012). The cnidarian provides the symbionts with protection from grazers and a stable position in the photic zone, as well as nutrients from coral waste (Weis 2008; Davy *et al*., 2012; Muller-Parker *et al*., 2015), whereas the symbiont provides the cnidarian host with photosynthetically-fixed carbon to support host growth, respiration and reproduction, and in the case of reef-building corals, stimulates skeletogenesis and the net accretion of coral reefs (Davy *et al*., 2012). The cnidarian can acquire its symbionts vertically (from a maternal source) or horizontally (from the environment) (Sachs and Wilcox 2006). Upon successful recognition of the symbiont by the cnidarian through a series of cell-cell signalling events, the symbiont becomes engulfed *via* phagocytosis into the host's gastrodermal cells (Fitt and Trench 1983a). Here, it is enclosed by a "symbiosome membrane complex" consisting of an outer host-derived membrane and several other multi-layered algal-derived membranes across which all inter-partner signalling and nutritional exchange occurs (Wakefield *et al*., 2000; Wakefield and Kempf 2001; Peng *et al*., 2010; Fransolet *et al*., 2012).

Once the symbiosis has been initiated, it is important that host and symbiont cell growth are carefully co-ordinated, in the first instance to allow symbiont proliferation and then to maintain symbiosis stability (Muscatine and Pool 1979; Neckelmann and Muscatine 1983; McAuley 1985a; Jones and Yellowlees 1997). The primary methods of symbiont population maintenance include both pre-mitotic (cell-cycle arrest) and post-mitotic (apoptosis, autophagy, and expulsion) mechanisms (Jones and Yellowlees 1997; Smith and Muscatine 1999; Baghdasarian and Muscatine 2000; Dunn *et al*., 2007; Davy *et al*., 2012) (Figure 4.1). These mechanisms allow the host to: winnow heterologous/novel symbiont types during the onset of symbiosis (Roth 2014); control their resident symbiont biomass levels for the maintenance of symbiosis (Gates and Muscatine 1992); shift their dominant symbiont genotype (Douglas 2003); and, abolish symbionts under periods of stress ("bleaching"), which is induced by either the host or symbiont, or both partners (Weis 2008; Lesser 2011).

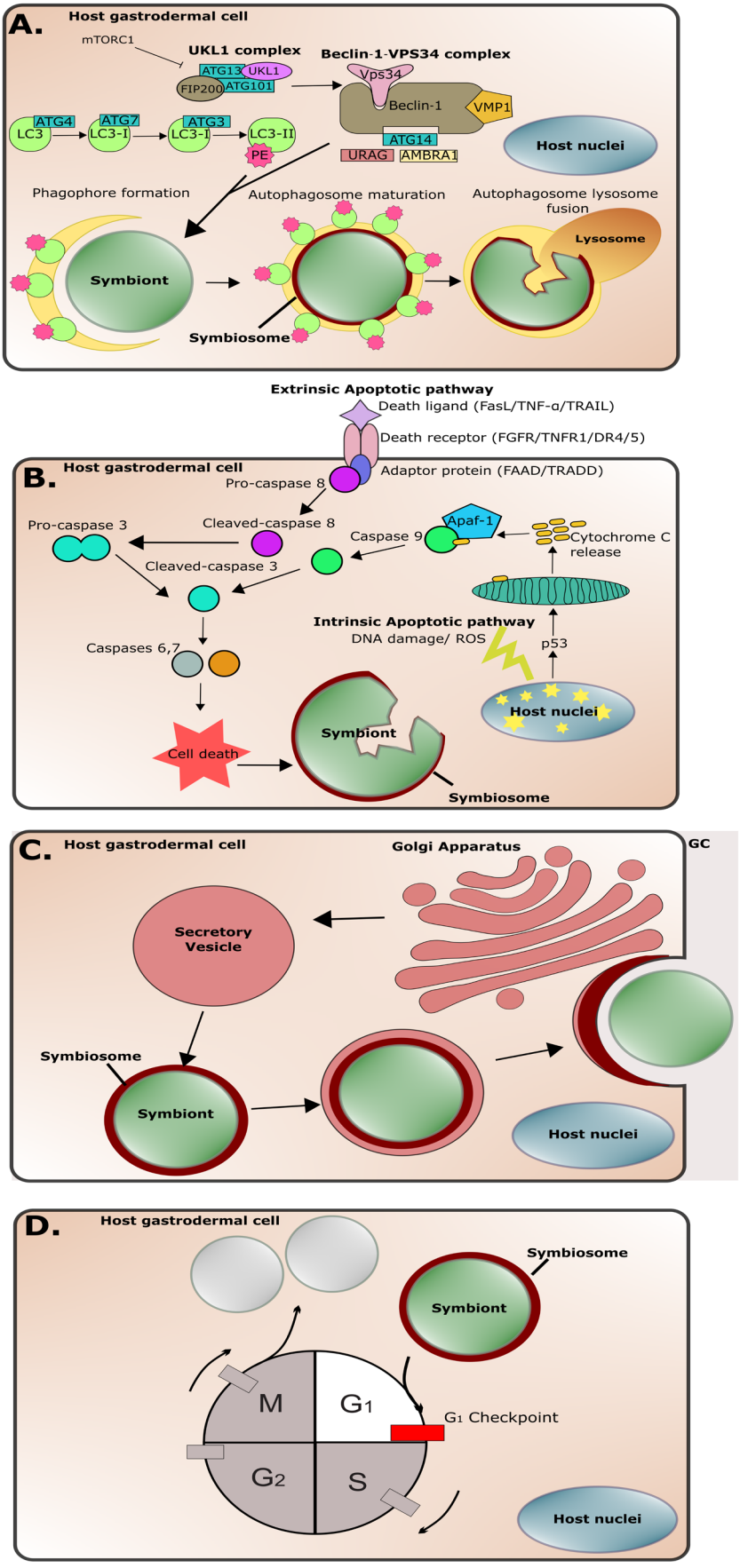

Figure 4.1. See over page for details.

Figure 4.1. Primary mechanisms hypothesised to control the resident symbiont population in the cnidarian-dinoflagellate symbiosis. **(A)** Host autophagy. During nutrient starvation or cellular stress, the inhibition of the mammalian target of rapamycin (mTOR) complex-1 (mTORC1) activates the autophagic cascade. This autophagic signal also increases the dephosphorylation of the UKL1 complex (a substrate of mTORC1) that leads to the induction of autophagy. This results in the disruption of the Beclin-1-Bcl-2 complex allowing it to form a complex with Vps34, so contributing to the induction and assembly of the autophagosome. Concomitantly, the cytosolic form of LC3 (LC3-I) becomes conjugated to phosphatidylethanolamine to form LC3-II. LC3-II is then relocated to the autophagosome membranes. Following this, autophagosomes fuse with lysosomes that degrade the components of the autophagosome using lysosomal hydrolase enzymes. (**B**) Host apoptosis. Apoptotic cascades are stimulated by the intrinsic and extrinsic apoptotic pathways. In the extrinsic apoptotic pathway, death ligands bind to death receptors on the cell surface and adaptor proteins contain death domains, allowing them to interact with death receptors and send the apoptotic signal to the death machinery within the cell. These death receptors can then bind to a homologous motif on Procaspase-8, which self-cleaves itself and becomes activated. Active caspase-8 then cleaves caspase-3, causing it to be activated which in turn activates caspase-7, committing the cell to apoptosis. The intrinsic apoptotic pathway begins when a cell becomes injured, such as *via* DNA damage, and the p53 protein senses this damage and activates the apoptotic cascade. p53 activates genes that contribute to increases in cellular ROS which in turn lead to mitochondrial damage. p53 also stimulates genes that change the permeability in the mitochondrial membrane allowing cytochrome *c* to be released into the cytosol. Upon release, cytochrome *c* binds to apoptotic protease activating factor 1 (Apaf-1) which activates caspase-9 and leads to the downstream activation of other caspases and hence cell death. (**C)** Expulsion *via* exocytosis. The Golgi apparatus within the host gastrodermal cell releases secretory vessels that engulf the symbiont/symbiosome and transport it to the cell membrane, where the secretory vessel fuses with the cell membrane and the symbiont becomes released from the host cell into the gastrovascular cavity (GC). (**D)** Symbiont cell-cycle arrest. Symbionts become arrested in the G_1 (growth) phase of the cell cycle *in hospite*, at the G_1/S checkpoint (red box). During normal cell-cycle progression, cells receive a signal for division. Upon this signal, the cells start to grow in the first growth phase (G_1) and must meet the requirements of the G_1 checkpoint in order to progress to the next stage. Once these criteria are met, cells can progress onto the DNA synthesis (S) phase. During the S phase there is an intra-S checkpoint where the cell checks for DNA breaks or/and damage. If the DNA is healthy the cell can progress through the S phase to the second growth (G_2) phase where the cell grows. The G_2 checkpoint checks for cell size and DNA damage and if the cell achieves a satisfactory size and does not contain any DNA damage it can progress to the mitosis (M) phase, where the cell splits its chromosomes into two equal copies. Following mitosis the cytoplasm splits during cytokinesis, allowing the mother cell to divide into two daughter cells.

The cell cycle is an evolutionary conserved pathway throughout eukaryotes. It is comprised of five stages: a quiescent phase (G_0) where the cell is dormant and does not progress through the cell cycle, a first gap phase (G_1) where cells grow, a DNA synthesis phase (S), a second gap phase (G_2) where DNA breaks are repaired, and finally a mitotic phase (M) where two equal copies of chromosomes are split between the two cells and the cells divide (Stark and Taylor

2004; Malumbres and Barbacid 2009). In cnidarians, ~80% of the symbiont population is typically arrested in the G_1 phase when *in hospite*, compared with 40-55% in culture (*ex hospite*) (Smith and Muscatine 1999). Both *ex hospite* and *in hospite*, the proportion of the symbiont population found in the G_1 phase differs between Symbiodiniaceae genotypes (Fujise *et al*., 2018; Tivey *et al*., 2020). Control of the symbiont cell cycle is only partially understood. For instance, *in hospite* nitrogen deprivation of the symbiont has been shown to control the proliferation of the symbiont population (Cook *et al*., 1988; Muscatine *et al*., 1989; Stimson and Kinzie 1991; Hoegh-Guldberg 1994). However, despite this, the proliferation rate of nitrogen replete symbionts *in hospite* is <20% of that in culture or at low population densities in the host (Smith and Muscatine 1999). These findings highlight that other mechanisms are behind the arrest of the symbiont cell cycle. Recent studies (**Chapter 2**; Cato *et al.*, 2019) have begun to investigate what symbiont cell-cycle genes and proteins are present, to understand how the host may control the symbiont cell cycle.

In addition to cell-cycle arrest, degradation of the symbiont population has been hypothesised to play a major role in maintaining the symbiont population, with estimates that at any one time ~1-6% of the resident symbiont population is being degraded by the host (Titlyanov *et al*., 1996). These pathways of degradation are hypothesised to include host autophagy and apoptosis (Dunn *et al*., 2007). The first of these pathways, apoptosis, is an evolutionarily-conserved mechanism of programmed cell death that allows the removal of aged or damaged cells (Weis 2008). Apoptosis is controlled by a series of pro-apoptotic and anti-apoptotic proteins (Dunn *et al*., 2006; Kvitt *et al*., 2016; Moya *et al*., 2016). If the expression of pro-apoptotic genes exceeds that of anti-apoptotic genes, enzymes known as caspases are stimulated (Kvitt *et al*., 2016). The apoptotic cascade can lead to chromatin condensation, DNA fragmentation and shrinking of the cell (Weis 2008). Under stable conditions, host cell apoptosis functions as an immune response to remove incompatible symbionts (Weis 2008; Weis *et al*., 2008; Dunn and Weis 2009), with baseline caspase rates being unique to each host-symbiont association (Tchernov *et al*., 2011; Hawkins *et al*., 2014). In addition to regulation of the resident symbiont population, apoptosis also functions in regulating the proliferation of symbionts after colonisation (Gates *et al*., 1992; Dunn and Weis 2009), removing incompatible symbionts (Weis 2008; Weis *et al*., 2008; Dunn and Weis 2009), and degrading resident symbionts during bleaching episodes (Dunn *et al*., 2004; Pernice *et al*., 2011; Tchernov *et al*., 2011; Paxton *et al*., 2013; Hawkins *et al*., 2014).

The second degradation pathway, autophagy, involves four main steps: autophagosome formation, autophagosome-lysosome fusion followed by autophagosome maturation, and finally degradation (Tanida 2011; Ao *et al*., 2014). As with apoptosis, autophagy is also an evolutionarily conserved process across eukaryotes and occurs during cellular starvation or disease, allowing the eukaryote to digest its own cells (Ao *et al*., 2014). Autophagy is also integral to the differentiation, structure, growth control and immune response within cells (Weis 2008). The autophagic and apoptotic pathways are interconnected and opposing in symbiotic cnidarians, with one's inhibition resulting in the other's initiation (Dunn *et al*., 2007). Similar to apoptosis, autophagy has been reported to be a primary mechanism utilised by the host during bleaching (Dunn *et al*., 2007; Downs *et al*., 2009). The molecular mechanisms behind this process are still unclear, although several recent studies have started to elucidate the changes in host autophagy during symbiosis e.g. cell-specific transcriptomics has confirmed that symbiosis inhibits the host autophagy pathway (Voss *et al*., 2019), and a set of genes associated with autophagy, Rab GTPases, were differentially associated with healthy and photosynthetically-damaged symbionts *in hospite* (Chen *et al*., 2003, 2004, 2005).

The final hypothesised regulatory mechanism is expulsion, in which the host removes healthy and non-healthy symbionts *via* exocytosis into the gastrovascular cavity and subsequent expulsion into the surrounding environment (Steele 1977; Steen and Muscatine 1987). Expulsion is a major regulatory mechanism in cnidarians, with rates of 0.1-4.6% of the resident symbiont population being expelled *per* day in scleractinian and soft corals (Hoegh-Guldberg *et al*., 1987; Jones and Yellowlees 1997; Baghdasarian and Muscatine 2000; Dimond and Carrington 2007). Symbionts with increased growth rates and horizontally-transmitted symbionts have been shown to be preferentially expelled from the host (McCloskey *et al*., 1996; Sachs and Wilcox 2006). In addition to autophagy and apoptosis, expulsion rates of symbionts increase under stressful conditions e.g. temperature increase (Baghdasarian and Muscatine 2000).

In addition to the knowledge gap surrounding the mechanisms of host regulation of the symbiont population, the influence that different Symbiodiniaceae species have on these host mechanisms remains unclear. Currently we know that symbiont species influence the regulatory mechanisms by: different Symbiodiniaceae species reaching different densities

within the same host at a steady state (Starzak *et al*., 2014; Yuyama and Higuchi 2014; Leal *et al*., 2015; Gabay *et al*., 2018); hosts preferentially expelling faster-growing Symbiodiniaceae species (McCloskey *et al*., 1996); different Symbiodiniaceae species eliciting different apoptotic rates within the same host species (Dunn and Weis 2009); and, different Symbiodiniaceae species having different proportions of their population in each cell-cycle phase in the same host (Tivey *et al*., 2020). However, we do not know how these mechanisms interact with each other and whether symbiont type affects the interaction of these regulatory mechanisms and whether time in symbiosis changes these mechanisms.

Thus, the aim of this chapter was to elucidate the relative importance of these host regulatory mechanisms (apoptosis, autophagy, expulsion, and cell-cycle arrest) during the onset, establishment, and maintenance of symbiosis, and how they combine to produce the colonisation patterns observed. Furthermore, I aimed to test how symbiont genotype influences these mechanisms and whether any differences are consistent across time in symbiosis. The model cnidarian Aiptasia was used due to its robustness in an experimental setting, allowing it to survive for long periods of time in an aposymbiotic state (Matthews *et al*., 2016). Aiptasia is able to form a successful symbiosis in the laboratory with several Symbiodiniaceae species (Chen *et al*., 2016; Hawkins *et al*., 2016; Gabay *et al*., 2018), making it an ideal candidate for modelling the influence of symbiont genotype on host physiology.

4.3. Materials and Methods

4.3.1. Aposymbiotic anemones

Specimens of Aiptasia were rendered aposymbiotic using the protocol of Matthews *et al*. (2016). Briefly, hosts were incubated with 800 µL menthol in 4 L of 0.22-µm filtered sea water (FSW) for 8 hours *per* day, 4 days a week, for 4-6 months. After 8 hours of incubation, menthol was replaced with 4 L 0.22-µm FSW and 200 µL dichloromethylurea. Hosts were kept under a 12 h light: 12 h dark cycle and fed biweekly. Aposymbiotic status was confirmed using confocal microscopy to check for absence of symbiont chlorophyll autofluorescence in anemones (n = 30 *per* tank) using × 10 and × 20 magnification on an Olympus Provis AX70 microscope. Chlorophyll fluorescence was excited using a 559 nm laser. After being rendered

aposymbiotic, Aiptasia were kept in 0.22-µm FSW in the dark and fed *Artemia* sp. nauplii biweekly until the start of the experiment.

4.3.2. Inoculation

Two weeks prior to inoculation, anemones were starved and put into jars (n = 150 Aiptasia *per* jar and n = 8 jars *per* treatment) containing 247 mL 0.22-µm FSW. Cultures of *Symbiodinium microadriaticum* (ITS2 type A1, strain CCMP2467), *Breviolum minutum* (B1, strain FlAp2), *Cladocopium goreaui* (C1, strain LHI-33) and *Durusdinium trenchii* (D1a, strain Ap2) were genotyped as below. One week before inoculation, cultures were refreshed with 50% f/2 medium in FSW to ensure that they were in the log-phase of growth during inoculation. On the day of inoculation, 50 mL of culture were aliquoted into a Falcon tube. This aliquot was then vortexed and suspended, of which 9990 µL of this suspension were added to 10 µL of formalin and this suspension used for symbiont cell counts using an InCell (Cytiva) microscope. Cell counts were measured by pipetting 20 µL of the suspension into individual wells (n = 10 wells *per* culture) in a 384-well plate for each sample. Then, using the Far Red laser to excite chlorophyll autofluorescence of the symbionts, images were taken of each well and cells from each image were counted using the cell counter function in the InCarta™ software. Following counts, cultures were concentrated by centrifugation to 1 million cells/mL, and freshly-hatched *Artemia* sp. nauplii added to the algal suspension to stimulate the uptake of algal cells by the anemones (Davy *et al*., 1997). This algal suspension was then pipetted into each jar of anemones to give a final symbiont cell density of 12,000 cells/mL and incubated for 24 hours. After this, the FSW was refreshed. Apoptosis, expulsion, and cell cycle measurements were then taken at Weeks 1 and 4 for anemones harbouring all Symbiodiniaceae species, Week 24 for hosts harbouring *B. minutum*, *C. goreaui* and *D. trenchii*, and Week 78 for anemones harbouring *B. minutum*. The absence in *S. microadriaticum* data at Week 24 is due to the COVID-19 pandemic (see note below[1]), while the absence of *C. goreaui* and *D. trenchii* at

[1] [Note: This current experiment was started in February 2020, during which the scale of the COVID-19 pandemic was only just being understood. New Zealand went into a national lockdown between Weeks 4 and 24 of the experiment. This lockdown meant that only minimal animal maintenance could be achieved, and no students could collect experimental data. Therefore, this resulted in the loss of the 12-week time point in this experiment and the bleaching of hosts harbouring *S. microadriaticum* between Weeks 4 and 24. Furthermore, the pandemic reduced the amount of time left to complete the project and therefore, although autophagy samples

Week 78 is due to unsuccessful maintenance of these symbioses past 24 weeks. Anemones were kept at 25 °C, under a 12 h light: 12 h dark cycle at 40 µmol photons m^{-2} s^{-1} and fed *Artemia* sp. nauplii biweekly. These measurements were also taken for unmanipulated symbiotic anemones (i.e., permanently in symbiosis with *B. minutum*), which were held under the same conditions as the inoculated anemones for four weeks prior to analysis.

4.3.3. Expulsion and cell density measurements

Expulsion was measured using the method of Perez *et al*. (2001) and the protocol was modified to include washing of anemones before and after harvesting of the symbiont cells to collect any symbionts that were attached to the animal. To summarise, the day before sampling, anemones (n = 5) were taken from each individual jar and washed with 0.22-µm FSW to remove any attached symbionts. After washing, 'clean' anemones (n = 5) were put into one-well of a 6-well plate. Each well contained 10 mL of 0.22-µm FSW and anemones were left for 24 hours to settle. On the day of sampling, the water previously surrounding the anemones was discarded, and the anemones were washed gently using a squeezy bottle with 0.22-µm FSW to remove any attached symbionts; each well was also cleaned with a cotton-tip to remove any attached symbionts. Ten millilitres of fresh 0.22-µm FSW were then added to the well at the start of the light period (T0 h). Anemones were maintained in the same conditions as the rest of the cohort during the experiment undergoing a 12 h light: 12 h dark cycle (Section 4.3.2). After 24 hours (T24 h), each anemone was removed from its well and washed with 0.22-µm FSW in a clean glass dish. This 'washing water' was retained, collecting any expelled symbionts that became attached to the anemone during this time. After washing, anemones were snap-frozen in a 1.5 mL Eppendorf tube in liquid nitrogen and held at -80 ˚C for subsequent analysis (see below). Each well was then scraped using a silicone spatula to dislodge any symbionts that may have stuck to its surface, and all the FSW in each well was then added to the 'washing water' from that well. This water, classed as the 'expelled symbiont' sample, was decanted into a 50 mL Falcon tube and centrifuged at 3900 × g for 10 min. The resulting supernatant was pipetted off until only 1 mL of supernatant remained, and the bottom

---

were taken at each time-point for anemones inoculated with each symbiont species (see **Appendix B** for description of method development), these samples could not be processed in time for the write-up of this thesis.]

of the Falcon tube scraped with a metal spatula and the tube vortexed to dislodge and suspend any remaining symbionts. This 1 mL sample was then transferred to a 1.5 mL Eppendorf, which was subsequently centrifuged at 10,000 × g for 10 min. The supernatant was pipetted off and the symbiont pellet fixed in 9990 µL 0.22-µm FSW and 10 µL formalin. Symbiont counts (n = 20 *per* sample) were performed as previously described (Section 4.3.2).

To estimate the *in hospite* symbiont density, snap-frozen anemones were thawed on ice, washed with 1 mL MilliQ water and vortexed. The MilliQ water was then removed and anemones were homogenised in 500 µL 3.3 × PBS. After homogenisation, the samples were kept on ice and centrifuged at 800 × g for 5 min at 4 °C, to separate host and symbiont. The host supernatant was stored at -80 ˚C for future protein quantification *via* the Bradford assay (see below). The symbiont pellet was washed by adding 1 mL 0.22 µm FSW, vortexing and spinning the sample down at 800 × g for 5 min to remove host contamination. The final symbiont pellet was again fixed in 9990 µL 0.22-µm FSW and 10 µL formalin, and symbiont counts performed as above.

For host protein content, Bradford protein quantification assays were performed (B6916, Sigma Aldrich). Briefly, 5- and 10-µL aliquots of host supernatant were added to 245- or 240-µL Bradford reagent, respectively. A bovine serum albumin (BSA) standard curve was generated using 1, 2, 4, 8, 10 and 20 µL BSA (1 mg/mL), and the remaining volume was adjusted to 250 µL using Bradford reagent. Plates were held for 15 min at room temperature and analysed using the 595 nm laser on a spectrophotometer.

4.3.4. Apoptosis – caspase assay

Apoptotic activity of samples containing 10 µg total host protein was measured using a caspase-3 colorimetric assay kit (CASP3C-1KT, SigmaAldrich) using the manufacturer's instructions, following the protocol by Hawkins *et al*. (2013). Briefly, anemones were collected between T4 h and T8 h and stored at -80 °C prior to analysis. For processing, anemones were washed in 1 mL MilliQ water. The MilliQ water was then decanted and the anemones homogenised in 150 µL 1 × lysis buffer. After homogenisation, the samples were kept on ice and centrifuged at 800 × g for 5 min at 4 °C, to separate host and symbiont. The symbiont pellet was washed in 1 mL MilliQ water and stored at -80 ˚C for future genotyping (see Section

4.3.6). The host supernatant was held on ice in the lysis buffer for 15 min and then centrifuged at 13,000 × g for 10 min, and the resulting pellet discarded. A Bradford protein assay was performed on the host supernatant, as previously described (Section 4.3.3). For each caspase assay, 10 µg of host protein were added to each well (n = 6) in a 96-well plate. Three of the wells contained 10 µg host supernatant which were adjusted to 90 µL total volume using 1x assay buffer, and 10 µL caspase substrate, acetyl-Asp-Glu-Val-Asp p-nitroanilide (Ac-DEVD-pNA). The other three wells were used as negative controls; these wells contained 10 µg host supernatant which were adjusted to 80 µL total volume using 1x assay buffer, 10 µL caspase substrate (acetyl-Asp-Glu-Val-Asp p-nitroanilide - Ac-DEVD-pNA) and 10 µL caspase-3 inhibitor, N-Acetyl-Asp-Glu-Val-Asp-al (Ac-DEVD-CHO). A p-nitroaniline standard curve was produced for each plate, which contained 0, 10, 20, 50, 100 and 200 µM p-nitroaline by adding 0, 1, 2, 5, 10 and 20 µL of 1mM p-nitroaline to each well and adding 1x assay buffer to make a total volume of 100 µL. The plates were then placed in an incubator at 37 °C for 180 min, and absorbance values were read on a spectrophotometer using a 405 nm laser at 90- and 180-min post-incubation.

4.3.5. Cell cycle analysis

Previous cell-cycle protocols (Wang *et al*., 2008; Fujise *et al*., 2018) were modified for cell-cycle analysis of Symbiodiniaceae, as below. At 4-h intervals over 24 hours at each experimental time-point, anemone were snap frozen (n > 5 *per* symbiont type). Host tissue samples were separated from symbiont samples as previously described (Section 4.3.3). Once separated and washed with 1 mL MilliQ water, 1 mL of methanol was added to each of the symbiont pellets, which were then kept at 4 °C overnight to extract chlorophyll. Cells were then centrifuged at 10,000 × g for 10 min to remove the methanol. Cells were washed twice with 3.3 × PBS. After washing, cells were incubated in a solution of 979 µL 3.3 × PBS, 10 µL DAPI stain (1 µg/µL), 10 µL RNase and 1 µL Triton X-100, and kept at 4 °C overnight in the dark. Cells were then centrifuged at 10,000 × g for 10 min and washed twice with 3.3 × PBS to remove any excess DAPI stain. Cells were analysed using flow cytometry (BD FACS Canto II) with the Pacific Blue laser, with a forward scatter voltage of 275, side scatter voltage of 357 and a Pacific Blue voltage of 230. A minimum event number of 10,000 cells was used *per* sample. The number of cells in each cell-cycle phase for each sample was determined using FlowJo ™ software version 10.7. Over each 24-hour period, the largest proportion of cells in

the G_1 phase was subtracted from the lowest proportion of cells in the G_1 phase to obtain an estimate for the number of cells cycling in and out of the G_1 phase over 24 hours.

4.3.6. Symbiont genotyping

After the experiment, symbiont identity was confirmed. The CTAB-chloroform protocol of Baker and Cunning (2016) was used to extract DNA and the protocol of Gabay *et al*. (2018) was used for PCR amplification of DNA. For PCR, 12.5 µL of 2 × MyTaq, 1 µL of 10 mM forward primer (ITSD; 5'- GTGAATTGCAGAACTCCGTG-3'), 1 µL of 10 mM reverse primer (ITSRev2; 5'- CCTCCGCTTACTTATATGCTT-3'), 1 µL 10 mg/mL BSA, and 7.5 µL PCR-grade water were added to 2 µL DNA template. Thermocycler conditions were: 3 min at 95 °C; 35 cycles of 15 s at 95 °C, 15 s at 56 °C and 10 s at 72 °C; and, a final 5 min at 72 °C. PCR products were sent to Macrogen (South Korea) for Sanger sequencing. Sequences were aligned with Geneious v.11.1.5 and a BLAST search was performed against the NCBI database to confirm Symbiodiniaceae genotypes.

4.3.7. Statistical Analysis

Expulsion and apoptosis data were log transformed, while cell-cycle data was arcsine transformed as in Fujise *et al*. (2018), to reduce variance. When three or more time-points or symbiont species were being compared for expulsion and apoptosis data, one-way ANOVA was performed on normal data with equal variance followed by the Tukey *post hoc* test. If the data were normal but did not harbour equal variance for expulsion and apoptosis data, a Welch ANOVA was performed followed by the Games-Howell *post hoc* test. If the data were not normal for expulsion and apoptosis data, the Kruskal-Wallis test was performed followed by Dunn's *post hoc* test. When two time-points or symbiont species were compared, a Students t-test was conducted on expulsion and apoptosis data, as the data were normally distributed in all cases. Due to the unequal variances in the cell-cycle datasets, after arcsine transforming the data, generalised least squares models were used followed by ANOVA to determine the significant influence and interaction of species and time interval on the data. Pairwise comparisons were then conducted with a Bonferroni correction to determine the differences.

4.4. Results

4.4.1. Symbiont density and colonisation success

Symbiont density in *B. minutum*-colonised anemones peaked at Week 4, when it was significantly higher than at all other time-points (Tukey *post hoc* one-way ANOVA, $F(3, 28) = 37.378$, $p < 0.001$). Moreover, it was nearly ten-fold higher at Week 4 than in the unmanipulated anemones (21603 ± 6079 *versus* 2407 ± 223 cells/µg host protein). Notably, however, the density after this peak declined to a level that was similar to that in the unmanipulated anemones and remained constant across time (Fig 4.2 A). The three heterologous symbiont species followed a similar colonisation pattern to that seen for *B. minutum*, all peaking at Week 4, though *S. microadriaticum* did not persist beyond this time-point (Fig 4.2 A). The density of *D. trenchii* then declined significantly by Week 24 (Games-Howell, $p \leq 0.001$), though the density of *C. goreaui* remained unchanged between these latter time-points (Tukey, $p > 0.05$).

While all the symbiont species followed the same general colonisation patterns, they achieved very different densities at each of the time-points (one-way ANOVA, $p < 0.001$ for each time-point). Notably, *B. minutum*-colonised anemones harboured significantly higher symbiont densities than anemones colonised by the various heterologous species at all time-points (Tukey, $p \leq 0.003$ for all comparisons). Of the heterologous symbionts, *D. trenchii* colonised Aiptasia more rapidly than the other two symbiont species during the earliest stages, reaching the highest cell density by Week 1 (Tukey, $p < 0.001$ for both comparisons). By Week 4, though, densities of *D. trenchii* and *S. microadriaticum* were similar, and both significantly exceeded those of *C. goreaui* (Tukey, $p \leq 0.026$ for both comparisons). However, given the marked decline in the density of *D. trenchii* seen between Weeks 4 and 24, and the plateauing of the density of *C. goreaui* between these time-points, the two symbiont species ultimately achieved the same population densities at Week 24 (699 ± 91 *versus* 936 ± 112 cells/µg host protein, respectively; Tukey, $p > 0.05$). Unlike anemones colonised by homologous *B. minutum*, those colonised by *C. goreaui* and *D. trenchii* for 24 weeks had lower symbiont cell densities than unmanipulated, permanently symbiotic anemones (Log transformed data, Kruskal-Wallis, $H(2) = 15.844$, $p < 0.001$, Dunn's Bonferroni correction *post hoc* $p < 0.05$).

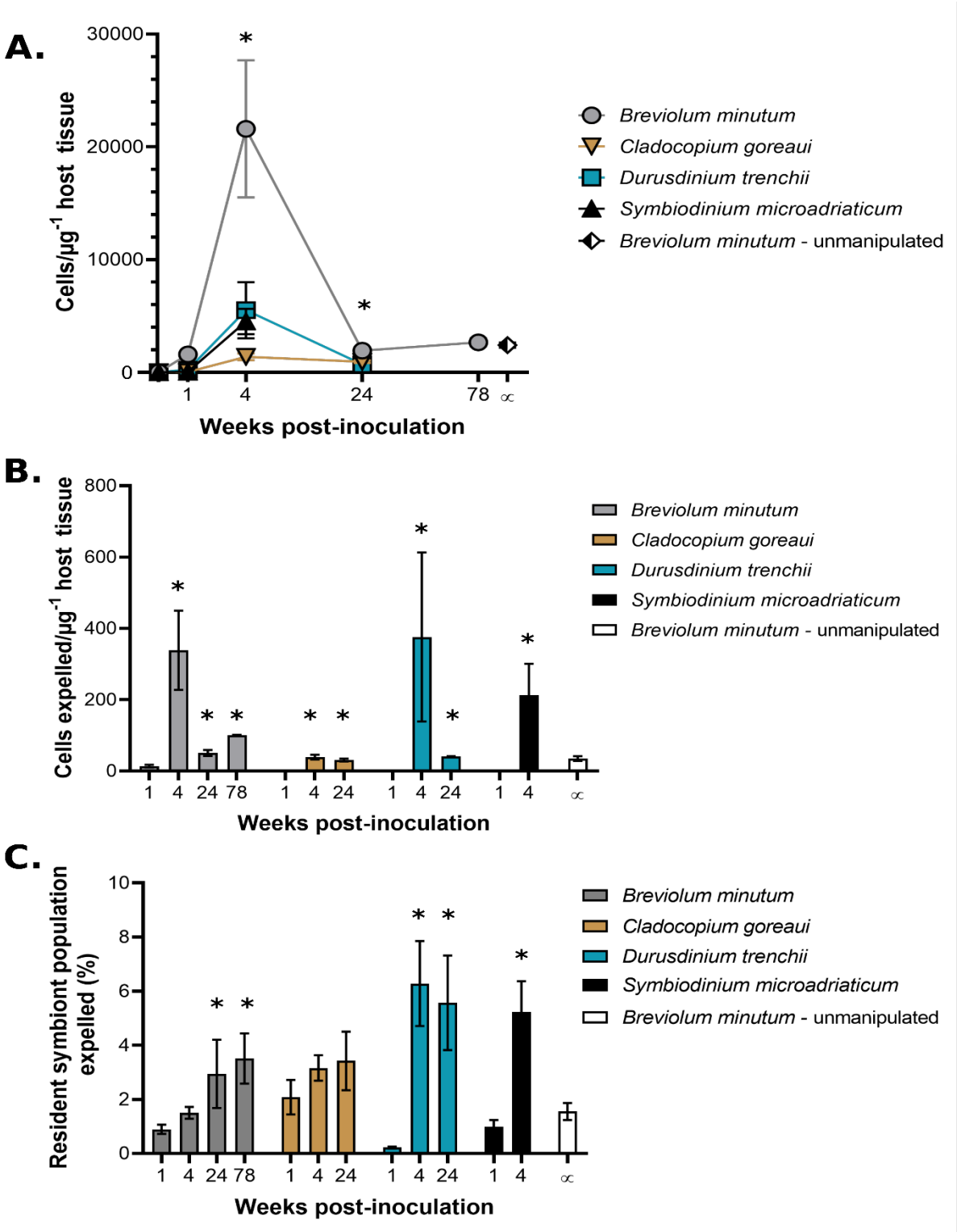

Figure 4.2. Colonisation success and expulsion rate (± S.E) during symbiosis establishment with Aiptasia, in anemones colonised by homologous *B. minutum*, and heterologous *C. goreaui*, *D. trenchii* and *S. microadriaticum*, at up to 1-, 4-, 24- and 78-weeks post-inoculation (maximum time-point dependent on colonisation success) (n = 7 – 8). (A) Cell density of symbionts *per* µg host tissue. (B) Symbiont cells expelled *per* µg host tissue. Bars that are not visible correspond to values < 1. (C) Overall proportion of the resident symbiont population expelled (%). Asterisk's correspond to a significant difference compared with Week 1 in each species ($p < 0.05$).

4.4.2. Expulsion

4.4.2.1. Symbiont expulsion rate

Symbiont expulsion rate (cells/ µg protein/ day) from *B. minutum*-colonised anemones changed significantly during the colonisation process (one-way ANOVA, $F(3, 28) = 18.419$, $p < 0.001$). Of note, the expulsion rate at Week 4 vastly exceeded that in the other weeks (Tukey, $p \leq 0.02$), after which it declined markedly, though to a level that still exceeded that seen at Week 1 (Tukey, $p \leq 0.017$) (Fig. 4.2 B). The expulsion rate at Weeks 24 and 78, although higher, was similar to that seen in unmanipulated anemones (51 ± 9, 101 ± 1, 35 ± 7 cells expelled/µg protein/day, respectively; Tukey test, $p > 0.05$ for both comparisons).

All heterologous symbiont species showed this same temporal pattern in expulsion rate as for the *B. minutum*-colonised anemones, with a peak at Week 4 (Fig. 4.2 B). For those species measured beyond Week 4, this peak was followed by a marked decline for *D. trenchii* between Weeks 4 and 24 (376 ± 237 *versus* 40 ± 1 cells expelled/µg host/day; Tukey *post hoc* one-way ANOVA, $p = 0.028$), but not *C. goreaui* (Dunn's Bonferroni correction *post hoc* Kruskal-Wallis, $p > 0.05$).

Given that the peak in symbiont expulsion coincided with the peak in symbiont density (Week 4), it is not surprising that expulsion rate correlated with symbiont population density for homologous and heterologous species (*B. minutum* - Spearman's Rank, $R_S = 0.773$, $n = 32$, $p < 0.001$; *S. microadriaticum* - Spearman's Rank, $R_S = 0.855$, $n = 14$, $p < 0.001$; *C. goreaui* - Spearman's Rank, $R_S = 0.871$, $n = 23$, $p < 0.001$; and *D. trenchii* - Pearson correlation coefficient = 0.900, $n = 22$, $p < 0.001$). Similarly, the expulsion rate was highest for those symbiont species that achieved the highest population density. For example, at Week 1, *B. minutum* was expelled at a faster rate than any of the heterologous symbiont species (Games Howell *post hoc* Welch ANOVA, $p < 0.001$), while *C. goreaui* was expelled less rapidly at Week 4 than either *B. minutum* or *S. microadriaticum* (Dunn's Bonferroni correction *post hoc* Kruskal-Wallis, $p \leq 0.04$). However, as symbiont density converged over time, so too did the expulsion rate, with there being no significant difference between the three symbiont species measured (*B. minutum*, *C. goreaui*, *D. trenchii*) at Week 24 (one-way ANOVA, $F(2,19) = 0.897$, $p > 0.05$). Unlike cell density, the number of cells expelled by *C. goreaui*- and *D.*

trenchii-colonised anemones at Week 24 was not different to that in unmanipulated, permanently symbiotic anemones (one-way ANOVA, $F(2,19) = 0.077$, $p = 0.927$).

4.4.2.2. Percent expulsion

The percentage of the resident symbiont population expelled *per* day (% expulsion) changed significantly with time during host colonisation by the homologous *B. minutum* (Kruskal-Wallis, $H(3) = 12.100$, $p = 0.007$), with a greater proportion of the population being expelled as time in symbiosis increased (from 0.89 ± 0.17 % at Week 1 to 3.51 ± 0.93 % at Week 78) (Dunn's Bonferroni correction, $p < 0.05$ for all comparisons; Figure 4.2 C). The percent expulsion in the fully re-established symbiosis (Weeks 24 and 78) was the same as that in the unmanipulated, permanently symbiotic state (Tukey *post hoc* one-way ANOVA, $p > 0.05$).

All heterologous symbionts exhibited the same trend as the homologous symbiont, with % expulsion increasing over time as colonisation progressed, before remaining consistent once the symbiont population density stabilised. For example, % expulsion increased from 2.1 to 3.2%, 1 to 5.2%, and 0.2 to 6.3% between Weeks 1 and 4 for *C. goreaui*, *S. microadriaticum* and *D. trenchii*, respectively. While this temporal change only trended towards significance for *C. goreaui* (one-way ANOVA, $F(2, 20) = 3.475$, $p = 0.051$), it represented a significant shift for the other two heterologous species (*S. microadriaticum*: Independent t-test, $T(13) = -4.784$, $p < 0.001$; *D. trenchii*: Kruskal-Wallis, $H(2) = 15.093$, $p < 0.001$).

While the general patterns of expulsion were very similar between symbiont species, symbiont identity clearly influenced % expulsion at Week 1 post-colonisation (Kruskal-Wallis, $H(3) = 17.085$, $p < 0.001$), as a greater proportion of both the *C. goreaui*- and *S. microadriaticum* populations were expelled than the *D. trenchii* population (Dunn's Bonferroni correction, $p < 0.05$ for both comparisons). Likewise, at Week 4, *B. minutum*-colonised anemones expelled a lower proportion of their resident symbiont population than *D. trenchii*- and *S. microadriaticum*-colonised anemones, but not *C. goreaui*-colonised anemones (Tukey *post hoc* one-way ANOVA, $p \leq 0.001$). As seen previously though, as symbiont expulsion rate became more similar across the different symbioses overtime, i.e. Week 24, so too did % expulsion (Kruskal-Wallis, $H(2) = 3.938$, $p = 0.14$); though while not significant, it is notable that the

average % expulsion of *D. trenchii* continued to be higher than that of the homologous *B. minutum* by about a factor of two. Moreover, at Week 24, anemones colonised by *D. trenchii* and *C. goreaui* expelled a greater proportion of their symbiont population than permanently symbiotic anemones (one-way ANOVA, $F(2,19) = 12.312$, $p < 0.001$, Tukey *post hoc* $p < 0.05$).

4.4.3. Apoptosis

In *B. minutum*-colonised anemones, apoptotic rate changed significantly with time in symbiosis (Kruskal-Wallis, $H(3) = 11.131$, $p = 0.011$) (Figure 4.3), with a marked (60% or more) dampening in apoptotic rate at Week 4 relative to the other time-points; the Week 4 value was significantly lower than for both Weeks 1 and 78 (Dunn's Bonferroni correction, $p < 0.05$ for both comparisons). Furthermore, apoptotic rate in the unmanipulated anemones was significantly higher than that in the re-colonised anemones at Week 4 (Games-Howell $p = 0.002$), though not the other weeks.

In *S. microadriaticum*-, *C. goreaui*- and *D. trenchii*-colonised anemones, apoptotic rates over time in symbiosis followed a similar pattern to that in *B. minutum*-colonised anemones (Fig. 4.3). *S. microadriaticum* induced a significantly dampened host apoptotic rate at Week 4 *versus* Week 1 (T-test, $T(11) = 3.837$, $p = 0.003$), while the mean apoptotic rate in *C. goreaui*-colonised anemones at Week 4 was only a third or less of that at Weeks 1 or 24, and significantly lower than the rate at 24 weeks (Games-Howell *post hoc* Welch ANOVA, $p = 0.05$). While time in symbiosis has a significant effect on apoptosis in *D. trenchii*-colonised anemones (one-way ANOVA, $F(2, 17) = 3.826$, $p = 0.042$), and apoptotic rate at Week 4 was only about 50% and 30% of that at Weeks 1 and 24, respectively, *post hoc* analysis failed to reveal any significant differences between time-points. In contrast to anemones colonised by *B. minutum*, those colonised by *C. goreaui* and *D. trenchii* had lower apoptotic rates at Week 24 than permanently symbiotic anemones (one-way ANOVA, $F(2,19) = 12.162$, $p < 0.001$, Tukey *post hoc* $p < 0.05$).

Apoptotic activity was somewhat variable (though not significantly so) between time-points in aposymbiotic anemones, perhaps masking some statistical differences with the various symbioses. For example, in all cases, symbiosis seemed to induce a decrease in apoptosis (50%

or more) at Week 4 relative to the aposymbiotic state that was not statistically supported. However, of particular interest, at Week 1, *D. trenchii* significantly depressed the host's apoptotic rate when compared to the aposymbiotic state (15.4 ± 8 *versus* 49.4 ± 7.7 µmol pNA released/min/mL) (Dunn's Bonferroni correction *post hoc* Kruskall-Wallis, $p = 0.05$), with this Week 1 rate also being lower than that seen in the symbioses with the other homologous and heterologous symbionts.

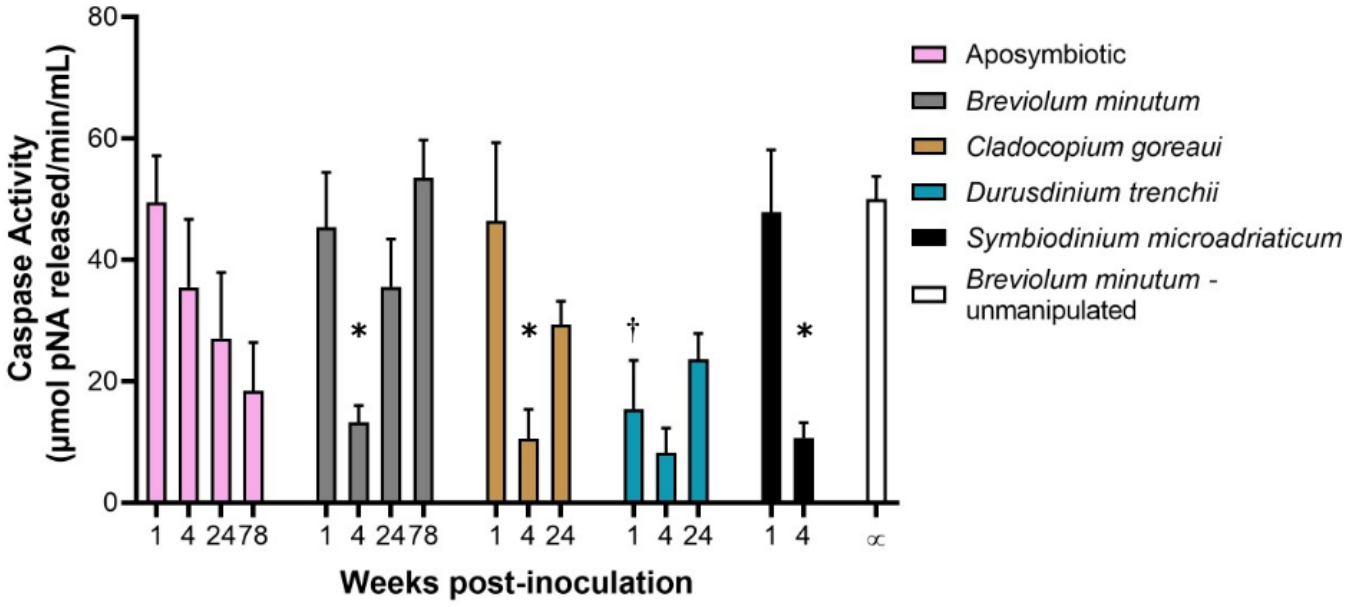

Figure 4.3. Host apoptotic rate over time measured by caspase activity (µmol pNA released/min/mL ± S.E.), during symbiosis establishment with Aiptasia when colonised by homologous *B. minutum*, and heterologous *C. goreaui*, *D. trenchii* and *S. microadriaticum*, at up to 1-, 4-, 24- and 78-weeks post-inoculation (maximum time-points dependent on colonisation success) ($n = 5$ - 8). Also shown are apoptotic rates in aposymbiotic anemones and unmanipulated/permanently symbiotic anemones harbouring *B. minutum*. Asterisks correspond to significant differences within a species at that time-point, whereas the dagger corresponds to a significant difference between species when compared with aposymbiotic anemones ($p < 0.05$).

4.4.4. Cell cycle

4.4.4.1. Cell cycle over time in symbiosis

In anemones colonised by homologous *B. minutum*, the length of time in symbiosis had a significant influence on the proportion of the symbiont population arrested in the G_1 phase (generalised least squares, one-way ANOVA, $F(3) = 84.75$, $p < 0.001$), with anemones at Week 24 possessing significantly more symbiont cells in the G_1 phase at all hourly intervals (T0-24 h) than at Week 1 (Bonferroni *post hoc* $p < 0.05$; Figure 4.4). This also reflects the difference in the number of cells cycling, with Week 1 having ~25% more of the symbiont population cycling through its cell cycle than at Week 4 (Figure 4.5). After Week 24, there was no significant difference in the proportion of the symbiont population arrested in the G_1 phase (Bonferroni *post hoc* $p > 0.05$, for Week 24 *versus* Week 78). The similar proportion of cells in the G_1 phase during these later time-points was reflected by the cell-cycle rate (Week 24: 4.54%; Week 78: 4.10%), with symbionts in permanently-symbiotic, unmanipulated *B. minutum* anemones behaving similarly. Ultimately, all anemones colonised by either *B. minutum* for 24 and 78 weeks, or unmanipulated anemones also containing *B. minutum*, had >85% of the resident symbiont population arrested in the G_1 phase of the cell cycle and ~4% of the symbiont population cycling through their cell cycle.

Time in symbiosis also influenced the proportion of the symbiont population in the G_1 phase for heterologous *C. goreaui*, *D. trenchii* and *S. microadriaticum*, with a similar pattern to that seen for *B. minutum* in all cases (Figure 4.4). For example, both *C. goreaui*- and *D. trenchii*-colonised anemones had a significantly higher proportion of their symbiont population in the G_1 phase at Week 24 compared with both Weeks 1 and 4 (Bonferroni *post hoc* $p < 0.05$). Although cell-cycle data for *S. microadriaticum*-colonised anemones were only collected until Week 4, the data showed a similar pattern, with anemones at Week 4 having significantly more of the symbiont population arrested in the G_1 phase at several hourly intervals (T0-8 h, T16 h) than at Week 1 (Bonferroni *post hoc* $p < 0.05$). Consistent with these patterns, cell-cycling rate decreased from ~8% at Week 1 to ~5% at Week 24 for both *C. goreaui* and *D. trenchii*, though in both cases there was an intermediate increase to ~13% at Week 4; this temporary peak was not seen in *S. microadriaticum*-colonised anemones (Figure 4.5).

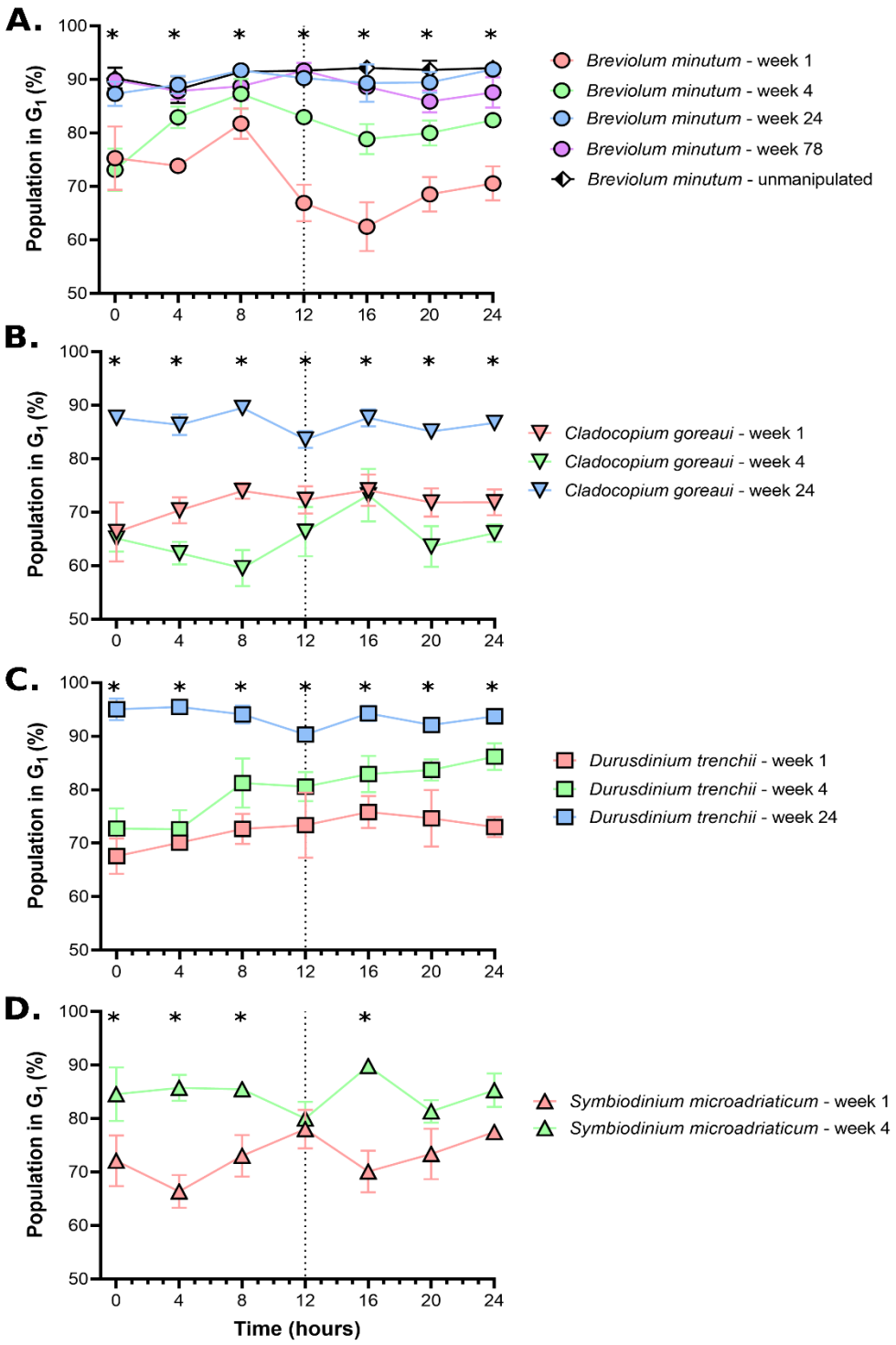

Figure 4.4. Symbiont population in the G_1 phase during symbiosis establishment, in Aiptasia colonised by homologous *Breviolum minutum* (A), and heterologous *Cladocopium goreaui* (B), *Durusdinium trenchii* (C) and *Symbiodinium microadriaticum* (D), at up to 1-, 4-, 24- and 78-weeks post-inoculation (maximum time-points dependent on colonisation success) (values are mean ± S.E; n = 3 - 8). Measurements were made across 24 hours (T0-24 h) on the day of sampling. Dotted line represents the end of the light phase (T0-12 h) and the start of the dark phase (T12-24 h). Asterisk's correspond to a significant difference compared to Week 1 for each species ($p < 0.05$).

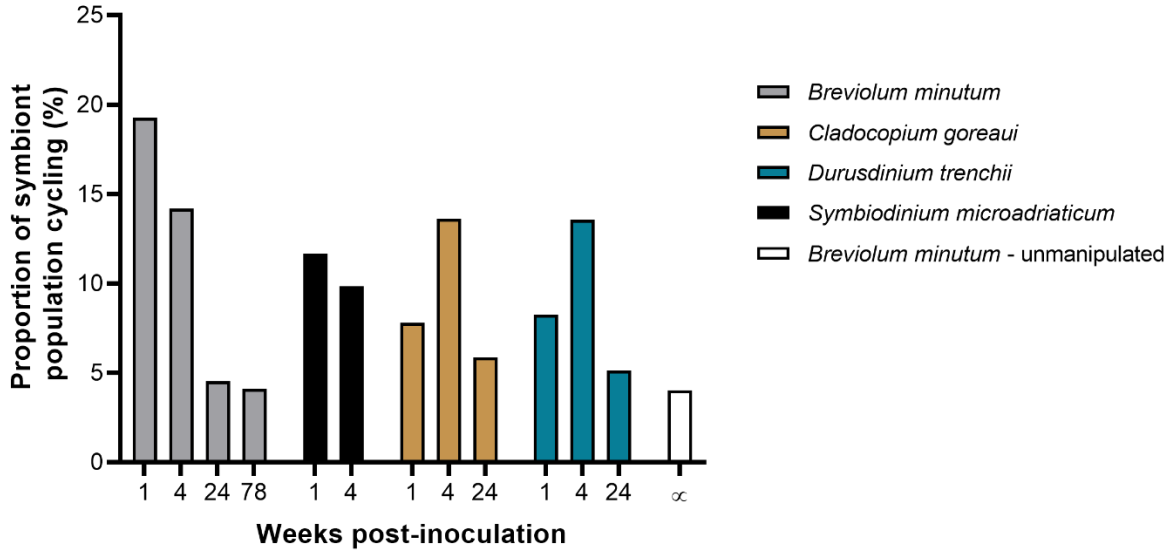

Figure 4.5. Proportion of the resident symbiont population cycling through its cell cycle, calculated by measuring the range between the highest and lowest proportion of the population in the G_1 phase at each time-point.

4.4.4.2. Cell cycle differences between species

At Week 1, symbiont identity did not have a significant influence on the proportion of the population in G_1 phase (generalised least squares, one-way ANOVA, $F(3) = 0.821$, $p = 0.4851$). In contrast to Week 1, at Weeks 4 and 24, symbiont identity *did* significantly influence the proportion of cells in G_1 phase (Week 4 - generalised least squares, one-way ANOVA, $F(3) = 66.686$, $p < 0.0001$; Week 24 - generalised least squares, one-way ANOVA, $F(2) = 63.77$, $p < 0.0001$). At Week 4, a greater proportion of both *B. minutum* and *S. microadriaticum* were in G_1 phase than *C. goreaui*, at most time-points during the day (Bonferroni *post hoc* $p < 0.05$). Likewise, *B. minutum*-colonised anemones had a significantly higher proportion of its population in the G_1 phase during several intervals at Week 4 (T4-12 h, T20-24 h) than *C. goreaui*-colonised anemones (Bonferroni *post hoc* $p < 0.05$). *D. trenchii* also had a relatively low proportion of its population in G_1 at Week 4, though it was only significantly lower than *B. minutum*- and *S. microadriaticum* on a couple of occasions (T0 and T4 h) (Bonferroni *post hoc* $p < 0.05$). At Week 24, *D. trenchii*-colonised anemones had >85% of the symbiont population arrested in the G_1 phase at all time-points (T0-24 h), which was more than in *C. goreaui* (T0-12 h, T20-24 h) and *B. minutum* at several time-points (T0, 4, 12, 24 h) (Bonferroni *post hoc* $p < 0.05$). Indeed, as at Week 4, *C. goreaui*-colonised anemones tended to have the lowest proportion of their symbiont population in G_1 phase at Week 24. Contrasting to *B.*

minutum-colonised anemones at Week 24, *D. trenchii*- and *C. goreaui*-colonised anemones had a significantly different number of cells in the G_1 phase at Week 24 compared with permanently-symbiotic anemones (generalised least squares, one-way ANOVA, $F(2) = 86.6$, $p < 0.0001$), with *D. trenchii* having significantly more of its population in G_1 phase at T4 h and *C. goreaui* having significantly less of its population in G_1 phase at T12 – 24 h compared with the unmanipulated symbiotic state (Bonferroni *post hoc* $p < 0.05$).

Although there was no influence of species identity on the proportion of symbionts in G_1 phase, cell-cycling rates seemed to be influenced by species identity at Week 1, with a greater proportion of *B. minutum* cells cycling through the cell cycle (19.28%) at Week 1 than any of the heterologous species (*C. goreaui* - 7.8%, *D. trenchii* - 8.25% and *S. microadriaticum* - 11.65%). As at Week 1, the proportion of *B. minutum* cells cycling through the cell cycle at Week 4 (14.19%) was higher than for the other symbiont species, though only just when compared with *C. goreaui* and *D. trenchii* (~ 13%); *S. microadriaticum* had the lowest rate of cell cycling (9.84%). By Week 24, cell-cycling rates had declined to a similar level in all species, with rates of 4-5%, not dissimilar to that witnessed in permanently symbiotic anemones (4.04%).

4.5. Discussion

The findings of this study highlight the importance of apoptosis and expulsion during the early onset and establishment in the cnidarian-dinoflagellate symbiosis as the symbiont population rapidly proliferates. However, once the symbiont population reaches a steady state, cell-cycle arrest becomes a major regulatory mechanism preventing the symbiont population from overgrowing the host. In addition to time in symbiosis, symbiont identity had a large influence on the host's regulatory mechanisms. For instance: heterologous *D. trenchii*-colonised anemones exhibited the earliest depression in host apoptotic rates; anemones inoculated with all heterologous symbiont species expelled a higher proportion of their resident population (%) at Week 4 compared with homologous *B. minutum*-colonised anemones; *B. minutum*-colonised anemones had the largest amount of their symbiont population cycling through their cell cycle at Weeks 1 and 4; and at Week 24, *D. trenchii*-colonised anemones had the largest proportion of their cell cycle in the G_1 phase. The following sections discuss these findings in more detail.

4.5.1. Symbiont population density

The homologous symbiont *B. minutum* reached a higher cell density in host tissues at all time-points than the various heterologous species. This observation agrees with past studies in symbiotic cnidarians, where homologous symbionts more rapidly colonise their hosts than other symbionts (Davy *et al*., 1997; Weis *et al*., 2001; Rodriguez-Lanetty *et al*., 2006b; Starzak *et al*., 2014; Gabay *et al*., 2018). Of the heterologous species, *D. trenchii* reached the highest population density during the onset and establishment of the symbiosis, however after 24 weeks in symbiosis *D. trenchii* had the lowest density of all symbiont species.

During the onset and establishment of the symbiosis (Weeks 1 and 4), the difference in cell density between Symbiodiniaceae species in Aiptasia is probably due, in part, to innate growth rate differences between species. For instance, in culture, *B. minutum* has been shown to have the fastest growth rate, followed by *D. trenchii* and then *C. goreaui* (Fujise *et al*., 2018), and these results mirror the cell densities recorded *in hospite* during this current study at Weeks 1 and 4. Inter-partner recognition may have also influenced the relatively rapid colonisation by *B. minutum*. In the cnidarian-dinoflagellate symbiosis, recognition involves interactions between signalling molecules on the host and symbiont cell surfaces, as well as signalling pathways once the symbiont is housed inside the host cell (Markell and Wood-Charlson 2010; Davy *et al*., 2012; Rosset *et al*., 2020). The composition of recognition molecules on the symbiont cell surface has been shown to be species-specific (Logan et al. 2010), perhaps contributing towards colonisation success (Lin *et al*., 2000; Wood-Charlson *et al*., 2006; but see Parkinson *et al*., 2018). Less is known about the signal molecules that pass between the partners *in hospite*, however studies are starting to elucidate this knowledge gap, allowing us to record symbiosis-associated molecules and how these molecules correspond to physiological shifts in the holobiont (Detournay and Weis 2011; Hambleton *et al*., 2019; Lawson *et al*., 2019; Rosset *et al*., 2020).

All Symbiodiniaceae species reached their highest density four weeks after uptake, consistent with previous work in Aiptasia (Gabay *et al*., 2018), and then declined. Such a population 'overshoot' and subsequent decline has been previously reported for a range of symbiotic

cnidarians (Davy *et al*., 1997; Starzak *et al*., 2014; Gabay *et al*., 2018). It seems probable that regulatory mechanisms were invoked by the host (and/or potentially the symbionts themselves) to reduce the symbiont population density once it reached this peak, with the lower ultimate density achieved by the heterologous *versus* homologous symbionts, potentially reflecting sub-optimal host-symbiont cellular integration and increased physiological cost, and the activation of regulatory processes (e.g. expulsion and cell-cycle arrest) to minimise this cost.

In support of this hypothesis, species from the genus *Durusdinium* (including *D. trenchii*, which achieved the lowest long-term density here) have been recorded to be more energetically costly to cnidarian hosts than other symbiont types. For example, colonisation by *Durusdinium* can reduce host growth and calcification rates under stable environmental conditions, potentially due to reduced fluxes of carbon and nitrogen from the symbiont to host (Cantin *et al*., 2009; Jones and Berkelmans 2010; Baker *et al*., 2013b; Pettay *et al*., 2015; Matthews *et al*., 2017, 2018). Moreover, hosting *D. trenchii* has been shown to induce oxidative stress in Aiptasia (Matthews *et al*., 2017, 2018).

4.5.2. Expulsion

The number of symbionts expelled (*per* µg host protein) was correlated with symbiont population density (also *per* µg host protein) in all species throughout the experiment, with both measurements peaking at Week 4. This relationship is unsurprising given the greater availability of cells for expulsion at higher population densities. However, the total proportion of the resident symbiont population expelled (% expulsion) did *not* correlate with the symbiont population density for all species, but rather increased with time in symbiosis. For the homologous *B. minutum*, % expulsion was 0.89 – 2.94% between Weeks 1 and 24 and increased to 3.51% at Week 78. These rates are consistent with past studies in other cnidarians, where daily expulsion rates of 0.1-4.6% have been reported for natural symbioses (Hoegh-Guldberg *et al*., 1987; Jones and Yellowlees 1997; Baghdasarian and Muscatine 2000). Why the % expulsion increased as colonisation proceeded is not known, but it seems plausible that, in the earlier stages of colonisation the cells were diving and proliferating rapidly through the host's vacant tissues and so expulsion was less necessary for regulating the symbiont population, despite the fact that hosts have previously been shown to expel dividing symbiont cells preferentially (Baghdasarian and Muscatine 2000). Indeed, this would be consistent with

the finite number of symbiont cells that can be housed by a host cell and space limitation in the host's tissues being a major driver of the symbiont population density (Jones and Yellowlees 1997; Muscatine *et al*., 1998; Davy *et al*., 2012; see Section 4.5.4. for further discussion).

Interestingly, permanently symbiotic Aiptasia containing *B. minutum* expelled a lower proportion of their symbiont population (1.55%) than anemones inoculated with *B. minutum,* both after 24 and 78 weeks, by which time they were fully colonised. This contrasts with the other regulatory mechanisms studied, where similar patterns were seen in the two symbiotic states (i.e. manipulated *versus* unmanipulated) by 24 weeks post-inoculation. Why this difference occurred is unknown, but it could be linked to the fact that in the unmanipulated symbiosis, the host was in symbiosis with its native symbiont species strain of *B. minutum*, possibly resulting in enhanced host-symbiont integration, and more effective control of the symbiont population, leading to lower expulsion rates.

For heterologous symbionts, the % expulsion was greater than for the homologous symbiont between Weeks 1 and 24, reaching 0.98 – 5.24% for *S. microadriaticum*, 0.22 – 6.28% for *D. trenchii* and 2.08-3.42% for *C. goreaui*. Combined with the lower population densities ultimately achieved by these symbionts, this suggests that the host was expelling a greater proportion of these non-native symbionts to limit their proliferation. As mentioned above, heterologous symbionts can cause increased cellular stress, reduced capacity for inter-partner signalling, and less beneficial nutritional fluxes in the host (Pernice *et al*., 2015; Matthews *et al*., 2018; Rädecker *et al*., 2018; Sproles *et al*., 2019, 2020). Of particular note with respect to symbiont expulsion, under cellular stress, stress molecules such as reactive oxygen species and nitric oxide are thought to be released in greater quantities from the symbiont cell and trigger downstream bleaching cascades if their levels surpass a threshold (Weis 2008; Hawkins *et al*., 2014; Krueger *et al*., 2015). Similarly, carbon limitation in the holobiont can lead to bleaching through the host exhausting its own carbon energy reserves and symbiont photosynthetic dysfunction triggering the bleaching cascade (Morris *et al*., 2019). This is especially interesting in the context of *D. trenchii*, which has previously been shown to assimilate significantly less carbon and to retain more host nitrogen than *B. minutum* when in Aiptasia (Sproles *et al*., 2020), while *Durusdinium* sp. was shown to fix and translocate less inorganic carbon than *Cladocopium* sp. in reef corals (Pernice *et al*., 2015). Ultimately, the physiological differences

between symbiont species are likely to underpin the different expulsion rates seen here under stable environmental conditions, though how these processes link to expulsion requires detailed exploration.

4.5.3. Apoptosis

The current study showed that, in symbiosis with either the homologous or heterologous symbionts, host apoptosis became depressed within four weeks after initial uptake. After this depression, apoptosis in all symbioses increased once colonisation was complete, peaking in *B. minutum*-colonised anemones at Week 78. Notably, these higher apoptotic rates were similar to those seen in permanently symbiotic anemones, implying that a higher level of apoptosis is a hallmark of maintaining a steady symbiont population, regardless of symbiont type.

Apoptosis has been shown previously to be a major regulatory mechanism for controlling the symbiont population in the cnidarian-dinoflagellate symbiosis, with previous studies showing that: host apoptotic genes are down-regulated during symbiosis (**Chapter 3;** Rodriguez-Lanetty *et al*., 2006a); increases in host apoptosis reduce the colonisation success of symbionts (Dunn and Weis 2009) ; and, the inhibition of host apoptosis allows symbionts to re-colonise a host after bleaching (Kvitt *et al*., 2016). The current study agrees with the hypothesis that dampening of host apoptosis facilitates symbiont proliferation, given that the depression of host apoptosis at Week 4 coincided with the peak symbiont density for all symbiont species studied. Likewise, the other pathway of symbiont degradation in hosts, autophagy, has been shown to be down-regulated during symbiont establishment in Aiptasia larvae (Voss *et al*., 2019). Thus, the down-regulation of symbiont degradation mechanisms during establishment in a host is probably an evolutionary mechanism evoked by the symbiotic state to allow successful colonisation of a host.

While apoptosis declined at Week 4 in most cases, it is notable that it declined as early as Week 1 in *D. trenchii*-colonised anemones. This earlier depression of apoptosis may have contributed to *D. trenchii* reaching the highest population density of all heterologous species during the first month of colonisation. If the response seen in Aiptasia also extends to other symbiotic systems, it perhaps explains , at least in part, *D. trenchii*'s success as a post-bleaching

opportunist (Stat and Gates 2010; Pettay *et al*., 2015). The mechanisms underlying this early suppression of apoptosis, and its links to *D. trenchii*'s opportunistic behaviour, are worthy of future work.

4.5.4. Cell cycle

Past studies have shown that, in culture, the Symbiodiniaceae cell cycle is intertwined with the light cycle, with cells entering G_1 during the light phase, and proceeding into G_2 and mitosis during the dark phase, with the total number of symbiont cells in the G_1/S and G_2/M phases peaking around five hours after light stimulation and five hours after dark stimulation, respectively (Wang *et al*., 2008; Fujise *et al*., 2018). During the current study, similar patterns were witnessed in the early stages of colonisation (and presumably log-growth phase of symbionts within host tissues) by the homologous *B. minutum,* where G_1 peaked eight hours after the light phase began, both one- and four-weeks post-colonisation.

At Weeks 1 and 4, 62.5-87.32% of the *B. minutum* population was in the G_1 phase, increasing to 87.34-91.88% at Week 24 when the symbiosis was fully-formed. This latter range is similar to that recorded at the long-term time point (78 weeks) as well as in the permanently-symbiotic anemones. Moreover, in a previous study of permanently-symbiotic Aiptasia, >80% of the resident symbiont population was in the G_1 phase (Smith and Muscatine 1999). When considered alongside the reduced rate of symbiont cell cycling as time in symbiosis progressed, it is apparent that, after 24 weeks in symbiosis, the symbiont population had reached a point where cell cycling was in homeostasis. As discussed above (Section 4.5.2), intracellular space limitation may again play a part in this pattern of events, with full occupancy of the host's cells eliciting the arrest of the symbiont cell cycle through an unknown mechanism (Jones and Yellowlees 1997), so operating in concert with the likes of expulsion and apoptosis to maintain symbiosis stability.

While cell-cycle arrest appeared to be important for maintaining host-symbiont biomass irrespective of symbiont identity, species-specific differences were apparent between the symbionts. Species-specific differences have been reported previously with, for example, homologous *B. minutum* having a larger proportion of its cells in the G_1 phase in Aiptasia than

another homologous symbiont, *Breviolum psygomophilum* (Tivey *et al*., 2020). In the current study, *B. minutum* passed through the cell cycle faster than any of the heterologous symbionts during the first month of colonisation. There is some evidence that this difference could be innate, as cultured *B. minutum* grows and progresses through its cell cycle more rapidly than *C. goreaui*, *D. trenchii* and *S. microadriaticum* when in log-phase growth (Klueter *et al*., 2017; Fujise *et al*., 2018). *D. trenchii*, in contrast, had the largest proportion of its population in the G_1 phase after six months in symbiosis. This suggests that cell-cycle arrest is a key mechanism for controlling proliferation of this opportunist, in addition to high rates of expulsion and host apoptosis. In addition to differences in innate growth rates between symbiont species, the differences in cell-cycle progression and the proportion of the population arrested in the G1 phase may be influenced by Symbiodiniaceae species possessing different cell-cycle genes (**Chapter 1**). However, even though we know that the state of symbiosis causes symbiont cell-cycle genes to differ in their expression in a homologous symbiosis (**Chapter 1**), whether the expression of these cell-cycle genes differs between Symbiodiniaceae species *in hospite* and corresponds to the differences observed here in the amount of cells in the G_1 phase, requires future investigation.

4.6. Conclusion

These findings emphasise that mechanisms employed to regulate host-symbiont biomass shift in their relative importance during the onset and establishment of symbiosis and are symbiont species-specific. A dampening of apoptosis may be important for facilitating the initial proliferation of the symbiont population, with symbiont expulsion increasing in relative importance at this time. Once the symbiosis is fully established though, the roles of cell-cycle arrest and increased host apoptosis become relatively more significant, working in concert with ongoing expulsion to regulate the long-term symbiosis. How these processes are co-ordinated at a cellular level, and how different symbionts induce the different responses observed, remains poorly understood and warrants future detailed exploration.

Chapter 5: General Discussion

5.1. Key findings

In addition to host-symbiont communication and optimal nutritional exchange between both partners, host-symbiont biomass co-ordination is integral to maintaining a stable symbiosis, ensuring that the algal symbiont does not outgrow the host but reaches densities sufficient to supply the host with the nutrients that it needs for its metabolism, growth, reproduction and survival (Muscatine 1990; Jones and Yellowlees 1997). The aim of this thesis was to further our understanding of how the host regulates its symbiont population on a molecular level, and how symbiont species and time in symbiosis influence this regulation. **Chapter 2** focused on the molecular mechanisms underpinning the symbiont cell cycle, as the arrest of the symbiont cell cycle has been proposed to be a major regulatory mechanism employed by the host to control its symbiont population (Smith and Muscatine 1999). **Chapter 2** also investigated whether this regulatory mechanism differed between different Symbiodiniaceae species. Key proteins involved in cell-cycle progression in eukaryotes are cyclins and cyclin-dependent kinases (CDKs), that regulate progression through cell-cycle checkpoints (Malumbres and Barbacid 2009). **Chapter 2** found several of these proteins across the Symbiodiniaceae, suggesting that they are indispensable for the symbiont cell cycle. One of these proteins (CDKB) was found across the majority of Symbiodiniaceae species studied and was related to both of the major cell-cycle CDKs found in yeast (*Saccharomyces cerevisiae*; Cdc28 and Pho85), emphasising that this protein may play a major regulatory role in the Symbiodiniaceae. The largest expansion of Symbiodiniaceae cyclin proteins found in **Chapter 2** was in groups related to the P/U cyclin proteins, which are also found in other single-celled eukaryotes. Several proteins were unique to certain Symbiodiniaceae species, such as cyclins found in *C. goreaui* and *D. trenchii,* which are both related to cyclins found in the opportunistic sister taxon, Apicomplexa. I found that several of the cell-cycle proteins discovered during my study switched in their expression in the symbiotic state. These findings emphasise how Symbiodiniaceae species have different protein repertoires that contribute to their proliferation and how the symbiotic association drastically alters the expression of genes involved in the progression of the symbiont cell cycle. These findings have progressed the field, by promoting our understanding of which Symbiodiniaceae cell-cycle genes are altered in the symbiotic state to arrest the symbiont cell cycle and maintain the stability of the symbiosis.

Chapter 3 focused on host-symbiont biomass co-ordination and how the presence of the symbiont induces gene expression changes in the host that allow host growth and the simultaneous persistence of the symbiont. Understanding the mechanisms that allow the persistence of a symbiont in the host and how these mechanisms may change under stress, leading to dysbiosis, is becoming increasingly important as coral bleaching is becoming more frequent due to climate change (Hughes *et al*., 2018). **Chapter 3** showed that the presence of a symbiont in the gastrodermal cells of a host leads to physiological changes in the host cell, e.g., reduced host cell division and DNA synthesis. Furthermore, the symbiont inhibited the expression of host genes that were upstream sensitisers of pathways that could lead to removal of the symbiont and dysbiosis e.g., ROS and apoptosis sensitisers. Moreover, genes that were involved in host immune responses to allow the persistence of 'non-self' cells were up-regulated in the gastrodermal cells, highlighting that the presence of a symbiont elicited an immune response in the host. Contrastingly, host cell division in the asymbiotic epidermal layer was stimulated by the presence of a symbiont in the gastrodermis, highlighting the nutritional benefits of the symbiosis to the whole polyp. These findings were further corroborated by microscopical analysis with an S-phase indicator (EdU), with significantly more host cells progressing through their cell cycle in the symbiotic gastrodermis and epidermis *versus* the aposymbiotic state.

Understanding how the host controls its symbiont population during the onset, establishment and maintenance of symbiosis, and how this control is impacted by the presence of heterologous (i.e. non-native) symbionts, provides important mechanistic information about the cellular events that underlie symbiosis success and host-symbiont specificity. **Chapter 4** reports that, during onset of symbiosis, symbiont identity influences the host's regulatory mechanisms, with the homologous symbiont (*B. minutum*) proliferating faster and reaching higher cell densities than heterologous symbionts. Meanwhile, while host apoptosis was dampened by the presence of all symbiont species, *D. trenchii* dampened host apoptosis earlier in the colonisation process than all other symbionts. This dampening of apoptosis allowed for proliferation of all symbiont species, with the relative importance of symbiont expulsion as a regulatory process increasing during this time. In contrast, symbiont cell-cycle arrest was not a major regulatory mechanism during symbiosis establishment, only becoming more important once the symbiosis was fully established. Nevertheless, symbiont species-specific differences

in the cell cycling rates were observed during symbiosis establishment, with more rapid proliferation of *B. minutum* being reflected in the highest rate of cell cycling.

While the findings described in this thesis represent an important step towards understanding host-symbiont biomass regulation and the stability of the cnidarian-dinoflagellate symbiosis, about which we previously knew little, we still have a long way to go. In particular, two broad questions arise from this thesis: (1) How can we leverage modern technologies to better understand the molecular and cellular events underlying host-symbiont regulation? And (2) what does our understanding of host-symbiont regulation tell us about the capacity for corals to adapt to climate change through acquiring new symbiotic partners that might be better adapted to the prevailing environmental conditions? Can we use this knowledge to aid efforts to conserve reefs? I will explore these questions further here.

5.2. How can we leverage modern technologies to help us to understand the molecular and cellular events underlying host-symbiont regulation?

A range of modern technologies have been developed that have the potential to accelerate our ability to understand the cnidarian-dinoflagellate symbiosis. Foremost among these are the 'omics', alongside advanced microscopical methods and gene editing approaches such as CRISPR/Cas9. The potential application of these technologies will be considered here in the context of the cnidarian-dinoflagellate symbiosis and Table 5.1 specifically refers to how these technologies can address further questions raised by the work done in this thesis.

Table 5.1. Questions arising in this thesis and proposed methods for addressing them.

Chapter	Questions raised	Technologies proposed to help address this question
Chapter 2	Which proteins correspond to specific cell-cycle checkpoints in Symbiodiniaceae, and do they differ between species?	Genomics Transcriptomics Proteomics Flow cytometry
	Does the expression of species-specific cell-cycle proteins correspond to the differences observed in cell-cycle progression and growth rates of different Symbiodiniaceae species both *ex* and *in hospite*?	Genomics Transcriptomics Proteomics Flow cytometry
	Do certain environmental conditions elicit a change in the expression of cell-cycle proteins *ex hospite* similar to the expression observed in *Breviolum minutum in hospite*, e.g. nitrogen starvation?	Genomics Transcriptomics Proteomics Flow cytometry
Chapter 3	How do symbionts move from one host cell to another during host cell division? Does host cell division disrupt vital structures of the symbiosis, i.e. symbiosome membrane complex? Does this explain why the presence of a symbiont reduces host cell division in the gastrodermis?	Live imaging confocal microscopy
	Would altering host genes that aid in the persistence of a compatible symbiont *in hospite* (apoptotic/ROS sensitisers and genes that allow persistence of 'non-self' cells) allow us to make a previously incompatible symbiont compatible? Or, allow a compatible but sub-optimal symbiont to colonise a host faster or reach densities similar to those of an optimal symbiont?	Gene editing technologies such as CRISPR/Cas9
Chapter 4	Do the patterns and mechanisms of host-symbiont biomass regulation, both during symbiosis establishment and maintenance, change under thermal stress?	Confocal microscopy Flow cytometry
	How do other aspects of the host-symbiont relationship, such as inter-partner signalling and nutritional exchange, change during symbiosis establishment and in what way are these linked to temporal shifts in the biomass regulation?	Genomics Transcriptomics Proteomics Metabolomics Confocal microscopy Flow cytometry

(a) 'Omics': Types of 'omics' technologies include, but are not limited to, genomics, transcriptomics, proteomics, and metabolomics (including lipidomics). These techniques allow us to characterise molecular networks and pathways, and assess how they are altered by a stimulus, so helping us to understand the phenotypic response of organisms to these stimuli (Joyce and Palsson 2006). In the cnidarian-dinoflagellate symbiosis, 'omics' methods have allowed us to understand the complex molecular interactions between host and symbiont, such as nutrient exchange, cell signalling and inter-partner communication, along with the regulation and co-ordination of host-symbiont biomass, and how variables such as environmental stress and symbiont identity influence these interactions (Meyer and Weis 2012; Parkinson *et al*., 2020; Rosset *et al*., 2020).

For instance, 'omics' have allowed us to understand the nutritional exchange that contributes to the symbiont supporting the host's metabolism and growth, including metabolomic confirmation of the forms in which photosynthate is translocated from symbiont to host (Burriesci *et al*., 2012; Chen *et al*., 2015; Hillyer *et al*., 2016) and proteomic characterisation of the transporters that regulate this translocation (Oakley *et al*., 2016). 'Omics' techniques have also allowed us to investigate the influence of symbiont identity on the nutritional flux and physiology of a symbiosis. For example, transcriptomic, proteomic and metabolomic analyses have revealed that symbiosis with a heterologous symbiont causes a reduction in the abundance and diversity of symbiosis-associated metabolites and signalling molecules in the host, and an up-regulation of oxidative stress and immunity pathways (Matthews *et al*., 2017, 2018; Sproles *et al*., 2019). This shift induces a physiological profile in the presence of heterologous symbionts that is midway between that in the presence of homologous symbionts and an aposymbiotic host (Matthews *et al*., 2017). Along with differences in nutritional fluxes and symbiosis-associated molecules, transcriptomics and proteomics have revealed that, in a compatible symbiosis, host gene expression does not differ greatly from that seen in aposymbiotic hosts, but differs greatly from that in a host containing a less compatible symbiont type (Barneah *et al*., 2006; Rodriguez-Lanetty *et al*., 2006a; Voolstra *et al*., 2009).

Inter-partner signalling between host and symbiont cells is a vital component of the formation and maintenance of a symbiosis, and is likely to involve many families of signalling molecules such as glycans, sterols, oxylipins and sphingolipids that have varying roles from phagocytosis

initiation to immune responses (Rosset *et al*., 2020). Different symbiont species have been shown to possess different compositions of signalling molecules on their cell surface (Parkinson *et al*., 2018), and the composition of these signalling molecules has been shown to influence a symbiont's success in the colonisation of a host (Bay *et al*., 2011; Parkinson *et al*., 2018). 'Omics' technologies have allowed us to start to document which host and symbiont signalling molecules change in their expression with symbiotic state, what host-symbiont signalling molecules are expressed during a successful symbiosis, and how symbiont identity or environmental stress influence this expression. For instance, transcriptomics and proteomics have revealed that, upon successful colonisation of a host, the presence of a homologous symbiont down-regulates the expression of host oxylipins (such as lipoxygenase) and host sphingolipid sphingosine-1-phosphate phosphatase (SPGG) (Lehnert *et al*., 2014), whilst the sterol transporter Niemann–Pick type C2-like protein (NPC2) is up-regulated (Oakley *et al*., 2016). However, this same expression of host oxylipins and NPC2 signalling molecules was not observed in symbiosis with a heterologous symbiont (Matthews *et al*., 2017; Sproles *et al*., 2019), highlighting species-specific differences in communication between the host and symbiont. 'Omics' have previously helped us to understand how the aspects underpinning a stable symbiosis (such as host-symbiont regulatory mechanisms and inter-partner signalling) are related, with transcriptomic analysis revealing that symbionts cause an increase in the accumulation of the pro-survival signalling molecule sphingosine-1-phosphate (S1P) rheostat in the host that leads to decreases in host pro-apoptotic genes and increases in host cell-cycle proliferation (Rodriguez-Lanetty *et al*., 2006a). My thesis built upon these findings using transcriptomics, investigating host gene expression on a tissue-specific level. I revealed that symbiont presence stimulates host cell-cycle progression in the epidermis but reduces cell division in the gastrodermis (**Chapter 3**), highlighting that signalling may vary between host tissue types.

In addition to fundamental functional aspects of the symbiosis, 'omics' technologies also allow us to predict population-wide responses to environmental factors such as climate change and other environmental stresses. For example, transcriptomics has demonstrated that elevated temperatures cause increased expression of genes involved in host growth arrest, nucleic acid stabilisation and repair, and calcification (DeSalvo *et al*., 2010; Kenkel *et al*., 2013). Proteomics has revealed that thermal stress induces a destruction of host proteostasis and an increased abundance of proteins involved in antioxidant pathways and the degradation of

damaged proteins (Oakley *et al*., 2017). Metabolomic analysis has shown that thermally-stressed symbionts continue to translocate photosynthetic products to the host at a cost to themselves by catabolising their own energy reserves (Hillyer *et al*., 2017). Heat stress has also been shown to influence the expression of cell signalling molecules in the host, with gene expression analysis revealing that initial thermal stress in a cnidarian host caused the suppression of pro-survival sphingolipid SPGG, though SPGG level increased after more prolonged stress (Kitchen and Weis 2017). The power of 'omics' for unravelling the complexities of symbiosis function and coral bleaching is therefore very clear. I recommend greater application of 'omics' technologies for increasing our understanding of host-symbiont biomass regulation, particularly focusing on the unanswered questions arising from this thesis (see Table 5.1).

(b) Advanced microscopical methods: Advances in the resolution of microscopy have allowed us to investigate the partner dynamics of the host and symbiont *in hospite*, with techniques such as fluorescent labelling and immunocytochemistry enabling us to measure parameters such as host and symbiont cell-cycle co-ordination or to locate symbiosis-related proteins. For example, a recent study used microscopy and fluorescent labelling to measure host and symbiont cell-cycle progression and co-ordination *in hospite* in Aiptasia (Tivey *et al*., 2020). This current study also used these techniques to measure, over time in symbiosis, symbiont expulsion and symbiont cell-cycle progression in Aiptasia colonised by different Symbiodiniaceae species (**Chapter 4**). These techniques have allowed me to investigate how cnidarian hosts regulate their symbiont population over time and how symbiont identity influences these regulatory mechanisms.

Microscopical advances, in conjunction with 'omics' technologies, have also allowed us to find genes or proteins of interest, predict their function and then to locate them in the symbiotic association (Meyer and Weis 2012; Dani *et al*., 2017). These methodological advances have facilitated preliminary investigations of especially challenging aspects of the cnidarian-dinoflagellate symbiosis, such as the nature of symbiosome-associated proteins. The symbiosome is fundamental and indispensable to the symbiotic relationship between the host and symbiont, as it is a gateway for nutrient trafficking in the symbiosis and communication between the two partners (Yellowlees *et al*., 2008). A previous study using proteomics has

identified possible symbiosome-associated proteins (Peng *et al*., 2010), and following this a study by Dani *et al*. (2017) used immunolocalisation and immunogold labelling combined with transmission electron microscopy that allowed the localisation of the sterol transporter NPC2 to the symbiosome membrane. Future work will need to repeat these methodologies in order to localise the full suite of transporters likely to exist at the symbiont-host interface.

In addition to further symbiosome-characterisation, which will inform our understanding of host-symbiont communication and biomass regulation, advances in microscopy coupled with 'omics' technologies can help to address some of the questions arising in this thesis (Table 5.1). For instance, **Chapter 3** highlighted that symbiosis alters many host genes to allow persistence of a symbiont in a gastrodermal cell, and that one of these changes is the down-regulation of host genes associated with host cell division in the gastrodermis. We still do not know how symbionts move between gastrodermal cells during host cell division. In addition, we do not know what happens to the symbiosome during host cell division. Thus, future work should use confocal live imaging microscopy to characterise these events. This work may help us to understand why DNA synthesis and mitosis are down-regulated in host gastrodermal cells during symbiosis.

(c) CRISPR gene editing: Gene-editing technologies are a logical next step from 'omics' technologies, which have pinpointed genes of interest in the cnidarian-dinoflagellate symbiosis in response to symbiont compatibility and environmental stress events. In recent years, a gene-editing technology known as CRISPR/Cas9 has been developed that allows more affordable, high-throughput gene-editing of organisms, and which is likely to have a profound impact on the cnidarian-dinoflagellate field. CRISPR allows us to pick a single gene to knock out and, once this gene is knocked out, researchers can compare between organisms that have been genetically altered ('mutants') and a control population that has not been manipulated ('wild type'), so elucidating gene function (Levin *et al*., 2017). CRISPR not only allows gene knock-out, but also allows genes to be edited. Studies have already started applying CRISPR gene-editing technologies to the cnidarian-dinoflagellate symbiosis and it has been shown to be effective in producing knock-outs in larvae of the coral *Acropora millepora* (Cleves *et al*., 2018) and the non-symbiotic sea anemone *Nematostella vectensis* (Ikmi *et al*., 2014). The successful knockout of genes in these cnidarians has meant that studies have now begun to

monitor the biological response of genes of interest. For example, a recent study has shown that the neuropeptide Wamide family elicits metamorphosis in *N. vectensis*, with its knock-out producing mutants with slower metamorphic progression (Nakanishi and Martindale 2018). Additionally, knock-out of the heat shock transcription factor HSF1 in *A. millepora* determined the survival rate of larvae under thermal stress, with mutants surviving at 27 °C but dying rapidly at 34 °C (Cleves *et al*., 2020). In the model cnidarian Aiptasia, successful microinjection of exogenous protein, mRNA and DNA into larvae has been achieved (Jones *et al*., 2018), allowing future studies to utilise this method for CRISPR/Cas9 gene editing. The successful genetic editing of the model organism Aiptasia will propel research on the cnidarian-dinoflagellate symbiosis, due to the ease of keeping Aiptasia under laboratory conditions (both in the symbiotic and aposymbiotic state) and the success in inoculating Aiptasia hosts with multiple different Symbiodiniaceae species (Weis *et al*., 2008; Chen *et al*., 2016; Hawkins *et al*., 2016; Gabay *et al*., 2018).

Although the future of applying CRISPR/Cas9 to advancing the field of the cnidarian-dinoflagellate symbiosis is becoming more optimistic, one hurdle to CRISPR/Cas9 technology will be optimising the method for Symbiodiniaceae, with efforts so far proving unsuccessful due to several obstacles. These obstacles include the condensed chromosomes of Symbiodiniaceae that could limit access to the site of interest, multi-copy genes in Symbiodiniaceae genomes making gene editing harder, as multi-copy genes have increased risk of DNA damage and cell death, and the unavailability of fully sequenced Symbiodiniaceae genomes (Levin *et al*., 2017). This being said, an analysis of possible candidate genes in Symbiodiniaceae that are suitable for gene-editing found 261 single-copy genes conserved across all three fully-sequenced Symbiodiniaceae genomes containing an optimal target site (Levin *et al*., 2017). Thus, although difficult, there are possibilities for Symbiodiniaceae genome editing and, coupled with the gene editing of cnidarian hosts, these techniques could provide a means of manipulating functional attributes of the symbiosis, so elucidating its function, including that of biomass regulation.

Ultimately, ‘omics’ technologies allow us to pinpoint genes of interest and to predict their function within biological pathways, and the advent of CRISPR/Cas9 gene editing allows us to investigate how altering these genes and their subsequent pathways can facilitate the

persistence and stabilisation of the cnidarian-dinoflagellate symbiosis. This would allow us to tailor previously suboptimal symbioses to a mutually beneficial symbiosis in the changing climate. Specifically, CRISPR/Cas9 could help further the understanding of host-symbiont biomass co-ordination by pinpointing genes found within this thesis (**Chapters 2 and 3**) that lead to the successful colonisation of a host through the interaction of the regulatory mechanisms shown in **Chapter 4**. For instance, would switching off host genes whose down-regulation allows the persistence of a symbiont, e.g. apoptotic and ROS sensitisers (**Chapter 3**), using CRISPR/Cas9, reduce the degradation and expulsion of a symbiont from the host (**Chapter 4**)? Or, would editing heterologous symbiont cell-cycle checkpoint proteins (CDKs and cyclins (**Chapter 2**)) to resemble those of a homologous symbiont, allow heterologous species to progress through their cell cycle faster *in hospite* similar to a homologous species, as seen in **Chapter 4**, and therefore reach higher densities in their host?

5.3. What does our understanding of host-symbiont regulation tell us about the capacity for corals to adapt to climate change? Can we use this knowledge to aid effort to conserve reefs?

Coral reefs are one of the world's most vulnerable ecosystems, facing extinction from climate change (Duarte *et al*., 2020). The adoption of the Paris Agreement has set limits to carbon dioxide emissions and global warming, aiming to limit global warming to under 1.5 °C above pre-industrial levels (Rogelj *et al*., 2016). However, globally, 71% of coral reefs have already warmed by 0.25 – 0.75 °C since the late nineteenth century (Hughes *et al*., 2017), and even under the most ambitious scenario of limiting warming to this 1.5 °C target, it is estimated that 70-90% of coral reefs will be subject to degradation (Hoegh-Guldberg *et al*., 2018). In addition to increased temperature, climate change is creating other risks to coral reefs, such as ocean hypoxia and acidification (IPCC 2013; Hughes *et al*., 2020). Ocean pH has already decreased by 0.1 pH units and the concentration of carbonate (that corals need in order to calcify their skeleton) is the lowest it has ever been during the last 420,000 years (Hoegh-Guldberg *et al*., 2007).

The main reason that corals are extremely vulnerable to climate change is that stressful conditions lead to the dysbiosis between the coral host and its symbionts, and the subsequent bleaching of the symbiont population, without which the coral cannot survive for extended

periods (Hoegh-Guldberg 1999). Bleaching occurs under stressful conditions, such as temperature stress, causing both the coral and its symbionts to release stress molecules such as nitric oxide and reactive oxygen species (ROS), and once the levels of these stress molecules surpass a threshold, a bleaching cascade is initiated (Weis 2008; Oakley and Davy 2018). To avoid post-bleaching in nutrient poor waters, there is a limited window of time for the coral to regain its complement of symbionts. There are currently two proposed mechanisms for this. One mechanism involves the coral 'switching' its whole resident symbiont population and developing an association with a more thermally tolerant one (Buddemeier and Fautin 1993; Baker 2003). However, whether symbiont switching occurs in the field has been contested (Cunning *et al*., 2015), although advances in the sensitivity of sequencing Symbiodiniaceae species is allowing more clarity into the debate of whether corals have the ability to switch their symbionts explicitly (see Boulotte *et al.*; Huang *et al*., 2020). Symbiont switching can however, be induced under laboratory conditions (Coffroth *et al*., 2010; Silverstein *et al*., 2015; Gabay *et al*., 2019). The second mechanism involves a coral 'shuffling' its resident symbiont community, causing a shift to a greater presence, or even dominance, of a more thermally tolerant symbiont species that previously represented a cryptic component of the resident symbiont population (Buddemeier and Fautin 1993; Baker 2003). Whatever the mechanism by which the symbiont community changes, a shift to a different dominant symbiont partner can, in some instances, induce physiological costs and stresses to the host (Starzak *et al*., 2014; Hawkins *et al*., 2016; Matthews *et al*., 2017; Baker *et al*., 2018; Sproles *et al*., 2019; Cunning and Baker 2020), as well as shifts in the competitive interactions between the different symbiont types (McIlroy *et al*., 2020). However, the potential to confer a degree of thermal resistance could nevertheless be of critical importance when considering the future survival of coral reefs (Cunning *et al*., 2015; Silverstein *et al*., 2015).

Chapter 4 provides further evidence that cnidarian hosts have the capacity to maintain a stable symbiosis with various heterologous symbiont species (at least under laboratory conditions), with the ability to regulate host-symbiont biomass in a co-ordinated manner. The precise timings and scales of these regulatory processes during the onset and establishment of the symbiosis does differ, however, between different symbiont types, meaning that some symbionts are more likely to dominate than others; innate differences in the growth rate of different Symbiodiniaceae species are also an important consideration in this regard (Fujise *et al*., 2018). For instance, does the earlier apoptotic suppression of a host by *D. trenchii* facilitate

its opportunistic colonisation of bleached hosts (Stat and Gates 2010; Leal *et al*., 2015; Pettay *et al*., 2015)? Or, does the high cell-cycling rate of *B. minutum* in Aiptasia allow it competitively to exclude other symbiont types, explaining the high degree of host-symbiont specificity seen in this anemone in the Pacific (Thornhill *et al*., 2013)? This latter scenario is certainly consistent with the dominance of this homologous symbiont species over heterologous symbionts (*D. trenchii* and *S. microadriaticum*) when these symbionts are inoculated simultaneously into Aiptasia under non-stressful conditions (Gabay *et al*., 2019). Further work should aim to elucidate the relative importance of various regulatory processes during symbiosis onset and establishment *via* mathematical modelling, expanding upon the statistical approach used in this thesis to understand better the control of uni- and multi-species symbiont populations, and the cellular basis of host-symbiont specificity. Moreover, such an approach could be applied to the symbiont population under a range of environmental scenarios, such as different irradiances and nutrient availabilities, and across a range of times. This would provide greater insight into how the symbiosis acclimatises and responds to environmental change, including climate change (Fig. 5.1).

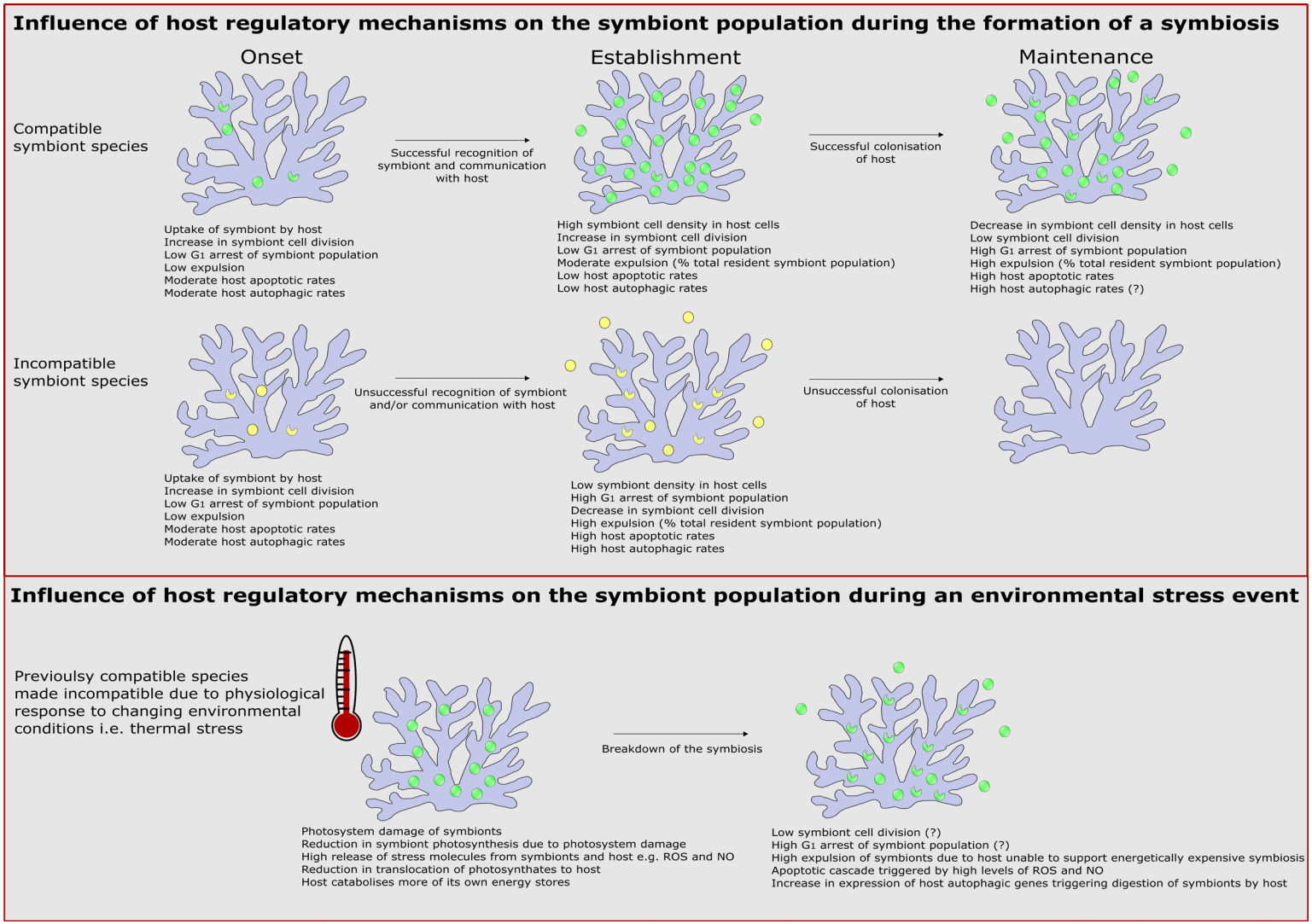

Figure 5.1. Influence of host regulatory mechanisms of the symbiont population during the formation of a symbiosis with a compatible and incompatible symbiont species and a thermal stress event. Question marks (?) correspond to hypothesised reactions.

Heat stress unquestionably influences host-symbiont biomass regulation, with more symbionts being actively expelled from the host (Fujise *et al*., 2014) and host apoptotic levels being elevated (Paxton *et al*., 2013) under heat stress. This highlights the need for future work to consider not only the underlying mechanisms of host-symbiont biomass regulation, but how thermal stress impacts these pathways. We should build upon **Chapter 4** by measuring host regulatory mechanisms under coral bleaching thresholds (≥ 0.4 - 1 °C above mean SST (Donner 2011)), as well as temperatures that reflect the predicted increase in the average temperature by 2100 years (~ +2°C (Hoegh-Guldberg *et al*., 2007)) and beyond. Moreover, to place findings from the model Aiptasia system into a broader ecological context, the impact of thermal regime (both short- and long-term) on host-symbiont biomass regulation needs to be tested in a range of coral species.

This approach will allow us, when combined with a suite of 'omics' approaches (see above), to confirm the elusive biochemical link(s) between the cellular stress pathways and the organismal events that lead to dysfunction and coral bleaching. Such knowledge might be critical, as it could provide a platform for engineering more thermally-resistant corals, for instance by CRISPR gene-editing (see above). When combined with improved understanding of nutritional exchange and inter-partner communication, a detailed understanding of host-symbiont biomass regulation might allow us to develop molecular tools by which less successful (but nutritionally beneficial) symbionts can be encouraged to form an optimal and persistent symbiosis with a new host (Parkinson *et al*., 2020; Rosset *et al*., 2020).

5.4. Conclusion

In conclusion, my thesis provides novel information on the molecular and cellular basis of biomass regulation in the cnidarian-dinoflagellate symbiosis, as well as the relative importance of the various regulatory mechanisms during symbiosis establishment and beyond. However, this is just a first step and we still have a huge amount to learn. In particular, sizeable knowledge gaps exist with respect to: (1) the cellular pathways that link inter-partner recognition to the discriminatory and regulatory processes that produce observable patterns of host-symbiont specificity; (2) how fixed these responses are to particular symbiont species and whether there is capacity for temporal shifts; and (3) what the implications might be for the adaptability of corals and other symbiotic cnidarians to adapt to climate change. Unravelling such

complexities is of paramount importance for understanding and predicting the future of the world's threatened coral reefs, and for potentially developing manipulative genomic (i.e. gene-editing) tools for enhancing the resilience of reefs to our warming climate.

References

Abraham RT (2001) Cell cycle checkpoint signaling through the ATM and ATR kinases. *Genes & Development*, **15**(17), 2177–96.

Alexa A, Rahnenführer J, Lengauer T (2006) Improved scoring of functional groups from gene expression data by decorrelating GO graph structure. *Bioinformatics*, **22**(13), 1600–1607.

Alexander A, Cai SL, Kim J, Nanez A, Sahin M, MacLean KH, Inoki K, Guan KL, Shen J, Person MD, Kusewitt D (2010) ATM signals to TSC2 in the cytoplasm to regulate mTORC1 in response to ROS. *Proceedings of the National Academy of Sciences USA*, **107**(9), 4153–58.

Alvarez CA, Suvorova ES (2017) Checkpoints of apicomplexan cell division identified in *Toxoplasma gondii*. *PLoS Pathogens*, **13**(7), e1006483.

Ang XL, Harper JW (2005) SCF-mediated protein degradation and cell cycle control. *Oncogene*, **24**(17), 2860-70.

Anisimova M, Gascuel O (2006) Approximate likelihood-ratio test for branches: a fast, accurate, and powerful alternative. *Systematic Biology*, **55**(4), 539–52.

Ao X, Zou L, Wu Y (2014) Regulation of autophagy by the Rab GTPase network. *Cell Death and Differentiation*, **21**(3), 348-58.

Aranda M, Li Y, Liew YJ, Baumgarten S, Simakov O, Wilson MC, Piel J, Ashoor H, Bougouffa S, Bajic VB, Ryu T (2016) Genomes of coral dinoflagellate symbionts highlight evolutionary adaptations conducive to a symbiotic lifestyle. *Scientific Reports*, **6**(1), 1-15.

Arriola MB, Velmurugan N, Zhang Y, Plunkett MH, Hondzo H, Barney BM (2018) Genome sequences of *Chlorella sorokiniana* UTEX 1602 and *Micractinium conductrix* SAG 241.80: implications to maltose excretion by a green alga. *The Plant Journal*, **93**(3), 566–86.

Atikukke G, Albosta P, Zhang H, Finley Jr RL (2014) A role for *Drosophila* Cyclin J in oogenesis revealed by genetic interactions with the piRNA pathway. *Mechanisms of Development*, **133**, 64–76.

Awasthi P, Foiani M, Kumar A (2015) ATM and ATR signaling at a glance. *Journal of Cell Science*, **128**(23), 4255–62.

Bäckhed F, Ley RE, Sonnenburg JL, Peterson DA, Gordon JI (2005) Host-bacterial mutualism in the human intestine. *Science*, **307**(5717), 1915–20.

Baghdasarian G, Muscatine L (2000) Preferential expulsion of dividing algal cells as a mechanism for regulating algal-cnidarian symbiosis. *The Biological Bulletin*, **199**(3), 278–86.

Bailey GF, Coelho JC, Poole AZ (2020) Differential expression of *Exaiptasia pallida* GIMAP genes upon induction of apoptosis and autophagy suggests a potential role in cnidarian symbiosis and disease. *Journal of Experimental Biology*, **223**(21), jeb229906.

Baker AC, Cunning R (2016) Bulk gDNA extraction from coral samples. *Protocols. io*. Available at: https://www.protocols.io/view/Bulk-gDNA-extraction-from-coral-samples-dyq7vv

Baker AC (2001) Reef corals bleach to survive change. *Nature*, **411**(6839), 765-6.

Baker AC **(**2003) Flexibility and specificity in coral-algal symbiosis: diversity, ecology, and biogeography of *Symbiodinium*. *Annual Review of Ecology, Evolution, and Systematics*, **34**(1), 661–89.

Baker AC, Glynn PW, Riegl B (2008) Climate change and coral reef bleaching: An ecological assessment of long-term impacts, recovery trends and future outlook. *Estuarine, Coastal and Shelf Science*, **80**(4), 435–71.

Baker DM, David M, Andras JP, Jordán-Garza AG, Fogel ML (2013b) Nitrate competition in a coral symbiosis varies with temperature among *Symbiodinium* clades. *The ISME Journal*, **7**(6), 1248-51.

Baker DM, Freeman CJ, Wong JCY, Fogel ML, Knowlton N (2018) Climate change promotes parasitism in a coral symbiosis. *The ISME Journal*, **12**(3), 921-30.

Baker DM, Weigt L, Fogel M, Knowlton N (2013a) Ancient DNA from coral-hosted *Symbiodinium* reveal a static mutualism over the last 172 years. *PLoS One*, **8**(2), e55057.

Bardin AJ, Amon A (2001) Men and sin: what's the difference? *Nature Reviews Molecular Cell Biology*, **2**(11), 815-26.

Barneah O, Benayahu Y, Weis VM (2006) Comparative proteomics of symbiotic and aposymbiotic juvenile soft corals. *Marine Biotechnology*, **8**(1), 11–16.

Barnum KJ, O'Connell MJ (2014) Cell-cycle regulation by checkpoints. In: Cell Cycle Control, Humana Press, New York (NY) 29–40.

Barott KL, Venn AA, Perez SO, Tambutté S, Tresguerres M (2015) Coral host cells acidify symbiotic algal microenvironment to promote photosynthesis. *Proceedings of the National Academy of Sciences USA*, **112**(2), 607–12.

Bashir T, Dorrello NV, Amador V, Guardavaccaro D, Pagano M (2004) Control of the SCF Skp2–Cks1 ubiquitin ligase by the APC/C Cdh1 ubiquitin ligase. *Nature*, **428**(6979), 190-93.

Bassermann F, Frescas D, Guardavaccaro D, Busino L, Peschiaroli A, Pagano M (2008) The Cdc14B-Cdh1-Plk1 axis controls the G_2 DNA-damage-response checkpoint. *Cell*, **134**(2), 256–67.
Baumgarten S, Simakov O, Esherick LY, Liew YJ, Lehnert EM, Michell CT, Li Y, Hambleton EA, Guse A, Oates ME, Gough J (2015) The genome of Aiptasia, a sea anemone model for coral symbiosis. *Proceedings of the National Academy of Sciences USA*, **112**(38), 11893–98.
Baumgarten S, Cziesielski MJ, Thomas L, Michell CT, Esherick LY, Pringle JR, Aranda M, Voolstra CR (2018) Evidence for mi RNA-mediated modulation of the host transcriptome in cnidarian–dinoflagellate symbiosis. *Molecular Ecology*, **27**(2), 403–18.
Bay LK, Doyle J, Logan M, Berkelmans R (2016) Recovery from bleaching is mediated by threshold densities of background thermo-tolerant symbiont types in a reef-building coral. *Royal Society Open Science*, **3**(6), 160322.
Bay LK, Cumbo VR, Abrego D, Kool JT, Ainsworth TD, Willis BL (2011) Infection dynamics vary between *Symbiodinium* types and cell surface treatments during establishment of endosymbiosis with coral larvae. *Diversity*, **3**(3), 356–74.
Bayer T, Aranda M, Sunagawa S, Yum LK, DeSalvo MK, Lindquist E, Coffroth MA, Voolstra CR, Medina M (2012) *Symbiodinium* transcriptomes: genome insights into the dinoflagellate symbionts of reef-building corals. *PloS One*, **7**(4), e35269.
Berner T, Baghdasarian G, Muscatine L (1993) Repopulation of a sea anemone with symbiotic dinoflagellates: analysis by *in vivo* fluorescence. *Journal of Experimental Marine Biology and Ecology*, **170**(2), 145–58.
Berthelier J, Schnitzler CE, Wood-Charlson EM, Poole AZ, Weis VM, Detournay O (2017) Implication of the host TGFβ pathway in the onset of symbiosis between larvae of the coral *Fungia scutaria* and the dinoflagellate *Symbiodinium* sp.(clade C1f). *Coral Reefs*, **36**(4), 1263–68.
Bertoli C, Skotheim JM, De Bruin RA (2013) Control of cell-cycle transcription during G_1 and S phases. *Nature reviews Molecular Cell Biology*, **14**(8), 518-28.
Bingham BL, Dimond JL, Muller-Parker G (2014) Symbiotic state influences life-history strategy of a clonal cnidarian. *Proceedings of the Royal Society of London B: Biological Sciences*, **281**(1789), 20140548.
Black CC, Burris JE (1983) Diurnal carbon-14 partitioning between zooxanthellae and the coral animal tissue of intact *Seriatopora hystrix* colonies. *Marine Biology*, **75**(2), 117–20.
Blackford AN, Jackson SP (2017) ATM, ATR, and DNA-PK: the trinity at the heart of the DNA damage response. *Molecular Cell*, **66**(6), 801–17.
Blackstone N (2009) Mitochondria and the redox control of development in cnidarians. *Seminars in Cell & Developmental Biology*, **20**(3), 330–36.
Blanc G, Duncan G, Agarkova I, Borodovsky M, Gurnon J, Kuo A, Lindquist E, Lucas S, Pangilinan J, Polle J, Salamov A (2010) The *Chlorella variabilis* NC64A genome reveals adaptation to photosymbiosis, coevolution with viruses, and cryptic sex. *The Plant Cell*, **22**(9), 2943–55.
Bolanos-Garcia VM, Blundell TL (2011) BUB1 and BUBR1: multifaceted kinases of the cell cycle. *Trends in Biochemical Sciences*, **36**(3), 141–50.
Boulotte NM, Dalton SJ, Carroll AG, Harrison PL, Putnam HM, Peplow LM, Van Oppen MJ (2016) Exploring the *Symbiodinium* rare biosphere provides evidence for symbiont switching in reef-building corals. *The ISME Journal*, **10**(11), 2693-2701.
Braun TE, Poole E, Sinclair J (2012) Depletion of cellular pre-replication complex factors results in increased human cytomegalovirus DNA replication. *PloS One*, **7**(5), e36057.
Bray NL, Pimentel H, Melsted P, Pachter L (2016) Near-optimal probabilistic RNA-seq quantification. *Nature Biotechnology*, **34**(5), 525–27.
Bremmer SC, Hall H, Martinez JS, Eissler CL, Hinrichsen TH, Rossie S, Parker LL, Hall MC, Charbonneau H (2012) Cdc14 phosphatases preferentially dephosphorylate a subset of cyclin-dependent kinase (Cdk) sites containing phosphoserine. *Journal of Biological Chemistry*, **287**(3), 1662–69.
Bretones G, Delgado MD, León J (2015) Myc and cell-cycle control. *Biochimica et Biophysica Acta (BBA)-Gene Regulatory Mechanisms*, **1849**(5), 506–16.
Brinkkoetter PT, Olivier P, Wu JS, Henderson S, Krofft RD, Pippin JW, Hockenbery D, Roberts JM, Shankland SJ (2009) Cyclin I activates CDK5 and regulates expression of Bcl-2 and Bcl-XL in postmitotic mouse cells. *The Journal of Clinical Investigation*, **119**(10), 3089–3101.
Brown BE, Le Tissier MDA, Bythell JC (1995) Mechanisms of bleaching deduced from histological studies of reef corals sampled during a natural bleaching event. *Marine Biology*, **122**(4), 655–63.
Buddemeier RW, Fautin DG (1993) Coral bleaching as an adaptive mechanism. *Bioscience*, **43**(5), 320–26.
Burriesci MS, Raab TK, Pringle JR (2012) Evidence that glucose is the major transferred metabolite in dinoflagellate–cnidarian symbiosis. *Journal of Experimental Biology*, **215**(19), 3467–77.
Cantin NE, van Oppen MJ, Willis BL, Mieog JC, Negri AP (2009) Juvenile corals can acquire more carbon from high-performance algal symbionts. *Coral Reefs*, **28**(2), 405.

Cao L, Chen F, Yang X, Xu W, Xie J, Yu L (2014) Phylogenetic analysis of CDK and cyclin proteins in premetazoan lineages. *BMC Evolutionary Biology*, **14**(1): 10.
Carroll AS, O'Shea EK (2002) Pho85 and signaling environmental conditions. *Trends in Biochemical Sciences*, **27**(2), 87–93.
Cato ML, Jester HD, Lavertu A, Lyman A, Tallent LM, Mitchell GC (2019) Genome-wide analysis of cell cycle-regulating genes in the symbiotic dinoflagellate *Breviolum minutum*. *G3: Genes, Genomes, Genetics*, **9**(11), 3843-3853.
Chance B, Sies H, Boveris A (1979) Hydroperoxide metabolism in mammalian organs. *Physiological Reviews*, **59**(3), 527–605.
Chaston J, Douglas AE (2012) Making the most of 'omics' for symbiosis research. *The Biological Bulletin*, **223**(1), 21–29.
Chen HK, Song SN, Wang LH, Mayfield AB, Chen YJ, Chen WNU, Chen CS (2015) A compartmental comparison of major lipid species in a coral-*Symbiodinium* endosymbiosis: evidence that the coral host regulates lipogenesis of its cytosolic lipid bodies. *PLoS One*, **10**(7), e0132519.
Chen HK, Wang LH, Chen WNU, Mayfield AB, Levy O, Lin CS, Chen CS (2017) Coral lipid bodies as the relay center interconnecting diel-dependent lipidomic changes in different cellular compartments. *Scientific Reports*, **7**(1), 1-13.
Chen J, Wu X, Lin J, Levine AJ (1996) Mdm-2 inhibits the G_1 arrest and apoptosis functions of the p53 tumor suppressor protein. *Molecular and Cellular Biology*, **16**(5), 2445–52.
Chen MC, Cheng YM, Hong MC, Fang LS (2004) Molecular cloning of Rab5 (ApRab5) in *Aiptasia pulchella* and its retention in phagosomes harboring live zooxanthellae. *Biochemical and Biophysical Research Communications*, **324**(3), 1024–33.
Chen MC, Cheng YM, Sung PJ, Kuo CE, Fang LS (2003) Molecular identification of Rab7 (ApRab7) in *Aiptasia pulchella* and its exclusion from phagosomes harboring zooxanthellae. *Biochemical and Biophysical Research Communications*, **308**(3), 586–95.
Chen MC, Hong MC, Huang YS, Liu MC, Cheng YM, Fang LS (2005) ApRab11, a cnidarian homologue of the recycling regulatory protein Rab11, is involved in the establishment and maintenance of the Aiptasia–*Symbiodinium* endosymbiosis. *Biochemical and Biophysical Research Communications*, **338**(3), 1607–16.
Chen WNU, Hsiao YJ, Mayfield AB, Young R, Hsu LL, Peng SE (2016) Transmission of a heterologous clade C *Symbiodinium* in a model anemone infection system via asexual reproduction. *PeerJ*, **4**, e2358.
Chen Y, González-Pech RA, Stephens TG, Bhattacharya D, Chan CX (2020) Evidence that inconsistent gene prediction can mislead analysis of dinoflagellate genomes. *Journal of Phycology*, **56**(1), 6-10.
Clair SS, Giono L, Varmeh-Ziaie S, Resnick-Silverman L, Liu WJ, Padi A, Dastidar J, DaCosta A, Mattia M, Manfredi JJ (2004) DNA damage-induced down-regulation of Cdc25C is mediated by p53 via two independent mechanisms: one involves direct binding to the cdc25C promoter. *Molecular Cell*, **16**(5), 725–36.
Clercq AD, Inzé D (2006) Cyclin-dependent kinase inhibitors in yeast, animals, and plants: a functional comparison. *Critical Reviews in Biochemistry and Molecular Biology*, **41**(5), 293–313.
Cleves PA, Strader ME, Bay LK, Pringle JR, Matz MV (2018) CRISPR/Cas9-mediated genome editing in a reef-building coral. *Proceedings of the National Academy of Sciences USA*, **115**(20), 5235–40.
Cleves PA, Tinoco AI, Bradford J, Perrin D, Bay LK, Pringle JR (2020) Reduced thermal tolerance in a coral carrying CRISPR-induced mutations in the gene for a heat-shock transcription factor. *Proceedings of the National Academy of Sciences USA*, **117**(46), 28899–905.
Clijsters L, Hoencamp C, Calis JJ, Marzio A, Handgraaf SM, Cuitino MC, Rosenberg BR, Leone G, Pagano M (2019) Cyclin F controls cell-cycle transcriptional outputs by directing the degradation of the three activator E2Fs. *Molecular Cell*, **74**(6), 1264–77.
Coffroth MA, Poland DM, Petrou EL, Brazeau DA, Holmberg JC (2010) Environmental symbiont acquisition may not be the solution to warming seas for reef-building corals. *PLoS One*, **5**(10), e13258.
Cook CB (1971) Transfer of ^{35}S-labeled material from food ingested by Aiptasia sp. to its endosymbiotic zooxanthellae. In: Experimental Coelenterate Biology, University of Hawaii Press, 218–24.
Cook CB (1972) Benefit to symbiotic zoochlorellae from feeding by green hydra. *The Biological Bulletin*, **142**(2), 236–42.
Cook CB, D'Elia CF (1987) Are natural populations of zooxanthellae ever nutrient-limited? *Symbiosis*, **4**, 199-212.
Cook CB, D'Elia CF, Muller-Parker G (1988) Host feeding and nutrient sufficiency for zooxanthellae in the sea anemone *Aiptasia pallida*. *Marine Biology*, **98**(2), 253–62.
Corellou F, Camasses A, Ligat L, Peaucellier G, Bouget FY (2005) Atypical regulation of a green lineage-specific B-type cyclin-dependent kinase. *Plant Physiology*, **138**(3), 1627–36.

Correa CC, Ballard JW (2016) Wolbachia associations with insects: winning or losing against a master manipulator. *Frontiers in Ecology and Evolution*, **3**, 153.
Cui G, Liew YJ, Li Y, Kharbatia N, Zahran NI, Emwas AH, Eguiluz VM, Aranda M (2019) Host-dependent nitrogen recycling as a mechanism of symbiont control in Aiptasia. *PLoS Genetics*, **15**(6), e1008189.
Cumbo VR, van Oppen MJ, Baird AH (2018) Temperature and *Symbiodinium* physiology affect the establishment and development of symbiosis in corals. *Marine Ecology Progress Series*, **587**, 117–27.
Cunning R, Baker AC (2020) Thermotolerant coral symbionts modulate heat stress-responsive genes in their hosts. *Molecular Ecology*, **29**(15), 2940–50.
Cunning R, Silverstein RN, Baker AC (2015) Investigating the causes and consequences of symbiont shuffling in a multi-partner reef coral symbiosis under environmental change. *Proceedings of the Royal Society B: Biological Sciences*, **282**(1809), 20141725.
Cziesielski MJ, Liew YJ, Cui G, Schmidt-Roach S, Campana S, Marondedze C, Aranda M (2018) Multi-omics analysis of thermal stress response in a zooxanthellate cnidarian reveals the importance of associating with thermotolerant symbionts. *Proceedings of the Royal Society B: Biological Sciences*, **285**(1877), 20172654.
D'Elia CF (1977) The uptake and release of dissolved phosphorus by reef corals. *Limnology and Oceanography*, **22**(2), 301–15.
D'Erfurth I, Jolivet S, Froger N, Catrice O, Novatchkova M, Mercier R (2009) Turning meiosis into mitosis. *PLoS Biology*, **7**(6), e1000124.
Dalton S, Whitbread L (1995) Cell cycle-regulated nuclear import and export of Cdc47, a protein essential for initiation of DNA replication in budding yeast. *Proceedings of the National Academy of Sciences USA*, **92**(7), 2514–18.
Dang CV (1999) c-Myc target genes involved in cell growth, apoptosis, and metabolism. *Molecular and Cellular Biology*, **19**(1), 1–11.
Dani V, Priouzeau F, Mertz M, Mondin M, Pagnotta S, Lacas-Gervais S, Davy SK, Sabourault C (2017) Expression patterns of sterol transporters NPC1 and NPC2 in the cnidarian–dinoflagellate symbiosis. *Cellular Microbiology*, **19**(10), e12753.
Darriba D, Taboada GL, Doallo R, Posada D (2011) ProtTest 3: fast selection of best-fit models of protein evolution. *Bioinformatics*, **27**(8), 1164–65.
Davy SK, Allemand D, Weis VM (2012) Cell biology of cnidarian-dinoflagellate symbiosis. *Microbiology and Molecular Biology Reviews*, **76**(2), 229–61.
Davy SK, Lucas IA, Turner JR (1997) Uptake and persistence of homologous and heterologous zooxanthellae in the temperate sea anemone *Cereus pedunculatus* (Pennant). *The Biological Bulletin*, **192**(2), 208–16.
Deane EM, O'Brien RW (1981) Uptake of sulphate, taurine, cysteine and methionine by symbiotic and free-living dinoflagellates. *Archives of Microbiology*, **128**(3), 311–19.
DeSalvo MK, Sunagawa S, Voolstra CR, Medina M (2010) Transcriptomic responses to heat stress and bleaching in the elkhorn coral *Acropora palmata*. *Marine Ecology Progress Series*, **402**, 97–113.
Detournay O, Schnitzler CE, Poole A, Weis VM (2012) Regulation of cnidarian–dinoflagellate mutualisms: evidence that activation of a host TGFβ innate immune pathway promotes tolerance of the symbiont. *Developmental & Comparative Immunology*, **38**(4), 525–37.
Detournay O, Weis VM (2011) Role of the sphingosine rheostat in the regulation of cnidarian-dinoflagellate symbioses. *The Biological Bulletin*, **221**(3), 261–69.
Dimond J, Carrington E (2008) Symbiosis regulation in a facultatively symbiotic temperate coral: zooxanthellae division and expulsion. *Coral Reefs*, **27**(3), 601–4.
Dimond JL, Pineda RR, Ramos-Ascherl Z, Bingham BL (2013) Relationships between host and symbiont cell cycles in sea anemones and their symbiotic dinoflagellates. *The Biological Bulletin*, **225**(2), 102–12.
Dimond J, Carrington E (2007) Temporal variation in the symbiosis and growth of the temperate scleractinian coral *Astrangia poculata*. *Marine Ecology Progress Series*, **348**, 161–72.
Dimova DK, Stevaux O, Frolov MV, Dyson NJ (2003) Cell cycle-dependent and cell cycle-independent control of transcription by the *Drosophila* E2F/RB pathway. *Genes & Development*, **17**(18), 2308–20.
Dobin A, Davis CA, Schlesinger F, Drenkow J, Zaleski C, Jha S, Batut P, Chaisson M, Gingeras TR (2013) STAR: ultrafast universal RNA-seq aligner. *Bioinformatics*, **29**(1), 15–21.
Donner SD (2011) An evaluation of the effect of recent temperature variability on the prediction of coral bleaching events. *Ecological Applications*, **21**(5), 1718–30.
Douglas AE (2003) Coral bleaching—how and why? *Marine Pollution Bulletin*, **46**(4), 385–92.
Downs CA, Kramarsky-Winter E, Martinez J, Kushmaro A, Woodley CM, Loya Y, Ostrander GK (2009) Symbiophagy as a cellular mechanism for coral bleaching. *Autophagy*, **5**(2), 211–16.
Downs CA, Fauth JE, Halas JC, Dustan P, Bemiss J, Woodley CM (2002) Oxidative stress and seasonal coral bleaching. *Free Radical Biology and Medicine*, **33**(4), 533–43.

Duarte CM, Agusti S, Barbier E, Britten GL, Castilla JC, Gattuso JP, Fulweiler RW, Hughes TP, Knowlton N, Lovelock CE, Lotze HK (2020) Rebuilding marine life. *Nature*, **580**(7801), 39–51.
Duncan RP, Feng H, Nguyen DM, Wilson AC (2016) Gene Family Expansions in Aphids Maintained by Endosymbiotic and Nonsymbiotic Traits. *Genome Biology and Evolution*, **8**(3), 753–64.
Duncker BP, Chesnokov IN, McConkey BJ (2009) The origin recognition complex protein family. *Genome Biology*, **10**(3), 214.
Dunn SR, Thomason JC, Le Tissier MDA, Bythell JC (2004) Heat stress induces different forms of cell death in sea anemones and their endosymbiotic algae depending on temperature and duration. *Cell Death and Differentiation*, **11**(11), 1213-22.
Dunn SR, Pernice M, Green K, Hoegh-Guldberg O, Dove SG (2012) Thermal stress promotes host mitochondrial degradation in symbiotic cnidarians: are the batteries of the reef going to run out? *PLoS One*, **7**(7), e39024.
Dunn SR, Schnitzler CE, Weis VM (2007) Apoptosis and autophagy as mechanisms of dinoflagellate symbiont release during cnidarian bleaching: every which way you lose. *Proceedings of the Royal Society of London B: Biological Sciences*, **274**(1629), 3079–85.
Dunn SR, Thomas MC, Nette GW, Dove SG (2012) A lipidomic approach to understanding free fatty acid lipogenesis derived from dissolved inorganic carbon within cnidarian-dinoflagellate symbiosis. *PLoS One*, **7**(10), e46801.
Dunn SR, Phillips WS, Spatafora JW, Green DR, Weis VM (2006) Highly conserved caspase and Bcl-2 homologues from the sea anemone *Aiptasia pallida*: lower metazoans as models for the study of apoptosis evolution. *Journal of Molecular Evolution*, **63**(1), 95–107.
Dunn SR, Weis VM (2009) Apoptosis as a post-phagocytic winnowing mechanism in a coral–dinoflagellate mutualism. *Environmental Microbiology*, **11**(1), 268–76.
Elowe S, Hümmer S, Uldschmid A, Li X, Nigg EA (2007) Tension-sensitive Plk1 phosphorylation on BubR1 regulates the stability of kinetochore–microtubule interactions. *Genes & Development*, **21**(17), 2205–19.
Fingar DC, Richardson CJ, Tee AR, Cheatham L, Tsou C, Blenis J (2004) MTOR controls cell-cycle progression through its cell growth effectors S6K1 and 4E-BP1/eukaryotic translation initiation factor 4E. *Molecular and Cellular Biology*, **24**(1), 200–216.
Fitt WK (2000) Cellular growth of host and symbiont in a cnidarian-zooxanthellar symbiosis. *The Biological Bulletin*, **198**(1), 110–20.
Fitt WK, Cook CB (2001) Photoacclimation and the effect of the symbiotic environment on the photosynthetic response of symbiotic dinoflagellates in the tropical marine hydroid *Myrionema amboinense*. *Journal of Experimental Marine Biology and Ecology*, **256**(1), 15–31.
Fitt WK, Trench RK (1983a) Endocytosis of the symbiotic dinoflagellate *Symbiodinium microadriaticum* Freudenthal by endodermal cells of the scyphistomae of *Cassiopeia xamachana* and resistance of the algae to host digestion. *Journal of Cell Science*, **64**(1), 195–212.
Fitt WK, Trench RK (1983b) The relation of diel patterns of cell division to diel patterns of motility in the symbiotic dinoflagellate *Symbiodinium microadriaticum* Freudenthal in culture. *New Phytologist*, **94**(3), 421–32.
Flesher JL (2013) Is there a change in expression of apoptosis and autophagy genes in Aiptasia sp. after thermal stress? Honors thesis, Oregon State University.
Fransolet D, Roberty S, Herman AC, Tonk L, Hoegh-Guldberg O, Plumier JC (2013) Increased cell proliferation and mucocyte density in the sea anemone *Aiptasia pallida* recovering from bleaching. *PLoS One*, **8**(5), e65015.
Fransolet D, Roberty S, Plumier JC (2012) Establishment of endosymbiosis: The case of cnidarians and *Symbiodinium*. *Journal of Experimental Marine Biology and Ecology*, **420**, 1–7.
Fransolet D, Roberty S, Plumier JC (2014) Impairment of symbiont photosynthesis increases host cell proliferation in the epidermis of the sea anemone *Aiptasia pallida*. *Marine Biology*, **161**(8), 1735–43.
Freeman CJ, Thacker RW (2011) Complex interactions between marine sponges and their symbiotic microbial communities. *Limnology and Oceanography*, **56**(5), 1577–86.
Fujise L, Yamashita H, Suzuki G, Sasaki K, Liao LM, Koike K (2014) Moderate thermal stress causes active and immediate expulsion of photosynthetically damaged zooxanthellae (*Symbiodinium*) from corals. *PLoS One*, **9**(12), e114321.
Fujise L, Nitschke MR, Frommlet JC, Serôdio J, Woodcock S, Ralph PJ, Suggett DJ (2018) Cell cycle dynamics of cultured coral endosymbiotic microalgae (*Symbiodinium*) across different types (species) under alternate light and temperature conditions. *Journal of Eukaryotic Microbiology*, **65**(4), 505-517.
Gabay Y, Parkinson JE, Wilkinson SP, Weis VM, Davy SK (2019) Inter-partner specificity limits the acquisition of thermotolerant symbionts in a model cnidarian-dinoflagellate symbiosis. *The ISME Journal*, **13**(10), 2489–99.

Gabay Y, Weis VM, Davy SK (2018) Symbiont identity influences patterns of symbiosis establishment, host growth, and asexual reproduction in a model cnidarian-dinoflagellate symbiosis. *The Biological Bulletin*, **234**(1), 1–10.
Ganot P, Moya A, Magnone V, Allemand D, Furla P, Sabourault C (2011) Adaptations to endosymbiosis in a cnidarian-dinoflagellate association: differential gene expression and specific gene duplications. *PLoS Genetics*, **7**(7), e1002187.
Gates RD, Muscatine L (1992) Three methods for isolating viable anthozoan endoderm cells with their intracellular symbiotic dinoflagellates. *Coral Reefs*, **11**(3), 143–45.
Gates RD, Baghdasarian G, Muscatine L (1992) Temperature stress causes host cell detachment in symbiotic cnidarians: implications for coral bleaching. *The Biological Bulletin*, **182**(3), 324–32.
Gavet O, Pines J (2010) Activation of cyclin B1–CDK1 synchronizes events in the nucleus and the cytoplasm at mitosis. *The Journal of Cell Biology*, **189**(2), 247–59.
Gheghiani L, Loew D, Lombard B, Mansfeld J, Gavet O (2017) PLK1 activation in late G2 sets up commitment to mitosis. *Cell Reports*, **19**(10), 2060–73.
Giacinti C, Giordano A (2006) RB and cell-cycle progression. *Oncogene*, **25**(38), 5220-7.
Giono LE, Resnick-Silverman L, Carvajal LA, St Clair S, Manfredi JJ (2017) Mdm2 promotes Cdc25C protein degradation and delays cell-cycle progression through the G_2/M phase. *Oncogene*, **36**(49), 6762-73.
Godinot C, Ferrier-Pagès C, Grover R (2009) Control of phosphate uptake by zooxanthellae and host cells in the scleractinian coral *Stylophora pistillata*. *Limnology and Oceanography*, **54**(5), 1627–33.
Golan A, Yudkovsky Y, Hershko A (2002) The cyclin-ubiquitin ligase activity of cyclosome/APC is jointly activated by protein kinases Cdk1-cyclin B and Plk. *Journal of Biological Chemistry*, **277**(18), 15552–57.
Golsteyn RM, Mundt KE, Fry AM, Nigg EA (1995) Cell-cycle regulation of the activity and subcellular localization of Plk1, a human protein kinase implicated in mitotic spindle function. *The Journal of Cell Biology*, **129**(6), 1617–28.
González-Pech RA, Vargas S, Francis WR, Wörheide G (2017) Transcriptomic resilience of the *Montipora digitata* holobiont to low pH. *Frontiers in Marine Science*, **12**(4), 403.
Gordon BR, Leggat W (2010) *Symbiodinium*—invertebrate symbioses and the role of metabolomics. *Marine Drugs*, **8**(10), 2546–68.
Griffin SV, Olivier JP, Pippin JW, Roberts JM, Shankland SJ (2006) Cyclin I protects podocytes from apoptosis. *Journal of Biological Chemistry*, **281**(38), 28048–57.
Guen VJ, Gamble C, Flajolet M, Unger S, Thollet A, Ferandin Y, Superti-Furga A, Cohen PA, Meijer L, Colas P (2013) CDK10/cyclin M is a protein kinase that controls ETS2 degradation and is deficient in STAR syndrome. *Proceedings of the National Academy of Sciences USA*, **110**(48), 19525–30.
Guevara T, Sancho M, Pérez-Payá E, Orzáez M (2014) Role of CDK5/cyclin complexes in ischemia-induced death and survival of renal tubular cells. *Cell Cycle*, **13**(10), 1617–26.
Guindon S, Gascuel O (2003) A simple, fast, and accurate algorithm to estimate large phylogenies by maximum likelihood. *Systematic Biology*, **52**(5), 696–704.
Guindon S, Dufayard JF, Lefort V, Anisimova M, Hordijk W, Gascuel O (2010) New algorithms and methods to estimate maximum-likelihood phylogenies: assessing the performance of PhyML 3.0. *Systematic Biology*, **59**(3), 307–21.
Habetha M, Anton-Erxleben F, Neumann K, Bosch TC (2003) The *Hydra viridis*/*Chlorella* symbiosis. Growth and sexual differentiation in polyps without symbionts. *Zoology*, **106**(2), 101–8.
Hambleton EA, Jones VAS, Maegele I, Kvaskoff D, Sachsenheimer T, Guse A (2019) Sterol transfer by atypical cholesterol-binding NPC2 proteins in coral-algal symbiosis. *Elife*, **8**, e43923.
Harland AD, Davies PS (1995) Symbiont photosynthesis increases both respiration and photosynthesis in the symbiotic sea anemone *Anemonia viridis*. *Marine Biology*, **123**(4), 715–22.
Hartwell LH, Kastan MB (1994) Cell cycle control and cancer. *Science*, **266**(5192), 1821–28.
Haupt Y, Maya R, Kazaz A, Oren M (1997) Mdm2 promotes the rapid degradation of p53. *Nature*, **387**(6630): 296-9.
Hawkins TD, Bradley BJ, Davy SK (2013) Nitric oxide mediates coral bleaching through an apoptotic-like cell death pathway: evidence from a model sea anemone-dinoflagellate symbiosis. *The FASEB Journal*, **27**(12), 4790–98.
Hawkins TD, Davy SK (2012) Nitric oxide production and tolerance differ among *Symbiodinium* types exposed to heat stress. *Plant and Cell Physiology*, **53**(11), 1889–98.
Hawkins TD, Davy SK (2013) Nitric oxide and coral bleaching: is peroxynitrite generation required for symbiosis collapse? *Journal of Experimental Biology*, **216**(17), 3185-88.
Hawkins TD, Krueger T, Becker S, Fisher PL, Davy SK (2014) Differential nitric oxide synthesis and host apoptotic events correlate with bleaching susceptibility in reef corals. *Coral Reefs*, **33**(1), 141–53.

Hawkins TD, Hagemeyer JC, Hoadley KD, Marsh AG, Warner ME (2016) Partitioning of Respiration in an Animal-Algal Symbiosis: Implications for Different Aerobic Capacity between *Symbiodinium* spp. *Frontiers in Physiology*, **7**, 128.
Hayman DS (1986) Mycorrhizae of nitrogen-fixing legumes. *MIRCEN Journal of Applied Microbiology and Biotechnology*, **2**(1), 121–45.
Hillyer KE, Dias DA, Lutz A, Roessner U, Davy SK (2017) Mapping carbon fate during bleaching in a model cnidarian symbiosis: the application of ^{13}C metabolomics. *New Phytologist*, **214**(4), 1551–62.
Hillyer KE, Tumanov S, Villas-Bôas S, Davy SK (2016) Metabolite profiling of symbiont and host during thermal stress and bleaching in a model cnidarian–dinoflagellate symbiosis. *Journal of Experimental Biology*, **219**(4), 516–27.
Hinds PW, Mittnacht S, Dulic V, Arnold A, Reed SI, Weinberg RA (1992) Regulation of retinoblastoma protein functions by ectopic expression of human cyclins. *Cell*, **70**(6), 993–1006.
Hoegh-Guldberg O, McCloskey LR, Muscatine L (1987) Expulsion of zooxanthellae by symbiotic cnidarians from the Red Sea. *Coral Reefs*, **5**(4), 201–4.
Hoegh-Guldberg O (1994) The population dynamics of symbiotic zooxanthellae in the coral *Pocillopora damicornis* exposed to elevated ammonium [$(NH_4)_2SO_4$] concentrations. *Pacific Science*, **48**, 263–72.
Hoegh-Guldberg O (1999) Climate change, coral bleaching and the future of the world's coral reefs. *Marine and Freshwater Research*, **50**(8), 839–66.
Hoegh-Guldberg O, Mumby PJ, Hooten AJ, Steneck RS, Greenfield P, Gomez E, Harvell CD, Sale PF, Edwards AJ, Caldeira K, Knowlton N (2007) Coral reefs under rapid climate change and ocean acidification. *Science*, **318**(5857), 1737–42.
Hoegh-Guldberg O, Jones RJ, Ward S, Loh WK (2002) Is coral bleaching really adaptive? *Nature*, **415**(6872), 601–2.
Hoegh-Guldberg O, Kennedy EV, Beyer HL, McClennen C, Possingham HP (2018) Securing a long-term future for coral reefs. *Trends in Ecology & Evolution*, **33**(12), 936–44.
Hoegh-Guldberg O, Smith GJ (1989) Influence of the population density of zooxanthellae and supply of ammonium on the biomass and metabolic characteristics of the reef corals *Seriatopora hystrix* and *Stylophora pistillata*. *Marine Ecology Progress Series*, 173–86.
Hoffman B, Liebermann DA (2008) Apoptotic signaling by c-MYC. *Oncogene*, **27**(50), 6462-72.
Houtgraaf JH, Versmissen J, van der Giessen WJ (2006) A concise review of DNA damage checkpoints and repair in mammalian cells. *Cardiovascular Revascularization Medicine*, **7**(3), 165–72.
Huang D, Moffat J, Wilson WA, Moore L, Cheng C, Roach PJ, Andrews B (1998) Cyclin partners determine Pho85 protein kinase substrate specificity *in vitro* and *in vivo*: control of glycogen biosynthesis by Pcl8 and Pcl10. *Molecular and Cellular Biology*, **18**(6), 3289–99.
Huang D, Friesen H, Andrews B (2007) Pho85, a multifunctional cyclin-dependent protein kinase in budding yeast. *Molecular Microbiology*, **66**(2), 303–14.
Huang YY, Carballo-Bolaños R, Kuo CY, Keshavmurthy S, Chen CA (2020) *Leptoria phrygia* in Southern Taiwan shuffles and switches symbionts to resist thermal-induced bleaching. *Scientific Reports*, **10**(1), 1–11.
Hughes DJ, Alderdice R, Cooney C, Kühl M, Pernice M, Voolstra CR, Suggett DJ (2020) Coral reef survival under accelerating ocean deoxygenation. *Nature Climate Change*, **10**(4), 296–307.
Hughes TP, Anderson KD, Connolly SR, Heron SF, Kerry JT, Lough JM, Baird AH, Baum JK, Berumen ML, Bridge TC, Claar DC (2018) Spatial and temporal patterns of mass bleaching of corals in the Anthropocene. *Science*, **359**(6371), 80–83.
Hughes TP, Baird AH, Bellwood DR, Card M, Connolly SR, Folke C, Grosberg R, Hoegh-Guldberg O, Jackson JB, Kleypas J, Lough JM (2003) Climate change, human impacts, and the resilience of coral reefs. *Science*, **301**(5635), 929–33.
Hughes TP, Barnes ML, Bellwood DR, Cinner JE, Cumming GS, Jackson JB, Kleypas J, Van De Leemput IA, Lough JM, Morrison TH, Palumbi SR (2017) Coral reefs in the Anthropocene. *Nature*, **546**(7656), 82-90.
Hume B, D'angelo C, Burt J, Baker AC, Riegl B, Wiedenmann J (2013) Corals from the Persian/Arabian Gulf as models for thermotolerant reef-builders: prevalence of clade C3 *Symbiodinium*, host fluorescence and *ex situ* temperature tolerance. *Marine Pollution Bulletin*, **72**(2), 313–22.
Hustedt N, Durocher D (2017) The control of DNA repair by the cell cycle. *Nature Cell Biology*, **19**(1), 1-9.
Ikmi A, McKinney SA, Delventhal KM, Gibson MC (2014) TALEN and CRISPR/Cas9-mediated genome editing in the early-branching metazoan *Nematostella vectensis*. *Nature Communications*, **5**(1), 1–8.
IPCC (2013) Climate Change 2013: The Physical Science Basis. Contribution of Working Group I to the Fifth Assessment Report of the Intergovernmental Panel on Climate Change. Cambridge University Press, 1535.

Ishikura M, Adachi K, Maruyama T (1999) Zooxanthellae release glucose in the tissue of a giant clam, *Tridacna crocea*. *Marine Biology*, **133**(4), 665–73.
Jang SH, Jeong HJ, Chon JK, Lee SY (2017) *De novo* assembly and characterization of the transcriptome of the newly described dinoflagellate *Ansanella granifera*: Spotlight on flagellum-associated genes. *Marine Genomics*, **33**, 47–55.
Jennings DH (1995) The Physiology of Fungal Nutrition. Cambridge University Press.
Jeong HJ, Lee SY, Kang NS, Yoo YD, Lim AS, Lee MJ, Kim HS, Yih W, Yamashita H, LaJeunesse TC (2014) Genetics and morphology characterize the dinoflagellate *Symbiodinium voratum*, n. sp.,(Dinophyceae) as the sole representative of *Symbiodinium* clade E. *Journal of Eukaryotic Microbiology*, **61**(1), 75–94.
Jiang M, Gao Y, Yang T, Zhu X, Chen J (2009) Cyclin Y, a novel membrane-associated cyclin, interacts with PFTK1. *FEBS Letters*, **583**(13), 2171–78.
Jimbo M, Yanohara T, Koike K, Koike K, Sakai R, Muramoto K, Kamiya H (2000) The D-galactose-binding lectin of the octocoral *Sinularia lochmodes*: characterization and possible relationship to the symbiotic dinoflagellates. *Comparative Biochemistry and Physiology Part B: Biochemistry and Molecular Biology*, **125**(2), 227–36.
Jimbo M, Yamashita H, Koike K, Sakai R, Kamiya H (2010) Effects of lectin in the scleractinian coral *Ctenactis echinata* on symbiotic zooxanthellae. *Fisheries Science*, **76**(2), 355–63.
Jones A, Berkelmans R (2010) Potential costs of acclimatization to a warmer climate: growth of a reef coral with heat tolerant vs. sensitive symbiont types. *PLoS One*, **5**(5), e10437.
Jones AM, Berkelmans R, van Oppen MJ, Mieog JC, Sinclair W (2008) A community change in the algal endosymbionts of a scleractinian coral following a natural bleaching event: field evidence of acclimatization. *Proceedings of the Royal Society of London B: Biological Sciences*, **275**(1641), 1359–65.
Jones NG, Thomas EB, Brown E, Dickens NJ, Hammarton TC, Mottram JC (2014) Regulators of *Trypanosoma brucei* cell-cycle progression and differentiation identified using a kinome-wide RNAi screen. *PLoS Pathogens*, **10**(1), e1003886.
Jones RJ (1997) Zooxanthellae loss as a bioassay for assessing stress in corals. *Marine Ecology Progress Series*, **149**, 163–71.
Jones RJ, Yellowlees D (1997) Regulation and control of intracellular algae (= zooxanthellae) in hard corals. *Philosophical Transactions of the Royal Society of London B: Biological Sciences*, **352**(1352), 457–68.
Jones VA, Bucher M, Hambleton EA, Guse A (2018) Microinjection to deliver protein, mRNA, and DNA into zygotes of the cnidarian endosymbiosis model *Aiptasia* sp. *Scientific Reports*, 8(1), 1–11.
Joubès J, Chevalier C, Dudits D, Heberle-Bors E, Inzé D, Umeda M, Renaudin JP (2000) CDK-related protein kinases in plants. *The Plant Cell Cycle*, 63–76.
Joyce AR, Palsson BØ (2006) The model organism as a system: integrating'omics' data sets. *Nature Reviews Molecular Cell Biology*, **7**(3), 198–210.
Kabeya Y, Mizushima N, Ueno T, Yamamoto A, Kirisako T, Noda T, Kominami E, Ohsumi Y, Yoshimori T (2000) LC3, a mammalian homologue of yeast Apg8p, is localized in autophagosome membranes after processing. *The EMBO Journal*, **19**(21), 5720–28.
Kahng SE, Maragos JE (2006) The deepest, zooxanthellate scleractinian corals in the world? *Coral Reefs*, **25**(2), 254.
Karakashian MW, Karakashian SJ (1973) Intracellular digestion and symbiosis in *Paramecium bursaria*. *Experimental Cell Research*, **81**(1), 111–19.
Karakashian SJ, Rudzinska MA (1981) Inhibition of lysosomal fusion with symbiont-containing vacuoles in *Paramecium bursaria*. *Experimental Cell Research*, **131**(2), 387–93.
Kastan MB, Bartek J (2004) Cell-cycle checkpoints and cancer. *Nature*, **432**(7015), 316-23.
Keeling PJ, Burki F, Wilcox HM, Allam B, Allen EE, Amaral-Zettler LA, Armbrust EV, Archibald JM, Bharti AK, Bell CJ, Beszteri B (2014) The Marine Microbial Eukaryote Transcriptome Sequencing Project (MMETSP): illuminating the functional diversity of eukaryotic life in the oceans through transcriptome sequencing. *PLoS Biology*, **12**(6), e1001889.
Kelly TJ, Brown GW (2000) Regulation of chromosome replication. *Annual Review of Biochemistry*, **69**(1), 829–80.
Kemp DW, Hernandez-Pech X, Iglesias-Prieto R, Fitt WK, Schmidt GW (2014) Community dynamics and physiology of *Symbiodinium* spp. before, during, and after a coral bleaching event. *Limnology and Oceanography*, **59**(3), 788–97.
Kenkel CD, Meyer E, Matz MV (2013) Gene expression under chronic heat stress in populations of the mustard hill coral (*Porites astreoides*) from different thermal environments. *Molecular Ecology*, **22**(16), 4322–34.
Kim JK, Diehl JA (2009) Nuclear cyclin D1: an oncogenic driver in human cancer. *Journal of Cellular Physiology*, **220**(2), 292–96.

Kitchen SA, Poole AZ, Weis VM (2017) Sphingolipid metabolism of a sea anemone is altered by the presence of dinoflagellate symbionts. *The Biological Bulletin*, **233**(3), 242–54.
Kitchen SA, Weis VM (2017) The sphingosine rheostat is involved in the cnidarian heat stress response but not necessarily in bleaching. *Journal of Experimental Biology*, **220**(9), 1709–20.
Klueter A, Trapani J, Archer FI, McIlroy SE, Coffroth MA (2017) Comparative growth rates of cultured marine dinoflagellates in the genus *Symbiodinium* and the effects of temperature and light. *PLoS One*, **12**(11), e0187707.
Kopp C, Pernice M, Domart-Coulon I, Djediat C, Spangenberg JE, Alexander DT, Hignette M, Meziane T, Meibom A (2013) Highly dynamic cellular-level response of symbiotic coral to a sudden increase in environmental nitrogen. *MBio*, **4**(3), e00052-13.
Kopp C, Domart-Coulon I, Escrig S, Humbel BM, Hignette M, Meibom A (2015) Subcellular investigation of photosynthesis-driven carbon assimilation in the symbiotic reef coral *Pocillopora damicornis*. *MBio*, **6**(1), e02299-14.
Kramer ER, Scheuringer N, Podtelejnikov AV, Mann M, Peters JM (2000) Mitotic regulation of the APC activator proteins CDC20 and CDH1. *Molecular Biology of the Cell*, **11**(5), 1555–69.
Krueger T, Hawkins TD, Becker S, Pontasch S, Dove S, Hoegh-Guldberg O, Leggat W, Fisher PL, Davy SK (2015) Differential coral bleaching—Contrasting the activity and response of enzymatic antioxidants in symbiotic partners under thermal stress. *Comparative Biochemistry and Physiology Part A: Molecular & Integrative Physiology*, **190**, 15–25.
Kvennefors ECE, Leggat W, Hoegh-Guldberg O, Degnan BM, Barnes AC (2008) An ancient and variable mannose-binding lectin from the coral *Acropora millepora* binds both pathogens and symbionts. *Developmental & Comparative Immunology*, **32**(12), 1582–92.
Kvennefors ECE, Leggat W, Kerr CC, Ainsworth TD, Hoegh-Guldberg O, Barnes AC (2010) Analysis of evolutionarily conserved innate immune components in coral links immunity and symbiosis. *Developmental & Comparative Immunology*, **34**(11), 1219–29.
Kvitt H, Rosenfeld H, Tchernov D (2016) The regulation of thermal stress induced apoptosis in corals reveals high similarities in gene expression and function to higher animals. *Scientific Reports*, **6**(1), 1-8.
Labib K, Diffley JF (2001) Is the MCM2–7 complex the eukaryotic DNA replication fork helicase? *Current Opinion in Genetics & Development*, **11**(1), 64–70.
Ladner JT, Barshis DJ, Palumbi SR (2012) Protein evolution in two co-occurring types of *Symbiodinium*: an exploration into the genetic basis of thermal tolerance in *Symbiodinium* clade D. *BMC Evolutionary Biology*, **12**(1), 1-13.
LaJeunesse TC, Loh WK, Van Woesik R, Hoegh-Guldberg O, Schmidt GW, Fitt WK (2003) Low symbiont diversity in southern Great Barrier Reef corals, relative to those of the Caribbean. *Limnology and Oceanography*, **48**(5), 2046–54.
LaJeunesse TC, Parkinson JE, Gabrielson PW, Jeong HJ, Reimer JD, Voolstra CR, Santos SR (2018) Systematic revision of Symbiodiniaceae highlights the antiquity and diversity of coral endosymbionts. *Current Biology*, **28**(16), 2570-2580.
Lane JD, Korolchuk VI, Murray JT, Rabanal-Ruiz Y, Otten EG (2017) mTORC1 as the main gateway to autophagy. *Essays in Biochemistry*, **61**(6), 565–84.
Larochelle S, Merrick KA, Terret ME, Wohlbold L, Barboza NM, Zhang C, Shokat KM, Jallepalli PV, Fisher RP (2007) Requirements for CDK7 in the assembly of CDK1/cyclin B and activation of CDK2 revealed by chemical genetics in human cells. *Molecular Cell*, **25**(6), 839–50.
Law CW, Chen Y, Shi W, Smyth GK (2014) voom: Precision weights unlock linear model analysis tools for RNA-seq read counts. *Genome Biology*, **15**(2), 1-17.
Lawson CA, Possell M, Seymour JR, Raina JB, Suggett DJ (2019) Coral endosymbionts (Symbiodiniaceae) emit species-specific volatilomes that shift when exposed to thermal stress. *Scientific Reports*, **9**(1), 1–11.
Le Dai J, Bansal RK, Kern SE (1999) G_1 cell cycle arrest and apoptosis induction by nuclear Smad4/Dpc4: phenotypes reversed by a tumorigenic mutation. *Proceedings of the National Academy of Sciences USA*, **96**(4), 1427–32.
Leal MC, Hoadley K, Pettay DT, Grajales A, Calado R, Warner ME (2015) Symbiont type influences trophic plasticity of a model cnidarian–dinoflagellate symbiosis. *Journal of Experimental Biology*, **218**(6), 858–63.
Leander BS, Keeling PJ (2004) Early evolutionary history of Dinoflagellates and Apicomplexans (Alveolata) as inferred from Hsp90 and actin phylogenies. *Journal of Phycology*, **40**(2), 341–50.
Lecointe A, Domart-Coulon I, Paris A, Meibom A (2016) Cell proliferation and migration during early development of a symbiotic scleractinian coral. *Proceedings of the Royal Society B: Biological Sciences*, **283**(1831), 20160206.

Lee MG, Nurse P (1987) Complementation used to clone a human homologue of the fission yeast cell cycle control gene cdc2. *Nature*, **327**(6117), 31-5.
Lee S, Thebault P, Freschi L, Beaufils S, Blundell TL, Landry CR, Bolanos-Garcia VM, Elowe S (2012) Characterization of spindle checkpoint kinase Mps1 reveals domain with functional and structural similarities to tetratricopeptide repeat motifs of Bub1 and BubR1 checkpoint kinases. *Journal of Biological Chemistry*, **287**(8), 5988–6001.
Lehnert EM, Mouchka ME, Burriesci MS, Gallo ND, Schwarz JA, Pringle JR (2014) Extensive differences in gene expression between symbiotic and aposymbiotic cnidarians. *G3: Genes, Genomes, Genetics*, **4**(2), 277–95.
Leonard M, Gates RD, Ingrid L (1994) Do symbiotic dinoflagellates secrete lipid droplets? *Limnology and Oceanography*, **39**(4), 925–29.
Lesser MP, Stat M, Gates RD (2013) The endosymbiotic dinoflagellates (*Symbiodinium* sp.) of corals are parasites and mutualists. *Coral Reefs*, **32**(3), 603–11.
Lesser MP, Stochaj WR, Tapley DW, Shick JM (1990) Bleaching in coral reef anthozoans: effects of irradiance, ultraviolet radiation, and temperature on the activities of protective enzymes against active oxygen. *Coral Reefs*, **8**(4), 225–32.
Lesser MP (2011) Coral bleaching: causes and mechanisms. *Coral Reefs: An Ecosystem in Transition*, 405–19.
Letunic I, Bork P (2019) Interactive Tree Of Life (iTOL) v4: recent updates and new developments. *Nucleic Acids Research*, **47**(1), 256–59.
Leung TLF, Poulin R (2008) Parasitism, commensalism, and mutualism: exploring the many shades of symbioses. *Vie et Milieu*, **58**(2), 107.
Levin RA, Beltran VH, Hill R, Kjelleberg S, McDougald D, Steinberg PD, van Oppen MJ (2016) Sex, scavengers, and chaperones: transcriptome secrets of divergent *Symbiodinium* thermal tolerances. *Molecular Biology and Evolution*, **33**(9), 2201–15.
Levin RA, Voolstra CR, Agrawal S, Steinberg PD, Suggett DJ, van Oppen, MJ (2017) Engineering strategies to decode and enhance the genomes of coral symbionts. *Frontiers in Microbiology*, **8**, 1220.
Li MO, Wan YY, Sanjabi S, Robertson AKL, Flavell RA (2006) Transforming growth factor-β regulation of immune responses. *Annual Review of Immunology*, **24**, 99–146.
Li S, MacLachlan TK, De Luca A, Claudio PP, Condorelli G, Giordano A (1995) The cdc2-related kinase, PISSLRE, is essential for cell growth and acts in G_2 phase of the cell cycle. *Cancer Research*, **55**(18), 3992–95.
Li W, Jaroszewski L, Godzik A (2001) Clustering of highly homologous sequences to reduce the size of large protein databases. *Bioinformatics*, **17**(3), 282–83.
Liang C, Stillman B (1997) Persistent initiation of DNA replication and chromatin-bound MCM proteins during the cell cycle in cdc6 mutants. *Genes & Development*, **11**(24), 3375–86.
Liang C, Weinreich M, Stillman B (1995) ORC and Cdc6p interact and determine the frequency of initiation of DNA replication in the genome. *Cell*, **81**(5), 667–76.
Liao Y, Smyth GK, Shi W (2014) FeatureCounts: an efficient general purpose program for assigning sequence reads to genomic features. *Bioinformatics*, **30**(7), 923–30.
Lim SK, Hoffmann FM (2006) Smad4 cooperates with lymphoid enhancer-binding factor 1/T cell-specific factor to increase c-myc expression in the absence of TGF-β signaling. *Proceedings of the National Academy of Sciences USA*, **103**(49), 18580–85.
Lim S, Kaldis P (2013) CDKs, cyclins and CKIs: roles beyond cell-cycle regulation. *Development*, **140**(15), 3079–93.
Lin KL, Wang JT, Fang LS (2000) Participation of glycoproteins on zooxanthellal cell walls in the establishment of a symbiotic relationship with the sea anemone, *Aiptasia pulchella*. *Zoological Studies*, **39**(3), 172–78.
Lin S, Cheng S, Song B, Zhong X, Lin X, Li W, Li L, Zhang Y, Zhang H, Ji Z, Cai M (2015) The *Symbiodinium kawagutii* genome illuminates dinoflagellate gene expression and coral symbiosis. *Science*, **350**(6261), 691–94.
Lipford JR, Bell SP (2001) Nucleosomes positioned by ORC facilitate the initiation of DNA replication. *Molecular Cell*, **7**(1), 21–30.
Liu H, Stephens TG, González-Pech RA, Beltran VH, Lapeyre B, Bongaerts P, Cooke I, Aranda M, Bourne DG, Forêt S, Miller DJ (2018) *Symbiodinium* genomes reveal adaptive evolution of functions related to coral-dinoflagellate symbiosis. *Communications Biology*, **1**(1), 1–11.
Liu Y, Hu H, Li Z (2013) The cooperative roles of Pho80-like cyclins in regulating the G_1/S transition and posterior cytoskeletal morphogenesis in *Trypanosoma brucei*. *Molecular Microbiology*, **90**(1), 130–46.
Logan DD, LaFlamme AC, Weis VM, Davy SK (2010) Flow-cytometric characterization of the cell-surface glycans of symbiotic dinoflagellates (*Symbiodinium* spp.). *Journal of Phycology*, **46**(3), 525–33.
Lõhelaid H, Samel N (2018) Eicosanoid diversity of stony corals. *Marine Drugs*, **16**(1), 10.

Luo RX, Postigo AA, Dean DC (1998) Rb interacts with histone deacetylase to repress transcription. *Cell*, **92**(4), 463–73.
Ma Z, Wu Y, Jin J, Yan J, Kuang S, Zhou M, Zhang Y, Guo AY (2013) Phylogenetic analysis reveals the evolution and diversification of cyclins in eukaryotes. *Molecular Phylogenetics and Evolution*, **66**(3), 1002–10.
MacDonald BT, Tamai K, He X (2009) Wnt/β-catenin signaling: components, mechanisms, and diseases. *Developmental Cell*, **17**(1), 9–26.
Maciejowski J, George KA, Terret ME, Zhang C, Shokat KM, Jallepalli PV (2010) Mps1 directs the assembly of Cdc20 inhibitory complexes during interphase and mitosis to control M phase timing and spindle checkpoint signaling. *The Journal of Cell Biology*, **190**(1), 89–100.
Malumbres M (2014) Cyclin-dependent kinases. *Genome Biology*, **15**(6), 122.
Malumbres M, Barbacid M (2005) Mammalian cyclin-dependent kinases. *Trends in Biochemical Sciences*, **30**(11), 630–41.
Malumbres M, Barbacid M (2009) Cell cycle, CDKs and cancer: a changing paradigm. *Nature Reviews Cancer*, **9**(3), 153–66.
Malumbres M, Harlow E, Hunt T, Hunter T, Lahti JM, Manning G, Morgan DO, Tsai LH, Wolgemuth DJ (2009) Cyclin-dependent kinases: a family portrait. *Nature Cell Biology*, **11**(11), 1275–76.
Malureanu LA, Jeganathan KB, Hamada M, Wasilewski L, Davenport J, van Deursen JM (2009) BubR1 N terminus acts as a soluble inhibitor of cyclin B degradation by APC/C Cdc20 in interphase. *Developmental Cell*, **16**(1), 118–31.
Manzoni R, Montani F, Visintin C, Caudron F, Ciliberto A, Visintin R (2010) Oscillations in Cdc14 release and sequestration reveal a circuit underlying mitotic exit. *The Journal of Cell Biology*, **190**(2), 209–22.
Maor-Landaw K, van Oppen MJ, McFadden GI (2020) Symbiotic lifestyle triggers drastic changes in the gene expression of the algal endosymbiont *Breviolum minutum* (Symbiodiniaceae). *Ecology and Evolution*, **10**(1), 451–66.
Markell DA, Wood-Charlson EM (2010) Immunocytochemical evidence that symbiotic algae secrete potential recognition signal molecules *in hospite*. *Marine Biology*, **157**(5), 1105–11.
Martín R, Miquel S, Ulmer J, Kechaou N, Langella P, Bermúdez-Humarán LG (2013) Role of commensal and probiotic bacteria in human health: a focus on inflammatory bowel disease. *Microbial Cell Factories*, **12**(1), 71.
Massagué J, Blain SW (2000) TGFβ signaling in growth control, cancer, and heritable disorders. *Cell*, **103**(2), 295–309.
Massagué J, Seoane J, Wotton D (2005) Smad transcription factors. *Genes & Development*, **19**(23), 2783–2810.
Matthews JL, Sproles AE, Oakley CA, Grossman AR, Weis VM, Davy SK (2016) Menthol-induced bleaching rapidly and effectively provides experimental aposymbiotic sea anemones (*Aiptasia* sp.) for symbiosis investigations. *Journal of Experimental Biology*, **219**(3), 306–10.
Matthews JL, Crowder CM, Oakley CA, Lutz A, Roessner U, Meyer E, Grossman AR, Weis VM, Davy SK (2017) Optimal nutrient exchange and immune responses operate in partner specificity in the cnidarian-dinoflagellate symbiosis. *Proceedings of the National Academy of Sciences USA*, **114**(50), 13194–99.
Matthews JL, Oakley CA, Lutz A, Hillyer KE, Roessner U, Grossman AR, Weis VM, Davy SK (2018) Partner switching and metabolic flux in a model cnidarian–dinoflagellate symbiosis. *Proceedings of the Royal Society B*, **285**(1892), 20182336.
McAuley PJ (1985a) Regulation of numbers of symbiotic *Chlorella* in digestive cells of green hydra. *Endocytosis Cell Research*, **2**, 179–90.
McAuley PJ (1985b) The cell cycle of symbiotic *Chlorella*. I. The relationship between host feeding and algal cell growth and division. *Journal of Cell Science*, **77**(1), 225–39.
McCloskey LR, Cove TG, Verde EA (1996) Symbiont expulsion from the anemone *Anthopleura elegantissima* (Brandt) (Cnidaria; Anthozoa). *Journal of Experimental Marine Biology and Ecology*, **195**(2), 173–86.
McFall-Ngai MJ (2014) The importance of microbes in animal development: lessons from the squid-vibrio symbiosis. *Annual Review of Microbiology*, **68**, 177–94.
McGuinness DH, Dehal PK, Pleass RJ (2003) Pattern recognition molecules and innate immunity to parasites. *Trends in Parasitology*, **19**(7), 312–19.
McIlroy SE, Wong JC, Baker DM (2020) Competitive traits of coral symbionts may alter the structure and function of the microbiome. *The ISME Journal*, **14**(10), 2424–32.
McQuin C, Goodman A, Chernyshev V, Kamentsky L, Cimini BA, Karhohs KW, Doan M, Ding L, Rafelski SM, Thirstrup D, Wiegraebe W (2018) CellProfiler 3.0: Next-generation image processing for biology. *PLoS Biology*, **16**(7), e2005970.
Measday V, Moore L, Retnakaran R, Lee J, Donoviel M, Neiman AM, Andrews B (1997) A family of cyclin-like proteins that interact with the Pho85 cyclin-dependent kinase. *Molecular and Cellular Biology*, **17**(3), 1212–23.

Medrano E, Merselis DG, Bellantuono AJ, Rodriguez-Lanetty M (2019) Proteomic Basis of Symbiosis: A Heterologous Partner Fails to Duplicate Homologous Colonization in a Novel Cnidarian–Symbiodiniaceae Mutualism. *Frontiers in Microbiology*, **10**, 1153.
Mendenhall MD, Hodge AE (1998) Regulation of Cdc28 cyclin-dependent protein kinase activity during the cell cycle of the yeast *Saccharomyces cerevisiae*. *Microbiology and Molecular Biology Reviews*, **62**(4), 1191–1243.
Mergaert P, Uchiumi T, Alunni B, Evanno G, Cheron A, Catrice O, Mausset AE, Barloy-Hubler F, Galibert F, Kondorosi A, Kondorosi E (2006) Eukaryotic control on bacterial cell cycle and differentiation in the *Rhizobium*–legume symbiosis. *Proceedings of the National Academy of Sciences USA*, **103**(13), 5230–35.
Meyer E, Weis VM (2012) Study of cnidarian-algal symbiosis in the 'omics' age. *The Biological Bulletin*, **223**(1), 44–65.
Morales F, Giordano A (2016) Overview of CDK9 as a target in cancer research. *Cell Cycle*, **15**(4), 519–27.
Morgan DO (1999) Regulation of the APC and the exit from mitosis. *Nature Cell Biology*, **1**(2), 47-53.
Morris LA, Voolstra CR, Quigley KM, Bourne DG, Bay LK (2019) Nutrient availability and metabolism affect the stability of coral–Symbiodiniaceae symbioses. *Trends in Microbiology*, **27**(8), 678–89.
Moya A, Sakamaki K, Mason BM, Huisman L, Forêt S, Weiss Y, Bull TE, Tomii K, Imai K, Hayward DC, Ball EE (2016) Functional conservation of the apoptotic machinery from coral to man: the diverse and complex Bcl-2 and caspase repertoires of *Acropora millepora*. *BMC Genomics*, **17**(1), 62.
Muller-Parker G, Cook CB, D'Elia CF (1990) Feeding affects phosphate fluxes in the symbiotic sea anemone *Aiptasia pallida*. *Marine Ecology Progress Series*, **60**(3), 283–90.
Muller-Parker G, McCloskey LR, Hoegh-Guldberg O, McAuley PJ (1994) Effect of ammonium enrichment on animal and algal biomass of the coral *Pocillopora damicornis*. *Pacific Science*, **48**(3), 273–83.
Muller-Parker G, D'Elia CF, Cook CB (2015) Interactions between corals and their symbiotic algae. *Coral Reefs in the Anthropocene*, 99–116.
Muller-Parker G, Davy SK (2001) Temperate and tropical algal-sea anemone symbioses. *Invertebrate Biology*, **120**(2), 104–23.
Muscatine L (1990) The role of symbiotic algae in carbon and energy flux in reef corals. *Coral Reefs*, **25**(1.29), 75-87.
Muscatine L, Ferrier-Pages C, Blackburn A, Gates RD, Baghdasarian G, Allemand D (1998) Cell-specific density of symbiotic dinoflagellates in tropical anthozoans. *Coral Reefs*, **17**(4), 329–37.
Muscatine L, Falkowski PG, Porter JW, Dubinsky Z (1984) Fate of photosynthetic fixed carbon in light-and shade-adapted colonies of the symbiotic coral *Stylophora pistillata*. *Proceedings of the Royal Society of London. Series B. Biological Sciences*, **222**(1227), 181–202.
Muscatine L, Falkowski PG, Dubinsky Z, Cook PA, McCloskey LR (1989) The effect of external nutrient resources on the population dynamics of zooxanthellae in a reef coral. *Proceedings of the Royal Society of London. B. Biological Sciences*, **236**(1284), 311–24.
Muscatine L, Pool RR 1979 Regulation of numbers of intracellular algae. *Proceedings of the Royal Society of London. Series B. Biological Sciences*, **204**(1155), 131–39.
Muscatine L (1967) Glycerol excretion by symbiotic algae from corals and *Tridacna* and its control by the host. *Science*, **156**(3774), 516–19.
Muscatine L, Cernichiari E (1969) Assimilation of photosynthetic products of zooxanthellae by a reef coral. *The Biological Bulletin*, **137**(3), 506–23.
Muscatine L, Hand C (1958) Direct evidence for the transfer of materials from symbiotic algae to the tissues of a coelenterate. *Proceedings of the National Academy of Sciences USA*, **44**(12), 1259–63.
Muscatine L, Karakashian SJ, Karakashian MW (1967) Soluble extracellular products of algae symbiotic with a ciliate, a sponge and a mutant *Hydra*. *Comparative Biochemistry and Physiology*, **20**(1), 1–12.
Muscatine L, Lenhoff HM (1965) Symbiosis of *Hydra* and algae. II. Effects of limited food and starvation on growth of symbiotic and aposymbiotic *Hydra*. *The Biological Bulletin*, **129**(2), 316–28.
Nakanishi N, Martindale MQ (2018) CRISPR knockouts reveal an endogenous role for ancient neuropeptides in regulating developmental timing in a sea anemone. *Elife*, **7**, e39742.
Nakayama KI, Nakayama K (2005) Regulation of the cell cycle by SCF-type ubiquitin ligases. *Seminars in Cell & Developmental Biology*, **16**(3), 323–33.
Neckelmann N, Muscatine L (1983) Regulatory mechanisms maintaining the *Hydra-Chlorella* symbiosis. *Proceedings of the Royal society of London. Series B. Biological Sciences*, **219**(1215), 193–210.
Neufeld TP, Edgar BA (1998) Connections between growth and the cell cycle. *Current Opinion in Cell Biology*, **10**(6), 784–90.
Newman MA, Sundelin T, Nielsen JT, Erbs G (2013) MAMP (microbe-associated molecular pattern) triggered immunity in plants. *Frontiers in Plant Science*, **4**, 139.

Nikoh N, Hosokawa T, Moriyama M, Oshima K, Hattori M, Fukatsu T (2014) Evolutionary origin of insect–*Wolbachia* nutritional mutualism. *Proceedings of the National Academy of Sciences USA*, **111**(28), 10257–62.
Nishitani H, Lygerou Z (2002) Control of DNA replication licensing in a cell cycle. *Genes to Cells*, **7**(6), 523–34.
Nitschke MR, Craveiro SC, Brandão C, Fidalgo C, Serôdio J, Calado AJ, Frommlet JC (2020) Description of *Freudenthalidium* gen. nov. and *Halluxium* gen. nov. to formally recognize clades Fr3 and H as Genera in the Family Symbiodiniaceae (Dinophyceae). *Journal of Phycology*, **56**(4), 923-940.
Nyholm SV, McFall-Ngai M (2004) The winnowing: establishing the squid–*Vibrio* symbiosis. *Nature Reviews Microbiology*, **2**(8), 632–42.
Oakenfull EA, Riou-Khamlichi C, Murray AH (2002) Plant D–type cyclins and the control of G_1 progression. *Philosophical Transactions of the Royal Society of London B: Biological Sciences*, **357**(1422), 749–60.
Oakley CA, Ameismeier MF, Peng L, Weis VM, Grossman AR, Davy SK (2016) Symbiosis induces widespread changes in the proteome of the model cnidarian Aiptasia. *Cellular Microbiology*, **18**(7), 1009–23.
Oakley CA, Davy SK (2018) Cell Biology of Coral Bleaching. In: Coral Bleaching, Springer, 189–211.
Oakley CA, Durand E, Wilkinson SP, Peng L, Weis VM, Grossman AR, Davy SK (2017) Thermal shock induces host proteostasis disruption and endoplasmic reticulum stress in the model symbiotic Cnidarian Aiptasia. *Journal of Proteome Research*, **16**(6), 2121–34.
Orford KW, Scadden DT (2008) Deconstructing stem cell self-renewal: genetic insights into cell-cycle regulation. *Nature Reviews Genetics*, **9**(2), 115-28.
Ortega S, Malumbres M, Barbacid M (2002) Cyclin D-dependent kinases, INK4 inhibitors and cancer. *Biochimica et Biophysica Acta (BBA)-Reviews on Cancer*, **1602**(1), 73–87.
Pardee AB (1989) G_1 events and regulation of cell proliferation. *Science*, **246**(4930), 603–8.
Parkinson JE, Baumgarten S, Michell CT, Baums IB, LaJeunesse TC, Voolstra CR (2016) Gene expression variation resolves species and individual strains among coral-associated dinoflagellates within the genus *Symbiodinium*. *Genome Biology and Evolution*, **8**(3), 665–80.
Parkinson JE, Tivey TR, Mandelare PE, Adpressa DA, Loesgen S, Weis VM (2018) Subtle differences in symbiont cell surface glycan profiles do not explain species-specific colonization rates in a model cnidarian-algal symbiosis. *Frontiers in Microbiology*, **9**, 842.
Parkinson JE, Baker AC, Baums IB, Davies SW, Grottoli AG, Kitchen SA, Matz MV, Miller MW, Shantz AA, Kenkel CD (2020) Molecular tools for coral reef restoration: Beyond biomarker discovery. *Conservation Letters*, **13**(1), e12687.
Parmesan C (2006) Ecological and evolutionary responses to recent climate change. *Annual Review of Ecology, Evolution and Systematics*, **37**, 637–69.
Passamaneck YJ, Martindale MQ (2012) Cell proliferation is necessary for the regeneration of oral structures in the anthozoan cnidarian *Nematostella vectensis*. *BMC Developmental Biology*, **12**(1), 34.
Patton JS, Abraham S, Benson AA (1977) Lipogenesis in the intact coral *Pocillopora capitata* and its isolated zooxanthellae: evidence for a light-driven carbon cycle between symbiont and host. *Marine Biology*, **44**(3), 235–47.
Paxton CW, Davy SK, Weis VM (2013) Stress and death of cnidarian host cells play a role in cnidarian bleaching. *Journal of Experimental Biology*, **216**(15), 2813–20.
Peng CY, Graves PR, Thoma RS, Wu Z, Shaw AS, Piwnica-Worms H (1997) Mitotic and G_2 checkpoint control: regulation of 14-3-3 protein binding by phosphorylation of Cdc25C on serine-216. *Science*, **277**(5331), 1501–5.
Peng L, Skylar A, Chang PL, Bisova K, Wu X (2014) CYCP2; 1 integrates genetic and nutritional information to promote meristem cell division in *Arabidopsis*. *Developmental Biology*, **393**(1), 160–70.
Peng SE, Wang YB, Wang LH, Chen WNU, Lu CY, Fang LS, Chen CS (2010) Proteomic analysis of symbiosome membranes in Cnidaria–dinoflagellate endosymbiosis. *Proteomics*, **10**(5), 1002–16.
Perez SF, Cook CB, Brooks WR (2001) The role of symbiotic dinoflagellates in the temperature-induced bleaching response of the subtropical sea anemone *Aiptasia pallida*. *Journal of Experimental Marine Biology and Ecology*, **256**(1), 1–14.
Perez S, Weis V (2006) Nitric oxide and cnidarian bleaching: an eviction notice mediates breakdown of a symbiosis. *Journal of Experimental Biology*, **209**(14), 2804–10.
Pernice M, Meibom A, Van Den Heuvel A, Kopp C, Domart-Coulon I, Hoegh-Guldberg O, Dove S (2012) A single-cell view of ammonium assimilation in coral–dinoflagellate symbiosis. *The ISME Journal*, **6**(7), 1314-24.
Pernice M, Dunn SR, Miard T, Dufour S, Dove S, Hoegh-Guldberg O (2011) Regulation of apoptotic mediators reveals dynamic responses to thermal stress in the reef building coral *Acropora millepora*. *PLoS One*, **6**(1), e16095.

Pernice M, Dunn SR, Tonk L, Dove S, Domart-Coulon I, Hoppe P, Schintlmeister A, Wagner M, Meibom A (2015) A nanoscale secondary ion mass spectrometry study of dinoflagellate functional diversity in reef-building corals. *Environmental Microbiology*, **17**(10), 3570–80.

Pettay DT, Wham DC, Smith RT, Iglesias-Prieto R, LaJeunesse TC (2015) Microbial invasion of the Caribbean by an Indo-Pacific coral zooxanthella. *Proceedings of the National Academy of Sciences USA*, **112**(24), 7513–18.

Pimentel H, Bray NL, Puente S, Melsted P, Pachter L (2017) Differential analysis of RNA-seq incorporating quantification uncertainty. *Nature Methods*, **14**(7), 687.

Piniak GA, Lipschultz F, McClelland J (2003) Assimilation and partitioning of prey nitrogen within two anthozoans and their endosymbiotic zooxanthellae. *Marine Ecology Progress Series*, **262**, 125–36.

Pochon X, Gates RD (2010) A new *Symbiodinium* clade (Dinophyceae) from soritid foraminifera in Hawai'i. *Molecular Phylogenetics and Evolution*, **56**(1), 492–97.

Pochon X, Lajeunesse TC, Pawlowski J (2004) Biogeographic partitioning and host specialization among foraminiferan dinoflagellate symbionts (*Symbiodinium*; Dinophyta). *Marine Biology*, **146**(1), 17–27.

Pochon X, Putnam HM, Gates RD (2014) Multi-gene analysis of *Symbiodinium* dinoflagellates: a perspective on rarity, symbiosis, and evolution. *PeerJ*, **2**, e394.

Quelle DE, Ashmun RA, Shurtleff SA, Kato JY, Bar-Sagi DMFR, Roussel MF, Sherr CJ (1993) Overexpression of mouse D-type cyclins accelerates G_1 phase in rodent fibroblasts. *Genes & Development*, **7**(8), 1559–71.

Quevillon E, Silventoinen V, Pillai S, Harte N, Mulder N, Apweiler R, Lopez R (2005) InterProScan: protein domains identifier. *Nucleic Acids Research*, **33**(2), 116–20.

Rädecker N, Raina JB, Pernice M, Perna G, Guagliardo P, Kilburn MR, Aranda M, Voolstra CR (2018) Using Aiptasia as a model to study metabolic interactions in cnidarian-*Symbiodinium* symbioses. *Frontiers in Physiology*, **9**, 214.

Rädecker N, Pogoreutz C, Voolstra CR, Wiedenmann J, Wild C (2015) Nitrogen cycling in corals: the key to understanding holobiont functioning? *Trends in Microbiology*, **23**(8), 490–97.

Redman RS, Dunigan DD, Rodriguez RJ (2001) Fungal symbiosis from mutualism to parasitism: who controls the outcome, host or invader? *New Phytologist*, **151**(3), 705–16.

Rehman AU, Szabó M, Deák Z, Sass L, Larkum A, Ralph P, Vass I (2016) *Symbiodinium* sp. cells produce light-induced intra-and extracellular singlet oxygen, which mediates photodamage of the photosynthetic apparatus and has the potential to interact with the animal host in coral symbiosis. *New Phytologist*, **212**(2), 472–84.

Reinhardt HC, Hasskamp P, Schmedding I, Morandell S, van Vugt MA, Wang X, Linding R, Ong SE, Weaver D, Carr SA, Yaffe MB (2010) DNA damage activates a spatially distinct late cytoplasmic cell-cycle checkpoint network controlled by MK2-mediated RNA stabilization. *Molecular Cell*, **40**(1), 34–49.

Ren B, Cam H, Takahashi Y, Volkert T, Terragni J, Young RA, Dynlacht BD (2002) E2F integrates cell-cycle progression with DNA repair, replication, and G_2/M checkpoints. *Genes & Development*, **16**(2), 245–56.

van Rhijn P, Fujishige NA, Lim PO, Hirsch AM (2001) Sugar-binding activity of pea lectin enhances heterologous infection of transgenic alfalfa plants by *Rhizobium leguminosarum* biovar *viciae*. *Plant Physiology*, **126**(1), 133–44.

Robinson MD, McCarthy DJ, Smyth GK (2010) EdgeR: a Bioconductor package for differential expression analysis of digital gene expression data. *Bioinformatics*, **26**(1), 139–40.

Rodriguez-Lanetty M, Loh W, Carter D, Hoegh-Guldberg O (2001) Latitudinal variability in symbiont specificity within the widespread scleractinian coral *Plesiastrea versipora*. *Marine Biology*, **138**(6), 1175.

Rodriguez-Lanetty M, Phillips WS, Weis VM (2006a) Transcriptome analysis of a cnidarian–dinoflagellate mutualism reveals complex modulation of host gene expression. *BMC Genomics*, **7**(1), 23.

Rodriguez-Lanetty M, Wood-Charlson EM, Hollingsworth LL, Krupp DA, Weis VM (2006b) Temporal and spatial infection dynamics indicate recognition events in the early hours of a dinoflagellate/coral symbiosis. *Marine Biology*, **149**(4), 713–19.

Rogers KT, Higgins PD, Milla MM, Phillips RS, Horowitz JM (1996) DP-2, a heterodimeric partner of E2F: identification and characterization of DP-2 proteins expressed *in vivo*. *Proceedings of the National Academy of Sciences USA*, **93**(15), 7594–99.

Rogelj J, Den Elzen M, Höhne N, Fransen T, Fekete H, Winkler H, Schaeffer R, Sha F, Riahi K, Meinshausen M (2016) Paris Agreement climate proposals need a boost to keep warming well below 2°C. *Nature*, **534**(7609), 631-639.

Roper C, Castro C, Ingel B (2019) *Xylella fastidiosa*: bacterial parasitism with hallmarks of commensalism. *Current Opinion in Plant Biology*, **50**, 140–47.

Roques M, Wall RJ, Douglass AP, Ramaprasad A, Ferguson DJ, Kaindama ML, Brusini L, Joshi N, Rchiad Z, Brady D, Guttery DS (2015) *Plasmodium* P-type cyclin CYC3 modulates endomitotic growth during oocyst development in mosquitoes. *PLoS Pathogens*, **11**(11), e1005273.
Rosset SL, Oakley CA, Ferrier-Pagès C, Suggett DJ, Weis VM, Davy SK (2020) The Molecular Language of the Cnidarian–Dinoflagellate Symbiosis. *Trends in Microbiology*, **29**(4), 320-333.
Rosset S, Wiedenmann J, Reed AJ, D'Angelo C (2017) Phosphate deficiency promotes coral bleaching and is reflected by the ultrastructure of symbiotic dinoflagellates. *Marine Pollution Bulletin*, **118**(1–2), 180–87.
Roth MS (2014) The engine of the reef: photobiology of the coral–algal symbiosis. *Frontiers in Microbiology*, **5**, 422.
Rowan R (1998) Diversity and ecology of zooxanthellae on coral reefs. *Journal of Phycology*, **34**(3), 407–17.
Rowan R, Knowlton N (1995) Intraspecific diversity and ecological zonation in coral-algal symbiosis. *Proceedings of the National Academy of Sciences USA*, **92**(7), 2850–53.
Rowan R, Knowlton N, Baker A, Jara J (1997) Landscape ecology of algal symbionts creates variation in episodes of coral bleaching. *Nature*, **388**(6639), 265–69.
Rowan R, Powers DA (1992) Ribosomal RNA sequences and the diversity of symbiotic dinoflagellates (zooxanthellae). *Proceedings of the National Academy of Sciences USA*, **89**(8), 3639–43.
Rubin SM, Gall AL, Zheng N, Pavletich NP (2005) Structure of the Rb C-terminal domain bound to E2F1-DP1: a mechanism for phosphorylation-induced E2F release. *Cell*, **123**(6), 1093–1106.
Sachs JL, Wilcox TP (2006) A shift to parasitism in the jellyfish symbiont *Symbiodinium microadriaticum*. *Proceedings of the Royal Society B: Biological Sciences*, **273**(1585), 425–29.
Salvador JM, Brown-Clay JD, Fornace AJ (2013) Gadd45 in stress signaling, cell cycle control, and apoptosis. In: Gadd45 Stress Sensor Genes, Advances in Experimental Medicine and Biology, Springer, 1–19.
Sampayo EM, Ridgway T, Bongaerts P, Hoegh-Guldberg O (2008) Bleaching susceptibility and mortality of corals are determined by fine-scale differences in symbiont type. *Proceedings of the National Academy of Sciences USA*, **105**(30), 10444-9.
Santamaría D, Barrière C, Cerqueira A, Hunt S, Tardy C, Newton K, Cáceres JF, Dubus P, Malumbres M, Barbacid M (2007) CDK1 is sufficient to drive the mammalian cell cycle. *Nature*, **448**(7155), 811-5.
Saragosti E, Tchernov D, Katsir A, Shaked Y (2010) Extracellular production and degradation of superoxide in the coral *Stylophora pistillata* and cultured *Symbiodinium*. *PLoS One*, **5**(9), e12508.
Schachter MM, Merrick KA, Larochelle S, Hirschi A, Zhang C, Shokat KM, Rubin SM, Fisher RP (2013) A CDK7-CDK4 T-loop phosphorylation cascade promotes G_1 progression. *Molecular Cell*, **50**(2), 250–60.
Schlichter D, Fricke HW, Weber W (1986) Light harvesting by wavelength transformation in a symbiotic coral of the Red Sea twilight zone. *Marine Biology*, **91**(3), 403–7.
Schmelzle T, Hall MN (2000) TOR, a central controller of cell growth. *Cell*, **103**(2), 253–62.
Schoenberg DA, Trench RK (1980) Genetic variation in *Symbiodinium* (= *Gymnodinium*) *microadriaticum* Freudenthal, and specificity in its symbiosis with marine invertebrates. I. Isoenzyme and soluble protein patterns of axenic cultures of *Symbiodinium microadriaticum*. *Proceedings of the Royal Society of London. Series B. Biological Sciences*, **207**(1169), 405–27.
Sherr CJ, Roberts JM (1995) Inhibitors of mammalian G_1 cyclin-dependent kinases. *Genes & Development*, **9**(10), 1149–63.
Sherr CJ, Roberts JM (1999) CDK inhibitors: positive and negative regulators of G_1-phase progression. *Genes & Development*, **13**(12), 1501–12.
Shi D, Gu W (2012) Dual roles of MDM2 in the regulation of p53: ubiquitination dependent and ubiquitination independent mechanisms of MDM2 repression of p53 activity. *Genes & Cancer*, **3**(3–4), 240–48.
Shoguchi E, Shinzato C, Kawashima T, Gyoja F, Mungpakdee S, Koyanagi R, Takeuchi T, Hisata K, Tanaka M, Fujiwara M, Hamada M (2013) Draft assembly of the *Symbiodinium minutum* nuclear genome reveals dinoflagellate gene structure. *Current Biology*, **23**(15), 1399–1408.
Shoguchi E, Beedessee G, Tada I, Hisata K, Kawashima T, Takeuchi T, Arakaki N, Fujie M, Koyanagi R, Roy MC, Kawachi M (2018) Two divergent *Symbiodinium* genomes reveal conservation of a gene cluster for sunscreen biosynthesis and recently lost genes. *BMC Genomics*, **19**(1), 458.
Shui W, Sheu L, Liu J, Smart B, Petzold CJ, Hsieh TY, Pitcher A, Keasling JD, Bertozzi CR (2008) Membrane proteomics of phagosomes suggests a connection to autophagy. *Proceedings of the National Academy of Sciences USA*, **105**(44), 16952–57.
Shupp A, Casimiro MC, Pestell RG (2017) Biological functions of CDK5 and potential CDK5 targeted clinical treatments. *Oncotarget*, **8**(10), 17373.
Siddiqui H, Solomon DA, Gunawardena RW, Wang Y, Knudsen ES (2003) Histone deacetylation of RB-responsive promoters: requisite for specific gene repression but dispensable for cell cycle inhibition. *Molecular and Cellular Biology*, **23**(21), 7719–31.

Silverstein RN, Cunning R, Baker AC (2015) Change in algal symbiont communities after bleaching, not prior heat exposure, increases heat tolerance of reef corals. *Global Change Biology*, **21**(1), 236–49.
Silverstein RN, Cunning R, Baker AC (2017) Tenacious D: *Symbiodinium* in clade D remain in reef corals at both high and low temperature extremes despite impairment. *Journal of Experimental Biology*, **220**(7), 1192–96.
Siu KT, Rosner MR, Minella AC (2012) An integrated view of cyclin E function and regulation. *Cell Cycle*, **11**(1), 57–64.
van der Sman J, Thomas NSB, Lam EWF (1999) Modulation of E2F complexes during G_0 to S phase transition in human primary B-lymphocytes. *Journal of Biological Chemistry*, **274**(17), 12009–16.
Smith GJ, Muscatine L (1999) Cell cycle of symbiotic dinoflagellates: variation in G_1 phase-duration with anemone nutritional status and macronutrient supply in the *Aiptasia pulchella–Symbiodinium pulchrorum* symbiosis. *Marine Biology*, **134**(3), 405–18.
Sorek M, Yacobi YZ, Roopin M, Berman-Frank I, Levy O (2013) Photosynthetic circadian rhythmicity patterns of *Symbiodinium*, the coral endosymbiotic algae. *Proceedings of the Royal Society B: Biological Sciences*, **280**, 20122942.
Sorek M, Schnytzer Y, Ben-Asher HW, Caspi VC, Chen CS, Miller DJ, Levy O (2018) Setting the pace: host rhythmic behaviour and gene expression patterns in the facultatively symbiotic cnidarian Aiptasia are determined largely by *Symbiodinium*. *Microbiome*, **6**(1), 83.
Sproles AE, Oakley CA, Matthews JL, Peng L, Owen JG, Grossman AR, Weis VM, Davy SK (2019) Proteomics quantifies protein expression changes in a model cnidarian colonised by a thermally tolerant but suboptimal symbiont. *The ISME Journal*, **13**(9), 2334–45.
Sproles AE, Oakley CA, Krueger T, Grossman AR, Weis VM, Meibom A, Davy SK (2020) Sub-cellular imaging shows reduced photosynthetic carbon and increased nitrogen assimilation by the non-native endosymbiont *Durusdinium trenchii* in the model cnidarian Aiptasia. *Environmental Microbiology*, **22**(9), 3741–53.
Stamatakis A (2014) RAxML version 8: a tool for phylogenetic analysis and post-analysis of large phylogenies. *Bioinformatics*, **30**(9), 1312–13.
Stark GR, Taylor WR (2004) Analyzing the G_2/M checkpoint. In: Checkpoint Controls and Cancer, Methods in Molecular Biology, Humana Press, **280**, 51–82.
Stark MJ, Hiraga SI, Donaldson AD (2016) Protein phosphatases and DNA replication initiation. In: The Initiation of DNA Replication in Eukaryotes, Springer, Cham, 461–77.
Starzak DE, Quinnell RG, Nitschke MR, Davy SK (2014) The influence of symbiont type on photosynthetic carbon flux in a model cnidarian–dinoflagellate symbiosis. *Marine Biology*, **161**(3), 711–24.
Stat M, Gates RD (2010) Clade D *Symbiodinium* in scleractinian corals: a 'nugget' of hope, a selfish opportunist, an ominous sign, or all of the above? *Journal of Marine Biology*, **2011**, 1-9.
Steele RD (1977) The significance of zooxanthella-containing pellets extruded by sea anemones. *Bulletin of Marine Science*, **27**(3), 591–94.
Steen RG (1986) Evidence for heterotrophy by zooxanthellae in symbiosis with *Aiptasia pulchella*. *The Biological Bulletin*, **170**(2), 267–78.
Steen RG, Muscatine L (1987) Low temperature evokes rapid exocytosis of symbiotic algae by a sea anemone. *The Biological Bulletin*, **172**(2), 246–63.
Stevaux O, Dyson NJ (2002) A revised picture of the E2F transcriptional network and RB function. *Current Opinion in Cell Biology*, **14**(6), 684–91.
Stimson J, Kinzie III (1991) The temporal pattern and rate of release of zooxanthellae from the reef coral *Pocillopora damicornis* (Linnaeus) under nitrogen-enrichment and control conditions. *Journal of Experimental Marine Biology and Ecology*, **153**(1), 63–74.
Suggett DJ, Warner ME, Smith DJ, Davey P, Hennige S, Baker NR (2008) Photosynthesis and production of hydrogen peroxide by *Symbiodinium* (pyrrhophyta) phylotypes with different thermal tolerances. *Journal of Phycology*, **44**(4), 948–56.
Sun T, Co NN, Wong N (2014) PFTK1 interacts with cyclin Y to activate non-canonical Wnt signaling in hepatocellular carcinoma. *Biochemical and Biophysical Research Communications*, **449**(1), 163–68.
Swain TD, Chandler J, Backman V, Marcelino L (2017) Consensus thermotolerance ranking for 110 *Symbiodinium* phylotypes: an exemplar utilization of a novel iterative partial-rank aggregation tool with broad application potential. *Functional Ecology*, **31**(1), 172–83.
Talevich E, Mirza A, Kannan N (2011) Structural and evolutionary divergence of eukaryotic protein kinases in Apicomplexa. *BMC Evolutionary Biology*, **11**(1), 321.
Tanaka H, Matsumura I, Ezoe S, Satoh Y, Sakamaki T, Albanese C, Machii T, Pestell RG, Kanakura Y (2002) E2F1 and c-Myc potentiate apoptosis through inhibition of NF-κB activity that facilitates MnSOD-mediated ROS elimination. *Molecular Cell*, **9**(5), 1017–29.

Tanaka Y, Miyajima T, Koike I, Hayashibara T, Ogawa H (2006) Translocation and conservation of organic nitrogen within the coral-zooxanthella symbiotic system of Acropora pulchra, as demonstrated by dual isotope-labeling techniques. *Journal of Experimental Marine Biology and Ecology*, **336**(1), 110–19.
Tanida I (2011) Autophagosome formation and molecular mechanism of autophagy. *Antioxidants & Redox Signaling*, **14**(11), 2201–14.
Tanida I, Ueno T, Kominami E (2008) LC3 and Autophagy. In: Autophagosome and Phagosome, Methods in Molecular Biology, Humana Press, **445**, 77–88.
Taylor DL (1974) Symbiotic marine algae: taxonomy and biological fitness. *Symbiosis in the Sea*, 245–62.
Tchernov D, Kvitt H, Haramaty L, Bibby TS, Gorbunov MY, Rosenfeld H, Falkowski PG (2011) Apoptosis and the selective survival of host animals following thermal bleaching in zooxanthellate corals. *Proceedings of the National Academy of Sciences USA*, **108**(24), 9905–9.
Team R Core (2020) R: A Language and Environment for Statistical Computing. R Foundation for Statistical Computing. Vienna, Austria. Available at: http://www.R-project.org.
Telles E, Seto E (2012) Modulation of cell-cycle regulators by HDACs. *Frontiers in Bioscience*, **4**, 831.
Thornhill, DJ, Howells EJ, Wham DC, Steury TD, Santos SR (2017) Population genetics of reef coral endosymbionts (*Symbiodinium*, Dinophyceae). *Molecular Ecology*, **26**(10), 2640-59.
Thornhill DJ, Xiang Y, Pettay DT, Zhong M, Santos SR (2013) Population genetic data of a model symbiotic cnidarian system reveal remarkable symbiotic specificity and vectored introductions across ocean basins. *Molecular Ecology*, **22**(17), 4499–4515.
Timofeev O, Cizmecioglu O, Settele F, Kempf T, Hoffmann I (2010) CDC25 phosphatases are required for timely assembly of CDK1/cyclin B at the G_2/M transition. *Journal of Biological Chemistry*, **285**(22), 16978-90.
Titlyanov EA, Titlyanova TV, Leletkin VA, Tsukahara J, Van Woesik R, Yamazato K (1996) Degradation of zooxanthellae and regulation of their density in hermatypic corals. *Marine Ecology Progress Series*, **139**, 167–78.
Tivey TR, Parkinson JE, Weis VM (2020) Host and Symbiont Cell-Cycle Co-ordination Is Mediated by Symbiotic State, Nutrition, and Partner Identity in a Model Cnidarian-Dinoflagellate Symbiosis. *MBio*, *11*(2), e02626-19.
Trench RK (1971) The physiology and biochemistry of zooxanthellae symbiotic with marine coelenterates. II. Liberation of fixed ^{14}C by zooxanthellae *in vitro*. *Proceedings of the Royal Society of London. Series B. Biological Sciences*, **177**(1047), 237–50.
Tu X, Wang CC (2005) Pairwise knockdowns of cdc2-related kinases (CRKs) in *Trypanosoma brucei* identified the CRKs for G_1/S and G_2/M transitions and demonstrated distinctive cytokinetic regulations between two developmental stages of the organism. *Eukaryotic Cell*, 4(4), 755–64.
Vermeulen K, van Bockstaele DR, Berneman ZN (2003) The cell cycle: a review of regulation, deregulation and therapeutic targets in cancer. *Cell Proliferation*, **36**(3), 131–49.
Vidal-Dupiol J, Adjeroud M, Roger E, Foure L, Duval D, Mone Y, Ferrier-Pages C, Tambutte E, Tambutte S, Zoccola D, Allemand D (2009) Coral bleaching under thermal stress: putative involvement of host/symbiont recognition mechanisms. *BMC Physiology*, **9**(1), 14.
Visintin R, Craig K, Hwang ES, Prinz S, Tyers M, Amon A (1998) The phosphatase Cdc14 triggers mitotic exit by reversal of Cdk-dependent phosphorylation. *Molecular Cell*, **2**(6), 709–18.
Vodermaier HC (2004) APC/C and SCF: controlling each other and the cell cycle. *Current Biology*, **14**(18), 787–96.
Voolstra CR, Schwarz JA, Schnetzer J, Sunagawa S, Desalvo MK, Szmant AM, Coffroth MA, Medina M (2009) The host transcriptome remains unaltered during the establishment of coral–algal symbioses. *Molecular Ecology*, **18**(9), 1823–33.
Voss PA, Gornik SG, Jacobovitz MR, Rupp S, Dörr MS, Maegele I, Guse A (2019) Nutrient-dependent mTORC1 signaling in coral-algal symbiosis. *BioRxiv*, 723312.
Wakasugi T, Nagai T, Kapoor M, Sugita M, Ito M, Ito S, Tsudzuki J, Nakashima K, Tsudzuki T, Suzuki Y, Hamada A (1997) Complete nucleotide sequence of the chloroplast genome from the green alga *Chlorella vulgaris*: the existence of genes possibly involved in chloroplast division. *Proceedings of the National Academy of Sciences USA*, **94**(11), 5967–72.
Wakefield TS, Farmer MA, Kempf SC (2000) Revised description of the fine structure of in situ" zooxanthellae" genus *Symbiodinium*. *The Biological Bulletin*, **199**(1), 76–84.
Wakefield TS, Kempf SC (2001) Development of host-and symbiont-specific monoclonal antibodies and confirmation of the origin of the symbiosome membrane in a cnidarian–dinoflagellate symbiosis. *The Biological Bulletin*, **200**(2), 127–43.
Wang J, Douglas AE (1998) Nitrogen recycling or nitrogen conservation in an alga-invertebrate symbiosis? *Journal of Experimental Biology*, **201**(16), 2445–53.

Wang JT, Douglas AE (1999) Essential amino acid synthesis and nitrogen recycling in an alga–invertebrate symbiosis. *Marine Biology*, **135**(2), 219–22.
Wang LH, Liu YH, Ju YM, Hsiao YY, Fang LS, Chen CS (2008) Cell-cycle propagation is driven by light–dark stimulation in a cultured symbiotic dinoflagellate isolated from corals. *Coral Reefs*, **27**(4), 823-35.
Wang LH, Lee HH, Fang LS, Mayfield AB, Chen CS (2013) Fatty Acid and Phospholipid Syntheses Are Prerequisites for the Cell Cycle of *Symbiodinium* and Their Endosymbiosis within Sea Anemones. *PLoS One*, **8**(8), e72486.
Warner BJ, Blain SW, Seoane J, Massagué J (1999) Myc down-regulation by transforming growth factor β required for activation of the $p15^{Ink4b}$ G_1 arrest pathway. *Molecular and Cellular Biology*, **19**(9), 5913–22.
Wasylyk C, Wasylyk B (2000) Defect in the p53-Mdm2 autoregulatory loop resulting from inactivation of TAFII250 in cell cycle mutant tsBN462 cells. *Molecular and Cellular Biology*, **20**(15), 5554–70.
Weis VM (2008) Cellular mechanisms of Cnidarian bleaching: stress causes the collapse of symbiosis. *Journal of Experimental Biology*, **211**(19), 3059–66.
Weis VM, Davy SK, Hoegh-Guldberg O, Rodriguez-Lanetty M, Pringle JR (2008) Cell biology in model systems as the key to understanding corals. *Trends in Ecology & Evolution*, **23**(7), 369–76.
Weis VM, Reynolds WS (1999) Carbonic anhydrase expression and synthesis in the sea anemone *Anthopleura elegantissima* are enhanced by the presence of dinoflagellate symbionts. *Physiological and Biochemical Zoology*, **72**(3), 307–16.
Weis VM, Reynolds WS, Deboer MD, Krupp DA (2001) Host-symbiont specificity during onset of symbiosis between the dinoflagellates *Symbiodinium* spp. and planula larvae of the scleractinian coral *Fungia scutaria*. *Coral Reefs*, **20**(3), 301–8.
Welchman DP, Aksoy S, Jiggins F, Lemaitre B (2009) Insect immunity: from pattern recognition to symbiont-mediated host defense. *Cell Host & Microbe*, **6**(2), 107–14.
Wernegreen JJ (2012) Endosymbiosis. *Current Biology*, **22**(14), 555–61**.**
Werner GD, Kiers ET (2015) Partner selection in the mycorrhizal mutualism. *New Phytologist*, **205**(4), 1437–42.
Wicks LC, Sampayo E, Gardner JP, Davy SK (2010) Local endemicity and high diversity characterise high-latitude coral–*Symbiodinium* partnerships. *Coral Reefs*, **29**(4), 989–1003.
Wilkinson CR, Fay P (1979) Nitrogen fixation in coral reef sponges with symbiotic cyanobacteria. *Nature*, **279**(5713), 527–29.
Wilkinson SP (2019) Aphid: an R package for analysis with profile hidden Markov models. *Bioinformatics*, **35**(19), 3829–30.
Wong OK, Fang G (2007) CDK1 phosphorylation of BubR1 controls spindle checkpoint arrest and Plk1-mediated formation of the 3F3/2 epitope. *The Journal of Cell Biology*, **179**(4), 611–17.
Wood-Charlson EM, Hollingsworth LL, Krupp DA, Weis VM (2006) Lectin/glycan interactions play a role in recognition in a coral/dinoflagellate symbiosis. *Cellular Microbiology*, **8**(12), 1985–93.
Wood DJ, Endicott JA (2018) Structural insights into the functional diversity of the CDK-cyclin family. *Open Biology*, **8**(9), 180112.
Xiang T, Nelson W, Rodriguez J, Tolleter D, Grossman AR (2015) *Symbiodinium* transcriptome and global responses of cells to immediate changes in light intensity when grown under autotrophic or mixotrophic conditions. *The Plant Journal*, **82**(1), 67–80.
Xiang T, Lehnert E, Jinkerson RE, Clowez S, Kim RG, DeNofrio JC, Pringle JR, Grossman AR (2020) Symbiont population control by host-symbiont metabolic interaction in Symbiodiniaceae-cnidarian associations. *Nature Communications*, **11**(1), 108.
Yagi K, Furuhashi M, Aoki H, Goto D, Kuwano H, Sugamura K, Miyazono K, Kato M (2002) c-myc is a downstream target of the Smad pathway. *Journal of Biological Chemistry*, **277**(1), 854–61.
Yam CH, Fung TK, Poon RY (2002) Cyclin A in cell cycle control and cancer. *Cellular and Molecular Life Sciences*, **59**(8), 1317–26.
Yan H, Merchant AM, Tye BK (1993) Cell cycle-regulated nuclear localization of MCM2 and MCM3, which are required for the initiation of DNA synthesis at chromosomal replication origins in yeast. *Genes & Development*, **7**(11), 2149–60**.**
Yellowlees D, Rees TA, Leggat W (2008) Metabolic interactions between algal symbionts and invertebrate hosts. *Plant, Cell & Environment*, **31**(5), 679–94.
Yuyama I, Higuchi T (2014) Comparing the effects of symbiotic algae (*Symbiodinium*) clades C1 and D on early growth stages of *Acropora tenuis*. *PLoS One*, **9**(6), e98999.
Zawel L, Le Dai J, Buckhaults P, Zhou S, Kinzler KW, Vogelstein B, Kern SE (1998) Human Smad3 and Smad4 are sequence-specific transcription activators. *Molecular Cell*, **1**(4), 611–17.

Zhan Q, Antinore MJ, Wang XW, Carrier F, Smith ML, Harris CC, Fornace AJ (1999) Association with Cdc2 and inhibition of Cdc2/Cyclin B1 kinase activity by the p53-regulated protein Gadd45. *Oncogene*, **18**(18), 2892-900.

Zhang HS, Postigo AA, Dean DC (1999) Active transcriptional repression by the Rb–E2F complex mediates G_1 arrest triggered by $p16^{INK4a}$, TGFβ, and contact inhibition. *Cell*, **97**(1), 53–61.

Zhao M, Mishra L, Deng CX (2018) The role of TGF-β/SMAD4 signaling in cancer. *International Journal of Biological Sciences*, **14**(2), 111.

Ziegler M, Order CM, Büchel C, Voolstra CR (2015) Mesophotic coral depth acclimatization is a function of host-specific symbiont physiology. *Frontiers in Marine Science*, **2**, 4.

Zook D (2015) Symbiosis—Evolution's Co-Author. In: Reticulate Evolution, Interdisciplinary Evolution Research, Springer, Cham, **3**, 41–80.

Appendix A: Supplementary Figures and Tables for Phylogenetic analysis of cell-cycle regulatory proteins within the Symbiodiniaceae

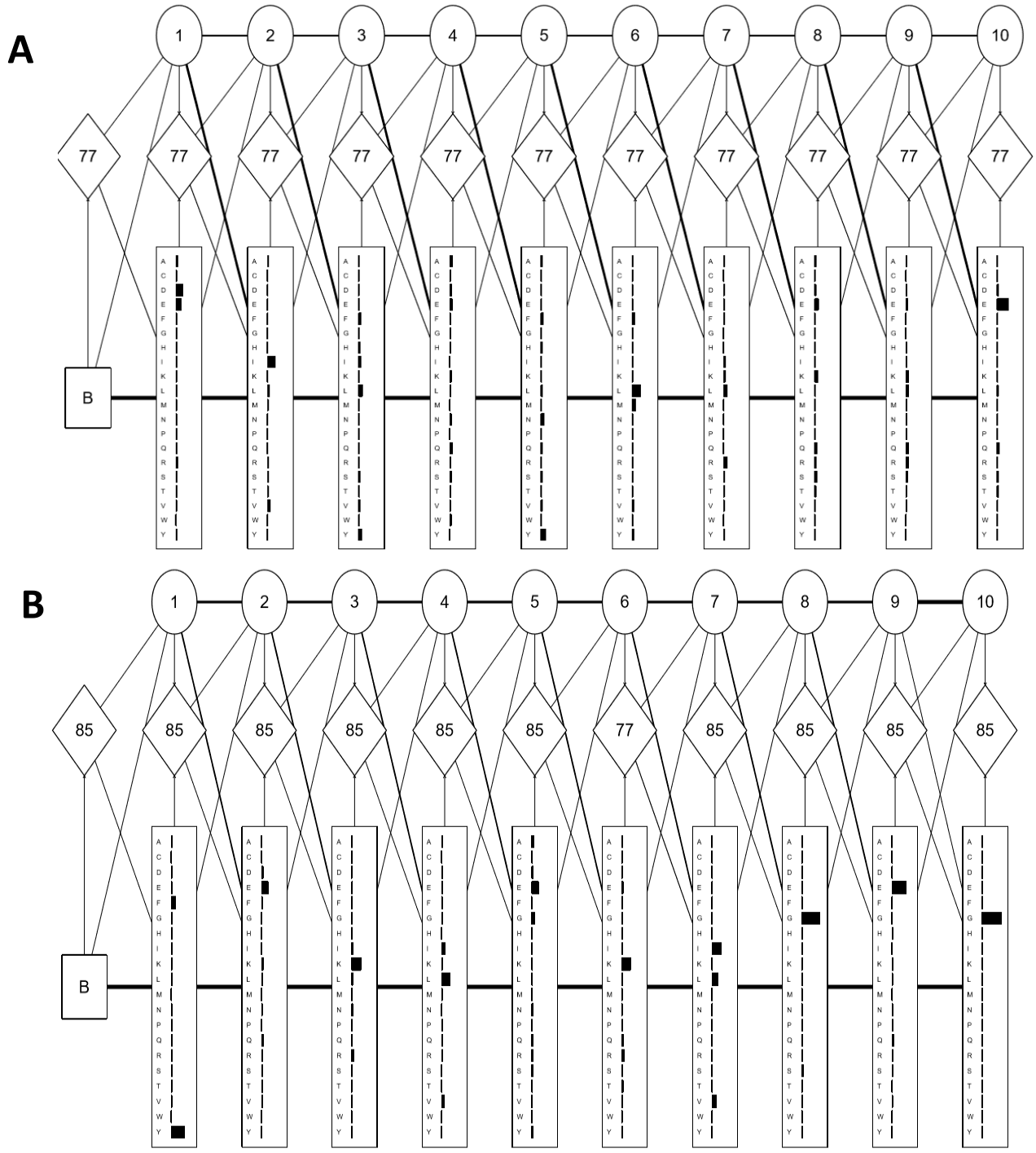

Fig A1. (A) Residues 1-10 of trained cyclin pHMM model for querying Symbiodiniaceae databases. (**B)** Residues 1-10 of trained cyclin-dependent kinase pHMM model for querying Symbiodiniaceae databases. Black horizontal bars represent the likelihood of an amino acid appearing at that residue. Match states are shown as rectangles, insert states as diamonds, and delete states as circles. Numbers in the delete states are simply model module numbers, while those in the insert states are the probabilities of remaining in the current insert state at the next emission cycle. Lines are weighted and directed where necessary to reflect the transition probabilities between states. The large "B" label is the silent begin state of the model.

Table A1. Cyclin- and CDK-specific roles and timing within the mammalian cell cycle. Class I refers to those involved directly in the cell cycle and Class II refers to those involved in transcription.

	Class (I/II)	Cell cycle stage	Role
CDK1 - Cyclin A/B	I	S/ G_2/M	CDK1 sequentially binds to cyclin A in the S phase and then binds to cyclin B in the M phase. Binding to cyclin B triggers the mitotic cascade (Gavet and Pines 2010).
CDK1 - Cyclin J	I	N/A	Expressed within ovaries and functions in egg chamber development in *Drosophila* (Atikukke et al. 2014)
CDK2 - Cyclin A	I	S	Phosphorylates replication substrates in S phase (Malumbres and Barbacid 2009; Yam et al. 2002). At the end of interphase, cyclin A activates CDK1 which is essential for progression into mitosis (Maciejowski et al. 2010).
CDK2 – Cyclin E	I	S	Phosphorylates retinoblastoma (Rb) and promotes S phase entry (Hinds et al. 1992; Siu et al. 2012)
CDK3	I	G_0/G_1	Phosphorylates retinoblastoma protein (pRb) leading to the expression of cyclins and CDKs, allowing quiescent cells to re-enter the cell cycle (Wood and Endicott 2018)
CDK4/6 - Cyclin D	I	G_1	Mitogenic sensors that pick up on extracellular cues (e.g. growth factors and nutrients) to elicit cell-cycle progression (Kim and Diehl 2009; Oakenfull et al. 2002; Quelle et al. 1993; Sherr and Roberts 1999)
CDK5	I	N/A	Activated by p25/p35 and p29/p39 and targets retinoblastoma protein (pRb) downstream (Shupp et al. 2017)
CDK5-Cyclin D/E	I	N/A	Cyclin D and E binding to CDK5 reduces its activity (Shupp et al. 2017)
CDK5 – cyclin I	I		Abundant in post-mitotic cells and serves anti-apoptotic/pro-survival function (Brinkkoetter et al. 2009; Griffin et al. 2006; Guevara et al. 2014)
CDK7 - Cyclin H	II	N/A	Forms the CDK-activating kinase (CAK) that activates the cell-cycle CDKs1/2/4/6 (Wood and Endicott 2018)

Table A1. continued.

CDK8-Cyclin C	II	N/A	Initiates gene transcription by phosphorylating heptad repeats in RNA polymerase II (Wood and Endicott 2018)
CDK9-Cyclin T/Cyclin K	II	N/A	Catalytic subunit of positive transcription elongation factor b (P-TEFb) which targets the carboxyl-terminal domain (CTD) of RNA polymerase II and is essential for the synthesis of mature mRNA (Morales and Giordano 2016)
CDK10-Cyclin M	II	G_2/M	Forms a complex with CDK10 (Guen et al. 2013) and regulates gene transcription by phosphorylating diverse substrates (Wood and Endicott 2018)
CDK11 – Cyclin L	II		Forms a complex with CDK11 and regulates RNA splicing (Wood and Endicott 2018)
CDK12 - Cyclin K	II	N/A	Initiates gene transcription by phosphorylating heptad repeats in RNA polymerase II (Wood and Endicott 2018). Regulates genes involved in the DNA damage response (Malumbres 2014)
CDK 13 – Cyclin K	II		Initiates gene transcription by phosphorylating heptad repeats in RNA polymerase II (Wood and Endicott 2018)
Cyclin F	I	S/G_2	Restricts E2F activity to the S phase which: prevents premature S phase entry; inhibits DNA damage; and, increases cell fitness (Clijsters et al. 2019)
Cyclin G	I	G_2/M	Triggers cell cycle arrest in response to DNA damage (Malumbres and Barbacid 2005)

Table A2. Symbiodiniaceae genome and transcriptome databases used.

Database	ITS2 type	Transcriptome (T) Genome (G)	Assembly	Gene number	Contig N50 (bp)	Source	Reference
Symbiodinium tridacnidorum (CCMP2430)	A3	T	MMETSP1117	39,104	1,163	iMicrobe - Marine Microbial Eukaryote Transcriptome Sequencing	Keeling *et al.* 2014
			MMETSP1115	47,757	1,551		
			MMETSP1116	40,140	1,187		
Cladocopium sp. #2	C	T	MMETSP1122	47,710	1,551		
			MMETSP1123	37,758	1,129		
			MMETSP1124	35,273	1,123		
			MMETSP1125	40,531	1,355		
Cladocopium goreaui	C1	T	MMETSP1367	48,210	1,424		
			MMETSP1369	48,216	1,377		
Cladocopium sp. C15	C15	T	MMETSP1370	44,616	1,194		
			MMETSP1371	51,910	1,190		
Symbiodinium sp. #2	A	T	MMETSP1374	43,062	1,297		
Durusdinium trenchii	D1a	T	MMETSP1377	56,916	852		
Fugacium kawagutii (CCMP2468)	F	T	MMETSP0132_2C	18,489	214		
Effrenium voratum (CCMP421)	E	T	MMETSP1110	77,821	1,725		
C. goreaui	C1	G		35,913	6,576	Reef genomics	Liu *et al.* 2018
F. kawagutii	F	G		26,609	35,743		
B. aenigmaticum	B1	T		45,343	1,355	Reef genomics	Parkinson *et al.* 2016
B. pseudominutum	B1	T		47,411	1,508	Reef genomics	
B. psygomophilum	B2	T		50,745	1,618	Reef genomics	
B. minutum	B1	T		51,199	1,579	Reef genomics	
B. minutum	B1	G		47,014	2,675	Shoguchi *et al.* 2013	
S. microadriaticum	A	G		49,109	3,987	Reef genomics	Aranda *et al.* 2016
Symbiodinium sp. #1 (CassKB8)	A	T		57,676	1,087	Bayer *et al.* 2012	
B. minutum	B1	T		56,198	741		
Cladocopium sp. #3	C	T		26,986	534		
Durusdinium sp. #1	D	T		23,777	920	Ladner *et al.* 2012	
Cladocopium sp. #1	C	T		55,588	687	González-Pech *et al.* 2017	

Table A2. continued.

Cladocopium goreaui – MI population	C1	T		106,097	1,239	Levin *et al.* 2016
Cladocopium goreaui – SM population	C1	T		93,377	1,323	
Breviolum sp. #1 (SSB01)	B	T		59,669	1,752	Xiang *et al.* 2015
Fugacium kawagutii	F	G		36,850	1,467	Lin *et al.* 2015
Symbiodinium tridacnidorum	A3	G		69,018	1,774	Shoguchi *et al.* 2018
Cladocopium sp. C92	C92	G		65,832	1,686	

Table A3. CDK motifs used to scan Symbiodiniaceae databases.

CDK Motif
PSTAIRE
PTTAIRE
PATAIRE
PTSFLRE
PSTALRE
PATALRE
PVSSIRE
PAVAMRE
PAVALRE
PRISLRE
PVSLLRE
PAHVLRE
PEQFQEE
PEKLKEE
PLSLLRE
PPYALRE
PSSSLRE
PEILERE
PLSSQRE
PQEVQRE
PSEIANE
PARFQRE
PARFQVE
PLCVERE
PSASLRE
PAVIRRE
PAATIRE
PCTAIRE
PISTVRE
PSSALRE
PLSTIRE
NRTALRE
SMSACRE
PITALRE
PISSLRE

PITSLRE
PFTAIRE

Table A3. continued.

PNQALRE
PPTALRE
PITAIRE
NFTALRE
SPTAIRE
SCTTLRE
PLTNLRE
PKNAIRE
HFTTLRE
PTSSLRE

Table A4. Candidate proteins used for custom BLAST searches performed on Symbiodiniaceae databases

Protein relation	Species	Database	Candidate gene ID	Candidate gene
Cyclin A	*Cladocopium goreaui*	MMETSP1367/1369(Keeling *et al.* 2014)	CAMPEP_0199578094	XMCATEVALSLKWPDNSHLMAPAGAACLPPKALAPRAAYHSRSGSLPALEVESTSGAIEHSGLDTRGAPDQGPKSCKGLKSMSVPKGRPAASTVLSLPVGGGTKMAAKVSSKALVGSAMAESAVPEPSTSMPVEDWTDVDKLNEMDPLAVSEYAQSICQHLRESELVKRPSSSYLERVQGDVNAKMRAILVDWLVEVTEEYTLCADTLYQAVNYIDRFLSTRVTTRAELQLVGVTCMWLSSKYEEIYPPTVSDFCFITDNTYTREQLIEMEEVVLKELKYELTVPTAKTFLRRMLQVCSPDELLHFLSNYLTELSLLDYAMLRYLPSTIAAAAIYLANVMLGREPWSANLRHYSTYAPEDIEECVLALAAVHKAATACPSLAAIRDKYAHPRFHEVSMISPVTAAAVTATL
Cyclin B	*Durusdinium trenchii*	MMETSP1377(Keeling *et al.* 2014)	CAMPEP_0196951544	HVNDPALVASYSADIYQYMREREECLLIDPNFLQRQSRVTAKNLAVLHDWLVQVHYKFELQLETLYITNAILLRYLSRVDTPRSKLQLYGVTAMLLASKYEDMYPPVVRDFAYITANAYKPREIIKAEMEMLTTLEFSLEQPLPLX
Cyclin D	*Cladocopium* sp. C15	MMETSP1370/1371(Keeling *et al.* 2014)	CAMPEP_0192418040	MELLCCEGPRVRYAYQDPVLLQDERVLRNLLTCEDKYIPSCRYFNIVQKEIEPHMRRMVTSWMLEVCEEQMCEEEVFPLAVNYLDRFLSVVPTRKCQLQLLGAVCMFIASKLKETSPLPAEKLCIYTDNSITCQELLDWEILVLGKLKWDLSAVTPYDFLEQIFSRLSLPNVSVIRKHAATFIALCCTDEKFLMYPPSMLAAASVCAAFTGLATEEQKSVWTRPMLFSFLQGLTNIEPEYLQSCQELMEEVLHFNVTEPPTSKVENGCSPSTPTDLQEIHF
Cyclin G/I	*Cladocopium* sp. C15	MMETSP1370/1371(Keeling *et al.* 2014)	CAMPEP_0192409796	MKVSCGLNVGKLLRVLQEGLLKEEAAHFAPLTCLVGNEDSDGISLSQRDNITTFMLNLSRRCGFHSETYSLSVNLLDRFLSVVKANPKYLPCMSICCLFLAIKMSEEDEDVPTAADFVKVSGLRFSSSDLLRMERIILDKLNWNLNATTPLYFLQVFHALGVAKGFLDHCPVNQHLQHITSLMEGLLCHHKFMFFKPSTLALALLSHELVYVSNNWFMATHYLQHEGKVSDAELWACSKLVNEHLNSVIQKHLPSFKTLPVTENEDKEFPVIEN

Table A4. continued.

Cyclin F	*Symbiodinium* sp. #2	MMETSP1374(Keeling *et al.* 2014)	CAMPEP_0196 858170	MVIESAPPSMFRQFVTRNTRPRRDPLDIR RGHHEAMMRSRSANPRAPLGDITNGVQ ADLPVKRRSLAPGDPASTALLDGPVWP RVEYSTDFMLNMLDAERKHRQPSADY MRHQNVVHEGMRSVLIDWLVDVHATY ELRIETLFLTISIIDQYLAQVKVSRRELQL IGVASMFIASKFEEIHPPEAKDFVYITAK SYSKQEIFDMELRILSQLQFKVARPTVA HFLQRLEAEASRASKPDSPRERVMQHLP WYLVELCMLDVGTLQFMPSCVAVAAL TLTRRLLNVNAAGPHQCMDLVGQTLAV EVLEECMNFMLNLLEAAPSTATTAAVR RKHSDQISVLGAPQEETEQAVAI
Cyclin L	*Cladocopium goreaui*	SM population – Levin *et al.* 2016	C1SM_TR46552 _c0_g1_i1_m.62 470	YSSPQPSGGPGSALMLALVPEDVLAAPP SREDGIDEDSEDQLRRFGANLIQRAGVL LRLPQLSVATASGLFQRFYFRKSFAEFE VRALAMASLTLASKLLEHPRKVVDVIQ VFYKLKMREAQEQDGSASFAGMPTPLL DPTKKEFHDAKKELLSAERNILRELGFE VHLLLDHPHRYAIEYIEHLQRPAELTQK VWNYLNDALQTSLCCAHQPRNIAGASL VLASKELGVNLPSKPPWWETFGVQIKD AELIANEMEELYQKKRPEYIEIPRRKREV FEPMTPFPSPPSGPGKSPSEEDDHVDGET SLARQDSNIDLEGLEEAMAQSVAALAR AKEGSPQRERPGEDKKEKLVENKLAQE QPQNAQHERSAKDRKKRDRQSEGSQSP KRKNAKKTRGS*
Cyclin P/U	*Breviolum minutum*	Parkinson *et al.* 2016	>m.6019 g.6019 ORF g.6019 m.6019 type:5prime_part ial len:218 (-) comp9819_c0_s eq1:142-795(-)	KTHLIFLQRRTWVAGHARACRPTGTVG VSMEMEDEQEDEPAYDDPGQQVANAG QSFVLALADVLTHLSSLRPPPTGQRVTK FHSVRPPQLPIRDYLFRIARYFQCSRECF VLCLVYIDRIVKLHPDFTICSLNIHRLLV TSVMLAVKFFDDVYYSNAYYAKVGGV RTKEVNALESHFLQLIEWKLHVTPEEFD QYRSHVCTVGAAQPVPRLADDALG*
Apicomplexan Mitotic Cyclin	*Cladocopium goreaui*	MI population – Levin *et al.* 2016	C1MI_TR14393 _c0_g1_i1_m.19 980	FRTRDDNAVNKPPGSTAVTGDVVTRAP VMTQPPISANSRDALPHHVVEYADEIVQ HLLEREQILFAMRAPDYLSAQPDVTERM RIILVDWLVDVHLKFKLHPETFFLAVDY VDRYLMTTKGERSTLQLIGVTAMLIAA KHEEIWPPEVKECVYISANTYQHQEILN MERDIVSALNFKLCVPTPYPFMLRLVEG TDATQDTRHLASYCLDLSSLDYSCLKFL PSTVGFASVLIANLVAENTRRSSNGRHP VAVPLISASDDAEALWTDEHGALSSIDR SQLGIVIECARSILGCASNVNTPTSRYHA VRRKYSSERFGEVASRYTLPPTI*
Dinoflagellate-specific Cyclin #1	*Cladocopium goreaui*	MMETSP1367/1 369 (Keeling *et al.* 2014)	CAMPEP_0199 568816	MAFQARRHANSENVNPNVGATRLGAP QARRKVATAKPQRGVNRAPLASLADIT NIQDARDMRKKPLREPLAPLAPLAPLER SLVTIRNREASPTPMEISNPELLAEAHDK VQSVAEYAPEIADQLFHDEAIFMPRADY MESQQDINGKMRAILVDWLVEVHMKY RLRPETLFLAVNLIDRYMSSLPVLRRRL QLLGVVAMFVAAKFEEIDPPKATDFVYI TDNTYSKDELFQMECNMLSTLEFQVVV PTAAHFVNQFVKANGCENPRHAEVIKYI MELALLDLRMIRHKASHLVAAAVLLSN ELFGRAIPWPEHMIQISRHTDAELRVCCE ELRQLVRQAPSQQLQAVRKKYMLAQH

				YQVARNAVLVAAXSHPMSFDFGRCWR RVAGARCNIGAASPRWRRVLANVGX

Table A4. continued.

Dinoflagellate-specific Cyclin #2	*Cladocopium goreaui*	MI population – Levin *et al.* 2016	C1MI_TR28979_c0_g1_i1_m.38873	ADLGKATAGGGHWSISMTRATSDHSVR SAAHLNILPVAMQPQVRPARRNAVLGDI TNTGPIGLGASGKVLGSEKSSLPSFAPMP SLKTTSVMGTGTTSAAGRCFRGKEDGQ LGLFSLGSAPQAHAREQHARFIRPASGD FMDVAMEEEPSEDPQHVAEYTKDIYAH MFAIEGSFQPRPHYLTEQREINAKMRAIL VDWLVEVHMKHRLRRETLFMAVSLIDR YLSVRQVARKRLQLCGVAAMFIAAKFE EIYPPEVKDFVYITDNAYTKDDILNMEV SMLRTLDFALCGPTAAHFLDRFHRANV CSEEQLHLMHYLAELALLEVQMLQYTP SHIAAAAALLSNKLLKFPTWPPCMAQFS KHSEGEIKACARELCGILESVDRSSLQAI RKKYSQERFKRVAKLSFGSS*
Dinoflagellate-specific Cyclin #3	*Cladocopium goreaui*	MMETSP1367/1369(Keeling *et al.* 2014)	CAMPEP_0199563964	MKRVLADITNELRLSPVRKVPREVHLEE FSDFTSPDVRGLKGWDDQELLHRRLAR LQLSPEPCGIDDDDPQGVAEYVADIFSK LEDDEIYHLSPQGVQLGRLWERERATA VDWMVEVQVLYGLRTETLFLAVSLLDS FLKLNEVNQVQLQLAVVCSLFVAAKFE EIEPPNVKDFVNMTNEVCNKQDILAME ATLLTSLEFSLCRPTAVHFLERGSRSPQR LFSRKMLQKHGFLTQYLLELALVDSQM LRFPPSLQVAAATMVSSRLLGSLVRVPR HDISGERSAMIYRCALEMCRLLEEVELS SHQAVRKKFLRPDYLSVAAMVSCT
Unidentified cyclin #1	*Symbiodinium* sp. #2	MMETSP1374 (Keeling *et al.* 2014)	CAMPEP_0196853782	XSRPPLRFFMEHRHLDAEAHKGMLRMI RSARSRLNKEAEDPSANFTSAVADGRD GGLPVSMHLSSRWRLEAGSLHQELKTA RTDRSESVGCTRPHASLLQHAVATGDSP THPVQRMRSDQRAVALEPQQPPLNDRA LKRGGQRSTFGGVGRPRLARSRSTADA LLATQGASENAVPAIQQADAPALPASQP LPHPAPQFVLSDVTNTAGHTGPPAAKLH AQTEPDANCVKPSVPPPTVTEPCAGHPA VASAVPSAPPLAPRGAPAPSRTAGGPRP SVVVAAQSPESRPSTEATDMEVDAVGID AEDPQVPVEYLADIYRHLDREEAHRLPR VLYMEKQTHVNAKMRAILIDWLVDVH KKYKLQTETLFLATSVVDGFLEQRVVQ RRHLQLVGVTGLLIAAKFEEMYPPQIND FVYVTAKAYKKEEVARMEVSMLNALD FNLCHPTAAHFLARYQCVNGCSEAHAD LAQYLLELTLVDYKMIRYAPSHLAAAAI LLSNKLLRRQPCWPASVVRHTKLTESAL KDCAKEICAALEQAENNPLQAVRKKFS QQKYHSVAKLNFTAAPSYVHAREGARR TSVRRSTANGSSQDSPSGQARQPSEGNP V
Unidentified cyclin #2	*Cladocopium goreaui*	MI population – Levin *et al.* 2016	C1MI_TR17217_c0_g1_i1_m.23333	MMDREDMMIEENNLSLEDIDEYDREDP QFCTEYVEEIFALLREKEQTNRVEAGYM ANQDDLIPSYRTKIVNWMGEVYMKFRL LSETLILAVNILDRFLMERPVSRSRLQLL GATAMLVACKFEEIYLPQIDDFVYLCAD AYSRKDFLRMENIILGTLNYNLAVPTPL HFLRRFSKAAFSDRKVHTLSKYITELSLS SYELLRFLPSQVAAAAVLVARNMSGITP LWNSTLRHYTQYKESDIMECAEMLNEM IRQVHEEA

Table A4. continued.

CDK1/2/3	*Cladocopium goreaui*	SM population – Levin *et al.* 2016	>C1SM_TR64037_c0_g1_i1_m.108940	EKRIEKGKMSIMEKYVKVEKPVGEGTY GVVYKARHKETGDIVALKKIRLEMEDE GVPSTALREISLLKELDHPNIVRLRDVEH QQQPKRLYLVFEWLEQDLRKHMDNLD GPMSNELIKSYMSQMLQGLDYCHCHGI FHRDLKPQNLLIDRTGTLKIADFGLARA FSLPFRTYTHEVVTLWYRAPEILLGQRR YGLPVDMWSVGTILAEMSNRRPLWPGE CEIDELYKIFRSLGTPDDSMWPGVASLP DYQDVFPNWSPQPLEKDVPRLEPMGIKL LAEMLKYDPATRISARNALRHEYFKDM *
CDK5	*Durusdinium trenchii*	MMETSP1377 (Keeling *et al.* 2014)	CAMPEP_0196914612	LLYKTYLLFFFLVVFISMISKSKLDKYEK LDKLGEGTYGVVYKAKDKTTGDLFALK KIRLESEDEGIPSTAIREIALLKELQHPNI VRIHDVIHTNKKLILVFEYVDYDLKKFL NSFDKGIDIKIAKSLLYQLVRGIAHCHQ MRVLHRDLKPQNLLVSKEGVLKLADFG LARAFGIPVKNYTNEVVTLWYRAPDILL GSKNYSTTVDIWSIGCIFVEMLNLKPLFP GSSEPDQLKKIFKIMGTPDPEKWPGLTE LPDYKPENFEGYTTEPLNKLCPSMPEDG LDLLDKMLRCNPAERITAKDALKHKFFE DIPENLKKLYN
CDK10	*Cladocopium goreaui*	Liu *et al.* 2018	SymbC1.scaffold196.6 SymbC1.scaffold196:164432-177259(+)	MSGLESGTYGTVYRARDTETGDIVALK KVRIHAEKEGFPRISLREIRLLKRLRHPNI VELREVACGRQSGSVFLVFEYCEHDVG ALLDLMERPFSQPEVKCLTLQLLKAVEC LHLASVIHRDIKLSNLLLNNKGVLKLAD FGLAREFVDFQTPITQNVVTLWYRAPEL LFGAKKYTVAVDMWSVGCNFGELLLK RPLLPGKCEEHQLVLTCELLGTPTPRIWP GVEKLPHYAASKLPENIYNNLGLKFPDL PDSCLDLLNRLLTFDPQKRSSASSSLQHL WFSEAPAPQEPHYMPTFREHRNETANPR GLPAAAKAPAKRPMVARSAVFAAAKK LKSCVF
CDK11	*Cladocopium goreaui*	Liu *et al.* 2018	SymbC1.scaffold1236.5 SymbC1.scaffold1236:119372-126370(-)	MATLDAADGEAAAKRQRVGGWAENCL NQGCRSVQCFRKLNRIDEGTYGVVYRA CEIDTGEVVALKQLKLGAVKSEEGFPVS SIREISLLLELNHPNVVQCREVVLGNTM QHVYMVMEYVEHELKVLITQQRFAVAE MKCLLRQLLLGLAHLHAMWIVHRDLK TSNILLDRNGILKICDFGLARHFGQPLRP YTHRVQSLWYRAPELLLGQRTYSNAID VWSSGCIFAEMLLRRPVFEGKAEMHQL GLIMGLVGLPDEESWPGCSELPHWKML ESFKDTMPGWRELFPEPPDSTLSELGLLL MRGLLECCPARRLAAADAVEHHYFQEV PQPQEPSMLPTFKESNSSTRGQR
CDK12/13	*Breviolum minutum*	Shogucchi *et al.* 2013	symbB.v1.2.023129.t1	MSTGKYQKVDDSPVGEGTYGTVWKGV NRENSAEVAMKKVVIRHPKEGLPTTAIR EIRALRTLQSHPNVVKMYDVYSEMPGS NGSVGDVYLIFEYAPHDLTGFMAYRKK LKLTEIKCLTAQLLEGLDYCHSLLVMHR DLKPSNILLTADGTLKLCDFGLCRLVKE AEPGAYTTRVITLWYRPPELLLGCQKYD FSVDIWSAGCIVGEMLFTVPLFPDSAEV QVLKKIRNRLTAFNADDWPSSMRKHQH WEKFWQQINRPVAPGENRDLYGDLKV

				KHGSLCVDFLKSFIHLDPAERKDTGTLL NHEFLDEEPLACGKKEMKMPPEGTNMK ELGIKRKAEEAGHGGKQRAPKRHADEG RLEPSPKRPRAP

Table A4. continued.

Alveolate-specific CDKA	*Cladocopium goreaui*	Liu *et al.* 2018	SymbC1.scaffold591.6 SymbC1.scaffold591:142736-143969(+)	MQVLADAGRSLLTERHLPELPDSPATDD RPDGADCSDVLLQAALHLQPWAVRGM EQYQKIEKVGEGTYGVVYKAQDSGGK VYALKTIRLEAEDEGIPSTAIREISLLKEL QHPNIVRLCDVIHTERKLTLVFEYLDQD LKKLLDMCEGGLDSATTKSFLYQLLRGI AYCHAHRVLHRDLKPQNLLINREGSLK LADFGLARAFGIPVRSYTHEVVTLWYR APDVLMGSRKYSTPVDIWSVGCIFAEM VNGRPLFPGDTDANQLQKIFRILGTPSAE TWPTITELPDWKPDFPVFEPQAWTSITPT LEPEGMDLMTKFLQYWPDRRISGKAAQ EHDYFKELSDAIKNMK
Alveolate-specific CDKB	*Cladocopium goreaui*	Liu *et al.* 2018	>SymbC1.scaffold10778.1 SymbC1.scaffold10778:323-3022(+)	MALKPRSSLEDFHGVENISHNLGDDEEN MQPGRQTPISQRRPLQQRFNFNCMALSP TKCRKQSHGLAEESPLKLAKDEVWISPA KLPEMRSGTFSLWLEVFRRLGARDIVSK AAPVCRQWRDVAQDRELWALARQHLR LVDCHVMLDKVVERRSKGRIFKCRALG SGDIVMLRMVDLELTNAGRDDGMPTSF LREAALLSELRHPNVIRHYGAEILDKRG VVCSEFVYENWTSWFKRLEVKFPCQRM EDIKGNFSQMLRGLNYLHHQGLMHRNL KPDNIFIDELGTVKVGDFTTTRMLDIPFQ AYTPEDPKERDRSGREMRRLWYRSPELI IREEIYGPKVDTWSVGCLFVEAATGRPL FQSDSEIDHLFRIFRLVGTPTLANWPGVV AAKNFSPKFPMYQGFSFAQVARAESLKP QSFEDQQRLWLQAQPDREEMLHQLIQIA RVVGVDGMFLLDRLITAAPLSRAGVEET LRMPFFAPSFGSEQGSLGSFGQGAQGRL QRNVQSFHPMTELWLGGRPVRLEEQRE QRPQPKNLENPEAKSYATPPTPATTLANI GSAQSQYPPMAIPSSLITSEMVWNILNV MLEQERSPSSVFATWSLPPGFDANARAV QVDFIIGLASSMNLRASTAHLACAVFDK YLSLQEKPVMPEQIKVVAATCLKVSDIF GEQSKEYYKQENSVEYTEAAVGKSITPS QMLSCEKEILPKLGFKLHHPTIRWFLQC YIAYARLSMFDAVGKTASFIADLMLLDF ELLLYTPSLKAQCAVLMAAFLVQQEAT LHQPHQPLDKAMKSLPNEDQSDKCKSI GPLQGYLSCLAYWDKNIRDAVCRANVA VDASMCLQAVVRMLLDKRREWKSLQL NAVEIKHAQLARALAYPDRFPVFKLLRY ILSDHQRSLVPE
Dinoflagellate-specific CDKA	*Breviolum aenigmaticum*	Parkinson *et al.* 2016	>m.43804 g.43804 ORF g.43804 m.43804 type:5prime_partial len:303 (-) comp28229_c0_seq1:90-998(-)	KLGEGTYGKVYKAACHQTGQVVALKRI PIVMDEDGVPATAIREVSLLKECDHPNV IRLHEVLSLDRALYLVFEYVDMDLRIFL KRNGAFKDPLALKNAAWQCIRGTAFCH GRQVLHRDLKPQNVLVDSTGCHLKLAD FGLARLLDVPLRAYTHEVVTLWYRAPEI LLGHRKYAMPTDIWSLGCIVAEMATAE VLFPGDSQIDTIFKIFRRLGTPSEEVWPGF STLKNFTEEFPKWSNTELVDVRSKAPSL GSRGVDMINACLRFNPVDRPSALKLLQ HKFFERAPLYEAVAVAEEAGRTSSC*

Table A4. continued.

Dinoflagellate-specific CDKB	*Breviolum minutum*	Parkinson *et al.* 2016	>m.48530 g.48530 ORF g.48530 m.48530 type:5prime_partial len:339 (-) comp39104_c0_seq1:385-1401(-)	LTIQRNVSFDMLGGRSHPMQRSMADLE DNLDEAEKAFESQYEKVEPSLLGEGTYG KVFKAKSIRTGELVAMKQMKLEGSEDG MPSTALREIALLKELKDHQNIVRLLNIFY KPNKLVLVFEFVENDLKKYMRSMGNNL SPGTVKNFAFQLFQGVQFCHANRILHRD LKPQNLLIDQRLRLKIADFGLARPFHVP VGEYTHEVVTVWYRPPEILLGSQKYSLP VDLWSIGCVIAEMATGSALFPGDSEIATI FKIFQRLGTPTEQMWPDITKLPYFKPSFP QWPAHSWSQIRNTLQQVGSDGCDLLDK LTYYDPRRRISAHRALQHAYFRDIDPRD GEV*
Dinoflagellate-specific CDKC	*Breviolum pseudominutum*	Parkinson *et al.* 2016	>pmin_comp22611_c0_seq1:82-1323(-)	MGFMETQDVAKRRRLDPPTDVDAFSGS NRTNSRPQLHPTPSTPSVGNAPPTAPGLR AGLHPQLHPNLQAASSLGSGSSSREELPS GPRYQTQCVLGRGSFGTVCKAIEVRSRK TVAIKTVASSGAGREMEVLRRLSGNPN VVSLLGAFEGTDPEARTLNFVLEYIEDT LGRIIKHHRQQGTEMDFNFVRIYMYQLL RGLGSLYREGIVHRDIKPANLLVDPQSY CLKVCDFGTAKWVNTNEVSQAYVCSRF YRAPELILSTRDHNTSVDMWAAGCVLG EMLLHQPLFAGKDGIDQLFKIMEILGTPS NQQLSQMNPFYDSAAVFTYVPPLKWSK VLRARWSGQAESLLTMMLQYDPKSRPH PMEAMATDFFAELRKSPPKVRIASEFFN FTDQEMSSCKPELLRKLMPEKRPL*
Dinoflagellate-specific CDKD	*Cladocopium goreaui*	Liu *et al.* 2018	>SymbC1.scaffold1699.6 SymbC1.scaffold1699:70847-80883(+)	MVNCDLSRTQDMDRAESLETAICAVQQ AIGHIGLSSEWTSVLSSKLRRPCELCPDV RRVLEKNGWVRGQFRSPPVRELLLREL REMANAANSAHAASAANADHGQSLLPI RLDDDRRFERQYTFEEKEAPVGEGTYG AVYRAFCNLSKKTVAIKRVKMEHEDEG MPSTAIREVAVLKAADHPNVVKLLDVA CSPGRLHLIFEFVDSNLKQYMKKFGLRL EAGVVRALHKQLMQGIDYCHARRIIHR DLKPQNILVDGQDNLKIADFGMARAFN LPIPKYTHEVVTTWYRPPEILFGCEDYSL GVDVWSAGCILGEMATGAALFHGDSEI DTIFQIFKKLGTPCEVEWPGLSELPDFKP SFPQWRKRPWSEIRNIVAQLGSAGTRLL DAMLRYDPLHRISARQTLLHEYFSVLDD VDANMTS
Unidentified CDK#1	*Cladocopium goreaui*	MI population – Levin *et al.* 2016	>C1MI_TR62820_c0_g1_i2_m.149847	LAPRPPAARLDNPVSHQELTNNNCCKK RRSSFLLHHTMSRYEKIEKVGEGTFGVV YKAKDRQTGELVALKRMRLEAEEEGIP CTAIREISLLKELRHDNVVRLHDVVHSD RKLTLVFEFLQMDLRDYMDKAGEGGL DPWSVQHFMRQLLLGIEYCHYRMVLHR DLKPQNLLISRDRVLKLADFGLGRAFEIP VHRMTHDVVTLWYRPPDVLLGSTKYSC NIDIWSAGCIFAEMAIGHALFNGRNDSD QLLKIFTFLGTPTQTEWPSMMDCPHSSA MLARDALHESFKTKSVEDLLAMGGGFE TLGALGCDLLLKMLQYEPQRRLCASEA LAHPYFQQRL*

Table A5. Selected unicellular marine organisms databases used for screening through for CDKs and cyclins.

Taxa	**Species**	**Source of Database**	**Free-living/Symbiotic/Parasitic**	**Heterotroph or photosynthetic**
Dinoflagellate	*Alexandrium fundyense*	MMETSP	Free-living	Photosynthetic
	Alexandrium monilatum		Free-living	Photosynthetic
	Lingulodinium polyedra		Free-living	Photosynthetic
	Karenia brevis		Free-living	Photosynthetic
	Amphidinium cartecea		Free-living	Photosynthetic
	Amphidinium		Free-living	Photosynthetic
	Peridinium aciculiferum		Free-living	Photosynthetic
	Pelagodinium bei		Symbiotic	Photosynthetic
	Kryptoperdinium foliaceum		Free-living	Photosynthetic
	Amoebophyra sp.		Parasitic	Heterotroph
	Brandtodinium nutricula		Symbiotic	Photosynthetic
	Polarella glacialis		Free-living	Photosynthetic
	Ceratium fusus		Free-living	Photosynthetic
	Ansanella granifera	Ensembl(Jang *et al*., 2017)	Free-living	Photosynthetic
Alveolate	*Perkinsus marinus*	NCBI ID:12737	Parasitic	Heterotroph
Diatom	*Licmophora paradoxa*	MMETSP	Symbiotic	Photosynthetic
	Nitzschia puncata		Free-living	Photosynthetic
Chlorophyta	*Chlorella variabilis*	NCBI ID:694 (Blanc *et al.*, 2010)	Symbiotic	Photosynthetic
	Chlorella sorokiniana	NCBI ID: 31394 (Arriola *et al.,* 2018)	Free-living	Photosynthetic
	Chlorella vulgaris	NCBI ID: 700 (Wakasugi *et al.,* 1997)	Symbiotic	Photosynthetic

Table A6. RNA-seq data taken from Maor-Landaw *et al.*(Maor-Landaw et al. 2020) of *Breviolum minutum* CDKs and cyclins that are differentially expressed (log_2 fold-change) in free-living *versus* symbiotic states that correspond to CDK and cyclin proteins found in our study. Values < 0 indicate a down-regulation in expression, whereas values > 0 indicate an up-regulation in expression.

Symbiodiniaceae gene	**log_2 fold-change**	**Adjusted p-value**
P/U-type Cyclin 1	0.34	<0.001
P/U-type Cyclin 2	-0.54	<0.001
CDKB1	0.367	0.0019
CDKB2	0.355	< 0.0001
CDKC	-0.6457	< 0.0001
CDKF	0.9921	< 0.0001
CDKG	0.398	0.01289
CDKH	0.697	< 0.0001
CDKI	-0.2309	0.0026
CDK7-related protein	0.363	0.0135
CDK9	0.1817	0.03014

Appendix B: Autophagy

Due to the COVID-19 pandemic happening during the experiment conducted in **Chapter 4,** autophagy analysis could not be conducted in the time required for the submission of this thesis. However, autophagy samples were taken at the same time points as the other measurements and are currently being analysed. This section will describe the methods used to analyse autophagy in *E. pallida*.

Although transmission electron microscopy can provide accurate images of autophagy in organisms, I wanted to use a more quantitative, and less subjective, method. The golden standard of autophagy flux in metazoans is to assess the turnover of the microtubule-associated protein 1A/1B-light chain 3 (LC3) using western blots as this is directly correlated with the number of autophagosomes in an organism (Kabeya et al. 2000). There are two forms of LC3, the pre-lipidated form of LC3 (LC3-I) and the post-lipidated form of LC3 (LC3-II). LC3-I is found in the cytoplasm and upon autophagic signal becomes lipidated and converted to LC3-II which is directly incorporated into the autophagosome membrane (Tanida et al. 2008). Autophagic flux can be measured by densitometry on western blots, comparing the ratio of LC3-I with LC3-II. Although a past study showed that Aiptasia LC3 is localised to mammalian LC3 (Flesher 2013), an antibody specific to Aiptasia LC3 has not been documented. Thus, I used the LC3 gene sequenced in Aiptasia and contacted Dr. Sean O'Sullivan at Thermofisher to help me to design an antibody for Aiptasia LC3 (Figures B1 and B2).

Antigen Profiler

Custom Antigen Information

Designed For: Lucy Gorman_MAP 1A1B LC3C

Sequence: Length: 128 amino acids.

Protein Sequence and Features

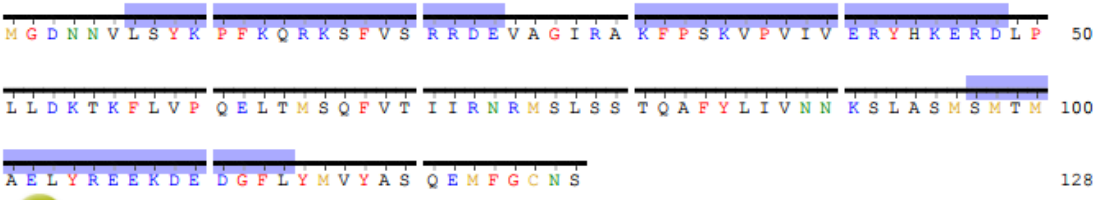

Antigen Peptide Candidates

Name	Peptide	Position	Length
OBS-7:24	LSYKPFKQRKSFVSRRDE	7	18
OBS-31:48	KFPSKVPVIVERYHKERD	31	18
OBS-97:114	SMTMAELYREEKDEDGFL	97	18

Figure B1. Peptide sequence of Aiptasia LC3 and proposed candidate antibodies.

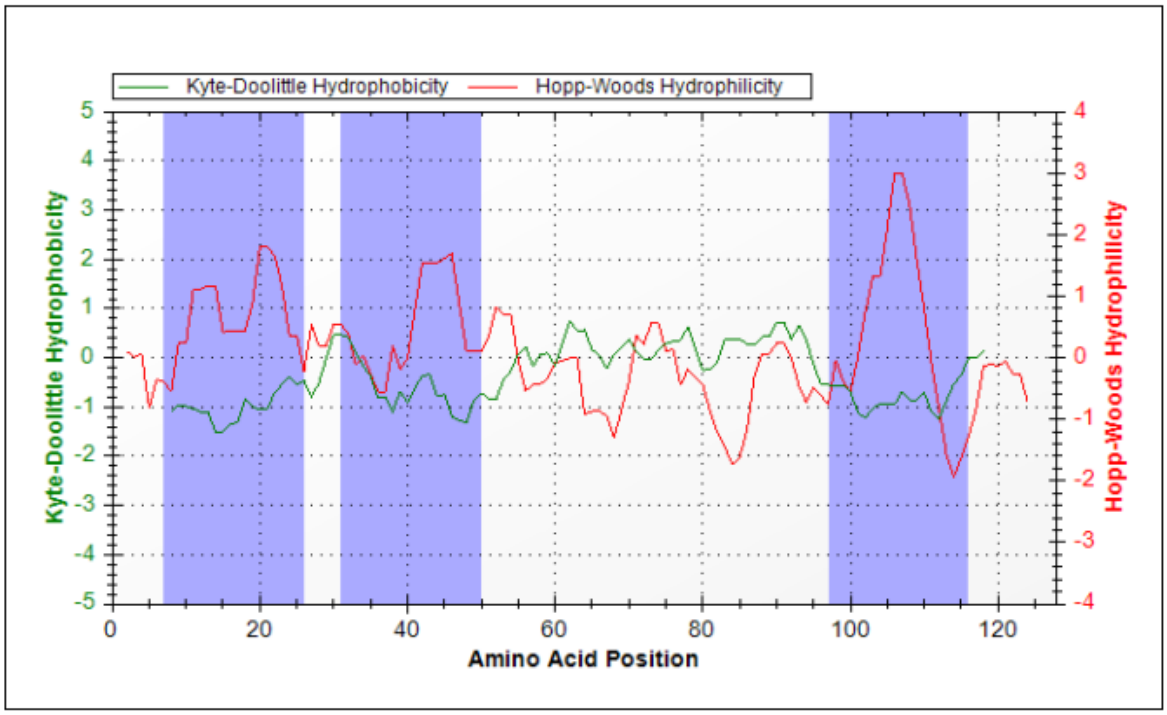

Figure B2. Corresponding hydrophobicity and hydrophilicity in Aiptasia LC3 peptide sequence. Purple boxes correspond to proposed candidate antibodies. Areas with more hydrophilicity are more likely to be on the exposed surface of the protein and therefore to have more antigenicity.

The most promising candidate for antibody design was the 'SMTMAELYREEKDEDGFL' sequence, due to its hydrophilicity and minor number of possible cross reactions with other proteins in the Aiptasia genome.

Protein extraction

Samples were stored at – 80 °C until protein extraction. On the day of the extraction, samples were taken from the freezer and thawed on ice. Once thawed, samples were vortexed in 500 µL ice cold grinding buffer pH 7.4 (100 mM Tris, 100mM NaCl, 10mM EDTA) to remove any salt from the samples. Samples were then re-suspended in 475 µL grinding buffer with 5% w/v SDS at room temperature and homogenised. Once homogenised, 25 µL of 2-mercaptoethanol was added to the samples and the samples were heated to 70 °C for 15 minutes. After heating, the samples were centrifuged for 10 min at 16,100 × g at 4 °C and the pellet was discarded. The supernatant was transferred to a new tube and 5 µL of this sample was used for protein quantification on a Qubit fluorometer.

Tricine-SDS-PAGE

After protein quantification, 20 µg of each sample was added to 4 × sample buffer (12% SDS (w/v), 5% mercaptoethanol (v/v), 30% glycerol (w/v), 0.05% Coomassie blue G-250 (Serva), 150 mM Tris/HCl (pH 7.0)) and heated for 4 min at 80 °C. Once the samples were denatured, they were loaded into gels (10% resolving gel and 4% stacking gel). The gels were then run at 30 V for 45 min and then 160 V for 30 min.

Western blots

The gel was then put into a submarine transfer and transferred at 25 V for 90 min at 4 °C, onto a 0.22 µm pore-size polyvinylidene fluoride (PVDF) membrane. After transfer, the membrane was blocked in TBST (Tris buffered saline + 0.1% Tween) with 5% w/v low fat milk for 60 min at room temperature (RT) or overnight at 4 °C on a shaker. Once blocked, the membrane was probed with the primary antibody at 1:5000/1:10,000 in TBST for 60 min at RT on a shaker. The membrane was then washed three times in TBST for 5 min. Following washing, the membrane was then probed with the secondary horseradish peroxidase conjugated antibody

incubated 1:40,000 in TBST for 60 min at RT on a shaker. The horseradish peroxidase chemiluminescence was induced by 5 min incubation at RT in non-commercial enhanced chemiluminescence solution (100 mM Tris/HCl pH 8.8, 2.5 mM luminol, 2.6 mM hydrogen peroxide and 0.4 mM 4-Iodophenylboronic acid (4-IPBA)). The target protein was then visualised on an Amersham Imager 680 CCD imager with ~10 min exposure time.

Results

The custom-made antibody for *Exaiptasia pallida* LC3 was found to be specific, producing two bands in the areas expected (Fig. B3). Future work will use this method to quantify the rate of autophagy in Aiptasia colonised by different symbiont species with time in symbiosis (Chapter 4).

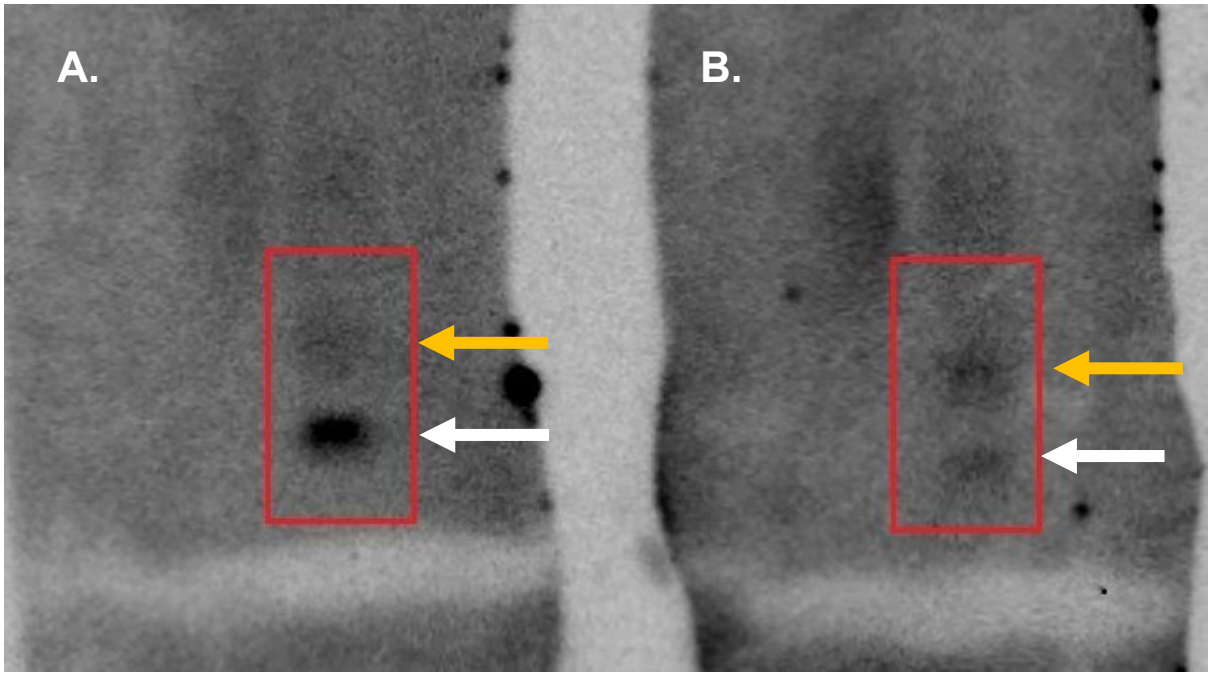

Figure B3. *Exaiptasia pallida* host protein run on a western blot and probed with LC3 antibody. Orange arrow corresponds to LC3-I (16-18 kDa) and white arrow corresponds to LC3-II (14-16 kDa). **(A)** Primary antibody concentration 1:5000. **(B)** Primary antibody concentration 1:10,000.

Appendix C: Cyclin expression in Symbiodiniaceae

During my PhD, I received funding to work with Professor Virginia Weis and the Weis Lab for 2 months. In these 2 months I attempted to further my bioinformatics work from **Chapter 2** by attempting to design qPCR primers for two groups of cyclin genes I had identified in *Breviolum minutum*, *Durusdinium trenchii* and *Symbiodinium microadriaticum*. The aim of this work was firstly to measure in each Symbiodiniaceae species when these cyclins were expressed in culture and to relate this to what cell cycle phase each of the populations were in. The second aim of this work was to measure whether the expression of these cell-cycle cyclins differed in the timing of their expression in symbiosis with the model cnidarian *Exaiptasia pallida*. Due to time restrictions from the COVID-19 pandemic this work could not be continued to a conclusion, however the work which was done on this project is outlined below.

Materials and Methods

Primer design

Two phylogenetically distinct cyclin groups in the 'Protist cyclin A/B' family were chosen from **Chapter 2** (Table C1).

Table C1. Cyclin genes chosen for qPCR.

Symbiodiniaceae species	**Database**	**Protist cyclin A/B group 1 gene**	**Protist cyclin A/B group 2 gene**
Breviolum minutum	Shoguchi *et al.* 2013	SymbB.v1.2.002641.t1	SymbB.v1.2.033807.t1
Durusdinium trenchii	MMETSP – Keeling *et al.* 2014	CAMNT_0042401863	CAMNT_0042328179
Symbiodinium microadriaticum	Aranda *et al.* 2016	Smic39017	Smic26768

Once chosen, the genes in each group were aligned in Geneious v.11.1.5 and the alignments were trimmed to get a consensus sequence for each group. Once a consensus sequence was made, primers recommended for the joint consensus sequence by Primer3 in Geneious v.11.1.5

were BLASTed against the databases for *B. minutum*, *D. trenchii* and *S. microadriaticum,* however no hits were found, therefore primers were designed for each individual cyclin sequence from each species (Table C2). The species-specific primers were then BLASTed against all other Symbiodiniaceae databases to check that the primers were specific to the individual Symbiodiniaceae species.

Table C2. Primer sequences for cyclin genes.

	Cyclin gene	**Forward primer (5' to 3')**	**Reverse primer (5' to 3')**
Group 1	SymbB.v1.2.002641.t1	AGGTGACATGCCTTTGGAGG	GGTGCCAATCAAAACCTGGG
	CAMNT_0042401863	AAGTGCACCGCTTTGATTGC	GCAGACACATCATCGCGTTG
	Smic39017	AGAATGTGGACACAGGGTGC	CCTGTTCGATCTCCAGGTCG
Group 2	SymbB.v1.2.033807.t1	ACCACAGGTACGTCAAGCAC	ATTCCCATCACAGCACTCGT
	CAMNT_0042328179	CACACATCTCCCGAGCACAT	TGATTCAGTACACGCCGTCA
	Smic26768	TTTCAGGTGTACGCAGGCAT	GCAGAACCAAAACCACCACC

A positive control primer for the oxygen-evolving enhancer 1 (OEE) gene was also used as it had been shown to change in its expression with the diurnal cycle in Symbiodiniaceae (Sorek *et al.* 2013).

RNA extraction

RNA was extracted from *B. minutum*, *D. trenchii* and *S microadriaticum* cultures following the methods by Parkinson *et al.* (2016) and Kitchen and Weis (2017). Firstly, 1×10^6 Symbiodiniaceae cells were spun down at 800 × g for 10 mins. The supernatant was discarded and the pellet was resuspended in 1 mL of 0.22 µm FSW and spun down at 10,000 × g for 2 mins and the supernatant was discarded. Then 350 µL of TriZol was added to the pellet in addition to 100 µL volume of glass beads. The sample was then milled for 20 secs. After milling, 350 µL of 100% ethanol was added to the sample and the sample was transfer to a spin column. The sample was spun at 13,000 × g for 30 secs and the flow through was discarded.

Then 400 µL of Direct-zol RNA pre-wash was added to the sample and the sample was centrifuged at 13,000 × g for 30 secs and the flow through was discarded. This step was repeated. After this, 700 µL of RNA wash buffer was added to the sample and the sample was spun at 13,000 × g for 2 mins and the flow through was discarded. Then 50 µL of nuclease-free water was added to the membrane in the spin column. The column was then centrifuged at 13,000 × g for 90 secs and the flow through was kept.

DNase treatment

For DNase treatment, 30 µl of RNA and nuclease-free water was added to 3 µl TURBO DNase Buffer and 3 µl of DNase. This mixture was then incubated at 37 °C for 30 mins. After incubation, 6 µl of inactivation reagent was added to the mixture and the mixture was vortexed. This mixture was left for 5 mins at room temperature and then centrifuged at 10,000 × g for 90 seconds. The supernatant (DNase treated RNA) was then aliquoted into a new tube and the pellet was discarded. RNA quantity was tested on a Qubit fluorometer and RNA quality was tested using a nanodrop.

RNA Clean-up

If contaminants were found in the RNA samples, RNA was cleaned up using the following protocol. For 30 µl of RNA sample, 3 µl of 3M sodium acetate (pH 5.2), 1.5 µl glycogen, and 75 µl of 100% ethanol were added and the sample was mixed gently. This sample was then incubated at -80 °C overnight. The next day, the sample was centrifuged at 9500 × g for 20 mins at 4 °C. The supernatant was then removed and 250 µl of 70% RNA-grade ethanol was added to the pellet. This sample was then centrifuged at 9500 × g for 5 mins at 4 °C. The supernatant was then removed, and the pellet was left to dry for 5 – 10 mins. The pellet was then re-suspended in 20 µl RNase free water.

cDNA synthesis

The Protoscript II cDNA kit was used to create cDNA from the extracted RNA. Briefly, 1 µL of RNA template was added to 10 µL of 2 × Protoscript II Reaction Mix, 2 µL of 10 × Protoscript II Enzyme Mix, 5 µL nuclease-free water and 2 µL of 10 µM oligo-dT primer

[d(T)$_{23}$VN]. This mix was then run on the thermocycler for 1 hour at 42 °C and 5 mins at 80 °C.

PCR for primer specificity

Once the cDNA for each species had been synthesised, PCR tests were conducted to check whether the designed primers worked. For this 1 µL cDNA was added to 0.5 µL of 20 mg/mL BSA, 1 µL of 10 µM forward primer, 1 µL of 10 µM reverse primer, 9.5 µL of nuclease-free water and 12 µL of 2 × GoTaq Green master mix. Samples were then run on the thermocycler for 2 mins at 95 °C, then 40 cycles of 45 secs at 94 °C, 45 secs at 52 °C and 30 secs at 72 °C, before ending with 5 minutes at 72 °C.

Rapid amplification of cDNA ends (RACE) PCR

RACE PCR was also attempted to investigate whether the full sequence of the cyclin genes of interest in the Symbiodiniaceae species could be retrieved. For this method, forward and nested primers were designed for the genes of interest (Table C3).

Table C3. RACE primers for cyclin genes.

	Cyclin gene	RACE 1st Primer	RACE Nested Primer
Cyclin group 1	symbB.v1.2.024610.t1	GGGCAGGAGATCAGCTTGAC	CGACGCAAAGCACCTTGAAA
	CAMNT_0042401863	GGAAGAAACTGGCACGACCT	CAAGATGCGGGCAATTCTCG
	Smic39017	TTCCTGCCTCGACCTTCCTA	CTGGAGCTTGCACTCATCGA
Cyclin group 2	symbB.v1.2.033807.t1	GACGCGAGCCACTTCTGAT	AACGAGTGCTGTGATGGGAA
	CAMNT_0042328179	GTTGCCATGGAGGAAGAGGA	TTGTCGATTGGCTGGTGGAG
	Smic26768	AGCGATCTCGGCTCAAGATG	AGCTTCAAGAAGTGGCTGCT

cDNA for RACE PCR was then synthesised using the following protocol. Template RNA (1 µL) was added to 4 µL of 5 × Protoscript II buffer, 2 µL of 0.1M dithiothreitol (DTT), 2 µL of 50 µM oligo-dT primer [d(T)$_{23}$VN], 1 µL of Protoscript II reverse transcriptase, 1 µL 10mM deoxyribose nucleotide triphosphate (dNTP) and 9 µL nuclease-free water.

After cDNA synthesis, PCRs were run using the RACE nested primers (Table B3). For this PCR, 2.5 µL of cDNA was added to 12.5 µL of 2 × GoTaq Green master mix, 5.5 µL of nucleas-free water, 2 µL of 5 µM nested (forward) primer, 2 µL of 5 µM abridged universal amplification primer (AUAP) (reverse) and 0.5 µL of 20 mg/mL BSA. Samples were then run on the thermocycler for 2 mins at 95 °C, then 40 cycles of 45 secs at 94 °C, 45 secs at 55 °C and 30 secs at 72 °C, before ending with 5 minutes at 72 °C.

Results

PCR for primer specificity

Bands in the 150 bp region (expected product size) were found in the primers designed for the *Breviolum minutum* and *Symbiodinium microadriaticum* cyclin genes in group 2 (Figure C1), however due to RNA contamination these results cannot be accurately confirmed to be the specific cyclin genes.

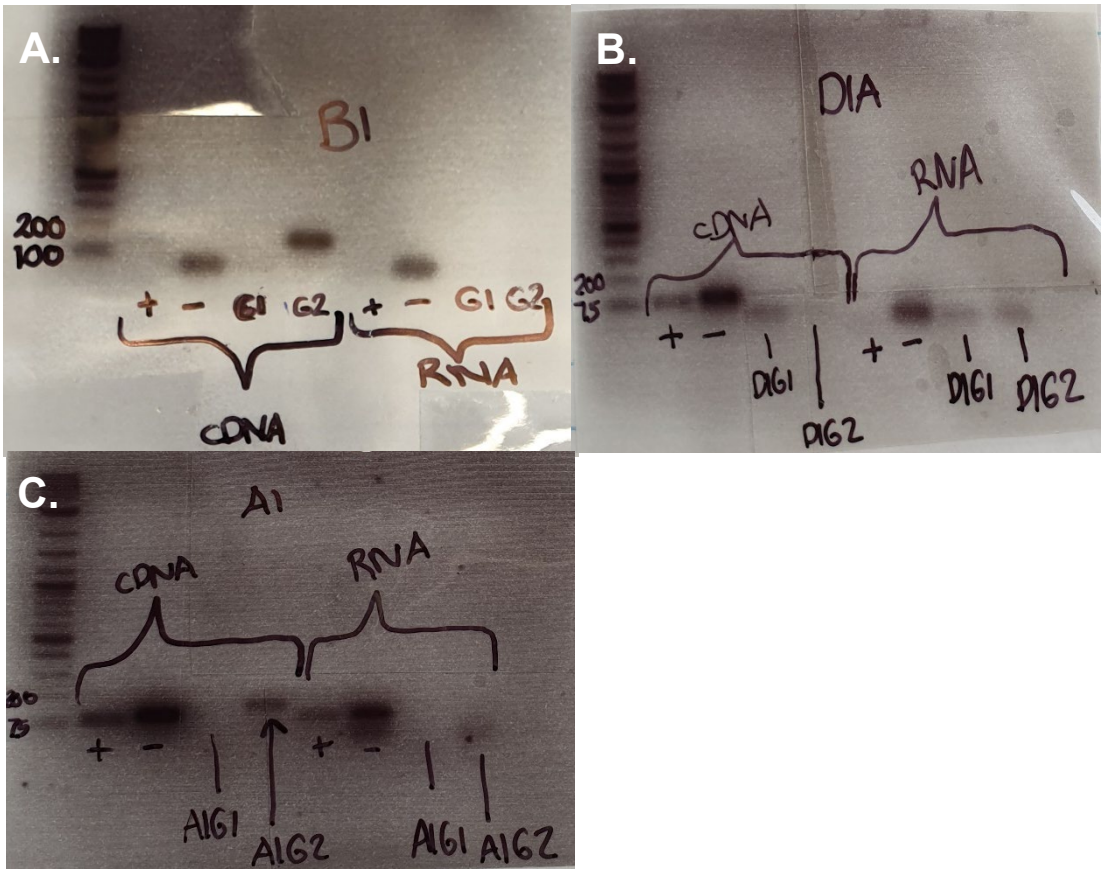

Figure C1. PCR results of primer specificity tests for cyclin group 1 'G1' and group 2 'G2' in (A) *Breviolum minutum*, (B) *Durusdinium trenchii* and (C) *Symbiodinium microadriaticum*. cDNA corresponds to samples run using cDNA of Symbiodiniaceae species whereas RNA corresponds to samples run using RNA template to check for genomic contamination in samples. The '+' corresponds to positive control OEE gene and the '-' corresponds to negative control run without any cDNA or RNA sample.

RACE PCR

Amplification using the nested primers in RACE PCR was witnessed in *B. minutum* nested primer cyclin group 1 and 2, and *D. trenchii* nested primer cyclin group 1 (Figure C2). However, time constraints meant these results could not be investigated further.

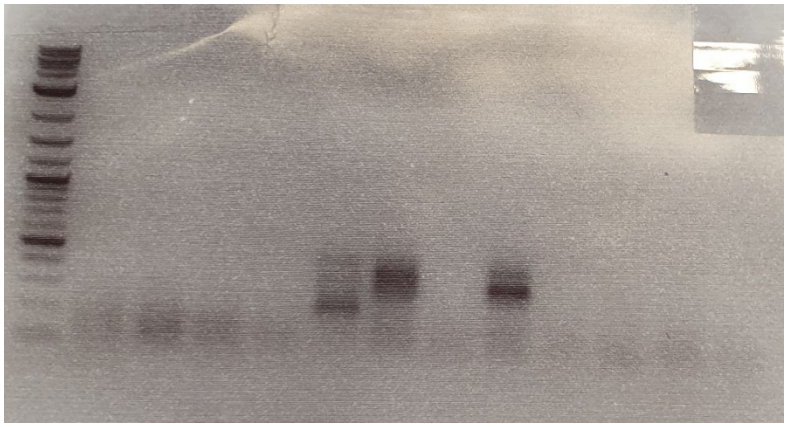

Figure C2. Results from the RACE PCR using nested primers. Lane 1 – ladder, lane 2 – *S. microadriaticum* nested primer cyclin group 1, lane 3 - *S. microadriaticum* nested primer cyclin group 2, lane 4 - *S. microadriaticum* nested primer cyclin group 1, lane 5 – *B. minutum* nested primer cyclin group 1, lane 6 *B. minutum* nested primer cyclin group 2, lane 7 – *B. minutum* nested primer cyclin group 1, lane 8 *B. minutum* nested primer cyclin group 2, lane 9 – *D. trenchii* nested primer cyclin group 1, lane 10 - *D. trenchii* nested primer cyclin group 2, lane 11 – *D. trenchii* nested primer cyclin group 1, lane 12 - *D. trenchii* nested primer cyclin group 2.

Appendix D: Expanded phylogenetic trees

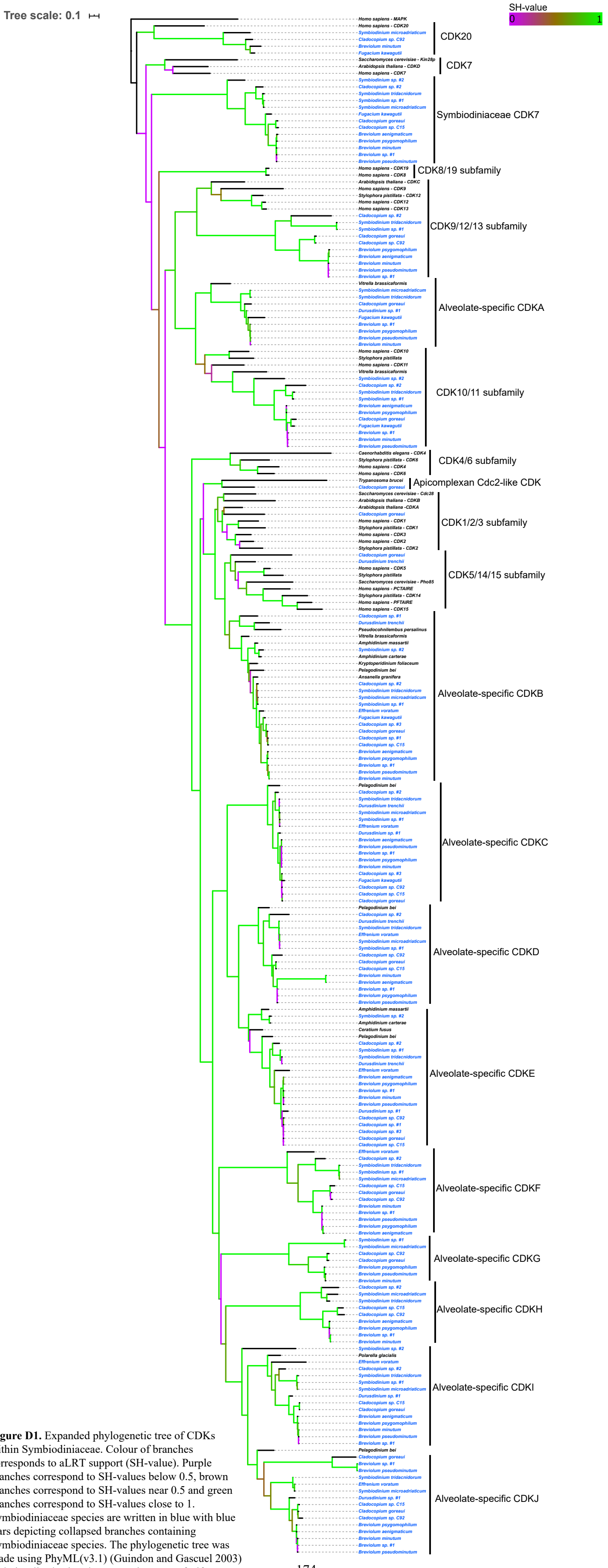

Figure D1. Expanded phylogenetic tree of CDKs within Symbiodiniaceae. Colour of branches corresponds to aLRT support (SH-value). Purple branches correspond to SH-values below 0.5, brown branches correspond to SH-values near 0.5 and green branches correspond to SH-values close to 1. Symbiodiniaceae species are written in blue with blue stars depicting collapsed branches containing Symbiodiniaceae species. The phylogenetic tree was made using PhyML(v3.1) (Guindon and Gascuel 2003) and visualised using the Interactive Tree of Life software (v.5.6.3) (Letunic and Bork 2019).

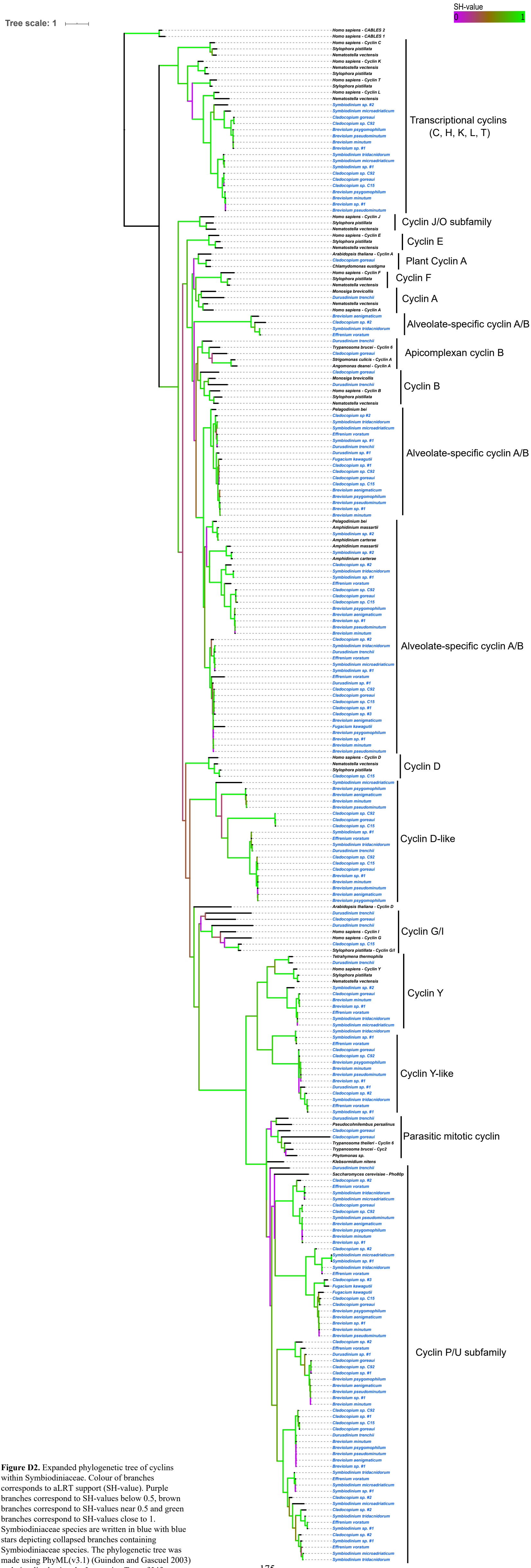

Figure D2. Expanded phylogenetic tree of cyclins within Symbiodiniaceae. Colour of branches corresponds to aLRT support (SH-value). Purple branches correspond to SH-values below 0.5, brown branches correspond to SH-values near 0.5 and green branches correspond to SH-values close to 1. Symbiodiniaceae species are written in blue with blue stars depicting collapsed branches containing Symbiodiniaceae species. The phylogenetic tree was made using PhyML(v3.1) (Guindon and Gascuel 2003) and visualised using the Interactive Tree of Life software (v.5.6.3) (Letunic and Bork 2019).

scientific reports

Check for updates

OPEN

Phylogenetic analysis of cell-cycle regulatory proteins within the Symbiodiniaceae

Lucy M. Gorman[1], Shaun P. Wilkinson[1], Sheila A. Kitchen[2], Clinton A. Oakley[1], Arthur R. Grossman[3], Virginia M. Weis[4] & Simon K. Davy[1]✉

In oligotrophic waters, cnidarian hosts rely on symbiosis with their photosynthetic dinoflagellate partners (family Symbiodiniaceae) to obtain the nutrients they need to grow, reproduce and survive. For this symbiosis to persist, the host must regulate the growth and proliferation of its symbionts. One of the proposed regulatory mechanisms is arrest of the symbiont cell cycle in the G_1 phase, though the cellular mechanisms involved remain unknown. Cell-cycle progression in eukaryotes is controlled by the conserved family of cyclin-dependent kinases (CDKs) and their partner cyclins. We identified CDKs and cyclins in different Symbiodiniaceae species and examined their relationship to homologs in other eukaryotes. Cyclin proteins related to eumetazoan cell-cycle-related cyclins A, B, D, G/I and Y, and transcriptional cyclin L, were identified in the Symbiodiniaceae, alongside several alveolate-specific cyclin A/B proteins, and proteins related to protist P/U-type cyclins and apicomplexan cyclins. The largest expansion of Symbiodiniaceae cyclins was in the P/U-type cyclin groups. Proteins related to eumetazoan cell-cycle-related CDKs (CDK1) were identified as well as transcription-related CDKs. The largest expansion of CDK groups was, however, in alveolate-specific groups which comprised 11 distinct CDK groups (CDKA-J) with CDKB being the most widely distributed CDK protein. As a result of its phylogenetic position, conservation across Symbiodiniaceae species, and the presence of the canonical CDK motif, CDKB emerged as a likely candidate for a *Saccharomyces cerevisiae* Cdc28/Pho85-like homolog in Symbiodiniaceae. Similar to cyclins, two CDK-groups found in Symbiodiniaceae species were solely associated with apicomplexan taxa. A comparison of *Breviolum minutum* CDK and cyclin gene expression between free-living and symbiotic states showed that several alveolate-specific CDKs and two P/U-type cyclins exhibited altered expression *in hospite*, suggesting that symbiosis influences the cell cycle of symbionts on a molecular level. These results highlight the divergence of Symbiodiniaceae cell-cycle proteins across species. These results have important implications for host control of the symbiont cell cycle in novel cnidarian–dinoflagellate symbioses.

Many cnidarians in the marine environment, including reef-building corals, form symbiotic relationships with photosynthetic dinoflagellates from the family Symbiodiniaceae[1]. These dinoflagellate symbionts are located in host gastrodermal cells inside symbiosomes (vacuoles consisting of a host-derived membrane)[2]. This closely integrated intracellular relationship indicates that symbiont population maintenance by the host was likely integral to the evolution of the symbiosis[1,3]. To date, most studies examining symbiont cell division *in hospite* have focused on nutrient availability[4–9]. However, symbiont growth rate appears to be controlled by more than nutrient limitation, as nutrient-replete symbionts *in hospite* still have a growth rate that is less than 20% of symbionts *ex hospite*[5].

Besides nutrient control, other proposed host regulatory mechanisms of symbiont growth and proliferation include pre-mitotic cell-cycle control and post-mitotic autophagy, expulsion and apoptosis[1,7,10,11]. However, the contribution of each mechanism towards the regulation of symbiont biomass, from the onset to the stabilisation of the symbiosis, is unknown. Smith and Muscatine[7] proposed that the main control of a dampened symbiont growth rate *in hospite* is from the cnidarian host arresting the cell cycle of its resident symbionts. In the eukaryotic cell cycle there is one quiescent stage (G_0) and four subsequent cycling phases: G_1 (gap 1) where cells grow and are sensitive to extracellular cues such as growth factors[12]; S (synthesis) where genomic DNA is replicated and synthesised[13]; G_2 (gap 2), where DNA breaks that occur during the S phase are repaired before mitosis[14];

[1]School of Biological Sciences, Victoria University of Wellington, Wellington 6140, New Zealand. [2]Division of Biology and Biological Engineering, California Institute of Technology, Pasadena, CA 91125, USA. [3]Department of Plant Biology, The Carnegie Institution for Science, Stanford, CA 94305, USA. [4]Department of Integrative Biology, Oregon State University, Corvallis, OR 97331, USA. ✉email: Simon.Davy@vuw.ac.nz

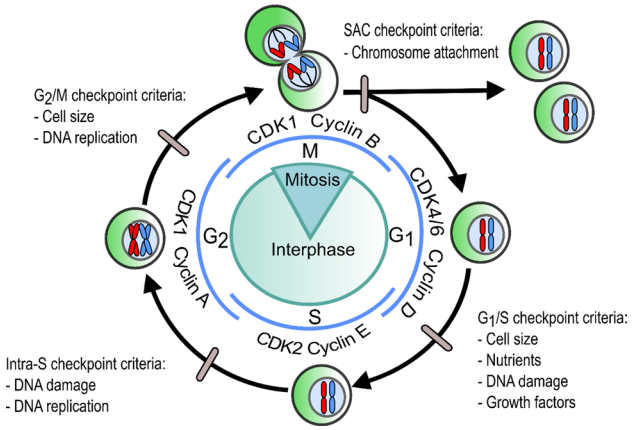

Figure 1. The generalised cell cycle in eumetazoans illustrating the cell-cycle phase and regulatory checkpoints (grey ovals) with their complementary criteria that must be met for the cell cycle to progress through that checkpoint. Blue lines depict the formation of cell-cycle phase associated CDK-cyclin complexes in *Homo sapiens*. *SAC* Spindle Assembly Checkpoint.

and M (mitosis), where two equal copies of the chromosomes are distributed between the two cells[13]. In the sea anemone *Exaiptasia pallida* ('Aiptasia'), 80% of the resident symbionts were shown to be arrested at the G_0/G_1 phase compared with 40–55% in culture[7].

Once a cell enters the cell cycle, it can be arrested at a series of cell-cycle checkpoints (Fig. 1). These checkpoints monitor the integrity and correct progression of the cell cycle with each checkpoint containing criteria that must be met for a cell to progress to the next stage of the cycle[15,16]. Each checkpoint is regulated by cyclin-dependent kinases (CDKs) and their partner cyclins[17]. Once a cell meets its checkpoint criteria, cyclins are synthesised and bind to their partner CDKs[17]. Cyclins regulate the catalytic activity of CDKs[18]. These CDK-cyclin complexes can directly trigger cell-cycle progression (Fig. 1) or indirectly trigger cell-cycle progression through a variety of other downstream events such as transcription, DNA damage repair, proteolytic degradation and metabolism[19]. Table S1 summarises the cell-cycle stage and roles of individual CDK and cyclin proteins. CDK-cyclin complexes in *Homo sapiens* are shown in Fig. 1; however, the type and quantity of CDKs and cyclins are specific to a particular species[17].

Identification of cell-cycle proteins in the Symbiodiniaceae is just beginning, with a study by Cato et al.[20] finding 10 distinct CDKs and 15 distinct cyclin genes in the genome of *Breviolum minutum*. In the same study[20], qPCR analysis revealed that a cyclin B2/CDK1 pair was expressed during the G_1/S phase transition in cultured *B. minutum*. As there are at least nine genera of Symbiodiniaceae[21,22], determining whether cell-cycle proteins present in *B. minutum* are conserved across the Symbiodiniaceae will inform our understanding of cell-cycle progression and cellular growth rates in this family. For example, a recent study[23] comparing cell-cycle progression between four Symbiodiniaceae genera (*Symbiodinium*, *Breviolum*, *Cladocopium* and *Durusdinium*) in culture, found that the proportion of the population progressing through the cell cycle was different between genera, resulting in differing growth rates. Similarly, different Symbiodiniaceae species have been shown to have different proliferation rates and reach different densities within the same host[24–27], with inherent differences in cell-cycle machinery between species being one possible explanation. The current study represents the first attempt to identify and describe cell-cycle proteins across diverse Symbiodiniaceae species and provides a basis for future research.

Materials and methods

Identification of Symbiodiniaceae CDKs and cyclins. Twenty-seven Symbiodiniaceae transcriptome and genome databases were acquired from publicly available sources (Table S2). Cyclins and CDKs from two free-living Symbiodiniaceae species, *Effrenium voratum*[28] and *Fugacium kawagutii*[29], were compared with symbiotic species (*Symbiodinium microadriaticum*, *S. tridacnidorum, Breviolum minutum, B. aenigmaticum, B. pseudominutum, B. psygmophilum, Cladocopium goreaui, Cladocopium* genotypes C15 and C92 and *Durusdinium trenchii*). Profile hidden Markov models (pHMMs) were obtained from the PFAM 31.0 database for the cyclin N terminal domain (PF00134) and CDK conserved domain (PF00069). The pHMM models were re-trained using CDKs and cyclins from eukaryotic organisms closely related to Symbiodiniaceae (e.g. Apicomplexa) using the aphid R package[30].

The Symbiodiniaceae databases were then queried with the updated pHMM models using an optimal alignment homology search to find putative cyclin and CDK sequences (Fig. S1). Sequences with log-odds similarity scores > 50 were retained for cyclins and CDKs. The cyclin model returned 119 sequences and the CDK model returned 6032 sequences. Due to the high abundance of Symbiodiniaceae CDK sequences returned from the model, the collected CDK sequences from the pHMM model were examined further using conserved CDK motifs (Table S3)[31–34]. If the CDK contained a motif that when BLASTp searched against the NCBI non-redundant database matched to a CDK, the sequence was retained for further analysis. All 119 cyclins retrieved by the model were also searched, and were included in the analysis if the highest-scoring sequence was annotated as a cyclin

or CDK and had an E value $\leq 1 \times 10^{-5}$. Owing to the lack of information available for CDKs and cyclins in other unicellular marine eukaryotes, several taxa (Table S5) were chosen for screening through the trained pHMM models to identify putative cyclin and CDK sequences, allowing possible alveolate-specific groups to be identified.

Sequence alignment and phylogenetic analysis. Phylogenetic trees were generated twice. The sequence alignment for the first set of trees was aligned to just the conserved cyclin N (PFAM ID:PF00134) and protein kinase domains (PFAM ID: PF00069), which were used to determine distinct phylogenetic groups of Symbiodiniaceae cyclins and CDKs. These were later used to identify other similar sequences from the Symbiodiniaceae databases.

The first trees were generated by aligning the putative CDKs and cyclins in the aphid R package[30] (along with other eukaryotic cyclins and CDKs) and the best substitution model was selected by ProTest (v3.4)[35]. Both alignments had an appropriate evolutionary model of PROTOGAMMAAUTO, which was then used to infer maximum-likelihood trees in RAxML (v8.2.12)[36]. Bootstrap support was used to find the distinct phylogenetic groupings among Symbiodiniaceae CDKs and cyclins ($n = 1000$) by using the topology of the tree with the highest log-likelihood score. Trees were rooted using the *H. sapiens* MAPK (NP_002737.2) gene for the CDK tree and *H. sapiens* CABLES1 (NP_112492.2) and *H. sapiens* CABLES2 (NP_001094089.1) for the cyclin tree based on a previous study on animal cyclins and CDKs[37]. Symbiodiniaceae candidate proteins from distinct phylogenetic CDK and cyclin groups were used to perform custom BLASTp searches (Table S4) in Geneious v.11.1.5 (Biomatters Ltd.) against the 27 Symbiodiniaceae databases used in this study, to ensure that all putative CDKs and cyclins were identified. The first 10 Symbiodiniaceae proteins with the highest E-value ($\leq 1 \times 10^{-5}$) that were not previously identified by the pHMM model, and that identified a CDK or cyclin on the NCBI nr database in BLASTp searches, were collected from each Symbiodiniaceae database for each of the candidate proteins. These newly identified Symbiodiniaceae sequences were added to the previously collected sequences through the pHMM models and together these were entered into CD-Hit v4.8[38] to remove isoforms and redundant proteins using a similarity threshold of 90%.

Once redundant proteins and isoforms were removed, Symbiodiniaceae sequences were submitted to InterProScan[39] to identify CDK and cyclin domains. Due to the low-quality annotations in Symbiodiniaceae databases[40], many sequences contained regions that coded other proteins, therefore the alignments were trimmed manually in Geneious v.11.1.5 to CDK- (PFAM ID: PF00069; PANTHER ID: PTHR24056) and cyclin-(PFAM ID:PF00134, PF02984, PF16899 and PF08613; PANTHER ID: PTHR10177) annotated domains. The final CDK alignment for the second phylogenetic analysis was 465 amino acids (aa) long, and contained 177 Symbiodiniaceae sequences and 50 CDKs from other eukaryotes (Supplementary File S1), whereas the cyclin alignment was 395 aa long and contained 191 Symbiodiniaceae sequences and 54 cyclins from other eukaryotes (Supplementary File S2). All CDK and cyclin families from *Homo sapiens* were included in the trees to create the correct topologies, and CDKs and cyclins from other model organisms, including *Saccharomyces cerevisiae* and *Arabidopsis thaliana,* were only included if Symbiodiniaceae proteins were related to them.

Final CDK and cyclin alignments were run through ProTest (v3.4)[35] as described previously. Maximum-likelihood trees were then run in PhyML (v3.1)[41] using the Akaike information criterion, which corresponded to the LG + I + G + F model for the CDK alignment with a proportion of invariable sites of 0.039 and a gamma shape parameter of 1.195, and the LG + G + F model for cyclin alignments with a gamma shape parameter of 2.331. Due to the quantity of sequences in the tree, an approximate likelihood ratio test (aLRT) was used for branch support instead of bootstrap support[42], however it has been shown to be very similar in calculating correct branch supports[43]. Based on a comparison of correct branch topologies determined by bootstrap support and SH-values[43], true Symbiodiniaceae CDK and cyclin homologs were determined by branches containing an SH-value > 0.8. Trees were rooted as described previously. Trees were edited in the Interactive Tree of Life (iToL) software v.5.6.3[44]. The nomenclature of protein groups that did not phylogenetically group with other well-classified CDKs or cyclins was attributed by using BLAST searches against the NCBI nr database.

Cyclin and CDK gene expression of *Breviolum minutum*. To explore expression of cyclins and CDKs in Symbiodiniaceae, RNA-Seq reads were analysed from a recent study by Maor-Landaw et al.[45] on the expression of cultured ($n = 3$) and freshly isolated *Breviolum minutum* ($n = 3$) from the sea anemone *Exaiptasia diaphana* (= *pallida*) (SRA PRJNA544863). Reads were aligned to the *B. minutum* genome assembly[46] using STAR v2.7.1a in two-pass mode[47] and read counts were extracted from the alignments with featureCounts v1.6.3[48]. Differential expression analysis was completed using the exact test in EdgeR[49] on TMM normalized counts of the cultured and isolated *B. minutum*. Differentially expressed genes (DEGs) were those with Benjamini–Hochberg adjusted p-values < 0.05. Cyclins and CDKs identified in *B. minutum* were selected from the list of DEGs to generate a heat map in the R environment[50], using the mean–variance modelling at the observational level (voom)[51] of $\log_2$-transformed counts *per* million (CPM).

Results and discussion

Characterisation and phylogenetic positioning of Symbiodiniaceae CDK sequences. Eukaryotic organisms contain different numbers of CDK proteins, ranging from three in premetazoans, to 20 in eumetazoans such as *Homo sapiens*[37]. A total of 177 unique Symbiodiniaceae CDK gene copies were identified across six genera (Table 1). CDK gene copy numbers were the highest in *Cladocopium goreaui*, which contained 16 CDK copies. Interestingly, no CDKs related to the CDK4/6 family nor their cyclin partners (cyclin E) were found in Symbiodiniaceae using the databases referenced in this study (Table 1; Fig. 2). This agrees with findings for plants and many protists, in which there is also an absence of the CDK4/6 family and cyclin E in most pre-metazoan lineages[37].

	Source of database	CDK1/2/3 subfamily	CDK4/6 subfamily	CDK5 subfamily (CDK5/14/15/Pho85)	CDK7	CDK8 subfamily (CDK8/19)	CDK9 subfamily (CDK9/12/13)	CDK10/CDK11 subfamily	CDK20	Alveolate-specific CDKA	Alveolate-specific CDKB	Alveolate-specific CDKC	Alveolate-specific CDKD	Alveolate-specific CDKE	Alveolate-specific CDKF	Alveolate-specific CDKG	Alveolate-specific CDKH	Alveolate-specific CDKI	Alveolate-specific CDKJ	Parasitic CDKA	Apicomplexan Cdc2-like CDK	Total
S. microadriaticum	G				1				1	1	1	1	1		1	1	1	1	1			11
S. tridacnidorum	G				1		1	1		1	1	1	1	1	1		1	1	1			12
Symbiodinium sp. #1	T				1		1	1			1	1	1	1	1	1		1				10
Symbiodinium sp. #2	T				1			1			1			1				1				5
B. minutum	G				1		1	1	1	1	1	1	1	1	1	1	1	1	1			14
B. aenigmaticum	T				1		1	1			1	1	1	1	1		1	1	1			11
B. pseudominutum	T				1		1	1		1	1	1	1	1	1	1		1	2			13
B. psygmophilum	T				1		1	1		1	1	1	1	1	1	1	1	1	1			13
Breviolum sp. #1	T				1		1	1		1	1	1	1	1	1		1	1	2			13
C. goreauii	G	1		1	1		1	1		1	1	1	1	1	1	1		1	2		1	16
Cladocopium sp. C15	T				1						1	1	1	1	1		1	1	1			9
Cladocopium sp. C92	G						1		1		1	1	1	1	1	1	1		1			10
Cladocopium sp. #1	T										1			1						1		3
Cladocopium sp. #2	T				1		1	1			1	1	1	1	1		1	1				10
Cladocopium sp. #3	T										1	1		1								2
D. trenchii	T			1							1	1	1	1						1		6
Durusdinium sp. #1	T									1		1		1				1	1			4
Effrenium voratum	T										1	1	1	1	1			1	1			7
Fugacium kawagutii	G				1			1	1	1	1	1										5
TOTAL		1	0	2	13	0	10	11	4	9	18	17	14	17	13	7	9	14	15	2	1	177

Table 1. Gene copies of CDKs in the Symbiodiniaceae.

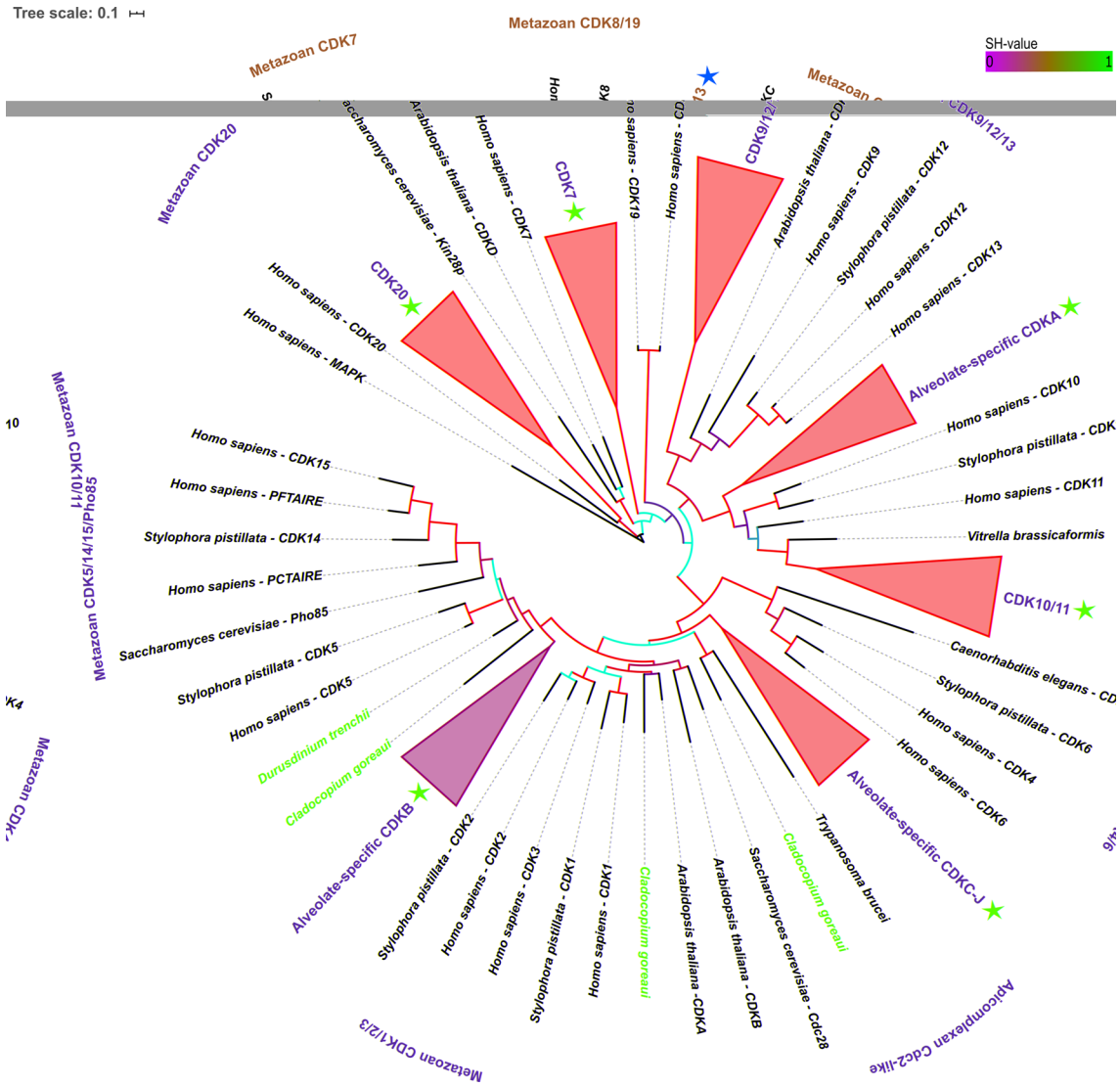

Figure 2. Collapsed phylogenetic tree of CDKs in the Symbiodiniaceae. Colour of branches corresponds to aLRT support (SH-value). Purple branches correspond to SH-values below 0.5, brown branches correspond to SH-values near 0.5, and green branches correspond to SH-values close to 1. Symbiodiniaceae species are written in blue, and blue stars depict collapsed branches containing Symbiodiniaceae species. The tree was made using PhyML(v3.1)[41] and visualised using the Interactive Tree of Life software (v5.6.3)[44].

Some of the Symbiodiniaceae CDKs showed high sequence similarity to eumetazoan CDKs, however the largest expansion of CDKs was within the alveolate-specific CDK groups (Table 1, Fig. 2). A previous study[20] investigating Symbiodiniaceae cell-cycle proteins found four *B. minutum*-specific CDKs. Here we show that three of those four CDKs are also present across other Symbiodiniaceae species (alveolate-specific CDKG/H/J—Table 1; Supplementary Fig. S2). In the previous study[20], the *B. minutum* CDKs (alveolate-specific CDKG/H/J) did not change their expression with cell-cycle phase when in a free-living state. However, our analysis of the previously published RNA-Seq data[45] shows that symbiosis alters the expression of *B. minutum* CDKG and CDKH, which were both up-regulated *in hospite* compared to when in culture (Table S6; Fig. 3).

The most common CDK identified in Symbiodiniaceae was an alveolate-specific CDK (CDKB) with gene copies found across 18 species in the five Symbiodiniaceae genera examined (Table 1). Symbiodiniaceae proteins in the CDKB group contained the canonical CDK motif PSTAIRE (Table 2). The CDKB sister clade is the Pho85/CDK5 subfamily (SH-value 0.95), which is sister to the metazoan CDK1/*S. cerevisae* Cdc28, with strong branch support (SH-value = 1; Supplementary Fig. S2). CDK1/Cdc28 is the primary cell-cycle regulator from yeast to humans[52–54], however Pho85 has been shown to have overlapping roles with Cdc28, phosphorylating many of the same substrates[55]. The primary roles of Pho85 include responding to environmental cues via the induction of signals that inform the cell whether conditions are adequate for cell division and nutrient metabolism [56]. As Symbiodiniaceae proliferate in response to increased nutrients[5], they may have evolved CDKs that possess similar functions for linking external stimuli (e.g. environmental nitrogen and phosphorus levels) to cell-cycle progression. Furthermore, our analysis of the RNA-Seq data comparing cultured *versus* freshly-isolated *B. minutum*[45]

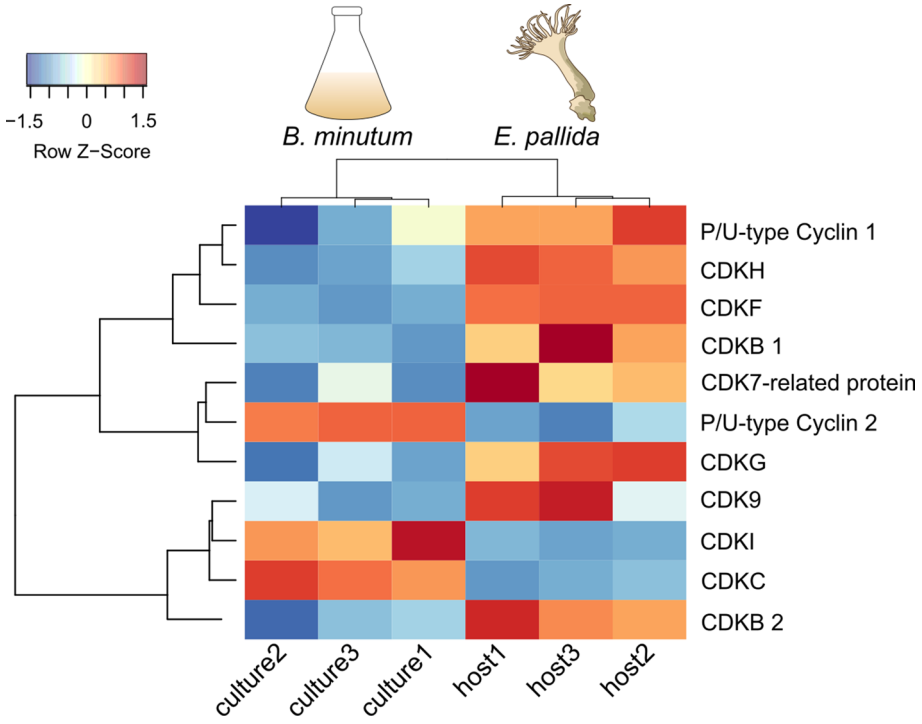

Figure 3. Heat map comparison of *Breviolum minutum* cyclin and CDK gene expression between culture and cells freshly isolated from *Exaiptasia pallida*. Red corresponds to a higher Z-score and gene up-regulation whilst blue corresponds to a lower Z-score and down-regulation.

CDK group	Symbiodiniaceae motif
CDK1/2/3 subfamily	PSTALRE
CDK4/6 subfamily	N/A
CDK5 subfamily (CDK5/14/15/Pho85)	PCTAIRE
CDK7	(G/S)TALRE
CDK8 subfamily (CDK8/19)	N/A
CDK9/12/13	P(A/T/S)T(S/A/C)(I/V)RE
CDK10/11	P(V/S)(P/A/S)S(L/I)RE
CDK20	PWFSAERE
Alveolate-specific CDKA	P(K/R)(I/S)SLRE
Alveolate-specific CDKB	PSTAIRE
Alveolate-specific CDKC	PSTAIRE
Alveolate-specific CDKD	PSTALRE/EHQLRRE
Alveolate-specific CDKE	P(G/S)TA(I/L)RE
Alveolate-specific CDKF	(S/P)(A/P)(T/H/Y/Q)(T/A/V)(I/L)RE
Alveolate-specific CDKG	S(A/T)Q(V/A)LRE
Alveolate-specific CDKH	(S/T)S(Y/F)(S/A)(L/I)RE
Alveolate-specific CDKI	P(T/A)(T/A)(S/T/A)(I/L)RE
Alveolate-specific CDKJ	P(T/A)TALRE; PAVA(L/M)RE
Parasite CDKA	PSTAIRE
Apicomplexan Cdc2-like CDK	PQTALRE

Table 2. Conserved motifs found in the Symbiodiniaceae CDK genes.

suggests that two CDKB genes are up-regulated in symbiosis (Table S6; Fig. 3). We hypothesise that, due to its phylogenetic grouping, conserved motif, widespread presence across Symbiodiniaceae and up-regulation in the symbiotic state, CDKB may be a homolog of Cdc28/Pho85 and a primary cell-cycle regulator in Symbiodiniaceae. This hypothesis requires confirmation.

	Cydin type	Symbiodiniaceae motif	*Symbiodinium microadriaticum*	*Symbiodinium triacnidorum*	*Symbiodinium* sp.#1	*Symbiodinium* sp. #2	*Breviolum minutum*	*Breviolum aenigmaticum*	*Breviolum pseudominutum*	*Breviolum psygmophilum*	*Breviolum* sp. #1	*Cladocopium goreaui*	*Cladocopium* sp. C15	*Cladocopium* sp. C92	*Cladocopium* sp. #1	*Cladocopium* sp.#2	*Cladocopium* sp. #3	*Durusdinium trenchii*	*Durusdinium* sp.#1	*Effrenium voratum*	*Fungacium kawagutii*	Total
Eumetazoan and plant cell-cycle cyclins	Cyclin A	(M/L)R(A/V)(I/A)L(V/I)DWL										1						1				2
	Cyclin B	YRTKIVNWM; NLAVLHDWL										1						1				2
	Cyclin D	MRRMVTSWM											1									1
	Plant Cyclin D-like	ERALAVDWL; DRQETLTWM; RRLDALEWL	1	1	1		2	2	2	2	1	2	2	2				1		1		20
	Cyclin E																					0
	Cydin G/I	GRRDLMIWL;QRDNITTFM;(W/N)R(R/D)(Q/D)(M/S)(I/T)(E/V)(W/F)(C/I)										1	1					2				4
	Cydin J/O																					0
	Cydin F																					0
Eumetazoan transcriptional cydins	Cyclin C																					0
	Cyclin H																					0
	Cydin K																					0
	Cydin L	LR(R/A)FG(V/G/N/S)VL(I/L)	2	1	1	1	2		2	2	2	2	1	2								18
	Cydin T																					0
	Cydin Y-like	LADEIYELL; S(K/T)E(T/A)ILDFL; REMVLDFL; HEAVL(T/A)FL		2	2		1		1	1	1	1		1		1		1	1	2		15
	Cydin Y	TVDNIYEFM; –IYDFL	1	1		1	1				1	1								1		7
Protist A/B cyclins	Cydin A/B	MR(G/A)ILVDWL; ER(A/G)(L/T/A/S/C/I)(A/V)(A/D/N)W(L/M); (S/Q)RA(V/T)(Q/L)(I/V)D(F/M)(M/I)	2	4	3	2	3	4	3	3	3	3	3	3	2	4	1	2	2	5	2	54
	Apicomplexan cyclin B	MR(T/I)ILVDWL										1						1				2
	Parasitic mitotic cyclin	PSINVADYL; PGITMPDFF; PPLSLADLG										2						1				3
	P/U cyclin	PSISVRSYL; PPIT(V/L)(R/K)DY(V/L); (E/D)PPDI(S/N)(A/Y/S)(Y/F)(I/V); (K/S)(N/A)MDLDDFI; E(S/T)(S/Q/V)DIEEYI; P(T/S)I(S/G)(V/I)(G/E)(E/D)YL; PKISV(R/L)(D/N)YL; PGIG(V/A/I)(A/E)(A/Q/L/V)YL; P(G/T/S)I(P/S)V(D/Q)(K/Q)YL	5	5	4		4	4	4	4	4	4	2	3	2	6	1	2	1	6	2	63
Total			11	14	11	4	13	10	12	12	12	19	10	11	4	11	2	12	4	15	4	191

Table 3. Gene copies of cyclins in the Symbiodiniaceae and complementary conserved motifs.

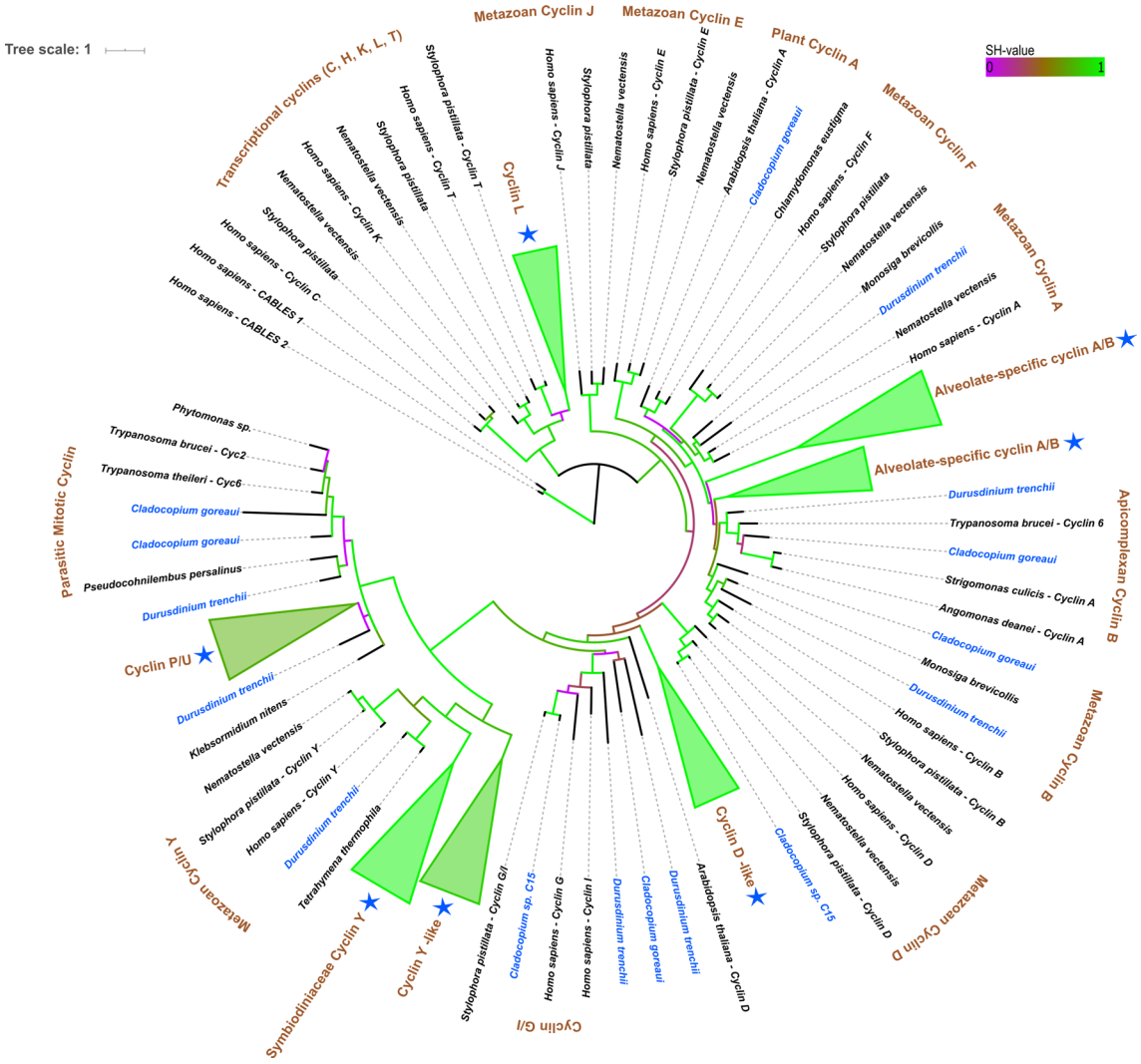

Figure 4. Collapsed phylogenetic tree of cyclins in the Symbiodiniaceae. Colour of branches corresponds to aLRT support (SH-value). Purple branches correspond to SH-values below 0.5, brown branches correspond to SH-values near 0.5, and green branches correspond to SH-values close to 1. Symbiodiniaceae species are written in blue, and blue stars depict collapsed branches containing Symbiodiniaceae species. The tree was made using PhyML(v3.1)[41] and visualised using the Interactive Tree of Life software (v.5.6.3)[44].

Proteins related to eumetazoan transcriptional CDK subfamilies (CDK9/12/13 (SH-value = 0.89), CDK10/11 (SH-value = 0.89) and CDK20 (SH-value = 0.93)) were also present in Symbiodiniaceae (Table 1; Supplementary Fig. S2). Amongst transcriptional roles, the CDK10/11 subfamily has also been proposed to have roles in cell-cycle progression during the G_2/M phase (Table S1)[57]. However, in *B. minutum,* CDK20, CDK9 and CDK11 expression did not change with cell-cycle phase[20], highlighting their similarity to metazoan CDK20, CDK9 and CDK11, which are predominantly transcriptional CDKs and indirectly related to the cell cycle[58]. Previous studies[20] have reported an absence of CDK7 in *B. minutum*, however this study found a CDK7-related gene (confirmed via BLAST searches on the NCBI nr database) across 13 different Symbiodiniaceae species (Supplementary Fig. S2). The difference in results may be explained, in part, by the Symbiodiniaceae CDK7 being phylogenetically distant from the metazoan CDK7 and yeast CDK7 homolog (Kin28p), grouping separately and with no concrete relationship to any other CDK included in this study, possibly owing to its divergence. CDK7 has been discovered in other basal organisms, such as the amoebozoan *Dictyostelium purpureum*[59]. In metazoans, CDK7 forms part of the cyclin kinase-activating (CAK) complex that activates other CDKs by phosphorylating their T-loop[60], and inhibition of CDK7 led to the arrest of the cell cycle in proliferating cells[61]. The previously published RNA-Seq data[45] show that the CDK7-related gene was up-regulated in symbiotic *B. minutum* (Table S6).

Symbiodinium sp. #2 contained CDKs and cyclins that are more similar to those of the free-living dinoflagellate *Amphidinium* (SH-value > 0.95) than other Symbiodiniaceae species (Supplementary Fig. S2). CDKs and cyclins that are not present in *Amphidinium* sp. but are present in *Symbiodinium* sp. #2 grouped next to, not with, the other Symbiodiniaceae species (SH-value > 0.78). This placement may reflect the basal status of *Symbiodinium* within the Symbiodiniaceae[21].

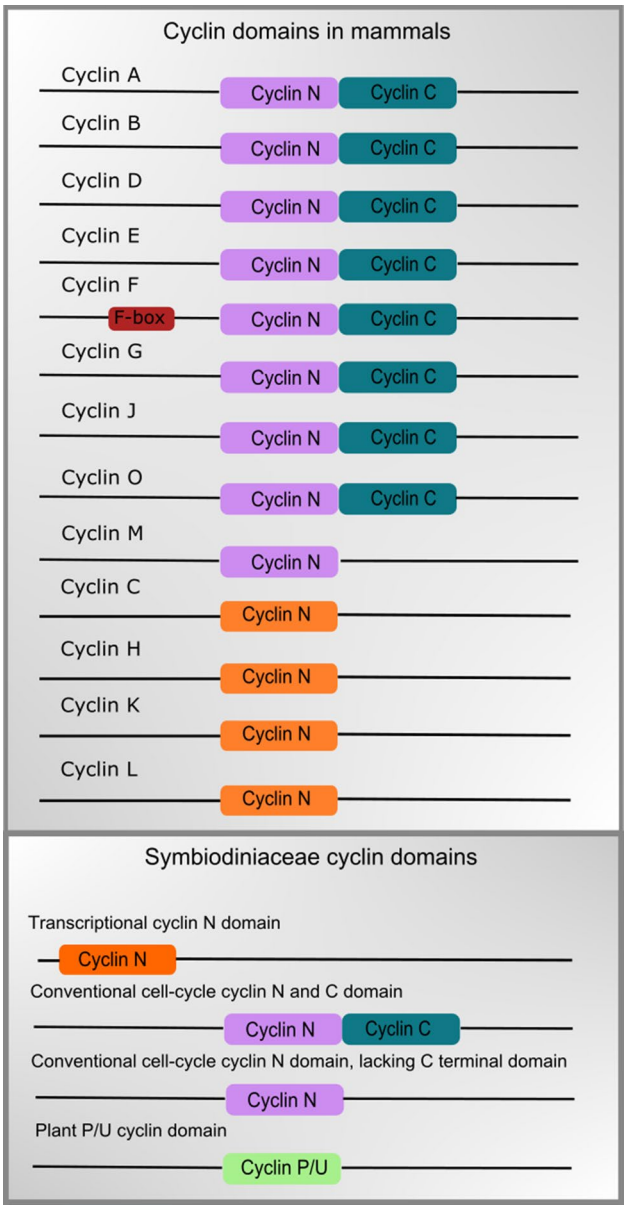

Figure 5. Domain structure of cyclin proteins present in the Symbiodiniaceae.

Several Symbiodiniaceae species contained CDKs found in parasitic taxa. A CDK protein that is related to a gene present in the free-living, facultative pathogenic marine ciliate *Pseudocohnilembus persalinus,* was found in both *D. trenchii* and *Cladocopium* sp. #1 (SH-value = 1), while *C. goreaui* harbours a CDK related to Cdc2-related kinase 6 (CRK6) from *Trypanosoma brucei* (SH-value = 0.97) (Fig. 2, Supplementary Fig. S2). Studies[62,63] have shown that the loss of *T. brucei* CRK6 slows cell growth but does not inhibit the cell cycle (contrasting with cell cycle indispensable CRK3 and CRK1), highlighting a function of CRK6 that may not be directly associated with the cell cycle.

Characterisation and phylogenetic positioning of Symbiodiniaceae cyclin sequences. Similar to CDKs, the number of cyclins differs across eukaryotes – from eight in premetazoans to 29 in *Homo sapiens*[37]. Across the six Symbiodiniaceae genera examined, 191 cyclins were identified (Table 3; Fig. 4). *C. goreaui* contained the most cyclin gene copies, harbouring 19 distinct copies. Differences in abundance of cell-cycle proteins (cyclins and CDKs) between different Symbiodiniaceae species could be a result of the different database information provided (genomes *versus* transcriptomes), as if CDKs and cyclins were not expressed at the time of transcriptomic analysis, these may have been missed, thus producing a bias towards genomes harbouring more cyclin and CDK gene copies. Another possible reason for the difference in cyclin and CDK gene copies in the Symbiodiniaceae are gene duplication events, which are followed by genetic drift over time, causing the formation of cell-cycle paralogs with functional divergence in the family.

All the cyclins found in the Symbiodiniaceae contained one of three distinct domains (Fig. 5): the conventional cell-cycle cyclin N and C domains; a cyclin N domain found nearer the amino terminus than the position of the conventional cell-cycle cyclin N domain which corresponded phylogenetically to transcriptional cyclins (specifically cyclin L); and a single plant P/U cyclin domain that is phylogenetically related to the analogous domain of the Pho80p cyclin in *S. cerevisiae*.

Proteins related to eukaryotic cell-cycle cyclins A, B, D and G/I, and transcriptional cyclin L were identified in the Symbiodiniaceae, along with proteins related to plant cyclin D, protist/plant P/U-type cyclin and cyclin Y, as well as genes related to Cyc2 and mitotic Cyc6 from the sister taxon Apicomplexa (Fig. 4; Supplementary Fig. S3). Three phylogenetically distinct groups of cyclins were also present in Symbiodiniaceae, that upon searching the NCBI nr database, matched to alveolate-specific cyclins A/B (Supplementary Fig. S3). Two cyclins previously reported to be *B. minutum*-specific[20] were found in other Symbiodiniaceae species and belong to the "Plant Cyclin D-like" grouping (Table 3; Supplementary Fig. S3). In metazoans and plants, cyclin D is required for G_1 phase progression[64].

An expansion of the protist/plant P/U-type cyclin groups was found within Symbiodiniaceae, with 63 gene copies being present across six Symbiodiniaceae genera (Table 3, Fig. 4, Supplementary Fig. S3). This finding agrees with the previous study[20], which found P-type cyclins in *B. minutum*. Genes within these groups were related to the *S. cerevisiae* Pho80p cyclin. In *S. cerevisiae,* the Pho80 subfamily of P/U-type cyclins (Pho80, Pcl6, Pcl7, Pcl8 and Pcl10[55]) links nutrient availability with cell-cycle progression[65]. In *A. thaliana,* P/U-type cyclins are implicated in the switch from heterotrophic to autotrophic growth[66]. RNA-Seq data[45] revealed that two of these P/U type cyclins had contrasting expression (one being up-regulated whilst the other was down-regulated) *in hospite versus* in culture in *B. minutum* (Table S6; Fig. 3). Given that nutritional exchange is a fundamental feature of the cnidarian–dinoflagellate symbiosis[1], and that P/U cyclins are involved in glycogen metabolism and carbon source utilisation[56,67], the differential expression of these cyclins *in hospite* is unsurprising. Whether the difference in expression is a response to environmental stimuli exclusively experienced in symbiosis, e.g. host-associated factors such as the pH of the symbiosome in which the alga resides[68], requires further study. Similar to Symbiodiniaceae, the apicomplexan *T. gondii* also lacks a cyclin E homolog and instead uses a P-type cyclin for G_1 phase progression[69]. Symbiodiniaceae may also use P-type cyclins in place of eumetazoan cyclin E, however this requires confirmation.

Twenty two cyclin Y-like gene copies were found across the Symbiodiniaceae. These encompassed two phylogenetic groups, one termed "Cyclin Y" which grouped with eumetazoan Cyclin Y (SH-value = 0.93), and one group of cyclins that grouped as a sister group with the conventional eumetazoan Cyclin Y (SH-value = 0.80) that were termed "Cyclin Y-like" (Fig. 4, Supplementary Fig. S3). Cyclin Y is absent in plants and fungi (being replaced by the Pcl class of cyclins in fungi) but is present in animals and protists[59]. In eumetazoans and fungi, cyclin Y and Pcl1 cyclins are the binding partners of CDK14 and Pho85, respectively[70,71]. In yeast, the cyclin Y homolog, Pcl1, is expressed during the G_1 phase of the cell cycle[70] and provides information to the cell, determining whether it passes the START checkpoint, where the yeast cell commits to mitosis[56]. In *Drosophila*, cyclin Y is required for Wnt signalling by localising the CDK14 kinase to the cell membrane[72]. As Wnt signalling is an indispensable pathway for the long-term viability of cells[73], the presence of cyclin Y and cyclin-Y like genes in most eukaryotes is predicted.

Uniquely, *C. goreaui* and *D. trenchii* both contain cyclins present in two phylogenetic groups that cluster with mitotic cyclins from the dinoflagellate sister taxon, the apicomplexans[74] (Fig. 4). One group is related to the B-type G_2/M phase-specific cyclin, Cyc6, in the apicomplexans (SH-value > 0.98), while the other clusters with Cyc2-like from *T. brucei*, which is involved in transition from both the G_1 to S and G_2 to M phases[75] (Fig. 4). The correlation in cell-cycle machinery of both cyclins and CDKs between pathogenic protists and *D. trenchii,* which is reported to colonise hosts during heat stress opportunistically[25,76] and has a fast growth rate *versus* other Symbiodiniaceae species in culture[23], is noteworthy and warrants future investigation.

Cladocopium sp. C15 harbours two cyclins (cyclin D and cyclin G/I) that are related to those in the symbiotic coral, *Stylophora pistillata*, with strong support (SH-value = 1). Both *Cladocopium* sp. C15 cyclin D and G/I share a similar identity (92.1% and 74.5%, respectively) and similarity (95.7% and 91.6%, respectively), across the full sequence length to *S. pistillata* cyclins. To account for possible contamination of host material in the *Cladocopium* sp. C15 transcriptome, the origin of this symbiont was traced[77]. The *Cladocopium* sp. C15 was found to have been freshly isolated from its host *Porites compressa,* so host contamination cannot be excluded. This being said, symbiosis has been suggested to drive the formation of paralogous genes involved in host-symbiont interactions due to selective pressure for a more mutualistic partnership between host and symbiont[78]. How the evolution of cell-cycle proteins that share a high similarity between host and symbiont affects biomass co-ordination is deserving of future attention.

Conclusions

Our study shows the divergence of cell-cycle proteins in the Symbiodiniaceae family and demonstrates that there are several conserved CDK and cyclin groups across the Symbiodiniaceae, though also marked species-specific differences. Which of these conserved cell-cycle proteins are indispensable for cell-cycle progression and which species-specific proteins influence proliferation rates in symbiosis remains unknown. Further study will be required to clarify which CDKs and cyclins are required for Symbiodiniaceae cell-cycle progression, and whether this differs between species and symbiotic states. As annotation of Symbiodiniaceae genomes is challenging[79], future studies should aim to apply the same comparative analysis across new Symbiodiniaceae genomes to inform cyclin and CDK gene prediction accurately.

Received: 11 April 2020; Accepted: 28 October 2020
Published online: 24 November 2020

References

1. Davy, S. K., Allemand, D. & Weis, V. M. Cell biology of cnidarian–dinoflagellate symbiosis. *Microbiol. Mol. Biol. Rev.* **76**, 229–261 (2012).
2. Wakefield, T. S. & Kempf, S. C. Development of host-and symbiont-specific monoclonal antibodies and confirmation of the origin of the symbiosome membrane in a cnidarian–dinoflagellate symbiosis. *Biol. Bull.* **200**, 127–143 (2001).
3. Jones, R. J. & Yellowlees, D. Regulation and control of intracellular algae (= zooxanthellae) in hard corals. *Philos. Trans. R. Soc. Lond. B.* **352**, 457–468 (1997).
4. Hoegh-Guldberg, O. & Smith, G. J. Influence of the population density of zooxanthellae and supply of ammonium on the biomass and metabolic characteristics of the reef corals *Seriatopora hystrix* and *Stylophora pistillata*. *Mar. Ecol. Prog. Ser.* **57**, 173–186 (1989).
5. Hoegh-Guldberg, O. The population dynamics of symbiotic zooxanthellae in the coral *Pocillopora damicornis* exposed to elevated ammonium (NH_4Cl) concentrations. *Pac. Sci.* **48**, 263–272 (1994).
6. Muller-Parker, G., McCloskey, L. R., Hoegh-Guldberg, O. & McAuley, P. J. Effect of ammonium enrichment on animal and algal biomass of the coral *Pocillopora damicornis*. *Pac. Sci.* **48**, 273–283 (1994).
7. Smith, G. J. & Muscatine, L. Cell cycle of symbiotic dinoflagellates: variation in G_1 phase-duration with anemone nutritional status and macronutrient supply in the *Aiptasia pulchella–Symbiodinium pulchrorum* symbiosis. *Mar. Biol.* **134**, 405–418 (1999).
8. Fitt, W. K. Cellular growth of host and symbiont in a cnidarian–zooxanthellar symbiosis. *Biol. Bull.* **198**, 110–120 (2000).
9. Xiang, T. *et al.* Symbiont population control by host-symbiont metabolic interaction in Symbiodiniaceae–cnidarian associations. *Nat. Commun.* **11**, 108 (2020).
10. Baghdasarian, G. & Muscatine, L. Preferential expulsion of dividing algal cells as a mechanism for regulating algal–cnidarian symbiosis. *Biol. Bull.* **199**, 278–286 (2000).
11. Dunn, S. R., Schnitzler, C. E. & Weis, V. M. Apoptosis and autophagy as mechanisms of dinoflagellate symbiont release during cnidarian bleaching: every which way you lose. *Proc. R. Soc. Lond. B* **274**, 3079–3085 (2007).
12. Pardee, A. B. G_1 events and regulation of cell proliferation. *Science* **246**, 603–608 (1989).
13. Nishitani, H. & Lygerou, Z. Control of DNA replication licensing in a cell cycle. *Genes Cells* **7**, 523–534 (2002).
14. Stark, G. R. & Taylor, W. R. Analyzing the G_2/M checkpoint. *Methods Mol. Biol.* **280**, 51–82 (2004).
15. Houtgraaf, J. H., Versmissen, J. & van der Giessen, W. J. A concise review of DNA damage checkpoints and repair in mammalian cells. *Cardiovasc. Revascularization Med.* **7**, 165–172 (2006).
16. Barnum, K. J. & O'Connell, M. J. Cell-cycle regulation by checkpoints. *Methods Mol. Biol.* **1170**, 29–40 (2014).
17. Malumbres, M. & Barbacid, M. Cell cycle, CDKs and cancer: a changing paradigm. *Nat. Rev. Cancer* **9**, 153–166 (2009).
18. Lim, S. & Kaldis, P. CDKs, cyclins and CKIs: roles beyond cell-cycle regulation. *Development* **140**, 3079–3093 (2013).
19. Vermeulen, K., Van Bockstaele, D. R. & Berneman, Z. N. The cell cycle: a review of regulation, deregulation and therapeutic targets in cancer. *Cell Prolif.* **36**, 131–149 (2003).
20. Cato, M. L. *et al.* Genome-wide analysis of cell-cycle-regulating genes in the symbiotic dinoflagellate *Breviolum minutum*. *Genes Genomes Genet.* **9**, 3843–3853 (2019).
21. LaJeunesse, T. C. *et al.* Systematic revision of Symbiodiniaceae highlights the antiquity and diversity of coral endosymbionts. *Curr. Biol.* **28**, 2570–2580 (2018).
22. Nitschke, M. R. *et al.* Description of *Freudenthalidium* gen. nov. and *Halluxium* gen. nov. to formally recognize clades Fr3 and H as Genera in the Family Symbiodiniaceae (Dinophyceae). *J. Phycol.* **56**, 927–943 (2020).
23. Fujise, L. *et al.* Cell-cycle dynamics of cultured coral endosymbiotic microalgae (*Symbiodinium*) across different types (species) under alternate light and temperature conditions. *J. Eukaryot. Microbiol.* **65**, 505–517 (2018).
24. Yuyama, I. & Higuchi, T. Comparing the effects of symbiotic algae (*Symbiodinium*) clades C1 and D on early growth stages of *Acropora tenuis*. *PLoS ONE* **9**, e98999 (2014).
25. Leal, M. C. *et al.* Symbiont type influences trophic plasticity of a model cnidarian–dinoflagellate symbiosis. *J. Exp. Biol.* **218**, 858–863 (2015).
26. Starzak, D. E., Quinnell, R. G., Nitschke, M. R. & Davy, S. K. The influence of symbiont type on photosynthetic carbon flux in a model cnidarian–dinoflagellate symbiosis. *Mar. Biol.* **161**, 711–724 (2014).
27. Gabay, Y., Weis, V. M. & Davy, S. K. Symbiont identity influences patterns of symbiosis establishment, host growth, and asexual reproduction in a model cnidarian–dinoflagellate symbiosis. *Biol. Bull.* **234**, 1–10 (2018).
28. Jeong, H. J. *et al.* Genetics and morphology characterize the dinoflagellate *Symbiodinium voratum*, n. sp., (Dinophyceae) as the sole representative of *Symbiodinium* clade E. *J. Eukaryot. Microbiol.* **61**, 75–94 (2014).
29. Liu, H. *et al. Symbiodinium* genomes reveal adaptive evolution of functions related to coral–dinoflagellate symbiosis. *Commun. Biol.* **1**, 1–11 (2018).
30. Wilkinson, S. P. aphid: an R package for analysis with profile hidden Markov models. *Bioinformatics* **35**, 3829–3830 (2019).
31. Joubes, J. *et al.* CDK-related protein kinases in plants. *Plant Mol. Biol.* **43**, 607–620 (2000).
32. Corellou, F., Camasses, A., Ligat, L., Peaucellier, G. & Bouget, F.-Y. Atypical regulation of a green lineage-specific B-type cyclin-dependent kinase. *Plant Physiol.* **138**, 1627–1636 (2005).
33. Malumbres, M. & Barbacid, M. Mammalian cyclin-dependent kinases. *Trends Biochem. Sci.* **30**, 630–641 (2005).
34. Talevich, E., Mirza, A. & Kannan, N. Structural and evolutionary divergence of eukaryotic protein kinases in Apicomplexa. *BMC Evol. Biol.* **11**, 321 (2011).
35. Darriba, D., Taboada, G. L., Doallo, R. & Posada, D. ProtTest 3: fast selection of best-fit models of protein evolution. *Bioinformatics* **27**, 1164–1165 (2011).
36. Stamatakis, A. RAxML version 8: a tool for phylogenetic analysis and post-analysis of large phylogenies. *Bioinformatics* **30**, 1312–1313 (2014).
37. Cao, L. *et al.* Phylogenetic analysis of CDK and cyclin proteins in premetazoan lineages. *BMC Evol. Biol.* **14**, 10 (2014).
38. Li, W., Jaroszewski, L. & Godzik, A. Clustering of highly homologous sequences to reduce the size of large protein databases. *Bioinformatics* **17**, 282–283 (2001).
39. Quevillon, E. *et al.* InterProScan: protein domains identifier. *Nucleic Acids Res.* **33**, 116–120 (2005).
40. Chen, Y., González-Pech, R. A., Stephens, T. G., Bhattacharya, D. & Chan, C. X. Evidence that inconsistent gene prediction can mislead analysis of dinoflagellate genomes. *J. Phycol.* **56**, 6–10 (2020).
41. Guindon, S. & Gascuel, O. A simple, fast, and accurate algorithm to estimate large phylogenies by maximum likelihood. *Syst. Biol.* **52**, 696–704 (2003).
42. Anisimova, M. & Gascuel, O. Approximate likelihood-ratio test for branches: a fast, accurate, and powerful alternative. *Syst. Biol.* **55**, 539–552 (2006).
43. Guindon, S. *et al.* New algorithms and methods to estimate maximum-likelihood phylogenies: assessing the performance of PhyML 3.0. *Syst. Biol.* **59**, 307–321 (2010).
44. Letunic, I. & Bork, P. Interactive tree of life (iTOL) v4: recent updates and new developments. *Nucleic Acids Res.* **47**, 256–259 (2019).

45. Maor-Landaw, K., van Oppen, M. J. H. & McFadden, G. I. Symbiotic lifestyle triggers drastic changes in the gene expression of the algal endosymbiont *Breviolum minutum* (Symbiodiniaceae). *Ecol. Evol.* **10**, 451–466 (2020).
46. Shoguchi, E. *et al.* Draft assembly of the *Symbiodinium minutum* nuclear genome reveals dinoflagellate gene structure. *Curr. Biol.* **23**, 1399–1408 (2013).
47. Dobin, A. *et al.* STAR: ultrafast universal RNA-seq aligner. *Bioinformatics* **29**, 15–21 (2013).
48. Liao, Y., Smyth, G. K. & Shi, W. featureCounts: an efficient general purpose program for assigning sequence reads to genomic features. *Bioinformatics* **30**, 923–930 (2014).
49. Robinson, M. D., McCarthy, D. J. & Smyth, G. K. edgeR: a Bioconductor package for differential expression analysis of digital gene expression data. *Bioinformatics* **26**, 139–140 (2010).
50. Team, R. C. R: A Language and Environment for Statistical Computing. Vienna: R Project. Available at: https://www.R-project.org (2020).
51. Law, C. W., Chen, Y., Shi, W. & Smyth, G. K. voom: precision weights unlock linear model analysis tools for RNA-seq read counts. *Genome Biol.* **15**, R29 (2014).
52. Santamaría, D. *et al.* CDK1 is sufficient to drive the mammalian cell cycle. *Nature* **448**, 811 (2007).
53. Lee, M. G. & Nurse, P. Complementation used to clone a human homologue of the fission yeast cell-cycle control gene cdc2. *Nature* **327**, 31 (1987).
54. Mendenhall, M. D. & Hodge, A. E. Regulation of Cdc28 cyclin-dependent protein kinase activity during the cell cycle of the yeast *Saccharomyces cerevisiae*. *Microbiol. Mol. Biol. Rev.* **62**, 1191–1243 (1998).
55. Huang, D., Friesen, H. & Andrews, B. Pho85, a multifunctional cyclin-dependent protein kinase in budding yeast. *Mol. Microbiol.* **66**, 303–314 (2007).
56. Carroll, A. S. & O'Shea, E. K. Pho85 and signaling environmental conditions. *Trends Biochem. Sci.* **27**, 87–93 (2002).
57. Li, S. *et al.* The cdc2-related kinase, PISSLRE, is essential for cell growth and acts in G_2 phase of the cell cycle. *Cancer Res.* **55**, 3992–3995 (1995).
58. Malumbres, M. Cyclin-dependent kinases. *Genome Biol.* **15**, 122 (2014).
59. Ma, Z. *et al.* Phylogenetic analysis reveals the evolution and diversification of cyclins in eukaryotes. *Mol. Phylogenet. Evol.* **66**, 1002–1010 (2013).
60. Schachter, M. M. *et al.* A CDK7-CDK4 T-loop phosphorylation cascade promotes G_1 progression. *Mol. Cell* **50**, 250–260 (2013).
61. Larochelle, S. *et al.* Requirements for CDK7 in the assembly of CDK1/cyclin B and activation of CDK2 revealed by chemical genetics in human cells. *Mol. Cell* **25**, 839–850 (2007).
62. Jones, N. G. *et al.* Regulators of *Trypanosoma brucei* cell-cycle progression and differentiation identified using a kinome-wide RNAi screen. *PLoS Pathog.* **10**, e1003886 (2014).
63. Tu, X. & Wang, C. C. Pairwise knockdowns of cdc2-related kinases (CRKs) in *Trypanosoma brucei* identified the CRKs for G_1/S and G_2/M transitions and demonstrated distinctive cytokinetic regulations between two developmental stages of the organism. *Eukaryot. Cell* **4**, 755–764 (2005).
64. Ortega, S., Malumbres, M. & Barbacid, M. Cyclin D-dependent kinases, INK4 inhibitors and cancer. *Biochim. Biophys. Acta* **1602**, 73–87 (2002).
65. Roques, M. *et al. Plasmodium* P-type cyclin CYC3 modulates endomitotic growth during oocyst development in mosquitoes. *PLoS Pathog.* **11**, e1005273 (2015).
66. Peng, L., Skylar, A., Chang, P. L., Bisova, K. & Wu, X. CYCP2;1 integrates genetic and nutritional information to promote meristem cell division in *Arabidopsis*. *Dev. Biol.* **393**, 160–170 (2014).
67. Huang, D. *et al.* Cyclin partners determine Pho85 protein kinase substrate specificity *in vitro* and *in vivo*: control of glycogen biosynthesis by Pcl8 and Pcl10. *Mol. Cell. Biol.* **18**, 3289–3299 (1998).
68. Barott, K. L., Venn, A. A., Perez, S. O., Tambutté, S. & Tresguerres, M. Coral host cells acidify symbiotic algal microenvironment to promote photosynthesis. *Proc. Natl. Acad. Sci.* **112**, 607–612 (2015).
69. Alvarez, C. A. & Suvorova, E. S. Checkpoints of apicomplexan cell division identified in *Toxoplasma gondii*. *PLoS Pathog.* **13**, e1006483 (2017).
70. Measday, V. *et al.* A family of cyclin-like proteins that interact with the Pho85 cyclin-dependent kinase. *Mol. Cell. Biol.* **17**, 1212–1223 (1997).
71. Jiang, M., Gao, Y., Yang, T., Zhu, X. & Chen, J. Cyclin Y, a novel membrane-associated cyclin, interacts with PFTK1. *FEBS Lett.* **583**, 2171–2178 (2009).
72. Sun, T., Co, N. N. & Wong, N. PFTK1 interacts with cyclin Y to activate non-canonical Wnt signaling in hepatocellular carcinoma. *Biochem. Biophys. Res. Commun.* **449**, 163–168 (2014).
73. MacDonald, B. T., Tamai, K. & He, X. Wnt/β-catenin signaling: components, mechanisms, and diseases. *Dev. Cell* **17**, 9–26 (2009).
74. Leander, B. S. & Keeling, P. J. Early evolutionary history of Dinoflagellates and Apicomplexans (Alveolata) as inferred from Hsp90 and actin phylogenies. *J. Phycol.* **40**, 341–350 (2004).
75. Liu, Y., Hu, H. & Li, Z. The cooperative roles of Pho80-like cyclins in regulating the G_1/S transition and posterior cytoskeletal morphogenesis in *Trypanosoma brucei*. *Mol. Microbiol.* **90**, 130–146 (2013).
76. Stat, M. & Gates, R. D. Clade D *Symbiodinium* in scleractinian corals: a "nugget" of hope, a selfish opportunist, an ominous sign, or all of the above?. *J. Mar. Biol.* **2011**, 1–10 (2010).
77. Keeling, P. J. *et al.* The Marine Microbial Eukaryote Transcriptome Sequencing Project (MMETSP): illuminating the functional diversity of eukaryotic life in the oceans through transcriptome sequencing. *PLoS Biol.* **12**, e1001889 (2014).
78. Duncan, R. P., Feng, H., Nguyen, D. M. & Wilson, A. C. C. Gene family expansions in aphids maintained by endosymbiotic and nonsymbiotic traits. *Genome Biol. Evol.* **8**, 753–764 (2016).
79. Chen, Y., González-Pech, R. A., Stephens, T. G., Bhattacharya, D. & Chan, C. X. Evidence that inconsistent gene prediction can mislead analysis of dinoflagellate genomes. *J. Phycol.* **1**, 95 (2019).

Acknowledgements

This research was supported by the Marsden Fund of the Royal Society Te Apārangi of New Zealand (Grant Number VUW1601), awarded to S.K.D., A.R.G., V.M.W. and C.A.O. and an associated PhD scholarship to L.M.G. Additional support was provided via strategic research funds from the School of Biological Sciences at Victoria University of Wellington to S.K.D.

Author contributions

The study was conceptualised by L.M.G., C.A.O., A.R.G., V.M.W., and S.K.D. L.M.G. wrote the manuscript, collected and analysed the sequence and phylogenetic data, and constructed all figures (apart from figure 3) and all tables. S.P.W. helped L.M.G. with data collection and analysis. S.A.K. conducted and analysed the expression analysis, constructed figure 3, helped revise the manuscript, and advised on methods, data analysis and

visualisation, C.A.O., V.M.W., S.K.D., A.R.G. helped edit and refine the manuscript. All authors reviewed the manuscript before submission.

Competing interests
The authors declare no competing interests.

Additional information
Supplementary information is available for this paper at https://doi.org/10.1038/s41598-020-76621-1.

Correspondence and requests for materials should be addressed to S.K.D.

Reprints and permissions information is available at www.nature.com/reprints.

Publisher's note Springer Nature remains neutral with regard to jurisdictional claims in published maps and institutional affiliations.